Evaluating rice performance in contrasting East African wetlands using an experimental and modelling approach

by Kristina Grotelüschen

Institute of Crop Science and Resource Conservation

UNIVERSITÄT BONN INRES

Evaluating rice performance in contrasting East African wetlands using an experimental and modelling approach

Dissertation
in fulfillment of the requirements for the degree of

'Doktorin der Agrarwissenschaften (Dr. agr.)'
at the Faculty of Agricultural Sciences
University of Bonn

by
Kristina Grotelüschen
born in Wildeshausen, Germany

Bonn, 2021

This dissertation was accepted by the Faculty of Agricultural Sciences at the University of Bonn.

Date of doctoral colloquium: 24.09.2021

Thesis reviewer:

Prof. Dr. Mathias Becker

Department of Plant Nutrition in the Tropics and Subtropics, Institute of Crop Science and Resource Conservation, University of Bonn, Germany

Thesis co-reviewer:

Dr. Thomas Gaiser

Department of Crop Science, Institute of Crop Science and Resource Conservation, University of Bonn, Germany

Associated promoters:

Prof. Dr. Matthias Langensiepen, Department of Plant Nutrition in the Tropics and Subtropics, Institute of Crop Science and Resource Conservation, University of Bonn, Germany

Dr. Kalimuthu Senthilkumar, Africa Rice Center (AfricaRice), P.O. Box 1690, Antananarivo, Madagascar

Dr. Donald S. Gaydon, CSIRO Food and Agriculture, Brisbane, Australia

Dr. Anthony M. Whitbread, International Crops Research Institute for the Semi-Arid Tropics (ICRISAT), P.O. Box 34441, Dar es Salaam, Tanzania

'Mkulima ni mmoja walaji ni wengi' (The farmer is one but those who eat the fruits of his labour are many)

Swahili Proverb (undated)

Kristina Grotelüschen

Evaluating rice performance in contrasting East African wetlands using an experimental and modelling approach, 171 pages.

Dissertation, University of Bonn, Bonn, Germany (2021)

With references, with summaries in English and German.

Acknowledgement

After many, many years in the making, this day has finally come and my PhD journey is coming to an end! It certainly wasn't a piece of cake but I am immensely grateful for all the happy memories and good friendships that will stay with me forever.

I am immensely grateful to Prof. Dr. Mathias Becker for his guidance and support throughout this study. Despite your busy schedule, you always made time for a quick coffee upon my return from the numerous field trips. And during our discussions, your enthusiasm, optimism and genuine humanity would lift my spirits every time I felt I had hit a dead end. Particularly during this last time, you helped me navigate the difficult waters and I will be forever thankful for that. I am also thankful to Dr. Thomas Gaiser who agreed to being the co-reviewer of this study – I hope you enjoyed the read! Kudos also to Prof. Dr. Matthias Langensiepen for his steady support throughout this study and to Dr Senthilkumar Kalimuthu who always made time to visit us in the field and was always there for guidance and support. Thank you both! Additionally, I want to thank Prof. Dr. Barbara Reichert and Prof. Dr. Thomas Döring for taking time out of their busy schedules to join my doctoral committee. Special thanks also to Prof. Dr. Salome Misana and Dr. Michael Ugen Adrigo for their support regarding field transportation and coordination in Tanzania and Uganda.

A huge shout out goes to the entire GlobE Wetlands family – I think we all value the bonds of friendship and tireless support to help navigate the (at times) treacherous waters of a PhD journey; namely Dr-to-be Kai Behn, Dr. Kristian Näschen, Dr. Katrin Wagner, Dr. Matian van Soest, Dr. Bisrat Haile Gebrekidan, and in particular my *work-wife* Dr-to-be Claudia Schepp. Claudia, while our 'Mission 2020' evidently failed, I wouldn't have succeeded with 'Mission 2021' without you – thank you for all the conversations during our field stays, extended lunch-breaks and beyond, and for your friendship – to many more adventures!

Special thanks to Susanne Ziegler, Dr. Julius Kwesiga, Dr. Geofrey Gabiri, Dr. Sonja Burghof, Dr-to-be Björn Glasner and Maureen Namugalu for successful collaboration in the field and subsequent discussions on field data or something completely else, data

exchange and for lending an ear whenever needed. It was a pleasure having worked with you! I would also like to thank Dr. Andrea Rechenburg, Dr. Carlos Angulo, Dr. Constanze Leemhuis, Dr, Daniel Neuhoff, Prof. Dr. Bernd Diekkrüger and Dr. Miguel Alvarez for continued discussions. Miguel, I really can't thank you enough for your everlasting patience in trying to bring R closer to me – certainly not an easy task. I would also like to thank Eike Kiene at the GlobE secretariat. Your constant support and tireless effort to keep the show going are highly appreciated, and so are all the off-topic conversations during coffee-breaks, *Feierabendbier*, and, let's face it, office hours.

Furthermore, I want to thank the additional Co-Authors of my publications in this thesis, namely Dr. Anthony Whitbread and Dr. Donald Gaydon. Anthony, I have always considered you a valuable mentor and I am grateful for all the support you provided during this study which I don't take for granted. Don, I am not sure I can express my sincere gratitude with words. Under no obligation whatsoever, you took me under your wings and even made me a part of your working group during my visit to Australia. I will never forget your humanity, the hospitality of your family, and our eye-to-eye discussions on all things APSIM. I simply couldn't have done it without you and will forever be grateful! I simply can't thank you enough - you are good people!

The completion of this study would not have been possible without the great and diligent work of all field assistants, particularly that of Lozio Makesa and John Massawe, and of Nagirinya Justine, Jesca Nassolo, Sam Okirya, Goodluck Munishi, Rashid Mutengela, Kayongo Augustine, Sandali Ali Milasi, Oswald Munishi, Ali Mbwiro, and all the casual labourers. I also want to thank the farmers who provided their land for the field experiments as well as Ms. Joyce Ligungulu and Aisha Nanozi for making the project houses a home.

My deepest gratitude, however, goes to my family, my fiancé Sean and my friends for their unwavering support and patience. Words can hardly express what I will forever be thankful for: being there every step of the way, never failing to believe that it can be done and accepting my moodiness during particularly stressful times. Mum, I will never forget you sending all the boxes of sweets to keep up morale during this last months. Sean, I can't thank you enough for putting up with me and this painfully long long-distance relationship. I am extremely blessed to have you all in my life and simply couldn't have done it without you! I love you!

Thank you! Asante sana! Mwebale nyo! Dankeschön!

Abstract

Rice (*Oryza* spp.) has become an important staple food crop across East Africa over recent decades and rice demand is steadily increasing. Continuous population growth, rural-urban migration with associated dietary changes, and economic advancements favour rice consumption, making rice both an important subsistence and cash-crop. Therefore, rice is now playing a pivotal role in regional food security and national economies. Attaining rice self-sufficiency has thus become imperative to many East African governments.

Wetlands cover about 0.17 million km^2 across East Africa, 80% of which are characterized as alluvial floodplains and inland valley swamps, and are anticipated to absorb much of the growing pressure for rice. Attributed with the greatest, yet largely unexploited scope to increase lowland rice production from sustained water availability and relative soil fertility, previously underutilized wetland sites have been increasingly converted. Indiscriminate agricultural wetland use, however, must be avoided as they provide an array of vital ecosystem services for surrounding and downstream communities, and, therefore, needs to be carefully balanced against potential negative impacts on ecosystem functioning.

Among the focal sites for rice intensification are the Kilombero floodplain in southeast Tanzania and the numerous inland valley swamps in central Uganda, and were thus the selected study sites. Despite generally favourable growth conditions, regional rice yields currently remain low, ranging between 1.8-2.2 Mg ha^{-1} in the floodplain and between 1.8-1.9 Mg ha^{-1} in the inland valleys. Low yields are largely the result of sub-optimal management practices, exacerbated by widespread soil nitrogen (N) deficiency and zero to low external organic and/or inorganic amendments. Therefore, this study combined multi-year agronomic field experiments with a modelling approach, using the APSIM model to assess the differential yield responses of lowland rice to improved management practices (land, crop, N and water management) and hydro-edaphic field conditions, as well as the use efficiencies and profitability of mineral N rates in both wetland types. Field positions were selected based on the origin, extend and duration of floodwater in the floodplain (fringe and middle positions) and as a toposequence cross-section in the inland valley (valley-fringe, mid-valley, and valley-bottom positions).

Attained rice yields ranged between 3.2-9.2 Mg ha^{-1} in the floodplain and between 1.9-6.3 Mg ha^{-1} in the inland valley, depending on management (rainfed 0 and 60 kg N ha^{-1}, irrigated 120 kg N ha^{-1} + 60 kg PK ha^{-1}), field position and year, and highlighting the

substantial scope to increase lowland rice production. In both wetlands, yields responded significantly to mineral N fertiliser, while hydro-edaphic field conditions modulated yield responses. Non-amended baseline yields (i.e., from field bunding, levelling and puddling, timely weeding and row-transplanting of improved rice varieties) were significantly higher in the floodplain's fringe (4.3 Mg ha^{-1}) as compared to the middle position (3.8 Mg ha^{-1}). In the inland valley, however, non-amended baseline yields did not differ significantly between field positions, ranging between 2.6-2.9 Mg ha^{-1}. Additional yield gains from mineral N fertiliser ranged between 2.2-2.3 Mg ha^{-1} and 0.4-1.1 Mg ha^{-1} from 60 kg N ha^{-1}, and between 3.7-4.4 Mg ha^{-1} and 2.3-2.7 Mg ha^{-1} from 120 kg N ha^{-1}, 60 kg PK ha^{-1} and supplemental irrigation in the floodplain and inland valley, respectively.

The APSIM model performed with a high level of accuracy in simulating grain yields, i.e., RMSEa of 0.92 and 0.78 Mg ha^{-1} (comparing favourably to observed standard deviations of 1.84 and 1.11 Mg ha^{-1}), r^2 of 0.76 and 0.71, and MAE of 0.13 and 0.42 Mg ha^{-1} in the floodplain ($n=$ 12) and the inland valley ($n=$ 18) during model validation, respectively. Additionally, APSIM accurately simulated so-called 'carry-over' effects, i.e., soil moisture contents (e.g., with r^2 >0.81 and >0.66 in the floodplain at 10 and 30 cm soil depth, respectively), and soil carbon dynamics and indigenous N supply via comparison of non-amended baseline yields. Results further highlighted the importance of shallow water tables for lowland rice production and sound model performance as they evidently attenuated drought events during low and variable rainfall years.

Simulated spatial-temporal abiotic stress patterns (water and N stress) further delineated yield determinants from hydro-edaphic field conditions, i.e., low soil N was generally the main yield constraint, but was less pronounced in the wetlands' fringes from more favourable topsoil C/N ratios and alternate soil wetting and drying that likely led to higher mineralization capacities. Water stress was generally more pronounced in the inland valley from lower seasonal rainfall as compared to the floodplain, and lower water table supply capacities. Comparatively, however, water stress was more pronounced towards both wetlands' fringes. Long-term (30-years) scenario analysis of yield responses to and partial gross margins of N fertiliser rates indicated high fertiliser use efficiencies, i.e., with yield gains of 1.7-4.5 Mg ha^{-1} in the floodplain and 1.0-3.2 Mg ha^{-1} in the inland valley, and profitable fertiliser use, i.e., at rates of 30-120 kg N ha^{-1} in the fringe and 30-90 kg N ha^{-1} in the middle position of the floodplain, and at rates of 60-150 kg N ha^{-1} in the inland valley. However, N fertiliser use was comparatively riskier in the valley-fringe position of the inland valley. Since supplemental irrigation generally increased yields and

reduced yield variability, particularly in the valley-fringe position, it may help boost N fertiliser use efficiency and profitability.

Overall, this study has shown the substantial scope to increase regional lowland rice production from adoption of improved management practices and mineral N fertiliser use in representative East African wetland types. The APSIM model has additionally proved a valuable tool in prioritizing production constraints, assessing management options and thus in guiding the decision-making on crop management in wetlands. These findings may help to align regional rice self-sufficiency and conservation targets through site- and system-specific targeting of management options.

Keywords: Alluvial floodplain, APSIM, inland valley swamp, *Oryza* spp., Tanzania. Uganda.

Kurzfassung

Reis (*Oryza* spp.) hat sich in den letzten Jahrzehnten in ganz Ostafrika zu einem wichtigen Grundnahrungsmittel entwickelt und die Nachfrage steigt stetig. Kontinuierliches Bevölkerungswachstum, Land-Stadt-Migration und damit verbundene Veränderungen der Ernährungsgewohnheiten sowie wirtschaftliche Fortschritte begünstigen den Reiskonsum und machen Reis zu einer wichtigen Subsistenz- und Cash-Crop-Kultur. Daher spielt Reis heute eine zentrale Rolle für die regionale Ernährungssicherheit und Volkswirtschaften. Das Erreichen der Selbstversorgung mit Reis ist daher für viele ostafrikanische Regierungen zu einer Notwendigkeit geworden.

Feuchtgebiete bedecken etwa 0,17 Millionen km^2 in ganz Ostafrika, von denen 80% als alluviale Überflutungsebenen und Talgrund-Feuchtgebiete charakterisiert sind und voraussichtlich einen Großteil der Ausweitung des Reisanbaus auffangen werden. Aufgrund günstiger klimatischer und edaphischer Bedingungen, hat der regenwassergespeiste Tieflandreisanbau das größte, bisher jedoch weitestgehend ungenutzte Potenzial zur Steigerung der Reisproduktion. Daher werden Feuchtgebiete zunehmend zu landwirtschaftlichen Nutzflächen umgewandelt. Eine unbedachte landwirtschaftliche Nutzung von Feuchtgebieten sollte jedoch vermieden werden, da sie viele essentielle Ökosystemdienstleistungen für die umliegenden und flussabwärts gelegenen Gemeinden bereitstellen, und sollte daher sorgfältig gegenüber möglicher negativer Auswirkungen auf die Ökosystemfunktionen abgewogen werden.

Die Kilombero-Überflutungsebene in Südost Tansania und die zahlreichen Talgrund-Feuchtgebiete in Zentraluganda gelten als Fokus-Standorte für die regionale Reisintensivierung und wurden daher als Untersuchungsgebiete für diese Studie ausgewählt. Trotz generell günstiger Wachstumsbedingungen sind die regionalen Reiserträge derzeit niedrig und liegen nur zwischen 1,8-2,2 Mg ha^{-1} in der Überflutungsebene und 1,8-1,9 Mg ha^{-1} in den Talgrund-Feuchtgebieten. Die niedrigen Reiserträge sind überwiegend das Ergebnis sub-optimaler Bewirtschaftungspraktiken, und werden von niedrigen Bodenstickstoffgehalten und geringen bis garkeinen organischen und/oder anorganischen Düngemittelmengen zusätzlich limitiert. Daher wurden in dieser Studie mehrjährige agronomische Feldversuchsdaten mit einem Modellierungsansatz unter Verwendung des APSIM-Modells kombiniert, um Ertragsreaktionen auf verbesserte Bewirtschaftungspraktiken (Land-, Reis-, Stickstoff (N)- und Wassermanagement) und hydro-edaphische Feldbedingungen, sowie die Nutzungseffizienz und Rentabilität von N-Dünger in beiden Feuchtgebietstypen zu bewerten. Die Feldpositionen wurden basierend

auf den Ursprung, Ausdehnung und Dauer des Hochwassers in der Überflutungsebene (Rand und Mitte) und als toposequentieller Querschnitt im Talgrund-Feuchtgebiet (Talrand, Talmitte und Talboden) ausgewählt.

Gemessene Reiserträge lagen zwischen 3,2-9,2 Mg ha^{-1} in der Überflutungsebene und zwischen 1,9-6,3 Mg ha^{-1} im Talgrund-Feuchtgebiet, abhängig von Bewirtschaftung (regenwassergespeist 0 und 60 kg N ha^{-1}, bewässert 120 kg N ha^{-1} + 60 kg PK ha^{-1}), Feldposition und Jahr, und verdeutlichen das Potenzial zur Ertragssteigerung von Tieflandreis. In beiden Feuchtgebietstypen steigerte mineralischer N-Dünger die Reiserträge signifikant, wobei die Ertragssteigerungen von hydro-edaphischen Feldbedingungen beeinflusst wurden. Ungedüngte Basisreiserträge (d.h. von Nivellierung des Bodens, Bau von wasserrückhaltenden Felddeichen, effiziente Unkrautbekämpfung und Reihenpflanzung verbesserter Reissorten) waren am Rand der Überflutungsebene (4,3 Mg ha^{-1}) signifikant höher als in der Mitte (3,8 Mg ha^{-1}). Im Talgrund-Feuchtgebiet unterschieden sich die ungedüngten Basisreiserträge zwischen den Toposequenzpositionen nicht signifikant und lagen zwischen 2,6-2,9 Mg ha^{-1}. Zusätzliche Reiserträge durch den Einsatz von N-Dünger lagen zwischen 2,2-2,3 Mg ha^{-1} und 0,4-1,1 Mg ha^{-1} von 60 kg N ha^{-1}, und zwischen 3,7-4,4 Mg ha^{-1} und 2,3-2,7 Mg ha^{-1} von 120 kg N ha^{-1}, 60 kg PK ha^{-1} und zusätzlicher Bewässerung in der Überflutungsebene bzw. im Talgrund-Feuchtgebiet.

APSIM zeigte eine gute Modellierleistung in beiden Feuchtgebietstypen, d.h. RMSEa von 0,92 und 0,78 Mg ha^{-1} (im Vergleich zu den gemessenen Standardabweichungen von 1,84 und 1,11 Mg ha^{-1}), r^2 von 0,76 und 0,71 und MAE von 0,13 und 0,42 Mg ha^{-1} in der Überflutungsebene (*n*= 12) bzw. im Talgrund-Feuchtgebiet (*n*= 18) während der Modellvalidierung. Zudem wurden "carry-over"-Effekte akkurat simuliert, d.h. Bodenfeuchtemuster (z.B. mit r^2 >0,81 und >0,66 in der Überflutungsebene in 10 bzw. 30 cm Bodentiefe), Bodenkohlenstoffdynamiken und die bodeneigene N-Versorgung. Ergebnisse betonten weiterhin die Bedeutung von Grundwasser für regenwassergespeisten Tieflandreis und eine gute Modellleistung, da sie Wassermängel in Jahren mit geringen und variablen Niederschlägen abschwächten.

Simulierte räumlich-zeitliche abiotische Stressmuster (Wasser- und N-Stress) unterschieden die Ertragsdeterminanten anhand hydro-edaphischer Feldbedingungen. Geringe Bodenstickstoffgehalte war die Hauptertragsbeschränkung, jedoch waren diese in den Randbereichen beider Feuchtgebiete aufgrund günstigerer C/N-Verhältnisses des Oberbodens und abwechselnder Bodenfeuchteverhältnisse, die wahrscheinlich zu größeren Mineralisierungskapazitäten führten weniger ausgeprägt. Gleichzeitig war der

Trockenstress im Talgrund-Feuchtgebiet aufgrund geringerer saisonaler Niederschläge im Vergleich zur Überflutungsebene und geringerer Versorgungskapazität des Grundwassers stärker ausgeprägt. Innerhalb beider Feuchtgebietstypen war der Trockenstress zudem stärker in den Randbereichen ausgeprägt. Die Szenario Analyse (30-Jahre) von Ertragssteigerungen durch und Analyse partieller Bruttomargen für den Einsatz von N-Dünger ergaben hohe Nutzungseffizienzen, d.h. mit Ertragssteigerungen von 1,7-4,5 Mg ha^{-1} in der Überflutungsebene und 1,0-3,2 Mg ha^{-1} im Talgrund-Feuchtgebiet, und profitable N-Raten von 30-120 kg N ha^{-1} am Rand und 30-90 kg N ha^{-1} in der Mitte der Überflutungsebene, und mit Raten von 60-150 kg N ha^{-1} im Talgrund-Feuchtgebiet. Allerdings war der Einsatz von N-Dünger am Talrand vergleichsweise risikoreicher. Eine zusätzliche Bewässerung erhöhte Erträge und reduzierte die Ertragsvariabilität, insbesondere in der Talrandlage, und könnte dazu beitragen, die Effizienz und Rentabilität von N-Dünger zu steigern.

Insgesamt hat diese Studie gezeigt, dass die regionale Tieflandreisproduktion durch die Einführung verbesserter Bewirtschaftungspraktiken und den Einsatz von mineralischem N-Dünger in repräsentativen Feuchtgebieten Ostafrikas erheblich gesteigert werden kann. Das APSIM-Modell erwies sich als wertvolles Hilfsmittel bei der Priorisierung von Ertragsbeschränkungen, der Bewertung von Bewirtschaftungspraktiken und somit als Entscheidungshilfe für die landwirtschaftliche Nutzung von Feuchtgebieten. Ergebnisse können daher dazu beitragen, die regionale Selbstversorgung mit Reis und Ziele des Naturschutzes durch standort- und systemspezifische Managementoptionen zu vereinbaren.

Schlüsselbegriffe: APSIM, *Oryza* spp., Talgrund-Feuchtgebiet, Tansania, Uganda, Überflutungsebene.

Table of contents

List of figures

List of tables

Abbreviations & units

Abbreviation	Definition	Unit
α	Slope of linear regression line	-
β	Intercept of linear regression line	-
ΔC_{org}	Change in soil organic carbon content	%
ΔN_{tot}	Change in soil total nitrogen content	%
AD	Anno Domini ('in the year of the Lord')	-
algact	Daily algal activity factor	0-1
ANOVA	Analysis of variance	-
APSIM	Agricultural Production Systems Simulator	-
APSRU	Agricultural Production System Research Unit	-
AWD	Alternate wetting and drying rice production system	-
BD	Bulk density	$g\ cm^{-3}$
biom	More active soil organic carbon pool	-
BVP	Vegetative development stage	-
CA	Conservation Agriculture	-
CARD	Coalition for African Rice Development	-
CEC	Cation exchange capacity	$cmol_c\ kg^{-1}$
CENTURY	Soil organic matter quantity and composition model	-
CERES	Crop-Environment Resource Synthesis	-
CFT	Central field trial	-
cm	Centimetre	cm
CN2	Curve number	-
C/N, CNR	Carbon nitrogen ratio	-
CO_2	Carbon dioxide	ppm
CONA	Second stage soil evaporation coefficient	mm
C_{org}	Soil organic carbon content	$g\ kg^{-1}$
CREAMS	Chemicals, Runoffm and Erosion from Agricultural Management Systems	-
CRM	Coefficient of residual mass	-
CropSyst	Cropping Systems Simulation	-
CSIRO	Commonwealth Scientific and Industrial Research	-
CV	Coefficient of variation	%
DAE	Days after emergence	day

Abbreviation	Definition	Unit
DAS	Days after sowing	day
DAT	Days after transplanting	day
DRC	Development rate constant	-
DSSAT	Decision Support System for Agrotechnology Transfer	-
DUL	Volumetric water content at drained upper limit for each soil layer	$cm^3\ cm^{-3}$
DVR	Development rate of crop	$°C\ day^{-1}$
DVRI	Development rate during photoperiod-sensitive phase	$°C\ day^{-1}$
DVRJ	Development rate during juvenile phase	$°C\ day^{-1}$
DVRP	Development rate during panicle development phase	$°C\ day^{-1}$
DVRR	Development rate in reproductive phase (post anthesis)	$°C\ day^{-1}$
DVS	Development stage of crop	-
EA	East Africa (Kenya, Rwanda, Tanzania und Uganda)	-
EC	Electrical conductivity	$µs\ m^{-1}$
e.g.	For example	-
EF	Modelling efficiency	-
EPIC	Erosion-Productivity Impact Calculator	-
ESA	Eastern and Southern Africa	-
ESS	Ecosystem services	-
Es	Soil evaporation	mm
et al.	Et alii (and others)	-
etc.	Et cetera	-
ex-situ	Off site	-
f_incorp	Fraction of residues incorporated into the soil	0-1
FAO	Food and Agriculture Organization of the United Nations	-
fBiom	Inert biomass carbon fraction	-
FDR	Frequency-Domain-Reflectometry	-
FOM	Fresh organic matter pool	-
fInert	Inert soil carbon fraction	-
FLV	Fraction of shoot dry matter allocated to leaves	0-1
FSO	Fraction of shoot dry matter allocated to storage organs	0-1
FST	Fraction of shoot dry matter allocated to stems	0-1
g	Gram	g
GAP	Good Agricultural Practice	-
GDD	Growing degree days	$°C\ day^{-1}$

Abbreviation	Definition	Unit
GDP	Gross domestic product	$
GFP	Grain-fill stage	-
ha	Hectar	ha
HU	Daily heat units effective for phenological development	°C day^{-1}
hum	Humic soil organic carbon pool	-
HSD	Honestly significant difference	-
i.a.	Inta alia	-
i.e.	That is	-
IL	Irrigated lowland rice system	-
in-situ	On site	-
IRM	Integrated Rice Management	-
IRRI	International Rice Research Instiute	-
K	Potassium	-
kg	Kilogram	kg
KJ	Kilo joule	KJ
KPL	Kilombero Plantation Limited	-
Ks	Saturated daily percolation rate	mm day^{-1}
LAI	Leaf area index	-
lestrs	Water stress factor reducing leaf expansion	0-1
LL15	Volumetric water content for each layer corresponding to a soil potential of 15 bar	cm^3 cm^{-3}
LVC	Lake Victoria Crescent	-
m	Metre	m
m^2	Square metre	m^2
MACROS	Modules of an Annual CROp Simulator	-
MAE	Mean absolute error	-
masl	Metres above sea level	m
maxt	Maximum temperature	°C
maxrate_pab	Unconstrained daily growth rate of PAB	kg ha^{-1} day^{-1}
max_pond	Maximum pond height before water runoff	mm
Mg	Megagram	Mg
mg	Milligram	mg
mint	Minimum temperature	°C
MJ	Mega joule	MJ
mm	Millimetre	mm

Abbreviation	Definition	Unit
MSE	Mean squared error	-
mwcon	Coefficient to restrict the over-saturated water flow through macro-pores allowed to drain per day	0-1
N	Nitrogen	-
NARS	National Agricultural Research Systems	-
NARC	National Agricultural Research Center	-
NCROP	Subroutine to calculate the N dynamics in crop and the nitrogen-stress factors	-
NE	Northeast	-
NERICA	New Rice for Africa	-
NH_3	Ammonia N	-
NH_4^+	Ammonium N	-
NH4_loss_fact	Ammonia volatilisation value	0.4
no.	Number	-
NO_3^-	Nitrate-N	-
N_{tot}	Soil nitrogen content	g kg^{-1}
NTRM	Nitrogen-Tillage-Residue Management	-
obs.	Observed	-
ORYZA1	Potential rice production model	-
ORYZA2000	Ecophysiological rice model	-
ORYZA-N	Nitrogen-limited rice production model	-
ORYZA_W	Water-limited rice production model	-
P	Phosphorus	-
PAB	Pond algal biomass	kg ha^{-1}
PAPRAN	Production of Arid Pastures limited by Rainfall and Nitrogen	-
PAWC	Plant available water capacity	mm
PEP	Panicle development stage	-
PERFECT	Productivity, Erosion and Runoff Functions to Evaluate Conservation Techniques	-
pH	Measure of hydrogen ion concentration	-
PHENOL	Subroutine to determine phenology of crop	-
PI	Panicle initiation (DVS 0.65)	-
PSP	Photoperiod-sensitive development stage	-
QSORG	Sorghum growth model	-

Abbreviation	Definition	Unit
QSUN	Sunflower growth model	-
R, Rain	Rainfall	mm
r^2	Coefficient of determination	-
rad	Incoming solar radiation	$MJ\ m^{-2}$
RCBD	Randomized complete block design	-
rd_biom	Potential rate of soil biomass minerallisation	day
rd_carb	Potential rate for carbohydrate decomposition	day
rd_cell	Potential rate for cellulose decomposition	day
rd_hum	Potential rate of humus mineralisation	day
rd_lingn	Potential rate for lignin decomposition	day
RGRLMN	Minimum value of relative growth rate of leaf area	$°C\ day^{-1}$
RGRLMX	Maximum value of relative growth rate of leaf area	$°C\ day^{-1}$
RL	Rainfed lowland rice system	-
$RMSE_a$	Absolute root mean square error	-
$RMSE_n$	Normalised root mean square error	-
rnstrs	Nitrogen stress factor reducing relativ leaf area growth	0-1
RU	Rainfed upland rice system	-
SAGCOT	Southern Agricultural Growth Corridor Tanzania	-
SARP	Simulation and systems analysis for rice production	-
Salb	Soil albedo	-
SALUS	System Approach to Land Use Sustainability	-
SAT	Volumetric water content at saturation for each soil layer	$cm^3\ cm^{-3}$
SD	Standard deviation	-
SE	Standard error	-
SGPCDT	Subroutine to calculate daily total gross assimilation	-
sim.	Smulated	-
SLA	Specific leaf area	$m^2\ kg^{-1}$
SOM	Soil organic matter	$kg\ ha^{-1}$
SOILWAT	Soil water module	-
SOILN	Soil nitrogen module	-
SRI	System of Rice Intensification	-
SSA	sub-Saharan Africa	-
SUCROS	Simple and Universal CROp Grwoth Simulator	-
SURFACEOM	Surface organic matter module	-

Abbreviation	Definition	Unit
SW	Soil water	mm
SWIM	Soil Water Infiltration and Movement	-
swcon	Coefficient to restrict the saturated water flow allowed to drain per day	0-1
T	Air temperature	°C
t	Ton	t
TAZARA	Tanzania Zambia Railways	-
tkw	Thousand kernel weight	mg
Tmax	Maximum air temperature	°C
Tmin	Minimum air temperature	°C
U	First stage soil evaporation coefficient	mm
vs.	Versus	-
WGRMX	Maximum individual grain weight	kg grain^{-1}
WLV	Dry weight of leaves	kg ha^{-1}
WOFOST	World Food Studies	-
WRR	Dry weight of rough rice (0% moisture content)	kg ha^{-1}
WSO	Dry weight of storage organs	kg ha^{-1}
WST	Dry weight of stems	kg ha^{-1}
WSTRESS	Subroutine to calculate actual crop transpiration and water stress factors	-
WTT	West Tanzanian Terrane	-
WWP	Working Wetland Potential Index	-

1.   General introduction

In sub-Saharan Africa (SSA), average rice self-sufficiency stands at only 60% (Senthilkumar *et al.*, 2020), and rice imports amounted to 53% of the total rice consumption in 2011 (Demont & Ndour, 2015). Since imports and dependencies on international markets drain foreign currency reserves and risk social stability, attaining rice self-sufficiency has become imperative to many governments in SSA (Arouna *et al.*, 2021). Across East Africa (Kenya, Rwanda, Tanzania, and Uganda), rice has largely not been a traditional food crop but has gained momentum both as an important subsistence and cash-crop in recent decades (Tsujimoto *et al.*, 2019). Continuous population growth, urbanization processes and associated dietary changes as well as economic advancements favour rice consumption and provide incentives for rice production (Balasubramanian *et al.*, 2007). Therefore, rice has become a main staple food alongside maize, sorghum and cassava, and is now playing a pivotal role in improving regional food security and boosting national economies (Nasrin *et al.*, 2015).

In Tanzania, rice cultivation started around 700 AD (Walshaw, 2010), but has been more widely practiced since the mid-19th century (Monson, 2000). The main rice growing regions include the lowlands of the Southern Highland Zone, i.e., Iringa and Mbeya, the Lake Zone, i.e., Mwanza and Shinyanga, the Northern Zone, i.e., Kilimanjaro and Manyara, and the Coastal Zone, i.e., Morogoro (Mbaga *et al.*, 2017). Emphasizing their national importance, the Mbeya, Morogoro and Mwanza rice-growing regions contribute about 48% to the national rice production (Mlengera *et al.*, 2015). Alluvial river floodplains are the predominant rice-growing areas in Tanzania, e.g., the irrigated Dakawa scheme in the Dakawa floodplain (Mbaga *et al.*, 2017), and the predominantly rainfed Kilombero floodplain that stretches along the Kilombero River and is one of the most important agricultural hubs and part of the Southern Agricultural Growth Corridor (SAGCOT) (Mwongera *et al.*, 2014).

In Uganda, rice farming is a fairly recent activity and has been actively encouraged by the Government since the 1970s through the implementation of commercial irrigated rice schemes, particularly in the Eastern region of the country, i.e., Kibima (Bugiri District), Doho (Butaleja District) and Olweny (Lira District) (Oonyu, 2011). Ever since the introduction of rice schemes the area under production has been steadily expanding, particularly in the densely populated Eastern region (Kijima, 2013). Additionally, in order to increase rice production nationwide, the Government actively supported the introduction of the New Rice for Africa (NERICA) rice varieties in 2002 (Kijima *et al.*, 2008). Although

the NERICA varieties were mainly aimed at upland-based production systems (Fungo *et al.*, 2013), progressive land degradation and associated production risks have led to a gradual shift into previously underutilized inland valleys across the country (Rodenburg, 2013; Turyahabwe *et al.*, 2013). In central Uganda, recent intensification efforts were largely driven by the Coalition for African Rice Development (CARD), involving national and international agricultural research institutes and NGOs, and aiming at accelerating the development of inland valley swamps for rice production (van Campenhout *et al.*, 2016).

While both Tanzania and Uganda attained near rice self-sufficiency in 2012, future projections indicate that market demands will exceedingly outpace domestic supply in (Van Oort *et al.*, 2015). Tanzania is the leading rice producer in East Africa, accounting for about of 80% of the total production (Rugumamu, 2014). In both Tanzania and Uganda,
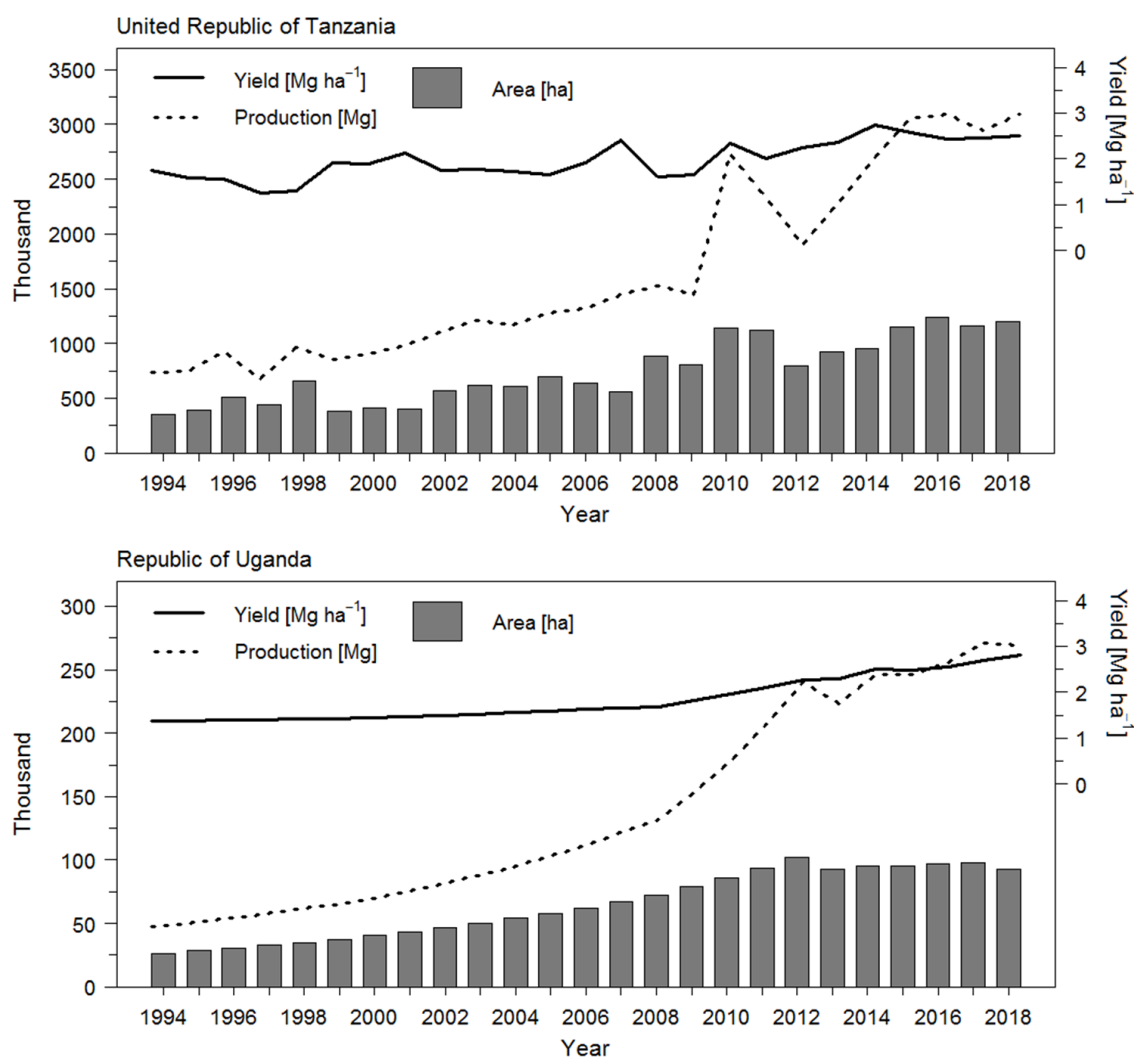
Figure 1.1 Mean annual national rice yields, total annual production in thousand tons and rice area in thousand hectares in Tanzania (top) and Uganda (bottom) from 1994 to 2018; data adapted from FAOSTAT (*www.fao.org/faostat*) and revised statistics for Uganda from Kikuchi *et al.* 2014.

the area under rice production has been increasing substantially over the past three decades, respresenting an area expansion of 250% in Tanzania and 400% in Uganda from 1994 to 2018 (**Figure 1.1**). Meanwhile, average national rice yields increased only marginally and remain low at <3 Mg ha^{-1}. Recent advancements in production have, therefore, largely been attributed to land expansion rather than increases in productivity (**Figure 1.1**) (Sekiya *et al.*, 2020).

Among upland, irrigated and rainfed lowland rice ecosystems, rainfed lowlands have been associated with the highest potential for productivity growth in East Africa (Kijima *et al.*, 2012). While upland ecosystems are attributed with high production risks from drought and soil degradation, and high regional costs of irrigation structures in irrigated lowland ecosystems impair sustainable rice production (Balasubramanian *et al.*, 2007), rainfed lowlands are generally considered favourable from sustained water availabilities and relative fertility (Nhamo *et al.*, 2014). Across East Africa, wetlands cover approximately 0.17 million km^2, 80% of which are categorized as alluvial floodplains and inland valley swamps (Leemhuis *et al.*, 2016). In recent years wetlands have, therefore, been progressively converted into sites of agricultural production, particularly for lowland rice (Sakané *et al.*, 2013). However, despite being generally considered favourable for lowland rice production (Balasubramanian *et al.*, 2007), wetlands are complex, transient and often fragile ecosystems that harbor a high level of biodiversity and provide an array of vital ecosystem services for surrounding and downstream communities (Dixon & Wood, 2003). Therefore, agricultural wetland use needs to be carefully balanced against potential negative impacts on ecosystem functioning (Rodenburg *et al.*, 2014).

Hence, sustainable rice intensification strategies are needed in order to align regional rice self-sufficiency and conservation targets. The Kilombero floodplain in southeast Tanzania and the numerous inland valley swamps in central Uganda are among the regional focal areas for sustainable lowland rice intensification, and are associated with substantial yet largely unexploited scope to increase rice productivity (Senthilkumar *et al.*, 2018; van Campenhout *et al.*, 2016).

1.1   Problem statement

Lowland rice production potentials and constraints of the Kilombero floodplain in Tanzania and of the inland valley swamps in Uganda remain largely unknown but are imperative to identify sustainable intensification strategies. Currently, regional rainfed lowland rice yields range only between 1.8-2.2 Mg ha^{-1} in the floodplain and between 1.8-1.9 Mg ha^{-1} in the inland valleys (Haneishi *et al.*, 2013a; Senthilkumar *et al.*, 2018). Predominantly produced by smallholders, social, economic and ecological constraints limit productivity, e.g., lack of knowledge, inputs, water control, and on-farm labour (Nhamo *et al.*, 2014), resulting in sub-optimal management practices (Mombo *et al.*, 2013). Particularly soil N deficiency constrains rice yields, aggravated by crop-residue removal, and zero to low external organic and/or inorganic amendments (Senthilkumar *et al.*, 2020). Additionally, rainfed lowland rice systems depend on seasonal rainfall and seasonally shallow water tables for production (Diagne *et al.*, 2013), and hydro-edaphic field conditions are anticipated to modulate rice yield responses to management practices and profitability of mineral N fertiliser use (Haefele *et al.*, 2013). Since most smallholders are highly risk-averse and operate on small economic margins (Jama *et al.*, 2017; Ragasa & Chapoto, 2017), fertiliser profitability will directly affect widespread adoption of improved management practices.

Agronomic field trials are thus invaluable to generate yield response data to management practices under prevalent environmental conditions. However, agronomic field trials are comparatively costly and usually only conducted for a limited time period and, therefore, lack long-term yield responses to management, climate and their effects on soil resources (Probert *et al.*, 1998). Crop growth models, however, are potentially useful tools to simulate such complex environment by management interactions on crop performance when thoroughly validated (Holzworth *et al.*, 2014). Additionally, the model can provide insights on abiotic yield determinants and long-term yield responses to management and environmental conditions, and thus in guiding the decision-making on crop management options. This study selected the Agricultural Production System Simulator (APSIM) modelling framework to complement and extrapolate experimental field data (Keating *et al.*, 2003). APSIM has a proven track record in simulating various cropping systems worldwide (e.g., Bahri *et al.*, 2019; Dutta *et al.*, 2020; Hoffmann *et al.*, 2020), including rice-based systems (e.g., Amarasingha *et al.*, 2017; Balwinder-Singh *et al.*, 2016; Gaydon *et al.*, 2021). To date, however, APSIM has not been used to simulate the performance of improved local rice varieties under prevalent hydro-edaphic field and weather conditions in rainfed lowland rice systems of East Africa.

1.2   Research hypotheses & objectives

The overall aim of this study was to combine extensive field experimental data and a modelling approach to assess rice performance under prevalent hydro-edaphic and climatic field conditions and in response to improved management practices in a floodplain and an inland valley wetland in East Africa. Therefore, the veracity of the APSIM model under variable hydro-edaphic conditions and management practices was assessed, yield determinants via spatial-temporal abiotic stress patterns (water and N stress) delineated, and the validated model subsequently used to simulate yield responses to and profitability of mineral N fertiliser rates over a 30-year simulation period.

Research hypotheses

The research hypotheses of this study were as follows:
   i. Improved land and crop management can boost regional lowland rice yields substantially.
   ii. The APSIM model is a useful tool to simulate rice responses to management practices in variable hydro-edaphic lowland systems.
   iii. Yield benefits from mineral N fertiliser use and supplemental irrigation vary from field positioning within the lowland system.
   iv. Long-term, model-based evaluation of mineral N fertiliser rates can help identify trade-offs between agronomic benefits and economic incentives for fertiliser use, and help assess production risks from hydro-edaphic and climatic conditions.

Research objectives

The research objectives of this study were as follows:
   i. Parameterise, calibrate and validate the APSIM model for improved local rice varieties, environmental conditions and management practices in a floodplain and an inland valley of East Africa.
   ii. Understand the relative effects of management practices and hydro-edaphic field conditions on rice yields and yield determinants.
   iii. Assess yield responses to mineral N fertiliser rates and supplemental irrigation, and production risks from hydro-edaphic and climatic conditions.
   iv. Identify the trade-offs between agronomic benefits and economic incentives for mineral N fertiliser use and supplemental irrigation at field level.

1.3   Research framework

The present study was embedded in the interdisciplinary research project 'GlobE – Wetlands in East Africa: Reconciling future food production with environmental protection', funded by the German Federal Ministry of Education and Research and the German Federal Ministry of Economic Cooperation and Development [FKZ: 031A250A-H]. The project focused on wetland functions, uses and associated risks in East Africa (Kenya, Rwanda, Tanzania and Uganda), and was organized in five clusters (**Figure 1.2**). The clusters focused on understanding the wetland systems (cluster A), identification of adapted wetland management options considering socio-economic and ecological boundary conditions (cluster B), identification, assessment and spatial targeting of innovative wetland use options (cluster C), development of an integrated assessment tool for regional wetland use options (cluster D), and recommendations for wetland use plans and implementation of capacity building measures (cluster E).
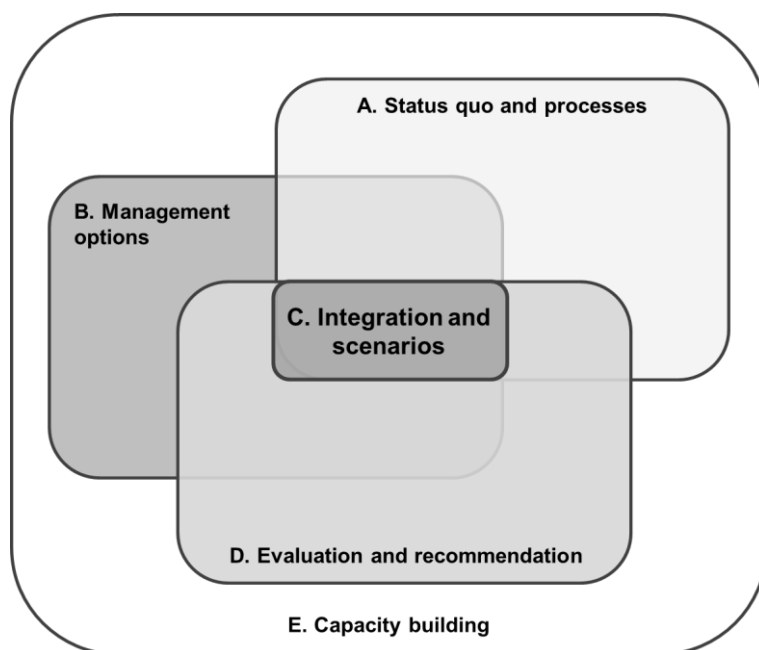
Figure 1.2 Conceptual overview of the five research clusters within the 'GlobE – Wetlands in East Africa' interdisciplinary project and their connections (GlobE Wetlands, 2013).

The present study is embedded in clusters A and B, and uses a modelling approach both to assess experimental yield response pattern to management and hydro-edaphic conditions, and to identify management recommendations from long-term climate records through balancing of agronomic benefits and economic incentives. Successful model validation and application required close interdisciplinary collaboration, i.e., to the works of Dr. Sonja Burghof (Burghof, 2017), Dr. Julius Kwesiga (Kwesiga, 2021), Dr. Geofrey Gabiri (Gabiri, 2018a), Susanne Ziegler and Björn Glasner.

1.4   Thesis outline

This thesis is a cumulative dissertation and consists of eight chapters. The focal areas of this study were (i) the Kilombero floodplain near Ifakara town in southeast Tanzania and (ii) an inland valley swamp near Namulonge town in Central Uganda.

Chapter 1 provides a **General introduction** into the status-quo of rice production, yields and deficits in Tanzania and Uganda. This chapter further includes the problem statement, research hypotheses and objectives.

Chapter 2 provides a brief **Introduction to the regions**, i.e., location and topography, climate, geology, soils, hydrology, vegetation, land use and land cover, socioeconomics and demographics, and an overview of current regional rice management practices and common constraints.

Chapter 3 provides a brief overview on **Wetlands for lowland rice production**, N-dynamics in wetland soils, and a compilation of vital wetland ecosystem services, functions and potential threats from agricultural (mis-) use.

Chapter 4 provides a detailed overview on the **Research approach**, i.e., the agronomic field experimental part and the cropping system modelling part. Details on the agronomic field experimental part include the experimental design, study sites, weather conditions, hydro-edaphic characteristics as well as the data collection protocols and field activities during the study period. Details on the cropping system modelling part include a brief history of the ORYZA2000 and the APSIM model, and descriptions of the APSIM modules Oryza, SoilWat, SoilN, SurfaceOM and Pond.

Chapter 5 contains the **Peer-reviewed journal publications** that were published and/or submitted to international peer-reviewed scientific journals and formatted to fit the style of this thesis.

Chapter 6 provides a **General Discussion** of the main findings in relation to the research hypotheses, remarks on experimental and modelling approaches in lowland rice systems, and finally an outlook and recommendations.

Chapter 7 provides a list of all **References** used in this thesis.

Chapter 8 provides the **Publication list** of the author's first- and co-authored peer-reviewed publications and conference contributions.

Chapter 9 provides the **Annex** of this thesis, i.e. supplementary material from journal publications, and APSIM input files and manager scripts.

2.   Introduction to the regions

Multi-year and multi-location field experiments were conducted in two representative and predominant East African wetland types. Both research locations represent the typical landscape attributes, including climatic and hydro-edaphic conditions of small inland valley swamps in the upper reaches of watersheds in the highlands and large river floodplains in the downstream areas of the tropical lowlands.

2.1   Study regions

2.1.1 Location & topography

Study sites were located in (i) the Kilombero floodplain near Ifakara town, Kilombero District, in southeast Tanzania (8.10°-8.18°S, 36.67°-36.76°E) and (ii) in a narrow inland valley swamp at the *National Crops Resources Research Institute* (*NaCRRI*) near Namulonge town, Wakiso District, in central Uganda (0.519°-0.522°N, 32.640°-32.344°E) (**Figure 2.1**). The floodplain forms the downstream alluvial extension of the Kilombero catchment which is part of the Rufiji River basin, the largest river basin in Tanzania (Näschen *et al.*, 2018). The Kilombero catchment is surrounded by the Udzungwa Mountains to the northwest and the Mahenge Highlands and Mbarika Mountains to the southwest (Kato, 2007). The total catchment covers about 40,240 km^2, of which 7,967 km^2 are covered by the seasonal floodplain (Leemhuis *et al.*, 2016). With altitudes of around 300 masl, the floodplain is the largest low-lying

Figure 2.1 Geographic location of both study sites in East Africa, i.e., near Ifakara town in southeast Tanzania and near Namulonge town in central Uganda.

freshwater wetland in East Africa (Kangalawe & Liwenga, 2005), however, altitudes within the catchment reach 2,576 masl in the Udzungwa Mountains and 1,516 masl in the Mahenge Highlands (Lyon *et al.*, 2015).

The Namulonge inland valley swamp is located in the Nasirye catchment which is a microscale headwater catchment in the upper reaches of the Lake Kyoga Basin (Gabiri *et al.*, 2020). The central stream of the inland valley, the Nasirye River, drains through the Sezibwa River floodplain into Lake Kyoga. The Nasirye catchment covers an area of approximately 31.1 km^2 and encompasses a wetland area of about 4.52 km^2 from the upper catchment in north-east direction towards the outlet (Gabiri *et al.*, 2017). Elevations range from 900 to 1,340 masl and narrow swampy bottomlands are widespread in the undulating landscape, characterised by flat-topped hills and broad valleys (Nsubuga *et al.*, 2011).

2.1.2 Climate

The climate at the study sites is described as sub-humid tropical and humid tropical in Tanzania and Uganda, respectively (Leemhuis *et al.*, 2016), and is classified as a tropical savanna (Aw) climate at both sites according to the updated Köppen-Geiger climate classification (Peel *et al.*, 2007). In the floodplain, rainfall pattern are predominantly mono-modal, however, many teleconnections influence the regional climate, resulting in shifts between mono-modal and bi-modal rainfall years and regional distinctions (Koutsouris *et al.*, 2016; Philippon *et al.*, 2002). Bi-modal rainfall years show a short (November-January) and a long rainy season (March-May), whereas mono-modal rainfall years lack the short rains (Msanya *et al.*, 2003). Climatic phenomenon's such as the El Niño-Southern
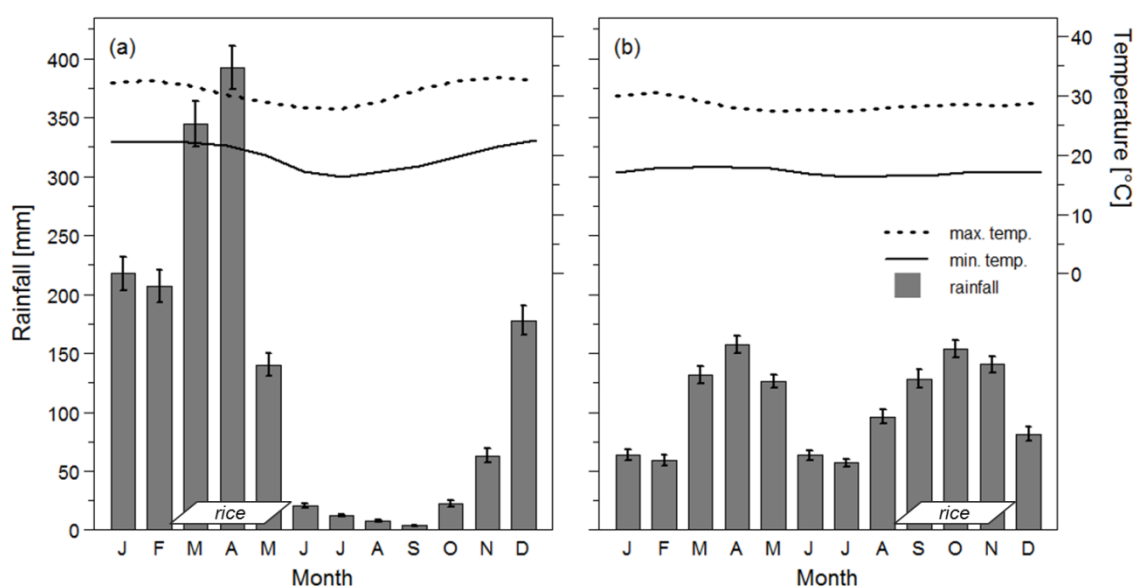
Figure 2.2 Mean monthly rainfall, and maximum and minimum temperatures from 1980 to 2010 in (a) Ifakara, Tanzania and in (b) Namulonge, Uganda; bars indicate standard deviations of the monthly rainfall means (*n*= 30); based on bias-corrected climate data from the AgMIP project (Ruane *et al.* 2015).

Oscillation and the Indian Ocean Zonal Mode (Indian Ocean Dipole) have been associated with the appearance of the short rains (Nicholson, 2017). Annual rainfall in the uplands of the Udzungwa Mountains and Mahenge Highlands exceed 2,000 mm, while annual rainfall within the floodplain ranges between 1,000-1,400 mm, however, with a large spatial-temporal variability (Wilson *et al.*, 2017). The mean annual temperature in the floodplain is about 24°C and about 17°C in the uplands (Näschen, 2020). From 1980 to 2010, the mean annual air temperature in Morogoro, Kilombero District, was 25.4°C, with October typically being the hottest (30.5°C) and July the coldest month (16.3°C) (**Figure 2.2**) (Ruane *et al.*, 2015).

In the Namulonge inland valley, climatic conditions are influenced by the movement of the Intertropical Convergence Zone (ITZ) with subtropical anticyclones and monsoonal easterly winds from the Indian Ocean and moist westerly winds from the Congo Basin (Ogallo, 1993). The rainfall pattern is bi-modal with a long (March-May) and a short rainy season (September-November) (Alibu *et al.*, 2019). However, the transitions from rainy to dry season are generally not distinctly pronounced, resulting in year-round monthly rainfall occurrences. Typically, the area receives an annual rainfall of around 1,170 mm (Nsubuga *et al.*, 2011). From 1980 to 2010, the mean annual rainfall in Namulonge was 1,259 mm, ranging from 846 to 1,826 mm (Ruane *et al.*, 2015). During the same period, mean annual air temperature was 22.9°C, with February typically being the hottest (30.5°C) and July the coldest (16.3°C) month (**Figure 2.2**).

2.1.3 Geology

As part of the Kilombero catchment, the floodplain is a SW-NE-trending depression and a southern extension of the eastern East African Rift System (Jätzold & Baum, 1968). The Kilombero River, the floodplains' lifeline, drains the valley. The floodplain is filled with Neogene sediments that are lying between crystalline basement rocks of the Neoproterozoic Mozambique Belt, characterised as alluvial sediments as well as Pliocene and Pleistocene deposits (Mruma, 2002). Typical structures include alluvial fans that are located at the northern and southern ends of the floodplain and mark the entry of tributaries to the Kilombero River into the floodplain (Burghof *et al.*, 2018). Located in the catchment's uplands, the Udzungwa Mountains are part of the Neoproterozoic Mozambique Belt and consist of metamorphic gneisses, while the Mahenge Highlands and Mbarika Mountains belong to the Eastern Granulite Cabo Degado Nappe of the Mozambique Belt and consist of complex igneous, metamorphic and sedimentary rocks (Sommer *et al.*, 2017). The study area is located in the alluvial fan of the Lumemo River in

the floodplain near Ifakara town that is marking the area of entry from the alluvial fan into the floodplain.

The Namulonge inland valley is located between the Kampala Suite of the West Tanzanian Terrane and the Buganda-Toro System, which are both dominated by Archean and Proterozoic rocks (Westerhof *et al.*, 2014). The study area has been exposed to deep weathering processes since the Miocene, resulting in a weathered mantle of 26 m thickness (geometric mean) (Taylor & Howard, 1998). Rocks of the Kampala Suite of the West Tanzanian Terrane include heterogeneous granitoids and banded ortho-gneisses, mainly of plutonic origin. Rocks of the Buganda-Toro System include Victoria and Nile formations. The Victoria formation is characterised by metamorphosed and deformed ortho-quartzites, sericite quartzites, and quartz rocks and while the Nile formation is characterised by slates, shales, and phyllites (Westerhof *et al.*, 2014). The study inland valley is filled with quaternary sediments, described as alluvium, swamp and lacustrine deposits (Burghof, 2017).

2.1.4 Soils

Predominant soils in the floodplain are eutric Fluvisols of variable soil textures depending on the velocity of the water upon sediment deposition (Jones *et al.*, 2013). Fluvisols are relatively young soils and characterised by high infiltration rates, sustained water availabilities and by recurrent deposition of sediments and nutrients during seasonal floods (Burghof, 2017). They are, hence, suitable for annual crops such as rice or for seasonal use as grazing pastures (Gabiri *et al.*, 2018b). The upland areas of the catchment are dominated by humic Nitisols which are soils of medium fertility, deep rooting-ability and high water holding capacity, e.g., in the Udzungwa Mountains, by Lixisols which are heavily weathered soils of low fertility, e.g., in the western part of the catchment, and by ferralic Cambisols which are of low fertility, e.g., in the lower eastern part of the catchment (Näschen *et al.*, 2019). The Nitisols in the northwestern part of the catchment are used for tea cultivation, while the Lixisols are used for annual crop cultivation but need fertilization to sustain production. At the bottleneck of the floodplain near Ifakara town, Arenosols are found in patches at the floodplain's fringe, while ferric, haplic and humic Acrisols are found in the southern part of the floodplain in a V-shaped distribution (Näschen, 2020).

Predominant soils in the Nasirye catchment include eutric rhodic Nitisols of colluvial character at the valley slopes, and eutric umbric Gleysols and eutric gleyic Fluvisols in the valley bottomland and hydromorphic fringes (Gabiri *et al.*, 2017). The Nitisols are formed

from quartzite, gneiss and laterite, and show a deep red colour with a well-developed nut-shaped structure (Gabiri, 2018a). They exhibit high water holding capacities, making them generally suitable for crop production although erosion and nutrient disorders are likely (Jones *et al.*, 2013). Within the valley bottomland, the eutric Gleysols are mainly formed from alluvium while colluvial materials from adjacent uplands govern soil characteristics. The eutric Gleysol typically has a high soil organic matter content and shows a humic topsoil (Windmeijer & Andriesse, 1993). The fertility status of the Gleysol depends upon physical attributes and land uses of valley slopes, i.e., nutrient mobilisation and subsequent translocation by subsurface water flows, and by the prevailing hydrological conditions, i.e., temporarily waterlogged conditions enhance availability of P, while permanently waterlogged conditions can cause low N availability and Fe-toxicity (Windmeijer & Andriesse, 1993).

2.1.5 Hydrology

Hydrological processes in the floodplain are governed by water influxes from various large rivers, including the Ugzungwa Mountain sourced Msolwa River as well as the Mnyera, Pitu and Ruhudji Rivers sourced in the southwestern Mbarika Mountains (Dinesen, 2016). The merger of the Ruhudji, Pitu and Mnyera River marks the beginning of the Kilombero River, which is flowing in a SW-NE direction. Upon entering the flat floodplain bottom, the Kilombero River bifurcates and meanders, forming a typical braided river system that further on is developing into a meandering river system due to a low slope gradient of 0.4‰ (Jätzold & Baum, 1968). The floodplain is a complex system of perennial and seasonal rivers and streams, swamps, ponds, lakes and oxbows (Lyon *et al.*, 2015). Perennial tributaries and seasonal streams from the NW and SE mountain areas additionally feed the Kilombero River (Burghof, 2017). The seasonal change in water flow in the floodplain is substantial, the central floodplain floods by up to 4.5 m above the riverbanks during the wet season from January to May. However, most parts of the floodplain dry up almost completely from June onwards, except for river margins, oxbow lakes and some permanent swamps (Dinesen, 2016; Lyon *et al.*, 2015). The Lumemo River is one of the major tributary of the Kilombero River and is draining into study area from N to S and marking the entry of the Kilombero River into a bottleneck structure before joining the Luwego River (Näschen *et al.*, 2019). The Luwego River flows south and later forms the Rufiji River, making the Kilombero River an important tributary catchment to the Rufiji River Basin, contributing 62% of the annual average basin water flow (Mwalyosi, 1990). In the study area, groundwater flows from N to S towards the Kilombero River and is recharged from *ex-situ* and *in-situ* rainwater infiltration, runoff and

subsurface inflows from adjacent mountain areas (Burghof *et al.*, 2018) (**Figure 2.3**). Seasonal flooding is caused by rainfall, overbank flow and groundwater-induced flooding, depending on the relative location within the floodplain, i.e., proximity to rivers or mountains (Gabiri *et al.*, 2018b) (**Figure 2.3**).
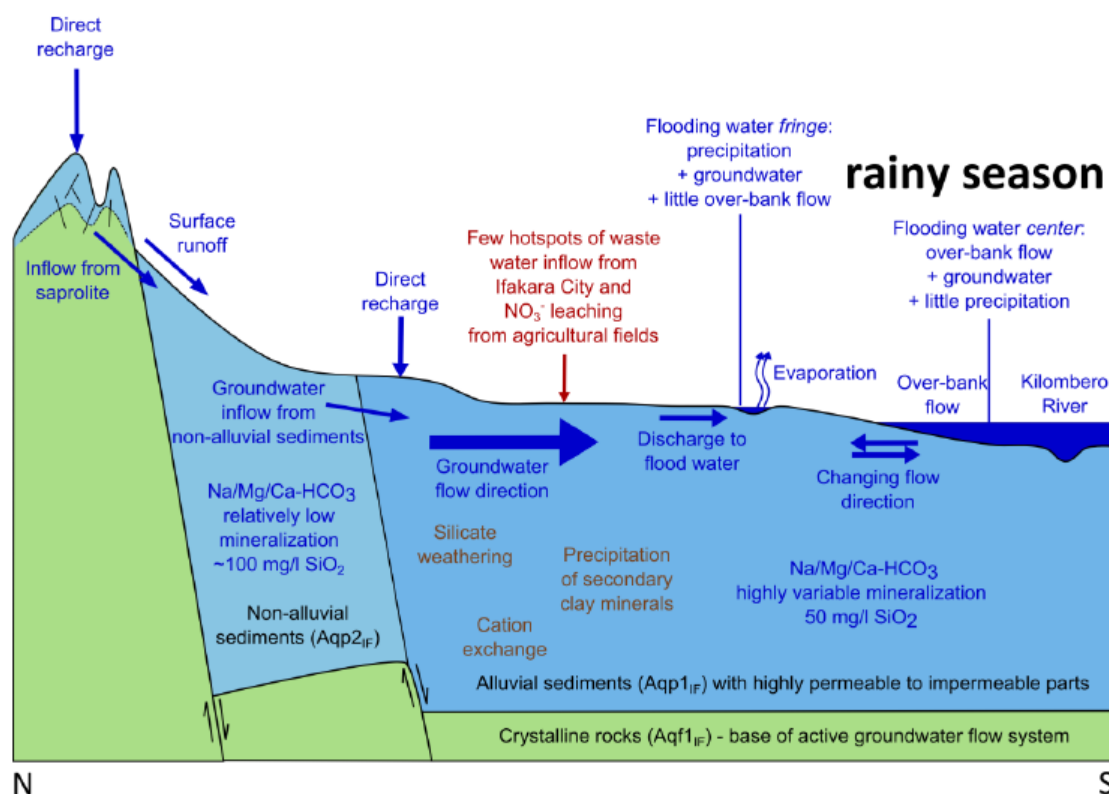
Figure 2.3 Conceptual hydrogeological model for the study site in the Kilombero floodplain in Ifakara, Tanzania. Water fluxes and compositions are represented in blue, hydrochemical processes in brown and anthropogenic influences in red; according to Burghof 2017.

The Namulonge inland valley lies within the Nasirye microscale catchment that is part of the Lake Kyoga Basin, the second largest drainage sub-basin and home of the third largest lake in Uganda that is the Lake Kyoga (Nsubuga *et al.*, 2014). The Lake Kyoga Basin consists of a vast network of diverse wetlands covering about 57,000 km^2 and contains abundant surface and groundwater resources (Gabiri *et al.*, 2019; Ojara *et al.*, 2020). However, from 1994 to 2008, the wetland coverage has declined by 27%, mainly due to the expansion of urban centres, industrial developments and agricultural encroachment (Nsubuga *et al.*, 2014). All streams in the study area, including natural and artificial streams from water drainage and channelling, are draining the Nasirye catchment and flow from the inlet in the NW to the outlet in the SE, where they merge into the Ssezibwa River, a tributary of the Lake Kyoga (Gabiri *et al.*, 2019). In the study inland valley, the Nasirye stream has been modified and diverted for irrigation and drainage purposes and thus follows only partly the local scale topography and natural water

pathways (Gabiri, 2018a). Major hydrological processes in the Nasirye catchment include evapotranspiration and runoff, i.e., surface runoff and lateral and subsurface inflows from the valley slopes and the uplands (Gabiri *et al.*, 2020) (**Figure 2.4**). Both runoff processes as well as direct recharge processes from the catchment and discharge processes from a deep groundwater table feed a permanently shallow water table in the study area (**Figure 2.4**). However, a micro-scale topography, distance to the stream and human activities, i.e., water diversion and channelling, affect water table dynamics and hydrological characteristics within the inland valley (Gabiri *et al.*, 2017).
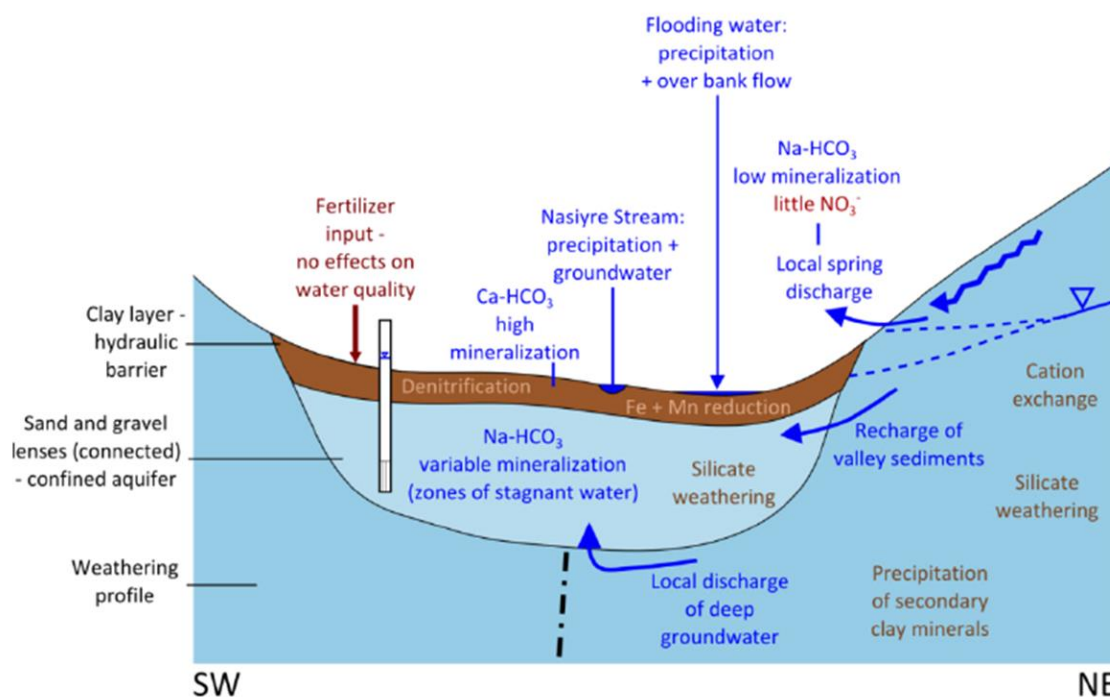
Figure 2.4 Conceptual hydrogeological model for the study site in the inland valley swamp in Namulonge, Uganda. Water fluxes and compositions are represented in blue, hydrochemical processes in brown and anthropogenic influences in red; according to Burghof 2017.

2.1.6 Vegetation, land use & land cover

The floodplain can be categorized into three main vegetative zones according to Kato (2007), i.e., the braided river and alluvial fan zone that are both part of the Zambezian flooded grassland ecoregion (Dinesen, 2016), and the marginal *miombo* woodland zone. The braided river zone is typically submerged during the wet season and the natural vegetation is composed of edaphic grasses such as *Hyparrhenia* spp. (thatching grass), *Panicum fluviicola* Steud.*, Panicum maximum* (guinea grass), *Phragmites mauritianus* Knuth (reed), and *Pensietum purpureum* (elephant grass) (Behn *et al.*, 2018; Nindi *et al.*, 2014). The alluvial fan zone experiences seasonal flooding from tributaries of the Kilombero River and the natural vegetation is composed of *Hyparrhenia* spp. (thatching

grass) and trees growing on termite hills such as the *borassus palm* (fan palms), *Ficus* spp. and the *Kigelia africana* (sausage tree) (Kato, 2007). Lastly, the southern fringes at the Mahenge Highland foothills are framed by the *miombo* woodland zone and the natural vegetation is composed of *Brachystegia* spp. (*miombo*) and *Julbernardia* spp. (*mnondo*) (Kangalawe & Liwenga, 2005). Since the floodplain boosts a high biodiversity (Nindi *et al.*, 2014), it has been repeatedly recognised for its ecological importance, i.e., by the International Union for Conservation of Nature (IUCN), and by designation as a Ramsar site in 2002 (Kangalawe & Liwenga, 2005). Therefore, the floodplain includes various conservation areas, i.e., the Udzungwa National Park, the Selous Game Reserve (World Heritage Site), the Kilombero Game Controlled Area, the Mbanrang'andu Wildlife Management Area and several forest reserves (Kangalawe & Liwenga, 2005; Wilson *et al.*, 2017). On the other hand, however, agricultural development in the floodplain has been actively encouraged since independence, and more recently with the establishment of the Southern Agricultural Growth Corridor (SAGCOT) in 2012 (Mwongera *et al.*, 2014). Today, the floodplain constitutes one of Tanzania's most important agricultural hubs, supporting various subsistence and commercial agricultural activities on small- and large-scale production schemes. In the drier floodplain fringes or on elevated areas, a large diversity of perennial fruits, i.e., oranges (*Citrus sinensis* L.), mangoes (*Mangifera* spp.), pawpaw (*Carica papaya* L.) and pineapples (*Ananas comosus* L.), and annual vegetables, i.e., okra (*Abelmoschus esculenthus* L.), amaranth (*Amaranthus* L.), tomatoes (*Solanum lycopsersicum* L.) and cabbage (*Brassica oleracea*) are cultivated (Nindi *et al.*, 2014). Tuber crops like sweet potatoes (*Ipomoea batatas* L.) and cassava (*Manihot esculenta*) are grown within the floodplain during the dry season on residual soil moisture (flood-recession cropping) and in the mountain foot-slopes. The dominant commercial crop in the area is sugarcane (*Saccharum officinarum*), grown on large production schemes following extensive soil drainage (Johansson & Abdi, 2020), but further include sesame (*Sesamum indicum*), sunflower (*Helianthus* spp.), and cocoa trees (*Theobroma cacao*) (Kangalawe & Liwenga, 2005). Rice (*Oryza* spp.) is the dominant cereal food crop and is typically produced in the alluvial fan zone on various production scales (Kato, 2007). A recent study by Näschen *et al.* (2018) has shown that agriculturally used land has been rapidly expanding within the floodplain, particularly at the wetland fringes and the western part of the catchment. In 2018, rice covered some 370,000 ha in the floodplain, encompassing >80% of the cropland area (Msofe *et al.*, 2019).

In the central Ugandan region, natural vegetation of the valley bottomlands are *Cyperus papyrus* L (papyrus) swamps and tropical gallery forests (Gabiri *et al.*, 2019; Lind *et al.*, 1974). However, the study area is located in proximity to the urban center of

Kampala city and thus the share of natural vegetation has been significantly reduced by human activities, particularly for agricultural production (Behn *et al.*, 2018). Agricultural intensification of bottomlands is driven by land scarcity with competing land uses from urban sprawls and demographic growth, and additionally from changing food demands of urban consumers. Hence, only small patches of the natural vegetation remain in the study area today. The study site itself is located within the premises of the *National Crop Resources Research Institute* (NaCRRI) research station. The surroundings, however, are characterised by intensive smallholder subsistence agriculture with a mosaic-type land use and management practices. While upland food crops such as maize (*Zea mays* L.), beans (*Phaseolus vulgaris* L.) and sweet potatoes (*Ipomoea batatas* L.) are typically cultivated on the valley slopes, mosaic-type land uses exist in the bottomlands, including rice (*Oryza* spp.) and taro (*Colocasia esculenta* L.) under saturated or near-saturated conditions. Additionally, bottomland farming practices include a diverse set of upland crops (including high-value vegetables) that are cultivated on raised ridges between shallow drainage channels (Gabiri *et al.*, 2017).

2.1.7 Socio-economics & demographics

The majority of inhabitants in the floodplain engage in agricultural activities, making it the most important economic and subsistence activity and employing about 79% of the local population (Johansson & Abdi, 2020). While rice and sugarcane are of leading economic importance, the floodplain also encompasses one of the country's largest inland fisheries (Kangalawe & Liwenga, 2005). Other activities of economic importance include forest products and animal husbandry (Thonfeld *et al.*, 2020). The indigenous population traditionally depended on fishery and small-scale valley slope cultivation for their livelihoods, and were of Bantu ethnical origin, i.e., the Ndamba, Mbunga, Ngindo, Pogoro, Hehe, and Bena tribes (Nindi *et al.*, 2014). However, the floodplain since underwent major developmental changes following Tanzania's independence in 1963, and with the establishment of the Kilombero Sugar Estate, the construction of the TAZARA railway, and the Kidatu Hydro-electricity scheme (Rebelo *et al.*, 2010), and most recently with the establishment of the SAGCOT in 2012 (Mwongera *et al.*, 2014). Economic development and the availability of cultivatable land have, hence, resulted in significant natural population growth and immigration (Rebelo *et al.*, 2010). Immigration is mainly from pastoralist and agro-pastoralist communities like the Masaai, Sukuma and Barbaig tribes but also from business people from across the country (Nindi *et al.*, 2014). This has led to a substantial rise is productivity, particularly of livestock products, but has also increased the pressures on wetland resources (Kangalawe & Liwenga, 2005; Thonfeld *et al.*, 2020).

The average annual population growth rate in the floodplain (Kilombero and Ulanga District) increased from 3.4 between 1978 and 1988 to 3.9% between 1988 and 2002 (Nindi *et al.*, 2014) In the Kilombero District, population thus increased from 71,826 in 1967 to 322.779 in 2002 (Rebelo *et al.*, 2010), and to 407,880 in 2012 (Johansson & Abdi, 2020), and is anticipated to increase to 1.2 million people within the next 20 years (Daconto *et al.*, 2018). Increased pressures on and decline of wetland resources have caused conflicts in the past and are expected to cause conflicts in the future. Conflicts arise among the indigenous population, immigrated communities, protected area authorities and large-scale foreign and domestic investment enterprises (Thonfeld *et al.*, 2020). The latter are increasingly perceived to displace small-scale farmers due to unequal power dynamics (Johansson & Abdi, 2020). For example, the Kilombero Plantation Limited (KPL) displaced 630 families upon their arrival in 2007, and drained and cleared 5,800 ha of land to implement large-scale irrigated rice schemes (Johansson & Abdi, 2020).

Similarly, the majority of people in the Wakiso District in the central Uganda engage in small-scale agriculture and retail (petty) trade (Kaye, 2006). The Wakiso District lies within the peri-urban reaches of Uganda's capital city Kampala, which is why it shows a gradient from peri-urban areas bordering Kampala city to typically rural areas with increasing distance to the capital city (Kaye, 2006). However, subsistence and commercial agricultural activities still provide 30-50% to household incomes (Mugisa *et al.*, 2017), and mainly cater to the market demands of the increasingly land-less population in Kampala city (Sabiiti & Katongole, 2016). The Wakiso District, for example, is the leading livestock producing district, accounting for 7.4 and 6.3% of the country's chicken and pig production, respectively (Sabiiti & Katongole, 2016). The largest ethnic group of the Wakiso District are the Baganda (17%), a Bantu-speaking tribe, however, influxes from the capital city have led to a heterogeneous population from various ethnicities (Kaye *et al.*, 2005). Meanwhile, the nationwide urbanisation level, particularly in and around Kampala city, is expected to increase from a current 12 to 30% by 2023 (Mugisa *et al.*, 2017). The peri-urban areas such as the Wakiso District are thus anticipated to host much of the expanding Kampala population, and its total population is expected to increase from 1,997,418 people in 2014 to 2,915,200 people in 2020 (UBOS, 2018). Hence, crop production in the Wakiso District is facing decreasing land availability and accessibility from urban encroachment as land is increasingly valued for housing development and recreational facilities (Sabiiti & Katongole, 2016). Additionally, land tenure systems are complex and confusing, and often the source of conflict between land owners and tenants (Van Soest, 2018). While the national law incorporated four tenure

systems in 1995, i.e., customary, freehold, leasehold and *mailo*, the latter is the most common in the central Ugandan region (Haneishi *et al.*, 2013c). The *mailo* system is a remnant of colonial times, encompassing an agreement between the British and the Buganda Government on ownership rights of some 50,764 km^2 of land in 1900 (Haneishi *et al.*, 2013c). While the landlords possess land ownership, tenants can lease land and obtain user rights, the so-called *kibanja* where both parties agree on rent, the so-called *busuulo* (Van Soest, 2018). Most people in the study area hold a *kibanja,* which can be sold, transferred, subdivided and inherited while land ownership remains out of reach for most. However, a landlord can only evict his tenants if he can prove development plans, reimburses his tenants for any investments, and provides an equivalent place to live and sustain their livelihood. Still, tenants perceive their land-use rights as fragile and are increasingly persuaded to accept deals by which they obtain legal ownership of parts of their *kibanja* but loose land-use rights of large parts. The *mailo* system, hence, discourages the tenants to substantially invest and improve the land, leaving fields underdeveloped (Bamwesigye *et al.*, 2020). While wetlands are usually state property and thus exempted from private or customary land tenure, land scarcity and lack of alternatives has accelerated agricultural wetland use, particularly by the landless poor (Kabumbuli & Kiwazi, 2009). Severe socio-economic implications, however, have led to a weak governmental enforcement to evict illegal wetland users (Kabumbuli & Kiwazi, 2009; Van Soest, 2018).

2.2   Regional smallholder rice management practices

Rice, both in the Kilombero District in Tanzania and the Wakiso District in Uganda, is commonly produced by smallholder farmers with farm sizes of less than 2 ha (Haneishi *et al.*, 2013b; Senthilkumar *et al.*, 2018). Average yields are generally low with only 1.8-2.2 Mg ha^{-1} in the Kilombero (Senthilkumar *et al.*, 2018), and 1.8-1.9 Mg ha^{-1} in the Wakiso District (Haneishi *et al.*, 2013a), while potential yields are estimated as high as 10 and 7 Mg ha^{-1}, respectively (Kwesiga *et al.*, 2020b). Rice production systems are predominantly rainfed and, hence, rely on rainfall and seasonally shallow water tables and/or flooding from rivers and streams for production (Nhamo *et al.*, 2014).

Low yields have repeatedly been associated to a myriad of abiotic, biotic, management-related and socio-economic production constraints (Rodenburg *et al.*, 2014; Senthilkumar *et al.*, 2020), and are summarized in **Table 2.1**, including:

Abiotic constraints. Drought and flood risks; nutrient deficiencies (N, available P, S, Zn), nutrient toxicities (Fe, Al, and Mn), low pH, CEC and organic carbon, cold and heat stress, soil organic matter accumulation.

Biotic constraints. Birds, rodents, and insect pests (e.g., stem borers, African rice gall midge, rice bugs), diseases (e.g., leaf blast, bacterial leaf blight, brown spot, *Rice Yellow Mottle Virus* (RYMV)), and weeds (e.g., *Echinochloa* spp., *Sphenoclea zeylanica*, *Ludwigia* spp., *Heteranthera callifolia*, including parasitic weeds like *Rhamphicarpa fistulosa*).

Management constraints. Crop establishment (broadcasting at high seeding rates or scatter transplanting of old seedlings), poor field levelling, lack of water control (i.e., bunds, drainage channels), poor soil fertility management (continued crop-residue removal, marginal use of mineral and/or organic amendments), untimely and/or ineffective weeding.

Socio-economic constraints. Lack of inputs, credits, water control and available on-farm labour, low level of mechanization, complex land tenure systems that often discriminate women.

On-farm labour limitations, cash constraints and knowledge gaps on improved management practices are the main culprits of sub-optimal field and crop management (Nhamo *et al.*, 2014). Additionally, the majority of farmers prefer using local varieties with aromatic grains, good cooking and milling qualities despite their inherently low yield potentials (±1.5 Mg ha^{-1}), long growing periods (<6 months) and risks of lodging from tall growth (Kafiriti *et al.*, 2003; Mbaga *et al.*, 2017). Slow dissemination of improved varieties is thus associated to a mismatch in farmer and consumer quality preferences, sub-optimal extreme climate adaptations and poor performance under local management practices (Senthilkumar *et al.*, 2020). Field surveys have shown that less than 50% of farmers have adopted improved modern rice varieties in Tanzania and Uganda (Senthilkumar *et al.*, 2020). Locally available and potentially high-yielding rice varieties include SARO-5 (Singh *et al.*, 2013) in Tanzania, introduced in 2002, and NERICA-4 (Jones *et al.*, 1997) in Uganda, introduced in 2004. Senthilkumar *et al.* (2020) have shown that 38% of farmers in their survey of 29 farms in the Kilombero Valley Floodplain have adopted SARO-5. Miyamoto *et al.* (2012) have shown that 70% of farmers in their survey of 47 farms in central Uganda have adopted NERICA varieties, mainly due to extensive NaCRRI promotion and regional dissemination efforts.

Table 2.1 Overview of the main rice production constraints related to field and crop management practices in the Kilombero District in Tanzania and the Wakiso District in Uganda.

Production system	Kilombero District, Tanzania	Reference	Wakiso District, Uganda	Reference
Production situation	rainfed lowland, alluvial river floodplain	Mbaga *et al.*, 2017	rainfed lowland, inland valley swamps	Haneishi *et al.*, 2013; Kijima *et al.*, 2012
Field management				
Land preparation	mechanical tillage, poor levelling, non-puddled	Senthilkumar *et al.*, 2018, 2020	manual tillage, poor levelling, non-puddled	Haneishi *et al.*, 2012; Makosa & Takayanagi, 2014; Miyamoto *et al.*, 2012
Water	no water control (i.e. bunds and/or drainage channels), lack of irrigation infrastructure, mainly rainfed	Mbaga *et al.*, 2017; Senthilkumar *et al.*, 2018, 2020	no water control (i.e. bunds and/or drainage channels), lack of irrigation infrastructure, mainly rainfed	Onaga *et al.*, 2012; Makosa & Takayanagi, 2014
Weed control	manual weeding with sub-optimal timing (twice/season), limited herbicide use	Senthilkumar *et al.*, 2018	manual one-time weeding (untimely), largely no herbicide use	Haneishi *et al.*, 2012; Onaga *et al.*, 2012
Residues	*in-situ* burning or residue incorporation	Kalala *et al.*, 2017; Senthilkumar *et al.*, 2020	*in-situ* burning or residue incorporation	Senthilkumar *et al*., 2020
Crop management				
Variety selection	poor seed quality, largely use of traditional varieties, i.e. *Kikese, Kalamata, Shingo ya mwali, Kabangala, Afaa, Kahogo, Sindano* and *Kilombero*	Kafiriti *et al.*, 2003; Kalala *et al.*, 2017; Mbaga *et al.*, 2017; Senthilkumar *et al.*, 2018, 2020	poor seed quality, largely use of traditional varieties, i.e. *Sindano, Kaiso, Benenego, Kyabukooli and Pakistan*	Haneishi *et al.*, 2012; Miyamoto *et al.*, 2012
Establishment	direct seeding exceeds scatter transplanting (seedling age 18-21 days)	Mbaga *et al.*, 2017; Senthilkumar *et al.*, 2018, 2020	direct seeding exceeds scatter transplanting (seedling age ≥ 27 days	Haneishi *et al.*, 2012; Miyamoto *et al.*, 2012
Nutrient management	largely no mineral or organic fertiliser use, max. use of 40 kg mineral N ha^{-1}, mean use of 11 kg mineral N ha^{-1}	Kalala *et al.*, 2017; Mbaga *et al.*, 2017; Senthilkumar *et al.*, 2018	largely no mineral or organic fertiliser, max. use of 53 kg mineral N ha^{-1}, mean use of 4 kg mineral N ha^{-1}	Fungo *et al.* 2013; Haneishi *et al.*, 2012; Onaga *et al.*, 2012
Pest and disease control	no bird and/or rat control, limited pesticide and fungicide use	Balasubramanian *et al.*, 2007; Mbaga *et al.*, 2017; Senthilkumar *et al.*, 2018	no bird and/or rat control, limited pesticide and fungicide use	Balasubramanian *et al.*, 2007; Haneishi *et al.*, 2013

3.   Wetlands for lowland rice production

Wetlands cover approximately 0.17 million km^2 in East Africa (Kenya, Rwanda, Uganda and Tanzania), 80% of which are characterized as alluvial floodplains and inland valley swamps (Leemhuis *et al.*, 2016), and were thus selected as focal sites for this study. Alluvial floodplains are wide and flat alluvial plains that border streams and rivers from which they flood periodically, and are characterised by oxbow depressions and natural levees (Leemhuis *et al.*, 2017). Inland valley swamps are seasonally water-logged linear depressions in head water zones of rivers and represent a toposequence of a valley bottom with its hydromorphic fringes and adjoining slopes that contribute lateral and subsurface runoff and seepage into the valley bottom (Leemhuis *et al.*, 2016). Thus, alluvial floodplains and inland valley swamps represent different flooding regimes, i.e., an overflow-flooding and inflow-flooding regime, respectively (Windmeijer & Andriesse, 1993). In the overflow-flooding regime, excessive rainfall in the upper catchment areas causes the water discharge to exceed the rivers capacity, resulting in riverbank overflow. In the inflow-flooding regime, seasonal flooding is caused by the accumulation of lateral and subsurface runoff, groundwater flow from adjacent uplands and rainfall.

Ecology	Upland	Lowland fringe (hydromorphic)	Lowland	Intensified lowland	Irrigated lowland
Main water supply	Rainfall	Rainfall + water table	Rainfall + water table + unregulated flood water	Regulated flood water	Irrigation
Agroecological zone	Guinea savannah–humid forest zone	Guinea savannah–humid forest zone	Sudan savannah to humid forest zone	Sudan savannah to humid forest zone	Sahel to humid forest zone
Main stresses	Drought Weeds Pests and diseases P and N deficiency Soil erosion Soil acidity	Drought Weeds Pests and diseases P and N deficiency Soil erosion Soil acidity Fe toxicity	Drought/flooding Weeds Pests and diseases P and N deficiency Fe toxicity	Drought/flooding Weeds Pests and diseases P and N deficiency Fe toxicity	Weeds Pests and diseases Salinity Alkalinity P and N deficiency Fe toxicity

Figure 3.1 Major rice environments and their attributes in Africa; according to Diagne *et al.* 2013.

Balasubramanian *et al.* (2007) additionally distinguished between four major rice ecosystems based on surface-water regimes, i.e., dryland, rainfed wetland, deep-water and mangrove swamps, and irrigated wetland. The focal study sites belong to the rainfed wetland rice ecosystem, i.e. lowlands of an alluvial floodplain, and lowlands and hydromorphic fringes of an inland valley swamp (Haefele *et al.*, 2013) (**Figure 3.1**). Rainfed wetland rice ecosystems are characterised by varying degrees of water control, and non-continuous flooding of variable depth and duration where rice is grown on level to slightly sloping, un-bunded or bunded fields (Saito *et al.*, 2013). Rice production depends on rainwater and stored groundwater (**Figure 3.1**), however, as the water supply conditions vary greatly within the wetland ecosystem, a sub-ecosystem classification was developed (Wade *et al.*, 1999):

- rainfed shallow, favourable,
- rainfed shallow, drought-prone,
- rainfed shallow, drought- and submergence-prone,
- rainfed shallow, submergence-prone, and
- rainfed medium deep, waterlogged.

Improved water management systems may entail primary and secondary drainage pathways, and outlining, levelling and bunding of individual fields (Rodenburg *et al.*, 2014). For inland valleys, different small-scale water management systems have additionally been identified, i.e., (1) the traditional random basin system, (2) the central drain system, (3) the interceptor-canal system, (4) the head-bund system, and (5) the contour-bund system, described in detail by Oosterbaan *et al.* (1986) (**Figure 3.2**).
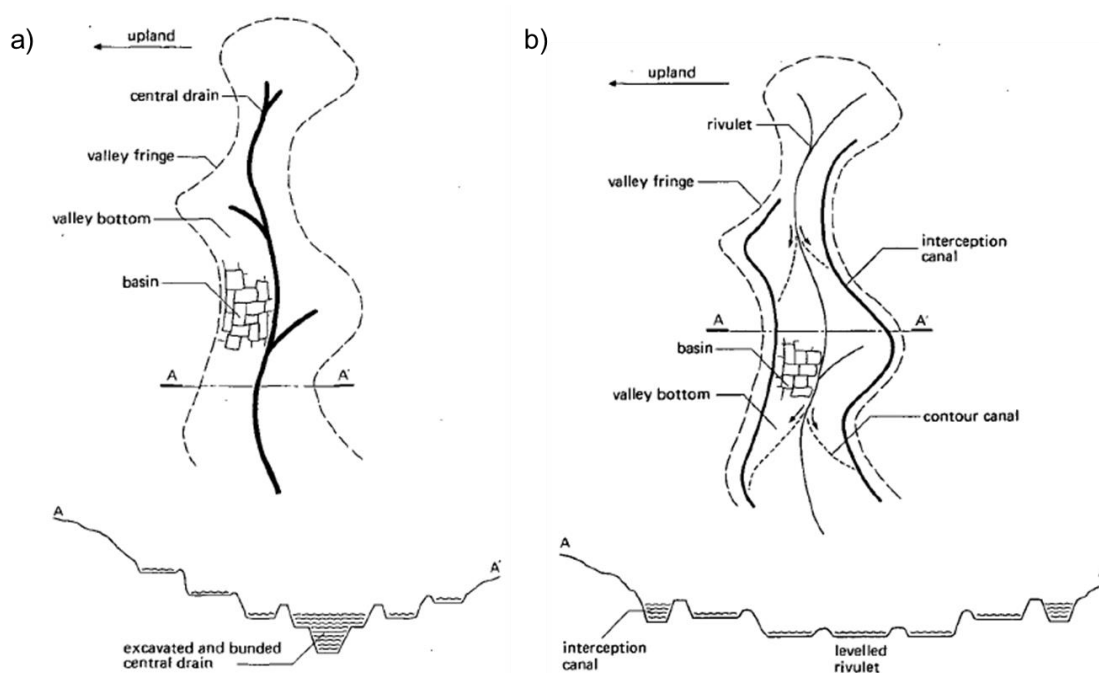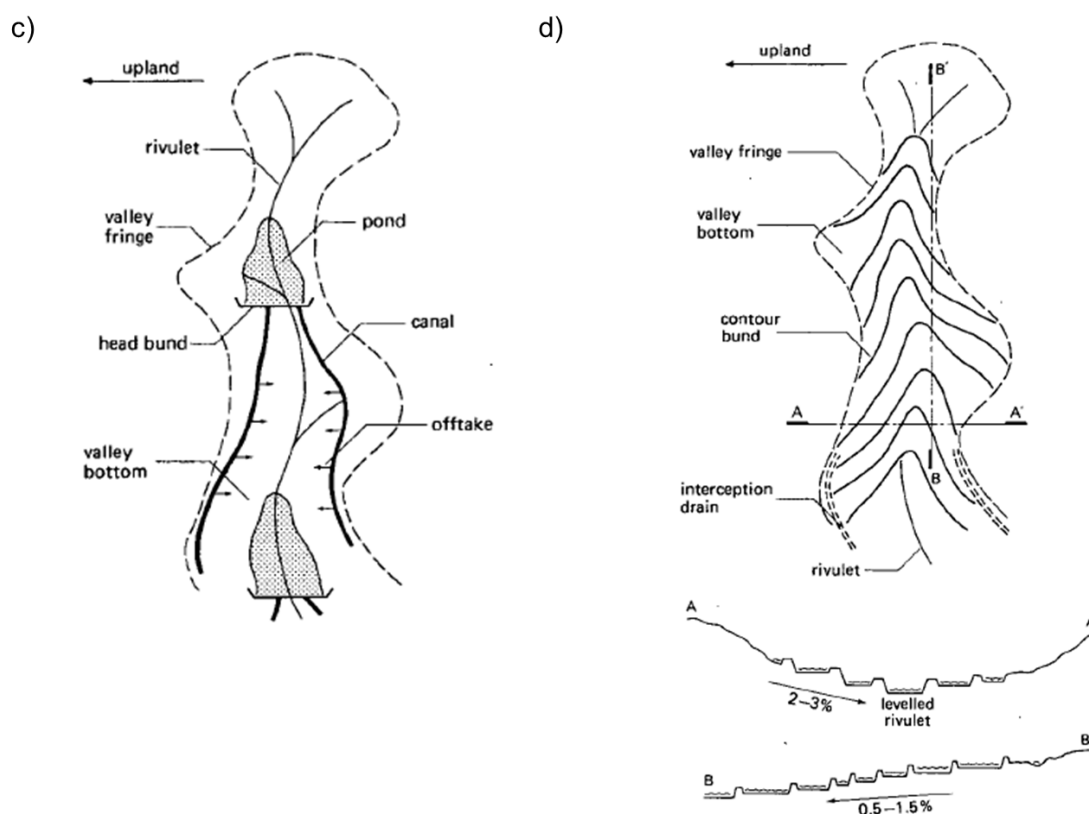
Figure 3.2 Schematic representation of small-scale water management systems for lowland rice production systems in inland valley wetlands, a) the central drain system, b) the interceptor-canal system, c) the head-bund system, and d) the contour-bund system; according to Windmeijer & Andriesse, 1993.

McCartney & Houghton-Carr (2009), for example, have proposed a working wetland potential (WWP) index method that uses a multi-criteria analysis to evaluate the agricultural wetland potential under consideration of the ecological character and conservation value, and the wetland's contribution to social welfare via the determination of biophysical and socio-economic suitability for agricultural production, and potential ecological and social hazards from agricultural use.

3.1   Nitrogen dynamics in wetland soils

Understanding nitrogen (N) dynamics in temporarily and/or permanently anaerobic wetland soils is imperative to increase N fertiliser use efficiencies and reduce the hazards of N losses (Wade *et al.*, 1999). Soil N transformation processes are largely governed by microorganisms, and plant-available N is predominantly inorganic, provided by N mineralization of organic matter and plant residues, N fixation from algae and bacteria, indigenous soil ammonium (NH_4^+) and nitrate (NO_3^-), and chemical fertilisers (**Figure 3.3**).

NH_4^+ is the predominant form of available N as the mineralization of organic N to NO_3^- does not proceed beyond the ammonia (NH_3) stage in the absence of oxygen.

Temporarily and/or permanently anaerobic soil conditions can, however, promote N fertiliser losses through denitrification, NH_3 volatilization and leaching. Belder *et al.* (2005) reported that most N fertiliser losses occur after application into the floodwater through NH_3 volatilization (**Figure 3.3**). NH_3 volatilization losses depend on soil pH, salinity and alkalinity, $CaCO_3$ content, CEC, buffering capacity, microbial activity and water management, and may thus range from negligible to substantial amounts (Gosh & Bhat, 1998). Some of the NH_3, however, is nitrified in the oxidized soil zones and the floodwater from where it moves into the reduced layers, denitrifies and is subsequently lost as N gas (N_2) and nitrous oxide (N_2O) (**Figure 3.3**). Therefore, NO_3^--based fertiliser are not recommended in anaerobic soils as the potential denitrification losses are high (Nurulhuda *et al.*, 2018). Factors affecting denitrification losses are soil temperature and pH, submergence period, nitrification rate and NO_3^--N content. N losses from leaching occur in coarse textured soils with a low CEC and predominantly affect NO_3^- as it moves easily by diffusion and percolation into the underlying reduced soil layers (Gosh & Bhat, 1998) (**Figure 3.3**). NH_4^+ on the other hand is less prone to leaching due to its adsorption in the
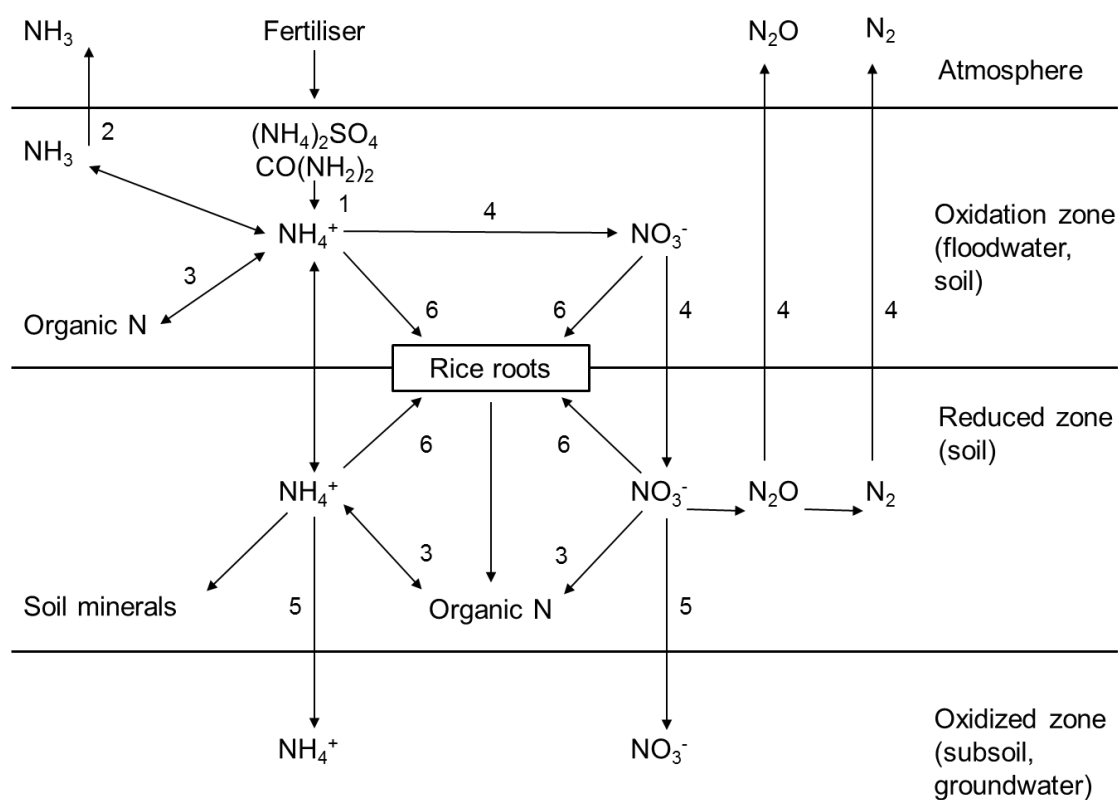
Figure 3.3 The fate of mineral N fertiliser in wetland soils. Numbers relate to the processes: 1= urea-N hydrolysis, 2= ammonia volatilization, 3= nitrogen immobilization, 4= denitrification, 5= leaching, 6= plant uptake; according to Gosh & Bhat, 1998.

cation exchange complex. Therefore, urea-N ($CO(NH_2)_2$) fertiliser remains the primary mineral N source in temporarily and/or permanently anaerobic wetland soils. In aerobic soils, however, the dominant form of N is NO_3^- as comparatively little NH_3 volatilization and NO_3^- leaching can be expected after fertiliser application. Alternating moist-dry soil conditions, however, may stimulate nitrification-denitrification processes, resulting in N loss through N_2 and N_2O diffusion, and NO_3^--leaching (Belder *et al.*, 2005).

3.2   Wetland functions & risks from agricultural (mis-)use

Wetlands provide an array of ecosystem services (ESS), i.e., provisioning, regulating, supporting and cultural services (Keddy *et al.*, 2009) (**Figure 3.4**). Additionally, wetlands are dynamic ecosystems and continuously evolve in response to local eco-hydrological processes, i.e., ecological, hydrological and geomorphological processes (Wood & Van Halsema, 2008). Throughout sub-Saharan Africa, rural and often poor communities depend on wetland services for their livelihoods (McCartney & Houghton-Carr, 2009; Rebelo *et al.*, 2010). Besides their potential for crop production from sustained water availability (Diagne *et al.*, 2013), wetlands support livelihoods through dry-season grazing, fishing, collection of freshwater and building materials (Dixon & Wood, 2003). Additionally,

Provisioning
Food & fodder production
Fisheries
Timber production, fuelwood
Building materials, medicinal plants
Freshwater

Cultural
Landscape aesthetics
Cultural sustenance
Recreation & spiritual enrichment
Science & education
Ecotourism

Wetland ecosystem services (ESS)

Regulating
Water & air quality
Flood mitigation & water regulation
Carbon sequestration
Micro-climate regulation
Habitat for endangered species
Disease and pest control
Pollination

Supporting
Water storage
Nutrient retention & cycling
Primary production
Hydric soil development (sediment retention & SOM accumulation)

Figure 3.4 Overview of the most important ecosystem services (ESS) provided by wetland ecosystems; according to Mitch *et al.* 2015 and Wood & van Halsema, 2008.

wetlands promote environmental stability, i.e., mitigate local floods through high water holding capacities, groundwater recharge and discharge, erosion and sedimentation control, carbon storage, and nutrient retention and cycling and thus reducing eutrophication (Johansson & Abdi, 2020; Keddy *et al.*, 2009). Wetlands also provide refuge to numerous, often endangered plant and animal species (Chapman *et al.*, 2001) (**Figure 3.4**). Therefore, indiscriminate development of wetlands for agricultural purposes should be avoided (Rodenburg, 2013), especially since unsustainable wetland use can cause a decline or irreversible destruction of wetland's ESS, placing both numerous livelihoods and environmental stability at risk (McCartney & Houghton-Carr, 2009). Hence, five environmental indicators have been developed by the IRRI to monitor ESS and ensure the long-term sustainability of rice farming systems in wetland areas (Balasubramanian *et al.*, 2007; IRRI, 2004):

Production. Combining balanced fertiliser use with adequate weed control to improve yields and maintain soil fertility. Implementation of conservation agriculture techniques, i.e., zero tillage and diversified cropping systems including legume fallows and dryland-rice cover crop rotations.

Biodiversity. Wetlands are important cradles of flora and fauna biodiversity (Chapman *et al.*, 2001), and natural vegetation is instrumental for the wetlands ability to actively attenuate wastewater, retain nutrients and dispense runoff water (Kansiime *et al.*, 2007). Agricultural activities such as slash-and-burn and shifting agriculture, however, are associated with progressive desertification and habitat loss (Nindi *et al.*, 2014). Hence, a priori impact assessments are essential, as are the alignment of food production with environmental protection (Rodenburg *et al.*, 2014).

Pollution. Excessive and untimely fertiliser use will cause eutrophication and adversely affect the wetland's ability to maintain and improve water quality (Oonyu, 2011), whilst threatening aquatic life (Nindi *et al.*, 2014). A study in the Kilombero floodplain by Materu & Heise (2019) has shown that agro-chemicals, particularly from commercial sugarcane and rice enterprises, have the potential to cause ecological damage to the river basin and aquatic ecosystem, and to contaminate surface- and groundwater. Since wetlands, shallow wells, rivers and streams are the main source for domestic water, water contamination can have to long-term human-health implications (Materu & Heise, 2019). Mitigation strategies should include site-specific nutrient management plans and integrated pest and disease management practices in a timely and appropriate manner.

Land degradation. Wetlands act as periodic or permanent sinks for inorganic sediments, nutrients and organic carbon as well as toxic substances, making them very vulnerable to land modifications (Kansiime *et al.*, 2007). Mitigation strategies should

include appropriate drainage to minimize risks of salinization and alkalization, and conservation agriculture techniques to prevent soil erosion and degradation.

Water use. Intensive agricultural wetland use typically includes large-scale irrigation water abstraction, water drainage and channeling (Dixon & Wood, 2003). Such practices reduce the hydraulic resistances, impair water recharge processes, drop groundwater levels, reduce the water storing capacities and cause more variable stream-flows (Lyon *et al.*, 2015). Hence, water removal accelerates and leads to amplified seasonal floods (Lankford & Franks, 2000), while the productivity and health of downstream lakes, streams and rivers may be negatively affected (Keddy *et al.*, 2009). Drainage is particularly harmful to seasonal wetlands and 60% of seasonal wetlands have reportedly been lost in Uganda as a consequence (Oonyu, 2011). Mitigation strategies should optimize water productivity, i.e., by implementation of alternate wetting and drying (AWD) systems, and use of water-efficient short-duration and aerobic rice varieties. Additionally, rainwater harvesting techniques (e.g., field bunds, farm ponds, small reservoirs and earth dams) are critical to increase infiltration and thus recharge groundwater as well as to revive small streams and rivers (Nhamo *et al.*, 2014).

Across East Africa, wetlands have been used extensively for centuries, while intensive agricultural encroachment accelerated in the 1950s, driven by population growth, resource constraints and lack of alternative livelihoods particularly in rural areas (Chapman *et al.*, 2001; Rebelo *et al.*, 2010). Therefore, traditional wetland use strategies, i.e., grazing, fishing, material collection and crop cultivation on wetland margins, is shifting towards more intensive usage, i.e., water drainage using permanent hydrological control structures and multi-cropping systems (Balasubramanian *et al.*, 2007). The shift from traditional to intensive agricultural wetland use is unlikely to be sustainable given the gradual degradation of wetland resources in Tanzania, and acceleration of downstream water flows from intensive drainage and cultivation in Uganda (Dixon & Wood, 2003). Besides agricultural wetland use, other human activities such as overgrazing, deforestation, illegal hunting and fishing, and bush fires additionally pose threats to wetland's ESS (Nindi *et al.*, 2014). Meanwhile, communities within both study regions have been shown to depend heavily on wetlands for their household food security and livelihoods, i.e., the Kilombero floodplain contributes to the food intake of some 98% of households (Rebelo *et al.*, 2010), while the Kyoga basin supports about 80% of all households through subsistence and commercial crop production (Turyahabwe *et al.*, 2013). Consequently, sustainable agricultural wetland use plans are needed, balancing both food production and preservation of the wetland's ESS (Rebelo *et al.*, 2010).

4.   Research approach

This study is composed of two integral parts, (i) an extensive field experimental part and (ii) a comprehensive cropping system modelling part. The agronomic field trials aimed at studying yield limiting factors, determining site- and year-specific non-amended baseline and attainable yields for rice-based lowland systems as affected by weather and hydro-edaphic field conditions (**Figure 4.1**). Agronomic field data were subsequently used to perform a multi-criteria model calibration and validation, i.e., testing the veracity of the APSIM model to simulate differential rice responses to management and hydro-edaphic conditions and to continuously simulate 'carry-over' effects (soil moisture contents, and soil carbon dynamics and indigenous soil N supply) during the study period. Upon model validation, various management scenarios were developed aiming at identifying site-specific 'best-bet' intensification options under consideration of agronomic and economic benefits for regional smallholder farming systems (**Figure 4.1**).
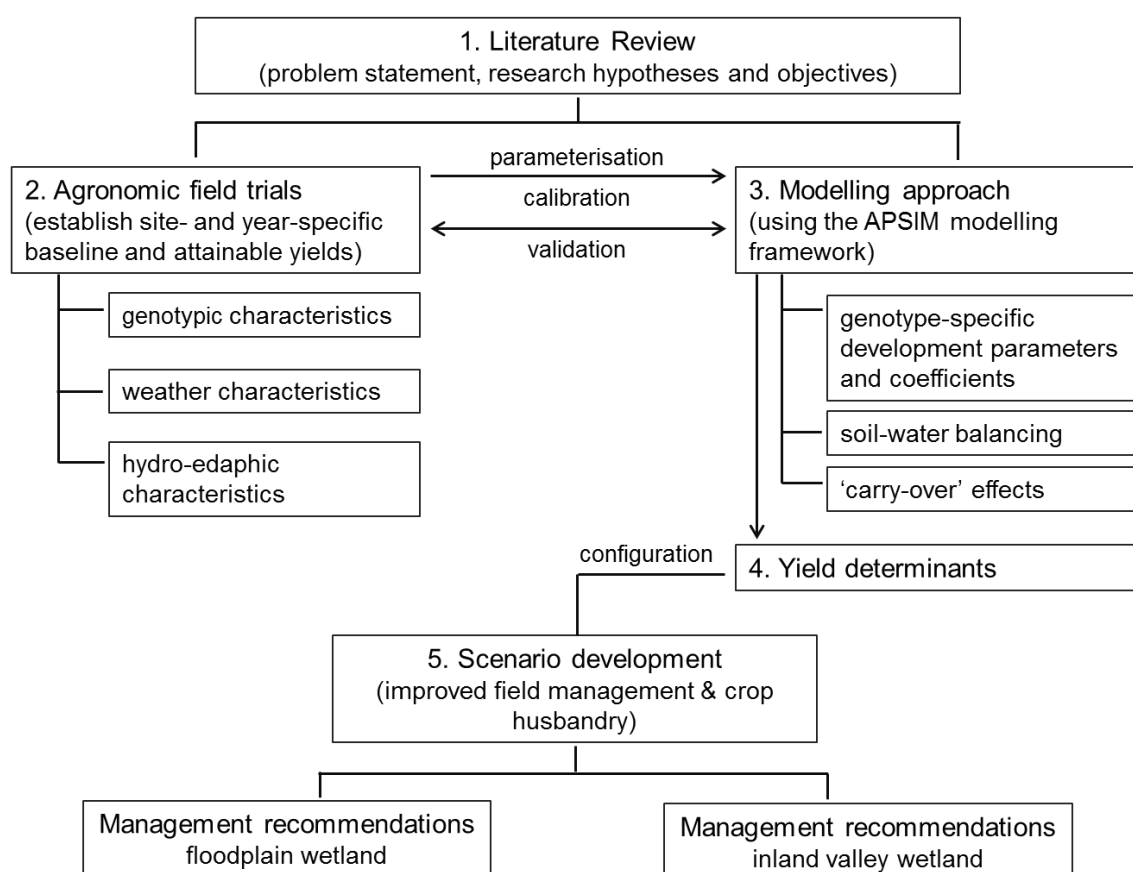
Figure 4.1 Conceptual presentation of research approach followed in this thesis.

4.1   Agronomic field trials

Agronomic field trials were implemented at various field positions within two contrasting wetland types, i.e., the Kilombero floodplain in southeast Tanzania and an inland valley swamp in central Uganda between 2014 to 2017 (**Table 4.1**).

Table 4.1 Geographical location, average annual air temperature and precipitation, and the predominant soil types of the study sites in the Kilombero floodplain in Ifakara, Tanzania, and the inland valley swamp in Namulonge, Uganda.

	Ifakara, Tanzania	Namulonge, Uganda
Wetland type	Alluvial floodplain	Inland valley swamp
Geographical location	8.10°- 8 .18°S, 36.67°- 36.76°E	0.519°- 0.522°N, 32.640°- 32.644°E
Altitude	255 masl	1,105 masl
Mean annual air temperature	25.6°C	22.2°C
Mean annual rainfall	1,177 mm	1,057 mm
Mean rainfall during rice-growth	757 mm	361 mm
Predominant soil	eutric Fluvisol	umbric Gleysol

The experimental design was a randomized complete block design (RCBD) with four replications per treatment and field position, and experiments were established for three consecutive years at both study sites. Treatments included: (i) a rainfed non-amended baseline treatment (0N); (ii) a rainfed 60 kg N ha^{-1} treatment (60N); and (iii) a manually irrigated, 120 kg N ha^{-1} and 60 kg PK ha^{-1} attainable yield treatment (120N+PK+I) (Senthilkumar *et al.*, 2018). N fertiliser was applied as Urea-N (46% N) in two split doses; 75 and 50% was applied basally and 25 and 50% at the panicle initiation stage (PI) in Tanzania and Uganda, respectively. As per local recommendations, P was applied basally as single super phosphate (SSP, 8.7% P) in Tanzania and as triple superphosphate TSP (19.7% P) in Uganda while K was applied basally as muriate of potash (KCl, 49.6% K). Individual plots measured 5x6 m, and were levelled, puddled and bunded (40 cm height and 20 cm width) to prevent surface water and nutrient flows. Locally available, improved rice varieties were used, i.e., the semi-dwarf, 120-day lowland rice (*O. sativa*) variety SARO-5 (TXD306; est. 2002) (Singh *et al.*, 2013) in Tanzania, and the drought-tolerant, 95-110-day rainfed rice (*O. sativa* x *O. gaberrima*) variety NERICA-4 (est. 1994) (Jones *et al.*, 1997) in Uganda. With the onset of the rainy seasons in February in Tanzania and August in Uganda, rice nurseries were established and experimental plots hand-ploughed, irrigated, puddled, and levelled prior transplanting. Two 16-30 day old seedlings per hill were transplanted at 20x20 cm in Tanzania, and three 21-27-day-old seedlings per hill at 15x30 cm spacing in Uganda. Weeds were removed manually 3, 6 and 9 weeks after transplanting while pests and diseases were controlled during the study period as required.

4.1.1 Experiments in the Kilombero floodplain in Tanzania

Study site

Experiments were conducted in farmer´s fields in the Kilombero floodplain near Ifakara town, in south-central Tanzania during 2015 and 2017 (**Figure 4.2**). The floodplain is one of Tanzania's most important agricultural hubs, supporting a number of agricultural activities on various scales and for both subsistence and commercial purposes, including animal husbandry, fishing, and crop production, e.g., sugarcane, maize and rice (Msofe *et al.*, 2019). Rainfed rice production is largely concentrated in the alluvial fans and dependent on the seasonal rainfall and flooding of the Kilombero River and its tributaries (Kato, 2007).
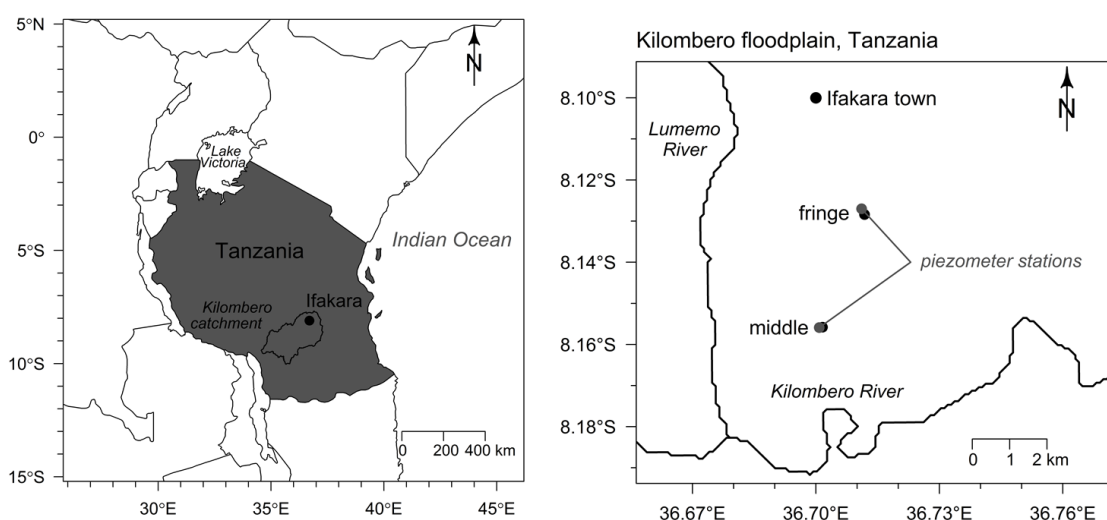
Figure 4.2 Geographic location of the study site (left) and field positions (right) in the Kilombero floodplain, Tanzania.

Weather conditions

During the study period from 2015 to 2017, weather data was obtained from an automatic weather station installed at the Ifakara Health Institute (IHI) (8.108°S, 39.665°E), about 5 km west of Ifakara town. Additionally, tipping buckets were installed at the respective field positions for more site-specific rainfall monitoring. During 2015 and 2017, annual rainfall ranged between 1,060 and 1,340 mm, with a mean annual average air temperature of 25.6°C (**Figure 4.3**). Some 80-90% of the annual rainfall occurred between December and April, while the dry periods from June to September received less than 10 mm of rain per month (Kwesiga *et al.*, 2019). During rice-growth, seasonal rainfall varied between 849, 809, and 1,049 mm at the fringe, and between 760, 536, and 1,167 mm at the middle

position in 2015, 2016, and 2017, respectively. Average monthly maximum and minimum temperatures during rice-growth were 31 and 21.6°C, respectively (**Figure 4.3**).

Figure 4.3 Average monthly rainfall, and minimum and maximum temperatures for the years (a) 2015, (b) 2016 and (c) 2017 at the study site in the Kilombero floodplain in Ifakara, Tanzania. Bars indicate standard deviations of the monthly rainfall means (*n*= 2), boxes indicate the main rice-growing period (March to May).

Hydro-edaphic characteristics

Experiments were established at the potentially drought-prone fringe and the potentially submergence-prone middle position based on the origin, extent and duration of the floodwater (Gabiri *et al.*, 2018b). Hydrology at the fringe position is characterised by *in-situ* rainfall and water table-induced flooding from lateral subsurface inflows from adjacent mountain ranges, while hydrology at the middle position is characterised by *in-situ* rainfall and seasonal river-bank overflows (Burghof *et al.*, 2018) (**Figure 2.3**). The water table fluctuated between 1.5 below surface and surface level, and between 3 m below and 1 m above surface level at the fringe and middle positions, respectively (**Figure 4.4**). Flooded conditions occurred annually between March and May at the fringe and between April and June at the middle position.

Soils at the study sites were formed from fluvial and alluvial sediments and according to the World Reference Base are classified as eutric Fluvisols (FAO, 2014). Seasonal flood events additionally deposit sediments and nutrients and soil attributes varied considerably between field positions. While the topsoil's texture was loamy in the fringe, it was more coarse-textured in the middle position, however, with an increasing clay content at both positions with increasing depth (**Table 4.2**). Topsoil in the fringe position showed a comparatively high soil organic C content with 24.5 g kg^{-1} and moderate soil N content with 1.2 g kg^{-1}. On the other hand, topsoil in the middle position showed low soil organic C and N contents with 6.5 and 0.5 g kg^{-1}, respectively. Soil pH was slightly acidic and ranged between 5.7 and 6.3 across sites. According to Senthilkumar *et al.* (2018), soil contents of 2 g N kg^{-1}, >5 mg P kg^{-1} and >59 mg K kg^{-1} are critical macro-nutrient levels for rice growth. Hence, soil N contents were only slightly above the critical level in the rooting zone (0-30 cm) (**Table 4.2**), while both P and K were sufficient (data not shown). Layer-wise soil properties were determined from a soil profiling campaign prior to the experimental trial in November 2014. Soil organic matter (SOM) contents were determined from the weight loss after dry combustion at 550°C for 2 hours. Soil N and C contents were determined by dry combustion method at 950°C using an Elemental Analyzer (vario-Elcube Elementar Analysesysteme GmbH, Langenselbold, Germany). Plant-available soil P and K contents were extracted using the Mehlich-3-extraction method and analysed colourimetrically using molybdenum-blue complex for P (Specord 50Plus, Analytik Jena AG, Jena) and ICP-OES for K (Spectro Arcos, Spectro Analytical Instruments GmbH, Kleve).

Data collection

Data collection included key phenological stages, i.e., panicle initiation (PI), 50% flowering and physiological maturity, and sequential biomass measurements at the early (30 DAT) and late vegetative stages (50 DAT), 50% flowering and physiological maturity. Sequential biomass samples from 2x6 hill clusters were used to determine biomass accumulation and partitioning, i.e., into green and dead leaf, stem and panicle parts, and were oven-dried at 90°C until constant weight. Biomass sub-samples of about 1 g were fine-ground and analysed for their C and N contents using an elemental analyser (EURO EA Elemental Analyser series 3000, EURO-EA Vector Pavia, Italy). Grain yields were determined from a 6 m^2 central harvest area as rough rice at 0% moisture content. Grain quality parameter further included the thousand kernel weight (tkw) and the percentage of filled spikelets per panicle, i.e., grains with a specific gravity ≥1.06 g cm^{-3} (Zakaria *et al.*, 2002). **Table 4.3** provides a detailed overview of all field activities during the study period.

Figure 4.4 Measured depth to water table in both field positions at the study site in the Kilombero floodplain in Ifakara, Tanzania (2015-2017); solid horizontal line represents the surface level; positive values are not implicitly related to water levels above the surface (floods). Modified from Gabiri *et al.* 2018.

Table 4.2 Soil chemical and physical properties at the study site and field positions in the Kilombero floodplain in Ifakara, Tanzania. Soil profiling was done in November 2014 prior to the onset of the experiments, data provided by Björn Glasner (unpublished).

Field position	Depth	Soil physical properties					Soil chemical properties			
		BD	Sand	Silt	Clay	Soil texture	pH	SOM	C_{org}	N_{tot}
	[cm]	[g cm^{-3}]	[%]	[%]	[%]	[WRB]	[H$_2$O]	[g kg^{-1}]	[g kg^{-1}]	[g kg^{-1}]
fringe	0-20	1.05	34.4	39.7	25.9	loam	5.96	87.02	24.51	1.21
	20-35	1.40	24.9	39.5	35.7	clay-loam	6.28	93.45	14.21	0.91
	35-50	1.41	21.6	40.2	38.2	clay-loam	6.30	95.46	11.63	0.81
	50-65	1.41	18.5	40.3	41.2	silty-clay	6.22	99.00	10.86	0.81
	65-80	1.42	10.9	43.2	45.9	silty-clay	6.19	101.89	10.66	0.71
	80-95	1.40	15.2	34.3	50.5	clay	6.17	100.77	9.73	0.71
	95+	1.39	12.7	34.1	53.1	clay	6.21	101.12	9.73	0.81
middle	0-20	1.34	68.0	15.5	16.5	sandy-loam	5.67	45.18	6.54	0.50
	20-25	n/a	43.5	25.4	31.0	clay-loam	5.88	78.83	9.27	0.71
	25-28	n/a	9.5	39.7	50.8	clay	5.84	107.19	12.05	0.91
	28-37	1.33	6.0	34.3	59.7	clay	5.80	111.96	12.20	1.11
	37-46	1.30	7.0	25.6	67.4	clay	5.77	113.04	11.74	0.91
	46-60	1.34	11.5	28.3	60.2	clay	5.86	106.42	12.00	0.40
	60-75	1.43	15.3	27.7	57.0	clay	6.17	93.08	7.88	0.61
	75-90	n/a	14.6	26.5	59.0	clay	6.35	94.07	4.22	0.91
	90-110	n/a	11.9	24.9	63.1	clay	6.47	103.51	4.99	0.50

BD, bulk density; soil texture definition according to the World Reference Base for Soil Resources (WRB): sand (63 to 2,000 µm), silt (2 to 63 µm), clay (<2 µm); pH, 1:2.5 (soil:water) suspension; SOM, soil organic matter; C_{org}, soil organic carbon content; N_{tot}, total soil N content.

Table 4.3 Field activities and data collection protocol at the study site in the Kilombero floodplain in Ifakara, Tanzania, and during the study period from 2015 to 2017.

Management	Field positon	Year 2015	DAT	Year 2016	DAT	Year 2017	DAT	Management details
		Rice growing seasons						
Nursery sowing	fringe middle	12-Feb 16-Feb	-24 -26	23-Jan 15-Mar	-30 -16	13-Feb 13-Feb	-16 -18	nursery set-up using pre-germinated seeds (soaked in water for 24 hour and incubated for 48 hours until shoot measured about 5 mm)
Transplanting	fringe middle	08-Mar 14-Mar	0 0	22-Feb 31-Mar	0 0	01-Mar 03-Mar	0 0	rice transplanting using about 25-day-old seedlings at an row and inter-row spacing of 20 by 20 cm (25 hills/m^2); two seedlings per hill
Basal fertiliser application (NPK)	fringe middle	08-Mar 14-Mar	0 0	22-Feb 31-Mar	0 0	01-Mar 03-Mar	0 0	75% of urea-N fertilizer application rate (46% N); 60 kg single super phosphate/ha (SSP, 8.7% P) and 60 kg muriate of potash/ha (KCl, 49.6% K)
Top dressing (N)	fringe middle	17-Apr 23-Apr	40 40	02-Apr 20-May	40 50	07-Apr 07-Apr	37 35	25% of urea-N fertilizer application rate (46% N); attempted at panicle initiation (PI)
First Weeding	fringe middle	28-Mar 04-Apr	20 21	13-Mar 21-Apr	20 21	27-Mar 28-Mar	26 25	manual weeding by hand-hoe
Second Weeding	fringe middle	17-Apr 23-Apr	40 40	02-Apr 11-May	40 41	14-Apr 07-Apr	44 35	manual weeding by hand-hoe
Third Weeding	fringe middle	08-May 13-May	61 60	23-Apr 31-May	61 61	01-May 03-May	61 61	manual weeding by hand-hoe
Data collection (30 DAT)	fringe middle	07-Apr 13-Apr	30 30	23-Mar 30-Apr	30 30	31-Mar 02-Apr	30 30	biomass accumulation and partitioning (12 hills), plant height (cm), number of tillers (nominal), chlorophyll content (SPAD), LAI, plant N
Data collection (50 DAT)	fringe middle	27-Apr 02-May	50 50	12-Apr 20-May	50 50	20-Apr 22-Apr	50 50	biomass accumulation and partitioning (12 hills), plant height (cm), number of tillers (nominal), chlorophyll content (SPAD), LAI, plant N
Data collection (50% flowering)	fringe middle	11-May - 21-May 18-May - 28-May	64- 74 65- 75	11-May - 22-May 08-Jun - 27-Jun	79- 90 69- 88	05-May - 10-May 05-May - 22-May	65- 70 63- 80	biomass accumulation and partitioning (12 hills), plant height (cm), number of tillers and panicles (nominal), chlorophyll content (SPAD), LAI, plant N
Data collection (physiological maturity)	fringe middle	20-Jun - 24-Jun 22-Jun - 27-Jun	104-108 100-105	14-Jun - 20-Jun 17-Jul - 26-Jul	113-119 107- 116	07-Jun - 18-Jun 11-Jun - 21-Jun	98-109 100- 110	biomass accumulation and partitioning (12 hills), plant height (cm), number of panicles (nominal), LAI, plant N, grain yield from 6 m^2, grain quality (tkw, % filled spickelets, filled grains per panicle)

4.1.2 Experiments in an inland valley in Uganda

Study site

Experiments were conducted in an inland valley swamp at the *National Crops Resources Research Institute* (NaCRRI) near Namulonge town in central Uganda during the years 2014 and 2017 (**Figure 4.5**). The regional topography is undulating and characterized with flat-topped hills that are dissected by broad valleys occupied with swamps (Nsubuga *et al.*, 2011). The study site lies within the Lake Victoria Crescent (LVC) agro-ecological zone and is commonly known for its banana-coffee system. Due to the proximity to Kampala markets, many farmers also engage in vegetable farming and animal husbandry (Mugisa *et al.*, 2017). However, recent market developments and extension efforts have led to a progressive utilisation of valley bottomlands for rice production (Miyamoto *et al.*, 2012).
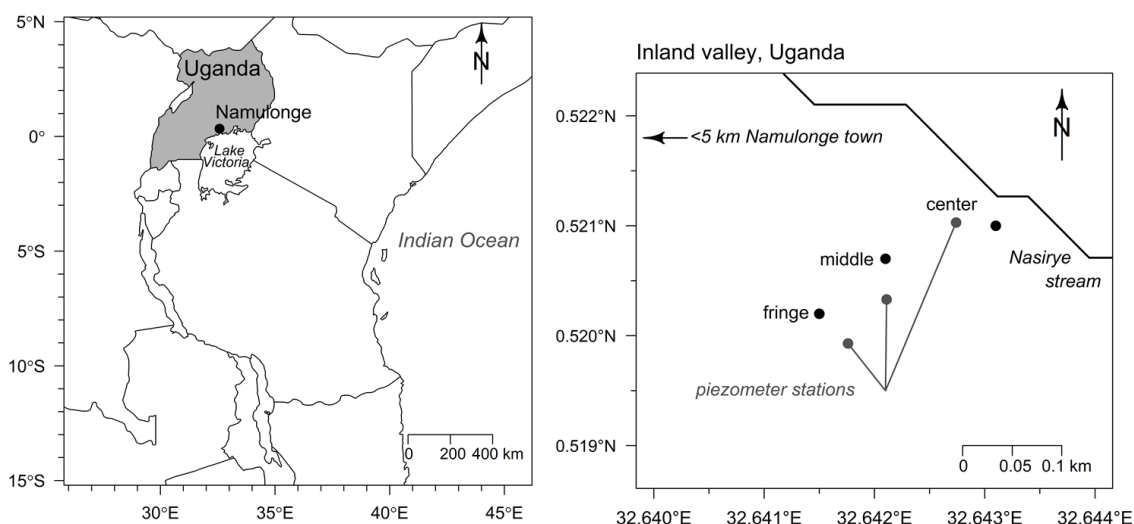
Figure 4.5 Geographic location of the study site (left) and field positions (right) in the inland valley swamp, Uganda.

Weather conditions

During the study period from 2014 to 2017, weather data was obtained from an automatic weather station installed at the NaCRRI station in Namulonge (0.520°N, 32.641°E), and additionally from a tipping bucket installed within the study inland valley. From 2014 to 2017, annual rainfall ranged between 775 and 1,300 mm, while the annual average air temperature showed low variability and averaged at 22.2C° (**Figure 4.6**). During rice-growth, seasonal rainfall varied between 480, 660, and 205 mm in 2014, 2015, and 2016, respectively. Average monthly maximum temperatures during rice-growth were 28.6°C while average monthly minimum temperatures were 17.7°C (**Figure 4.6**).
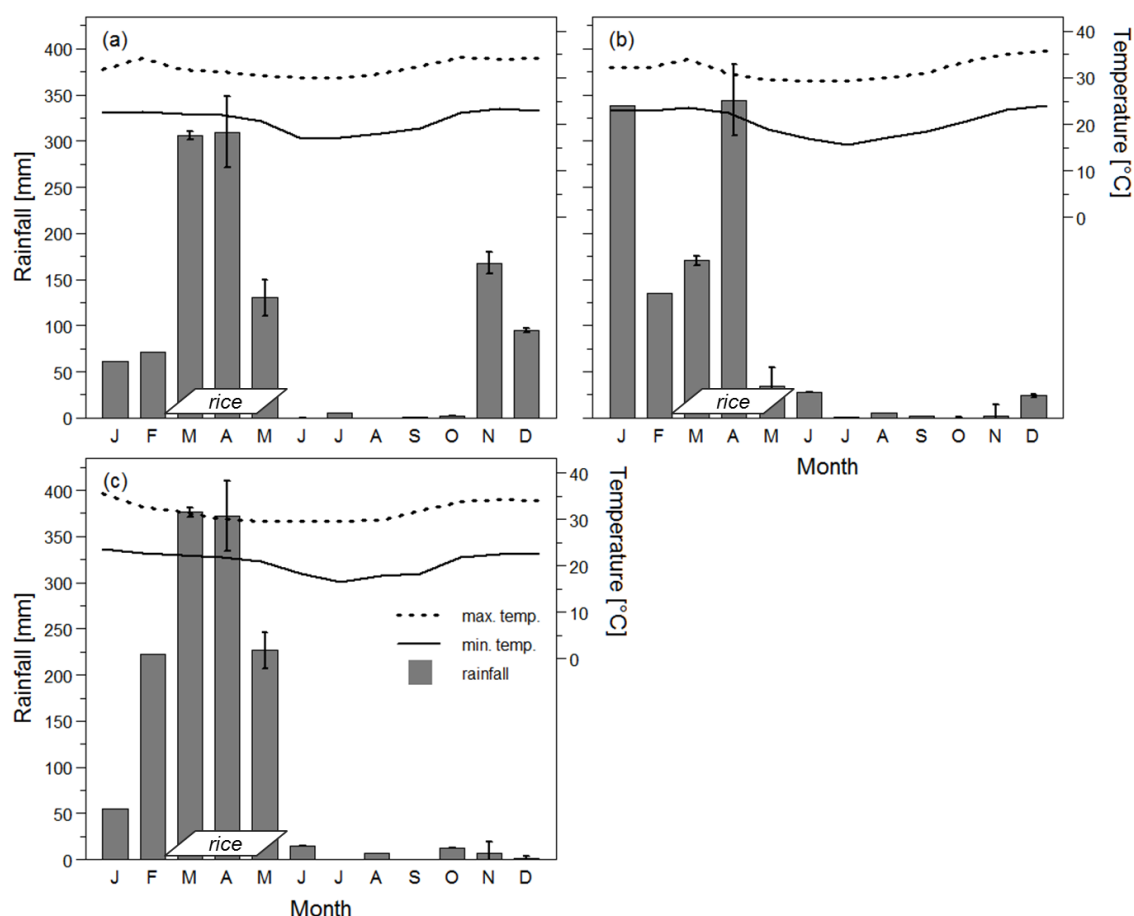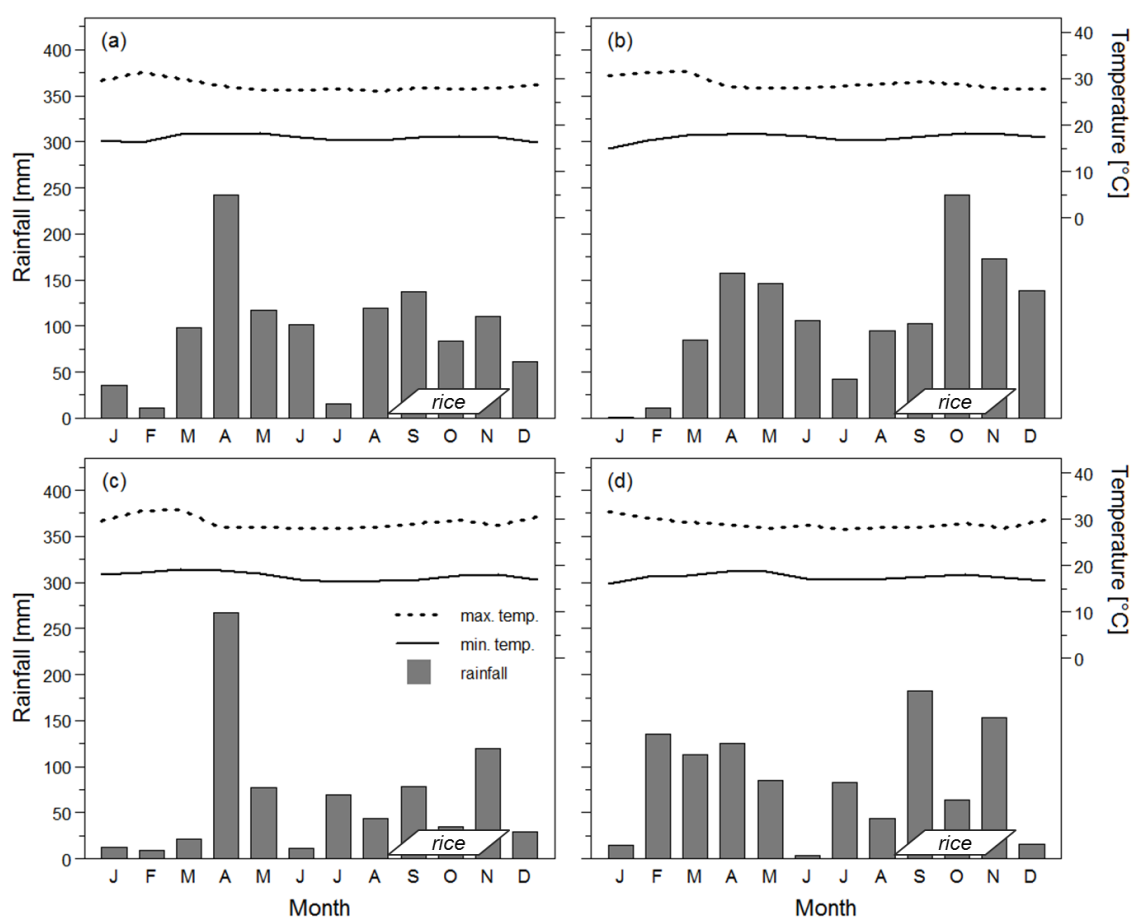
Figure 4.6 Average monthly rainfall, and minimum and maximum temperatures for the years (a) 2014, (b) 2015, (c) 2016 and (d) 2017 at the study site in the inland valley swamp in Namulonge, Uganda. Boxes indicate the main rice-growing period (September to November).

Hydro-edaphic characteristics

Experimental sites were established as a toposequence cross-section of the inland valley, i.e., at the valley-fringe, mid-valley and valley-bottom positions (Gabiri *et al.*, 2017) (**Figure 4.5**). Due to high spatio-temporal variability in soil moisture regimes, no clear hydrological delineation between field positions was possible. Variability was caused by a microscale topography, heterogenous soil properties and human activities such as water channeling and drainage (Gabiri *et al.*, 2017). The water table is replenished directly from the upper catchment, a deep groundwater table as well as subsurface and overland flows from adjacent valley slopes. The amplitude of the water table dynamics ranged between 0.6 m above and 0.9 m below surface level across all field positions, and saturated conditions occurred annually from October to January and from April to June (**Figure 4.7**).

Dominant soils in the inland valley are characterized as eutric Gleysols. The Gleysols were formed under the influence of a fluctuating shallow water table and showed

an umbric horizon (Gabiri *et al.*, 2017). In the valley-fringe and mid-valley positions, the Gleysols were overlaid by colluvial deposits from the Nitisols of adjacent valley slopes. Soil texture was generally loamy (**Table 4.4**), however, a study done by Gabiri *et al.* (2017) has shown that soil properties were highly heterogeneous among and within field positions. Since 1995, the inland valley was largely a long-term fallow and only used sporadically for crop production. Hence, initial topsoil C and N values were high. The topsoil's soil organic C content varied between 45.7, 28.9 and 57.0 g kg^{-1}, the soil N content varied between 3.5, 2.3 and 5.3 g kg^{-1} in the valley-fringe, mid-valley and valley-bottom position, respectively (**Table 4.4**). Soil pH was slightly acidic and varied between 4.3 and 5.2. In accordance with critical macro-nutrient levels for rice growth, soil N, P and K levels were found to be largely sufficient (data not shown). Layer-wise soil properties were determined from a soil profiling campaign prior to the experimental trial in September 2014. Soil organic matter (SOM) contents were determined from the weight loss after dry combustion at 550°C for 2 hours. Soil N and C contents were determined by dry combustion method at 950°C using an Elemental Analyzer (vario-Elcube Elementar Analysesysteme GmbH, Langenselbold, Germany). Plant-available soil P and K contents were extracted using the Mehlich-3-extraction method and analysed colourimetrically using molybdenum-blue complex for P (Specord 50Plus, Analytik Jena AG, Jena) and ICP-OES for K (Spectro Arcos, Spectro Analytical Instruments GmbH, Kleve).

Data collection

Data collection included key phenological stages, i.e., panicle initiation (PI), 50% flowering and physiological maturity, and sequential biomass measurements at the early (28 DAT) and late vegetative stages (56 DAT), 50% flowering and physiological maturity. Sequential biomass samples from 2x6 hill clusters were used to determine biomass accumulation and partitioning, i.e., into green and dead leaf, stem and panicle parts and were oven-dried at 90°C until constant weight. Biomass sub-samples of about 1 g were fine-ground and analysed for their C and N contents using an elemental analyser (EURO EA Elemental Analyser series 3000, EURO-EA Vector Pavia, Italy). Grain yields were determined from a 5 m^2 central harvest area as rough rice at 0% moisture content. Grain quality parameter further included the thousand kernel weight (tkw) and the percentage of filled spikelets per panicle, i.e., grains with a specific gravity ≥1.06 g cm^{-3} (Zakaria *et al.*, 2002). **Table 4.5** provides a detailed overview of all field activities during the study period.
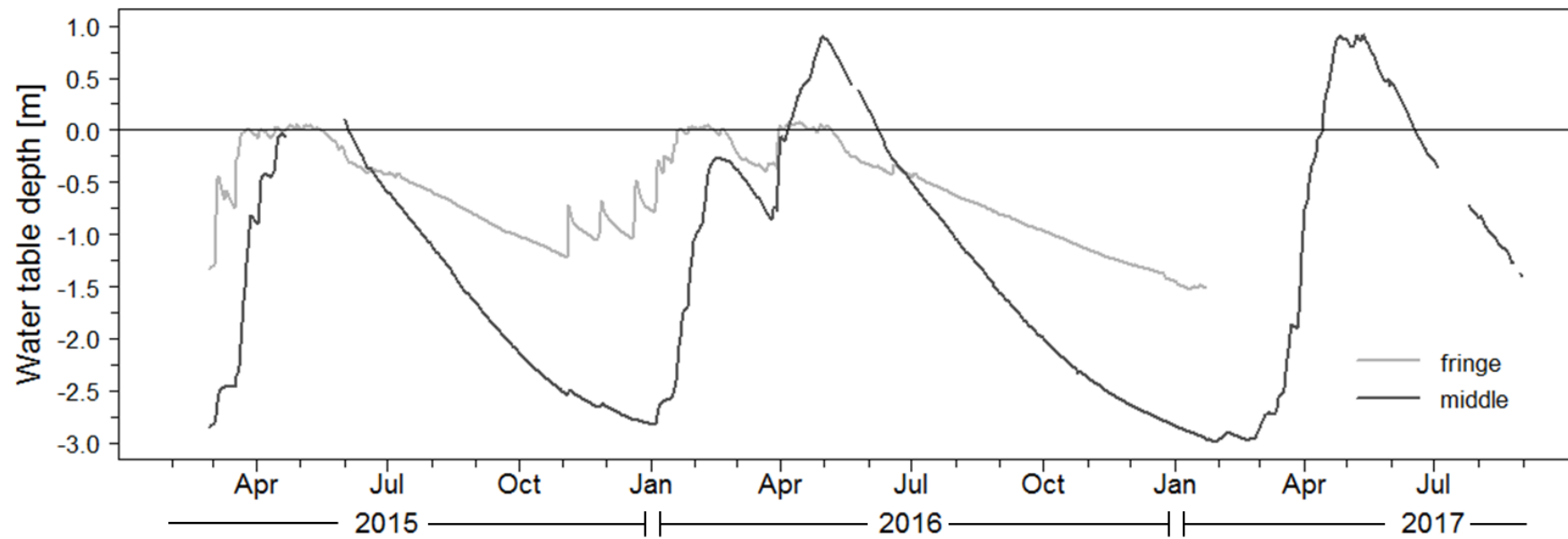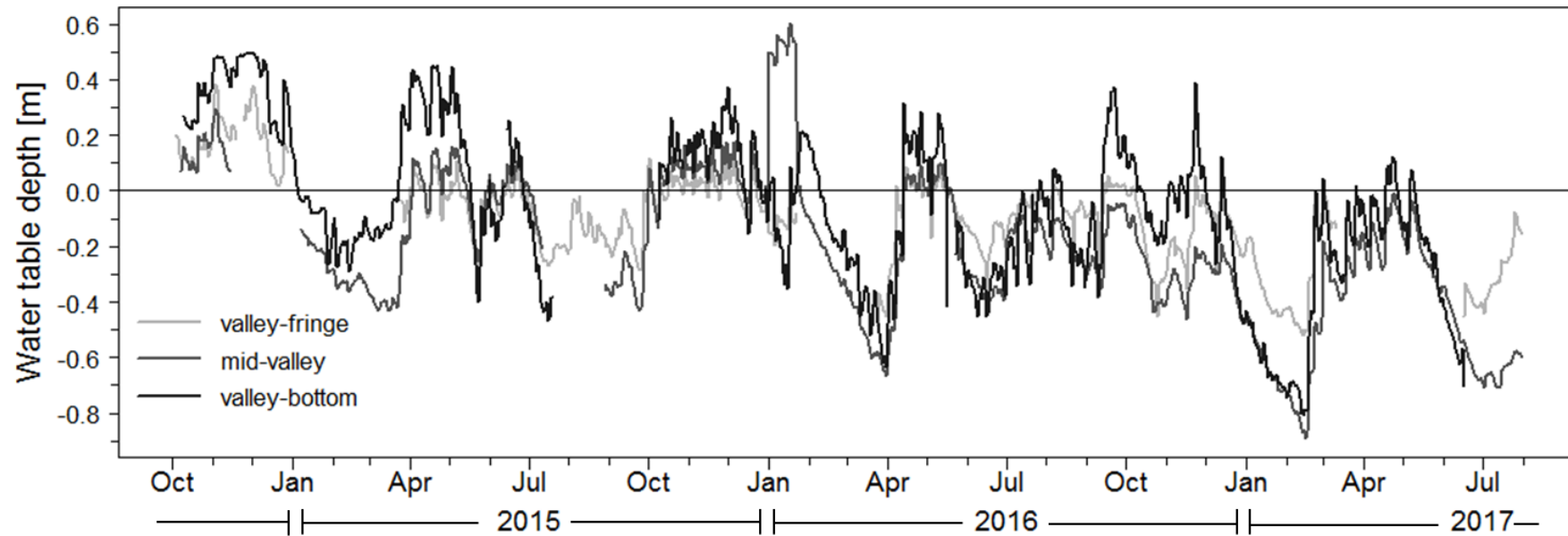
Figure 4.7 Measured depth to water table in the field positions at the study site in the inland valley swamp in Namulonge, Uganda (2014-2017); solid horizontal line represents the surface level; positive values are not implicitly related to water levels above the surface (floods). Modified from Gabiri *et al.* 2017.

Table 4.4 Soil chemical and physical properties at the study site and field positions in the inland valley swamp in Namulonge, Uganda. Soil profiling was done in September 2014 prior to the onset of the experiments, data provided by Björn Glasner (unpublished).

		Soil physical properties					Soil chemical properties			
Field position	Depth	BD	Sand	Silt	Clay	Soil texture	pH	SOM	C_{org}	N_{tot}
	[cm]	[g cm^{-3}]	[%]	[%]	[%]	[WRB]	[H$_2$O]	[g kg^{-1}]	[g kg^{-1}]	[g kg^{-1}]
valley-fringe	0-23	0.87	28.3	43.2	28.4	clay-loam	4.88	111.63	45.71	3.51
	23-30	1.13	29.1	43.7	27.3	clay-loam	4.84	85.23	33.13	2.17
	30-35	1.33	38.2	41.6	20.1	loam	5.09	48.26	13.86	0.62
	35-45	1.68	61.2	25.8	12.9	sandy-loam	4.78	19.32	3.15	0.31
	45-65	1.68	49.9	31.2	18.8	loam	4.58	23.85	2.36	0.31
	65-80	1.68	34.4	27.0	38.6	clay-loam	4.54	46.25	3.05	0.31
	80-100	n/a	25.7	21.9	52.4	clay	4.40	60.12	3.74	0.41
mid-valley	0-20	1.00	36.9	34.2	28.8	clay-loam	5.02	76.80	28.90	2.27
	20-30	1.44	49.0	25.0	26.1	loam	5.09	42.63	9.14	0.72
	30-45	1.51	48.5	18.7	32.8	clay-loam	5.18	38.38	3.34	0.41
	45-60	1.52	42.6	18.8	38.6	clay-loam	5.14	41.85	2.46	0.31
	60-85	1.52	41.1	17.8	41.1	clay	5.00	43.31	2.46	0.31
	85-100	1.50	39.9	15.8	44.3	clay	4.78	45.08	2.56	0.21
valley-bottom	0-22	0.72	16.0	31.9	52.1	clay	4.91	149.08	57.02	5.26
	22-34	0.89	31.3	30.1	38.6	clay-loam	5.02	83.12	27.62	2.06
	34-48	1.57	52.3	27.7	20.0	sandy-clay-loam	4.84	28.00	3.74	0.31
	48-60	1.53	50.1	18.0	31.9	sandy-clay-loam	4.99	38.24	2.95	0.31
	60-80	1.54	38.3	26.3	35.4	clay-loam	4.10	38.67	2.46	0.31
	80-100	1.53	39.8	22.3	37.9	clay-loam	4.26	39.60	2.06	0.21

BD, bulk density; soil texture definition according to the World Reference Base for Soil Resources (WRB): sand (63 to 2,000 µm), silt (2 to 63 µm), clay (<2 µm); pH, 1:2.5 (soil:water) suspension; SOM, soil organic matter; C_{org}, soil organic carbon content; N_{tot}, total soil N content.

Table 4.5 Field activities and data collection protocol at the study site in the inland valley swamp in Namulonge, Uganda, and during the study period from 2014 to 2017.

Management	Field position	Rice growing seasons						Management details
		Year 2014/15	DAT	Year 2015/16	DAT	Year 2016/17	DAT	
Nursery sowing	valley-fringe		-26		-25		-27	nursery set-up using pre-germinated seeds (soaked in water for 24 hour and incubated for 48 hours until shoot measured about 5 mm)
	mid-valley	22-Aug	-25	18-Aug	-23	30-Aug	-25	
	valley-bottom		-23		-21		-23	
Transplanting	valley-fringe	17-Sep	0	12-Sep	0	26-Sep	0	rice transplanting using about 25-day-old seedlings at an row and inter-row spacing of 15 by 30 cm (22 hills/m^2); three seedlings per hill
	mid-valley	16-Sep	0	10-Sep	0	24-Sep	0	
	valley-bottom	14-Sep	0	08-Sep	0	22-Sep	0	
Basal fertiliser application (NPK)	valley-fringe	17-Sep	0	12-Sep	0	26-Sep	0	50% of urea-N fertiliser application rate (46% N); 60 kg triple super phosphate/ha (TSP, 19.7% P) and 60 kg muriate of potash/ha (KCl, 49.6% K)
	mid-valley	16-Sep	0	10-Sep	0	24-Sep	0	
	valley-bottom	14-Sep	0	08-Sep	0	22-Sep	0	
Top dressing (N)	valley-fringe	23-Oct	36	30-Oct	48	05-Nov	40	50% of urea-N fertiliser application rate (46% N); attempted at panicle initiation (PI)
	mid-valley	22-Oct	36	30-Oct	50	03-Nov	40	
	valley-bottom	20-Oct	36	31-Oct	53	01-Nov	40	
First Weeding	valley-fringe	18-Oct	31	07-Oct	25	19-Oct	23	manual weeding by hand-hoe
	mid-valley	08-Oct	22	06-Oct	26	17-Oct	23	
	valley-bottom	07-Oct	23	05-Oct	27	15-Oct	23	
Second Weeding	valley-fringe	25-Oct	38	30-Oct	48	04-Nov	39	manual weeding by hand-hoe
	mid-valley	24-Oct	38	29-Oct	49	02-Nov	39	
	valley-bottom	23-Oct	39	28-Oct	50	31-Oct	39	
Third Weeding	valley-fringe	20-Nov	64	21-Nov	70	28-Nov	63	manual weeding by hand-hoe
	mid-valley	19-Nov	63	20-Nov	71	26-Nov	61	
	valley-bottom	18-Nov	64	19-Nov	72	26-Nov	65	
Data collection (28 DAT)	valley-fringe	15-Oct	28	10-Oct	28	24-Oct	28	biomass accumulation and partitioning (12 hills), plant height (cm), number of tillers (nominal), chlorophyll content (SPAD), LAI, plant N
	mid-valley	14-Oct	28	08-Oct	28	22-Oct	28	
	valley-bottom	12-Oct	28	06-Oct	28	20-Oct	28	
Data collection (56 DAT)	valley-fringe	13-Nov	57	07-Nov	56	21-Nov	56	biomass accumulation and partitioning (12 hills), plant height (cm), number of tillers (nominal), chlorophyll content (SPAD), LAI, plant N
	mid-valley	12-Nov	56	05-Nov	56	19-Nov	56	
	valley-bottom	09-Nov	55	03-Nov	56	17-Nov	56	
Data collection (50% flowering)	valley-fringe	26-Nov - 30-Nov	69-73	18-Nov - 01-Dec	67-80	01-Dec - 09-Dec	66-74	biomass accumulation and partitioning (12 hills), plant height (cm), number of tillers (nominal), number of panicles (nominal), chlorophyll content (SPAD), LAI, plant N
	mid-valley	28-Nov - 30-Nov	72-74	18-Nov - 03-Dec	69-85	01-Dec - 14-Dec	68-81	
	valley-bottom	27-Nov - 28-Nov	74-75	18-Nov - 03-Dec	71-86	28-Nov - 12-Dec	67-81	
Data collection (physiological maturity)	valley-fringe	01-Jan	105	01-Jan	111	29-Dec - 09-Jan	94-105	biomass accumulation and partitioning (12 hills), plant height (cm), number of panicles (nominal), LAI, plant N, grain yield from 5 m^2, grain quality (tkw, % filled spikelets, filled grains per panicle)
	mid-valley	01-Jan	106	30-Dec - 31-Dec	112-113	28-Dec - 11-Jan	95-109	
	valley-bottom	02-Jan	110	31-Dec	113	27-Dec - 06-Jan	96-106	

4.2   Cropping system modelling

This study applied a cropping system modelling approach to complement experimental field data and analyse complex interactions between management, genotype and environment. From a wide range of available crop models with application in rice-based systems, the Agricultural Production Systems Simulator (APSIM) modelling framework was selected. As distinct from other system models, soil processes rather than crops and the effects of management on soil resources become central in APSIM (Probert *et al.*, 1998), making APSIM particularly suited to evaluate long-term effects of cropping systems on soil resources and yield performances. Therefore, APSIM has a proven track record in simulating diverse cropping systems worldwide (e.g., Hoffmann *et al.*, 2015 and Mohanty *et al.*, 2020), including rice (e.g., Amarasingha *et al.*, 2017 and Dutta *et al.*, 2020). Additionally, APSIM was selected as the generic manager module provides the flexible simulation environment needed to freely code and combine system particulars and describe management practices (Holzworth *et al.*, 2014).

4.2.1 The origin of rice in APSIM: ORYZA2000

ORYZA2000 is a daily time-step, dynamic eco-physiological rice model with application under potential, water-limited and nitrogen-limited production conditions (Bouman *et al.*, 2001). Detailed explanations and program codes are documented and explained by Bouman *et al.* (2001). Additionally, a detailed description for potential and nitrogen-limited production is provided by Bouman & Van Laar (2006). ORYZA2000 is a product of the 'School of de Wit' research group based at Wageningen University that, starting in the 1980s, developed an array of crop growth models (Bouman *et al.*, 1996; Van Ittersum *et al.*, 2003) (**Figure 4.8**). The ORYZA2000 model is the latest of the ORYZA model series and integrates previous ORYZA models while incorporating recent technical and scientific improvements (Bouman *et al.*, 2001). The ORYZA model series includes the ORYZA1 model for potential production (Kropff *et al.*, 1994), the ORYZA-N model for nitrogen-limited production (Drenth *et al.*, 1994), and the ORYZA_W model for water-limited production (Wopereis *et al.*, 1996) (**Figure 4.8**). The ORYZA model series was initially founded on the SUCROS (Simple and Universal Crop Growth Simulator) (Van Keulen *et al.*, 1982), the WOFOST (World Food Studies) (Van Keulen & Wolf, 1987) and the MACROS (Modules of an Annual Crop Simulator) models (Penning de Vries *et al.*, 1989). While SUCROS and WOFOST are products of the 'School of de Wit', MACROS is a product of the SARP (Simulation and Systems Analysis for Rice Production) project. The SARP project started in 1984 as a collaboration of 15 national agricultural research

centres (NARC's) from eight Asian countries, the IRRI and the Wageningen research group, aiming to develop crop models to sustainably increase the productivity of rice-based systems in the developing world (Ten Berge & Kropff, 1995). MACROS is a generic rice model that uses a modular framework and includes modules for potential, water-limited and puddled as well as non-puddled production conditions (Bouman *et al.*, 1996). The MACROS model can be traced back to the WOFOST and the SUCROS model, which were the first summary models for potential and water-limited production conditions. In SUCROS, crop production is simulated daily based on incoming radiation and temperature, while it is using a generic crop template, i.e., phenological development stage parameters and biomass partitioning coefficients (Van Keulen *et al.*, 1982). Biomass is partitioned among roots, leaves, stems and storage organs as a function of phenological development stage (Van Keulen *et al.*, 1982). WOFOST followed SUCROS in 1986, having inherited the generic crop descriptions, but using a more application-oriented approach, i.e., a user-friendly interface to select soil, crop, management and weather particulars easily (Van Ittersum *et al.*, 2003) (**Figure 4.8**).
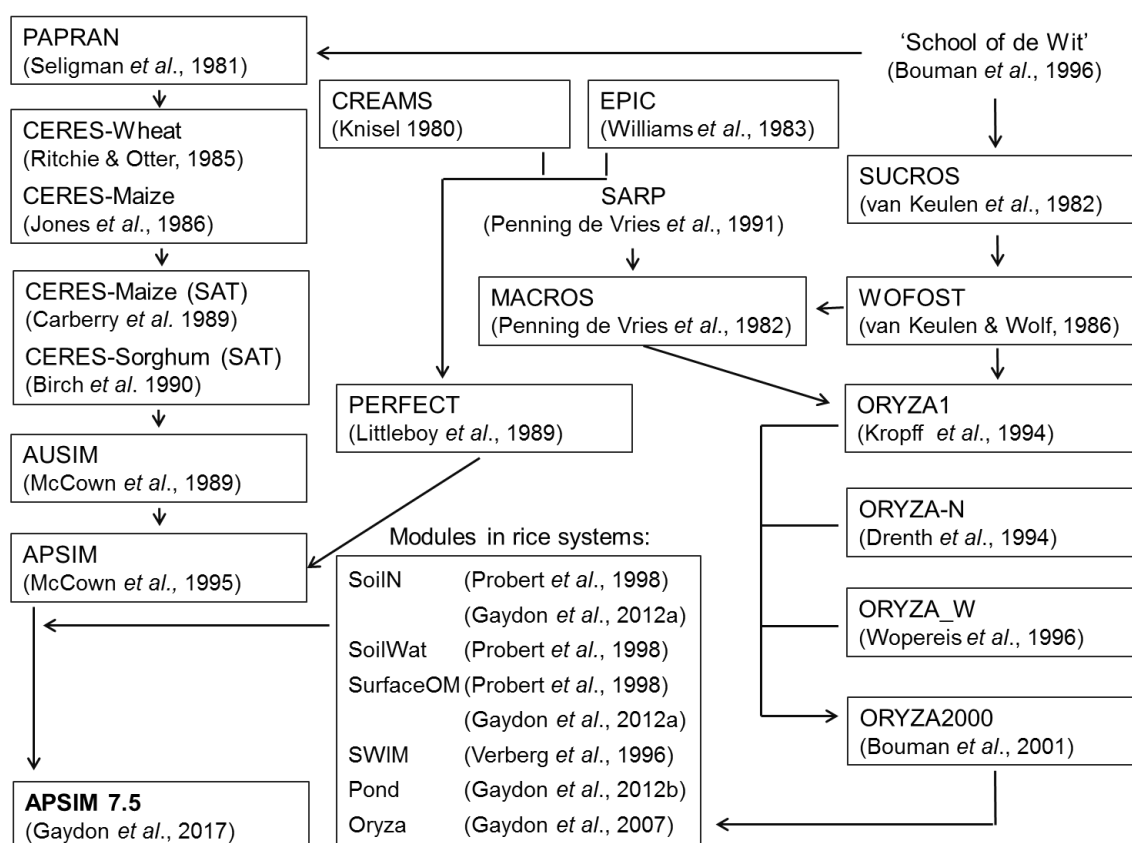
Figure 4.8 Schematic and chronological overview of the APSIM and ORYZA200 model development for application in rice-based cropping system; according to Bouman *et al.* 1996, Holzworth *et al.* 2014, Keating *et al.* 2003 and McCown *et al.* 1995.

ORYZA1

The physiological development of rice in ORYZA2000 is simulated in the ORYZA1 module that further contains a number of subroutines and sub-subroutines to manage different processes. Subroutines include for example PHENOL for the calculation of phenological development rates, WSTRESS for the effect of water stress on development, SGPCDT for the calculation of daily total gross assimilation, and NCROP for the effect of N stress on development (Bouman *et al.*, 2001). Daily phenological development rates are a function of daily average temperature and photoperiod, while daily assimilation rates are dependent on incoming radiation, temperature and leaf area index (Bouman *et al.*, 2001). Under N- or water-limited production conditions, both daily assimilation and phenological development rates are additionally affected by water and N limitations. With temperature being the main driver for phenological development (Van Keulen *et al.*, 1982), the daily development rate (DVR, °C day^{-1}) is a function of development stage (DVS, -), daily effective heat units (HU, °C day^{-1}) and photoperiod (Jones & Kiniry, 1986). The concept of effective heat units is based on a linear relationship between phenological development rate and daily mean temperature, and assumes phenological development increases linearly from a base to an optimum temperature beyond which it decreases to a maximum temperature (Kiniry *et al.*, 1990). The 'cardinal' temperatures for rice are reported as 8, 30 and 42°C for the base, optimum and maximum temperature, respectively. No phenological development is assumed below the base and above the maximum temperature. The phenological development of rice is described in four distinct development stages (DVS) those rate constants (DVR) are variety-specific:

 i. Vegetative stage (BVP); from emergence to start of photoperiod-sensitive stage (DVS 0.0-0.4), DVR constant is DVRJ;
 ii. Photoperiod-sensitive stage (PSP); from the end of vegetative stage to panicle initiation (DVS 0.4-0.65), DVR constant is DVRI;
 iii. Panicle development stage (PEP); from panicle initiation to 50% flowering (DVS 0.65-1.0), DVR constant is DVRP;
 iv. Grain-fill stage (GFP); from 50% flowering to physiological maturity (DVS 1.0-2.0), DVR constant is DVRR.

Daily canopy CO_2 assimilation rates are calculated from daily radiation, leaf area index and temperature, and obtained by integrating instantaneous rates of leaf CO_2 assimilation over the day and canopy layers using the Gaussian integral function (Bouman & Van Laar, 2006). Leaf area growth includes both a source- and sink-limited phase.

While the leaf area is not limited during the vegetative growth phase and grows exponentially as a function of temperature sum times a relative leaf growth rate, leaf area growth becomes limited when DVS >1 due to limited carbohydrate availability. Leaf photosynthesis is dependent on leaf N content, radiation intensity, stomatal CO_2 concentration and temperature. The net daily growth rate (kg carbohydrate ha^{-1} day^{-1}) is, hence, the result of the gross assimilation rates minus maintenance respiration requirements. Carbohydrates are converted to and partitioned among roots, leaves, stems, and storage organs according to variety-specific partitioning coefficients as a function of DVS and follow equations by Penning de Vries, F. W. & Van Laar (1982).

4.2.2 The APSIM framework

APSIM is a modelling framework aimed at simulating copping systems in response to the biophysical environment and management practices (Keating *et al.*, 2003). Operating on a daily time-step, APSIM is characterized by its modular design around a central engine that drives the simulation process and ensures the communication between all modules. The modular design uses a '*plug in–pull out*' approach (McCown *et al.*, 1995), ensuring the systems flexibility and ability to accommodate ongoing software and science improvements (Holzworth *et al.*, 2014). Additional flexibility is provided by the Manager module, which uses a simple '*if-then-else*' logic, and, hence, allows the user to freely code and combine systems particulars and practices (McCown *et al.*, 1996). Focusing on Australian cropping systems at first, APSIM has since evolved into an agricultural systems model that is being used worldwide for a range of cropping and management systems and in numerous biophysical environments (Holzworth *et al.*, 2014). The most recent, comprehensive APSIM evaluation for Asian rice-based systems was done by Gaydon *et al.* (2017).

A brief history

The development of APSIM started in the early 1990s by the APSRU (Agricultural Production System Research Unit) research group, a collaboration between the CSIRO (Commonwealth Scientific and Industrial Research Organisation) and Queensland State Government agencies (Keating *et al.*, 2003). APSIM owes much of its functionality and simulation routines to the PERFECT (Productivity, Erosion and Runoff Functions to Evaluate Conservation Techniques) (Littleboy *et al.*, 1989) and the AUSIM (McCown & Williams, 1989) model (**Figure 4.8**). PERFECT is a cropping system model that integrates the dynamics of soil and crop processes, and was developed to primarily simulate the effects of erosion on the productivity of Australian Vertisols (McCown *et al.*, 1996). The

model owes much of its routines to the EPIC (Erosion-Productivity Impact Calculator) model for estimating long-term effects of erosion on crop productivity (Williams *et al.*, 1989), and to the CREAMS (Chemicals, Runoff, and Erosion from Agricultural Management Systems) model for prediction of surface hydrology, and sediment, pesticide and nutrient movement from continuous agricultural use (Knisel, 1980) (**Figure 4.8**). Hence, PERFECT adds to the APSIM soil water module through alternative infiltration, runoff and erosion routines (McCown *et al.*, 1995). AUSIM is a cropping system model developed for dryland maize and sorghum cropping systems in the tropics that originates from the CERES-Maize (Crop-Environment Resource Synthesis) model (Jones & Kiniry, 1986), however, with modifications for maize (Carberry *et al.*, 1989) and sorghum (Birch *et al.*, 1990) production systems in the semi-arid tropics. Re-engineered routines from CERES-Maize as well as simplified routines from the sorghum QSORG (Hammer & Muchow, 1991) and the sunflower QSUN (Chapman *et al.*, 1993) models were used in APSIM to develop a generic crop growth template. CERES was additionally used as a template for the soil water and N routines (McCown *et al.*, 1995) that in return originate from the PAPRAN (Production of Arid Pastures limited by RAinfall and Nitrogen) model (Seligman & Van Keulen, 1981). However, the strengths of models like CENTURY (Parton *et al.*, 1987) and NTRM (Nitrogen-Tillage-Residue Management) (Shaffer *et al.*, 1991) from dealing with long-term dynamics of soil resources were further recognised in the development of APSIM (Keating *et al.*, 2003). Such stenghts include estimates for soil fertility and crop performance as affected by tillage, organic matter decomposition and N transformation processes. Due to the focus on dryland farming systems, APSIM lacked the capability to simulate rice-based cropping systems at first (Keating *et al.*, 2003). However, with APSIM evolving over the past decades, rice-based cropping as well as agroforestry systems and crop-livestock interactions are now part of the APSIM suite of modules (Holzworth *et al.*, 2014).

Oryza module

The rice physiological routines and parameters of the ORYZA1 module from the ORYZA2000 module were fully integrated into the APSIM framework by Gaydon *et al.* (2006), and validated in several studies (Zhang *et al.*, 2007). A brief overview is provided on **page 44**, while detailed descriptions and program codes are provided by Bouman *et al.* (2001), and additionally by Bouman & Van Laar (2006) for potential and N-limited production conditions.

SoilWat module

The SoilWat module simulates daily water dynamics and solute movements in the soil, i.e., runoff, evaporation, transpiration and drainage, and the saturated, un-saturated and over-saturated water flows. The soil water balancing uses a multi-layer cascading approach following its precursor CERES (Jones & Kiniry, 1986), and including routines to simulate the effects of residues on runoff and evaporation established in PERFECT (Littleboy *et al.*, 1989). Layer-wise water retention characteristics are defined as lower limit (LL15, permanent wilting point), drained upper limit (DUL, field capacity) and saturation (SAT) in cm^3 cm^{-3}. Any soil water exceeding the layers saturation capacity automatically cascades down into the next soil layer et cetera (Probert *et al.*, 1998). The soil's water retention characteristics are dependent on bulk density, soil texture and organic matter content. Water runoff is calculated using a modified USDA curve number (CN2) approach, and takes into account the effects of soil moisture status, residue and plant cover, and the roughness of the soil due to tillage (Mokus, 1972). Soil evaporation is described as a two-stage process, i.e., energy-limited and water-limited, based on potential evapotranspiration and quantified as the constant (U, cumulative evaporation) and the falling rate stage (CONA, ΔU) (Ritchie, 1972). Enhancements beyond CERES and PERFECT include the differentiation of saturated and unsaturated vertical water flows. In APSIM, saturated water flows occur when a layers' soil water exceeds field capacity and is specified via the *swcon* coefficient, quantifying the amount of water allowed to drain into the next layer per day. *Swcon* is dependent on soil texture; heavy clay soils with poor water conductivity typically have values <0.5, while sandy soils with higher water conductivity have values >0.8. Unsaturated water flows occur when soil water drops below field capacity and is specified via the diffusivity constant and the slope parameter, typically set to 40 and 16 for cracking clay soils, respectively (Dalgliesh *et al.*, 2016). Oversaturated water flow occurs when soil water exceeds saturation and is specified either via the *mwcon* coefficient or empirical saturated percolation rates K_S (mm day^{-1}), and describe the macro-flow conductivity, i.e., the water flow rate through the macro-pores (Asseng *et al.*, 1997). Restricted vertical water flow from low *mwcon* or K_S values are essential to simulate perched water tables and ponded conditions. A perched water table is determined as the proportion of soil water between DUL and SAT directly adjoining a saturated soil layer, and are the result of point-scale rainfall and/or irrigation events. Ponded conditions develop by water accumulation towards the surface and beyond from restricted vertical water flow and a user-defined pond depth (*max_pond*) that defines the maximum height of standing surface water before excess water is subjected to runoff. The

redistribution of solutes, i.e., nitrate-N and urea-N, is simulated simultaneously with the saturated and unsaturated water flows. An alternative module for the simulation of water dynamics and solute movement in APSIM is the SWIM module. The SWIM module is based on the Richard's equation in which water potential gradients are driving water transport. The module is documented in detail in Ross (1990), while a comprehensive evaluation of both SoilWat and SWIM was done by Verburg (1996).

SoilN module

The SoilN module simulates the dynamics and transformations of C and N in the soil and, thus, the available N to a crop from the soil and from residues/roots of previous crops. These transformation processes include soil organic matter (SOM) decomposition, N immobilization and mineralization, nitrification, denitrification and urea-N hydrolysis (**Figure 4.9**). The SoilN module has evolved from the CERES family, notably CERES-Maize (Jones & Kiniry, 1986), however, featuring distinct modifications. In non-flooded cropping systems, layer-wise parameter values for *fBiom* and *Finert* initiate the proportions of the three SOM pools and their mineralisation capacities, i.e., the fresh organic matter (*fom*), the *biom* and the *hum* pools. The *biom* pool is the more labile pool, representing the soil
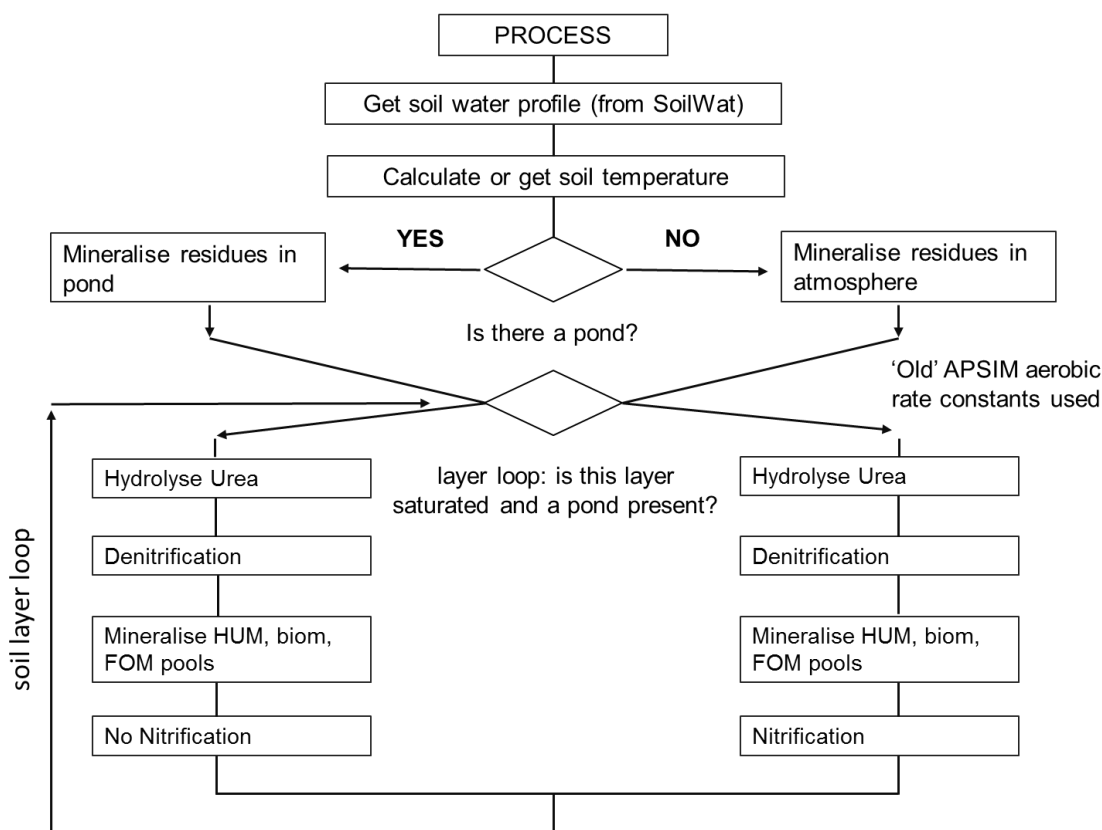
Figure 4.9 Logic daily process simulation within the APSIM SoilN module. If there is no 'pond', the process path corresponds to aerobic conditions; according to Gaydon *et al.* 2012a.

microbial biomass and products, while the *hum* pool is the more inert pool, representing the more stable pool of the remaining organic matter. Flows between the SOM pools are calculated in terms of carbon, while the corresponding N flows are calculated based on the C/N ratio of the receiving pool. The C/N ratio of the *biom* is constant, while the C/N ratio of the *hum* is derived from the soil based on input data. The efficiency coefficients *fInert* and *fBiom*, soil temperature and soil water content govern the decomposition rates of the *hum* and *biom* pool. Mineral-N mineralisation and immobilisation is determined as a balance between supply through decomposition and immobilisation through microbial synthesis and humification. Once the mineral-N supply is found inadequate to meet immobilization demand, the decomposition process is halted. A detailed description of all transformation processes in the soil is provided by Probert *et al.* (1998). The differentiation into three organic matter pools presents a major difference to the CERES-Maize model, where SOM is treated equally susceptible to decomposition (Probert *et al.*, 1998).

For rice-based systems, the SoilN module was recently updated to account for changes in N transformation processes and decomposition rates from temporarily or permanently submerged soil conditions (**Figure 4.9**). Gaydon *et al.* (2012a) introduced the anaerobic decomposition rate constants *rd_biom*, *rd_hum*, *rd_carb*, *rd_cell* and *rd_lign* on the basis of Jing *et al.* (2010) to account for decreased decomposition rates of soil biomass and humus mineralisation under anaerobic conditions (2-3 times slower than aerobic decomposition). Anaerobic conditions are assumed to develop rapidly after flooding with the microorganisms adapting without time lag. Anaerobic and aerobic decomposition rates transition seamlessly with the appearance and disappearance of a pond. In flooded conditions, N is assumed only to be available for plant uptake once it has been transported into the soil layers (Gaydon *et al.*, 2012a).

SurfaceOM module

In contrast to CERES, APSIM simulates the faith of aboveground organic matter in an individual module called SurfaceOM to account for their effect on runoff and evaporation (Probert *et al.*, 1998), and following procedures retained from PERFECT. Aboveground organic matter (residues, mulch) can either be burnt, incorporated into the soil, or decompose *in-situ* (Probert *et al.*, 1998). When incorporated, i.e., though tillage, the proportion of residues incorporated (*f_incorp*) and incorporation depth are user-defined and residues turn into *fom* and the transformation processes are handled in SoilN. When residues are left to decompose *in-situ*, the *biom* and *hum* products are transferred into the topsoil layer and transformation processes are consequently handled in SoilN as well. Potential decomposition rates are dependent on mineral N content, C/N ratio, temperature

and moisture availability (Probert *et al.*, 1998). Meanwhile, the effects of aboveground residues on runoff and evaporation processes are handled in the SoilWat module and dependent on soil coverage, e.g., while bare soils have a CN2 of 75, the CN2 reduces to 55 at 80% residue cover, thus inhibiting water transport during runoff events. A detailed description is provided by Probert *et al.* (1998).

Under flooded conditions, a lower potential decomposition rate of residues is considered by a constant moisture factor of 0.5, as compared to the moisture factor of 1 under aerobic conditions (Gaydon *et al.*, 2012a). The mineral-N demand for immobilisation of submerged residues is sought from the Pond module, thus, mineral-N in the floodwater is limiting the decomposition of surface residues (Gaydon *et al.*, 2012a).

Pond module

While the SoilWat module handles water flows in the soil and the pond (floodwater) as a continuum and the chemical processes in the soil, the Pond module simulates key chemical and biological processes in the pond. The Pond module is a transient module, i.e., it only activates once a pond is present. Effectively, the Pond module may be described as a 'filter' of nutrients by not allowing all applied N to reach the crop due to volatilisation losses and algal uptake, while additionally simulating C and N losses and gains through algal activity (Gaydon *et al.*, 2012a). The simulation of algal activity in the pond is using the approach of CERES-Rice (Godwin & Singh, 1991), however, extending its functionality by additionally considering C and N gains to rice systems through algal activity (Gaydon *et al.*, 2012b). Floodwater temperature and pH drives the transformation processes in the pond. The dynamic floodwater temperature and pH balance is calculated daily as an energy balance between atmosphere, floodwater, soil temperature and incoming radiation (Gaydon *et al.*, 2012b), following CERES-Rice and based on the soil temperature routine of the SALUS (System Approach to Land Use Sustainability) model (Schulthess & Ritchie, 1996). Gaydon *et al.* (2012b) explained the functionality in detail; however, a brief explanation is provided here:

Urea-N hydrolysis. The breakdown of applied urea-N fertiliser to NH_4^+ is described as a function of pond temperature and a soil-determined hydrolysis rate, i.e., dependent on either the algal activity rate or the topsoil's organic carbon content, whichever is greater (Godwin & Singh, 1991).

Ammonia volatilization. Pond ammonia (NH_3) exists in equilibrium with pond ammonium (NH_4^+), concentrations of NH_3 and NH_4^+ are calculated using floodwater temperature and pH; the partial pressure of NH_3 is determined from the overalll NH_3

concentration and can cause NH_3 volatilisation and atmospheric N losses as a function of wind and floodwater depth (Godwin & Singh, 1998); however, in absence of wind data, the calibrated surrogate constant *NH_4_loss_fact* is used.

Algae growth and turnover. Godwin & Singh (1991) described an algal activity factor *algact* that is influencing urea-N hydrolysis and floodwater pH. Based on *algact*, the daily algal growth and biomass accumulation (*dlt_pab*) is calculated using the maximum daily growth rate of algae (*maxrate_pab*) of ± 20 kg ha^{-1} day^{-1} (Godwin & Singh, 1991; Roger, 1996). *Algact* is a function of available radiation, floodwater temperature, P, and mineral-N availability. Pond algal biomass (PAB) is assumed to have a C/N ratio of 8 and is allowed to reach a maximum of 500 kg dry matter ha^{-1} after which any subsequent daily growth is matched by algal senescence and added to the SurfaceOM pool (Roger, 1996). PAB growth is sustained from mineral-N uptake from the floodwater and, when found insufficient, met by biologically-fixed N_2 (BNF). PAB is added to the *fom* pool for decomposition or incorporation into the soil after draining the rice paddock. In alternate wetting and drying systems, PAB stays viable for a 5-day period without a present pond after which, however, it is added to the *fom* pool.

Immobilization of pond mineral N. In the presence of a pond, immobilisation demand is sought from the mineral-N pools of the Pond module that are received through decomposition processes; however, under ponded conditions, the moisture factor for decomposition of residues is set to 0.5 to account for the lower potential decomposition rates.

Fluxes of solutes to/from the soil. Urea-N, NH_4^+ and NO_3^- are transferred to the soil daily via mass flow, diffusion, and adsorption. In case of the highly soluble NO_3^- and urea-N, NO_3^- and urea-N pond and soil solution concentrations are compared and concentration gradients invoke a 'diffusion process' to determine the flux. NH_4^+ is transferred via adsorption and the flux is dependent on the soil cation exchange capacity (CEC) (Godwin & Singh, 1998).

Nitrification and denitrification. Following the CERES-Rice approach, nitrification of NH_4^+ to NO_3^- and denitrification processes in the floodwater were neglected due to a more simplified representation of the floodwater environment (Godwin & Singh, 1991).However, both processes are simulated in APSIM once the solutes enter the soil profile and governed by soil water content, temperature and pH, following Michaelis-Menton kinetics as described by Probert *et al.* (1998).

5.   Peer-reviewed journal publications

This chapter consists out of two sub-chapters, which have been published, accepted or submitted to peer-reviewed and international high standard referenced journals. For citation of the sub-chapter's **5.1** to **5.2**, please use the references provided below:

Grotelüschen, K., Gaydon, D.S., Ziegler, S., Kwesiga, J., Langensiepen, M., Senthilkumar, S., Whitbread, A.M. and Becker, M. (2021). Assessing the effects of management and hydro-edaphic conditions on rice in contrasting East African wetlands using experimental and modelling approaches. *Agric. Water Manag.* 258, 107146. 10.1016/j.agwat.2021.107146.

Grotelüschen, K., Gaydon, D.S., Senthilkumar, K., Langensiepen, M. and Becker, M. (2021). Model-based evaluation of rainfed lowland rice responses to N fertiliser in variable hydro-edaphic wetlands of East Africa. *Field Crops Res.* (in revision).

5.1   Assessing effects of management & hydro-edaphic conditions on rice in contrasting East African wetlands using experimental & modelling approaches

Abstract

Lowland rice yields in East Africa remain low despite favourable hydro-edaphic conditions as benefits from improved cultural management vary between and within wetland types and interactions are poorly understood. Hence, multi-year agronomic field experiments were established to assess the differential responses of lowland rice to management (rainfed 0 and 60 kg N ha^{-1}, and irrigated 120 kg N ha^{-1} + 60 kg PK ha^{-1}) and field position within a floodplain in Tanzania (fringe and middle positions) and an inland valley in Uganda (valley-fringe, mid-valley and valley-bottom positions). We then calibrated and validated the Agricultural Production System Simulator (APSIM), evaluated the importance of external water table data as model input and assessed the relative effects of water and N stress on yield as affected by wetland type and field position. Yields of 3.2-9.2 Mg ha^{-1} were attained in the floodplain and of 1.9-6.3 Mg ha^{-1} in the inland valley, highlighting the substantial scope to boost yields beyond current regional means of around 2 Mg ha^{-1}. The model estimated grain yields in both wetlands well within the experimental uncertainty during model validation (n= 12, r^2= 0.76, RMSEa= 0.92 Mg ha^{-1} in the floodplain; n= 18, r^2= 0.71, RMSEa= 0.72 Mg ha^{-1} in the inland valley). Results further emphasised the importance of external water table data for sound model performance as they evidently alleviated seasonal droughts. Simulated abiotic stress patterns additionally highlighted hydro-edaphic differences from field positioning within and between both wetlands. While low soil N was generally the main yield constraint, water stress was comparatively more pronounced in the inland valley and supplemental irrigation thus more beneficial on yield. Hydro-edaphic field conditions favoured rice production in the floodplain's fringe with comparatively lower N stress, while large spatial-temporal variabilities prevented a distinct delineation based on toposequential field positions in the inland valley.

Keywords: APSIM, floodplain, inland valley, *Oryza* spp., Tanzania, Uganda

5.1.1 Introduction

Over recent decades, rice (*Oryza* spp*.*) has become a major staple food across East Africa and is now considered a key commodity for achieving regional food security (Nasrin *et al.*, 2015) and alleviating rural poverty (Balasubramanian *et al.*, 2007). Wetlands are particularly suited for lowland rice production due to sustained water supply from high seasonal rainfall and/or seasonally shallow water tables, and relatively fertile soils (Kijima *et al.*, 2012), and have thus increasingly become the focus of agricultural intensification efforts (Nhamo *et al.*, 2014).

In East Africa (Kenya, Rwanda, Tanzania and Uganda), wetlands cover an area of about 0.17 million km^2, 80% of which are comprised of alluvial floodplains and inland valley swamps (Leemhuis *et al.*, 2016), and were thus our selected focal sites. The Kilombero floodplain is Tanzania's most important lowland rice-growing area. Rice production is largely concentrated in the alluvial fans and depends on seasonal rainfall and overbank flooding of the Kilombero River and its tributaries (Kato, 2007). In central Uganda, swampy bottomlands of small inland valleys are the main rice-producing environments and production depends on seasonal rainfall and subsurface interflows from adjacent valley slopes (van Campenhout *et al.*, 2016). At both sites, farms tend to be small (0.5-2 ha) and average yields are low, with 1.8-2.2 Mg ha^{-1} in the floodplain in Tanzania (Senthilkumar *et al.*, 2018) and 1.8-1.9 Mg ha^{-1} in the inland valleys in central Uganda (Haneishi *et al.*, 2013a). In smallholder farming systems, yields are often constrained by economical, social and ecological factors, resulting in inadequate management practices, e.g., inappropriate varietal selection (Kafiriti *et al.*, 2003), untimely weeding (Rodenburg *et al.*, 2015), poor field levelling and water control (Rodenburg, 2013), and consequently in large regional yield gaps (Senthilkumar *et al.*, 2020). However, soil nitrogen (N) deficiency is reportedly the main culprit of low yields and is exacerbated by low external N application rates (Haefele *et al.*, 2013; Saito *et al.*, 2019). While improved crop and field management are likely to substantially increase lowland rice productivity (Saito *et al.*, 2013), variable hydro-edpahic and rainfall conditions have shown to differentially affect rainfed lowland rice yields and yield variability within wetlands, both in inland valleys (Touré *et al.*, 2009), and floodplains (Kwesiga *et al.*, 2019; Senthilkumar *et al.*, 2021). Particularly shallow water tables have been recognised to alleviate production risks from variable seasonal rainfall in rainfed systems (Worou *et al.*, 2012), and to reduce water requirements in irrigated systems (Schmitter *et al.*, 2015). Indiscriminate agricultural wetland use, however, should be avoided and production potentials carefully balanced against potential negative impacts on ecosystem functions

(Dixon & Wood, 2003). Additionally, wetland use plans should consider hydro-edpahic conditions to boost regional yields and reduce yield variability.

Crop models are potentially useful tools to analyse such complex environmental interactions in cropping systems and assess crop performances (Holzworth *et al.*, 2014). From a range of available rice models, including CERES-Rice (Godwin & Singh, 1991) and EPIC (Jones *et al.*, 1991), the Agricultural System Simulator (APSIM) (Keating *et al.*, 2003) was selected for this study. The APSIM model was selected as the generic manager module provides the flexible simulation environment needed to freely code and combine system particulars and describe management interventions (Holzworth *et al.*, 2014). Additionally, APSIM has a proven track record in simulating diverse cropping systems worldwide, e.g., oilseed rape in Germany (Hoffmann *et al.*, 2015) and soybean-wheat systems on long-term soil organic carbon sequestration in India (Mohanty *et al.*, 2020). In rice-based systems, APSIM has, for example, been used to assess the effects of improved water management practices on rice yields in Sri Lanka (Amarasingha *et al.*, 2017) and on rice-maize systems in India (Dutta *et al.*, 2020).

Despite the increasing importance of wetlands for regional rice production and the relative advantage of model applications as decision-support tools to identify site-specific production constraints and optimum management practices (Balwinder-Singh *et al.*, 2016), modelling studies on differential yield responses to imposed management practices and relative positioning within the wetland are currently lacking. However, in order to derive at sound management recommendations, the ability of APSIM to simulate rice growth and development under variable hydro-edaphic field conditions and in response to imposed management practices requires evaluation. Therefore, the objectives of this study were (i) to parameterise, calibrate and validate the APSIM model for improved local rice varieties, and diverse environmental conditions and management treatments and (ii) to subsequently use the validated model to help understand the relative effects of management and hydro-edaphic field conditions on rice yields and yield determinants in a floodplain and an inland valley wetland of East Africa.

5.1.2 Material and methods

Study sites

Field experiments were conducted between 2014 and 2017 in (i) an alluvial floodplain, i.e., the Kilombero floodplain near Ifakara in south-central Tanzania (8.10°-8.18°S and 36.67°-36.76°E, 255 masl), and (ii) an inland valley swamp at the *National Crops Resources Research Institute* (NaCRRI) near Namulonge in central Uganda (0.519°-0.522°N and 32.640°-32.644°E, 1,105 masl) (**Figure 5.1**). The floodplain lies at about 300 masl and covers around 7,967 km^2 (Näschen *et al.*, 2018). Besides the Kilombero River, a vast network of tributaries causes seasonal flooding from overbank flow (Dinesen, 2016). The topography in central Uganda is undulating, ranging from 900 to 1,340 masl and is characterised by inland valleys occupied with narrow swampy bottomlands (Miyamoto *et al.*, 2012). The studied inland valley covers 4.5 km^2 and is one of the headwater micro-catchments of the Lake Kyoga basin (Gabiri *et al.*, 2020).

Climate

The climate at the study sites is sub-humid tropical and humid tropical in the floodplain and the inland valley, respectively (Leemhuis *et al.*, 2016). In the floodplain, annual rainfall of 1,200-1,400 mm is received in a largely mono-modal pattern from December to May (Näschen *et al.*, 2018). In the inland valley, mean annual rainfall of about 1,200 mm is received in a bi-modal pattern from September to November and from March to May (Nsubuga *et al.*, 2011). During the main rice-growing periods from 1980-2010, monthly mean daily maximum and minimum temperatures ranged from 31.9° to 28.9°C and 22.1° to 20.0°C between March and May in the floodplain, and from 28.4° to 28.3°C and 17.1° to 16.6°C between September and November in the inland valley (Ruane *et al.*, 2015). Daily rainfall (mm), maximum and minimum temperatures (°C) and solar radiation (MJ m^{-2}) were recorded by automatic weather stations near Ifakara town in Tanzania (8.06°S and 36.39°E) and at the NaCRRI in Uganda (0.522°N and 32.642°E) from 2014 to 2017. Additional tipping buckets were installed at the respective field positions to monitor the within-site rainfall variability more precisely .
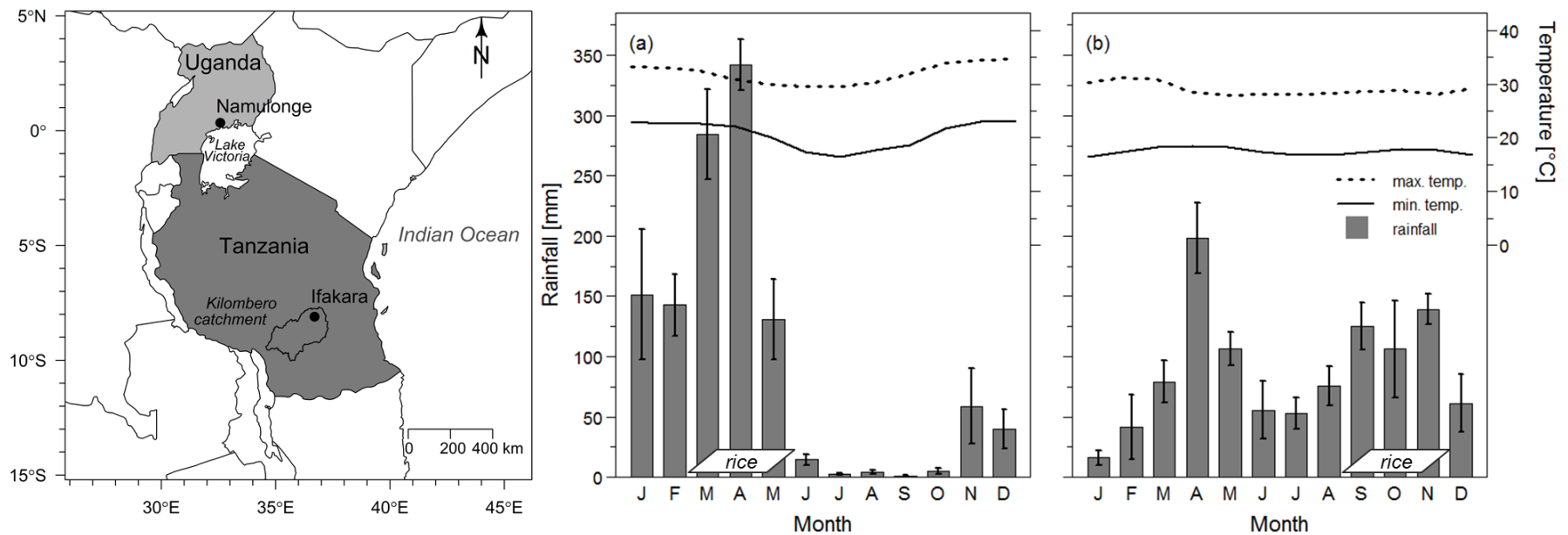
Figure 5.1 Geographical location of the study sites in the floodplain in south-east Tanzania and the inland valley in central Uganda (left), and average monthly rainfall, minimum and maximum temperatures during the study period (right) at the study sites in (a) the floodplain (2015-2017, *n*= 3) and (b) the inland valley (2014-2017, *n*= 4). Bars indicate standard errors of monthly rainfall means, boxes indicate the main rice-growing periods in the floodplain (March to May) and the inland valley (September to November).

Experimental design

Experiments were established along the hydrological gradient in the floodplain, i.e., at the fringe and middle positions based on the origin, extent and duration of floodwater (Kwesiga *et al.,* 2019), and as a toposequence valley cross-section in the inland valley, i.e., at the valley-fringe, mid-valley and valley-bottom positions (Gabiri *et al.*, 2017). A randomised complete block design with four replications per treatment and field position was used and established for three consecutive years, i.e., from 2015-2017 in the floodplain and from 2014-2016 in the inland valley. Management treatments included: (i) a rainfed non-amended baseline treatment (0N), (ii) a rainfed 60 kg N ha^{-1} treatment (60N), and (iii) a manually irrigated, 120 kg N ha^{-1} and 60 kg PK ha^{-1} attainable yield treatment (120N+PK+I) (Kwesiga *et al.*, 2019). N was applied as urea-N in two splits, with 75 and 50% being applied basally and 25 and 50% at panicle initiation (PI) in the floodplain and the inland valley, respectively. As per local recommendations, P was applied basally as single superphosphate in the floodplain and as triple superphosphate in the inland valley, while K was applied basally as muriate of potash. Manual supplemental irrigation aimed at maintaining near-saturated soil conditions from transplanting to ripening stages. Individual plots measured 5x6 m and were levelled, puddled and bunded (40x20 cm height and width). Weeds were removed manually at 3, 6 and 9 weeks after transplanting. With the onset of the rainy seasons in February in the floodplain and August in the inland valley, rice nurseries were established and experimental plots were ploughed with hand hoes, puddled, and levelled. Two 16-30-day-old seedlings per hill were transplanted at 20x20 cm spacing in the floodplain, and three 21-27-day-old seedlings per hill at 15x30 cm spacing in the inland valley. Recommended, potentially high-yielding and locally available rice genotypes were used, i.e., the semi-dwarf, 120-day lowland rice (*O. sativa*) variety SARO-5 (Singh *et al.*, 2013) in the floodplain, and the drought tolerant, 95-110-day rainfed rice (*O. sativa* x *O. glaberrima*) variety NERICA-4 (Jones *et al.*, 1997) in the inland valley. Sequential biomass accumulation and rice N uptake were determined at the early vegetative, PI, 50% flowering and physiological maturity stages from 2x6 opposing hill clusters outside the central harvest area. Phenological key stages, i.e., PI, 50% flowering and physiological maturity were observed by primordial initiation, emergence of 50% of panicles and yellow-colouring of 90% of grains, respectively (De Datta, 1981). Plants were partitioned into individual organs and oven-dried at 90°C until constant weight. Rice N uptake was determined by analysing ground dry matter sub-samples for their N content and multiplication with their weight as described in Kwesiga *et al.* (2020a). Central harvest

areas for grain yield determination (reported at 0% moisture content) measured 6 m^2 in the floodplain and 5 m^2 in the inland valley.

Hydro-edaphic characteristics

Predominant soils were Fluvisols in the floodplain (Gabiri *et al.*, 2018b) and Gleysols in the inland valley (Gabiri *et al.*, 2017). The Fluvisols were of alluvial origin and generally heavy-textured. Topsoil organic carbon (C_{org}) contents varied between 25 g kg^{-1} in the fringe and 7 g kg^{-1} in the middle position (**Table 5.1**). The soil N (N_{tot}) content was low and only slightly above the critical N content for rice growth of 2 g kg^{-1} (Senthilkumar *et al.*, 2018). The Gleysols were mostly of colluvial origin with an umbric horizon and largely loamy-textured although texture and nutrient contents varied considerably within and among field positions (Gabiri *et al.*, 2017). Topsoil C_{org} and N_{tot} contents were higher compared to the floodplain Fluvisols, with up to 57 g C kg^{-1} and 8 g N kg^{-1} (**Table 5.1**). At both sites, plant-available P and exchangeable K were largely sufficient for rice growth, exceeding the critical limit for rice growth of <8 mg P kg^{-1} and <60 mg K kg^{-1} according to Mehlich-3 soil extraction (Kwesiga *et al.*, 2019). A detailed description of soil analysis methods is provided by Kwesiga *et al.* (2020a).

In the floodplain, annual water tables fluctuated between surface level and 1.5 m below surface at the fringe, between 1 m above and 3 m below surface at the middle position, and between 0.6 m above and 0.9 m below surface across all field positions in the inland valley (**Figure A.B1**). Flooding occurred from April to July in the floodplain and from October to January and April to June in the inland valley (**Figure A.B1**). At all field positions, daily water table depths and volumetric soil moisture contents (10 and 30 cm depth) were aggregated from hourly piezometer pressure logger and Frequency-Domain-Reflectometry (FDR) profile probe data, respectively. A detailed instrumentation description is provided by Gabiri *et al.* (2018b) and Gabiri *et al.* (2019). Due to continuous pressure data logger failure in the floodplain's fringe position in 2017, data from 2015 were used. Remaining missing data were filled using the Kalman imputation method (Moritz & Bartz-Beielstein, 2017).

Table 5.1 Topsoil properties of the Fluvisols in the floodplain and the Gleysols in the inland valley used for APSIM parameterisation.

Site	Field position	Depth [cm]	BD [g cm^{-3}]	LL15 [cm^3 cm^{-3}]	DUL [cm^3 cm^{-3}]	SAT [cm^3 cm^{-3}]	Soil texture [WRB]	C_{org} [g kg^{-1}]	N_{tot} [g kg^{-1}]	*fBiom* [0-1]	*fInert* [0-1]
Floodplain, Tanzania	fringe	0-20	1.05	0.198	0.364	0.501	loam	24.51	1.21	0.040	0.620
		20-35	1.30	0.240	0.370	0.508	clay-loam	14.21	0.91	0.030	0.650
		35-50	1.41	0.248	0.373	0.468	clay-loam	11.63	0.81	0.020	0.700
	middle	0-20	1.34	0.137	0.237	0.401	sandy-loam	6.54	0.50	0.070	0.350
		20-25	1.30	0.223	0.354	0.508	clay-loam	9.27	0.71	0.060	0.400
		25-28	1.34	0.299	0.393	0.494	clay	12.05	0.91	0.060	0.450
		28-37	1.33	0.337	0.397	0.498	clay	12.20	1.11	0.015	0.500
		37-46	1.30	0.337	0.401	0.509	clay	11.74	0.91	0.010	0.550
Inland valley, Uganda	valley-fringe	0-23	0.97	0.205	0.380	0.479	clay-loam	45.71	3.51	0.040	0.700
		23-30	1.13	0.201	0.304	0.390	clay-loam	33.13	2.17	0.030	0.750
		30-35	1.33	0.152	0.298	0.497	loam	13.86	0.62	0.020	0.850
		35-45	1.68	0.093	0.175	0.366	sandy-loam	3.15	0.31	0.015	0.900
	mid-valley	0-20	1.05	0.212	0.371	0.514	clay-loam	28.90	2.27	0.040	0.420
		20-30	1.44	0.181	0.301	0.526	loam	9.14	0.72	0.030	0.450
		30-45	1.51	0.216	0.327	0.430	clay-loam	3.34	0.41	0.020	0.500
	valley-bottom	0-22	1.10	0.208	0.420	0.520	clay	57.02	5.26	0.040	0.780
		22-34	1.09	0.257	0.401	0.474	clay-loam	27.62	2.06	0.030	0.750
		34-48	1.57	0.139	0.245	0.408	sandy-clay-loam	3.74	0.31	0.020	0.850

BD, bulk density; layer-wise volumetric water content at wilting point (LL15), field capacity (DUL) and saturation (SAT); soil texture definition according to the World Reference Base for Soil Resources (WRB): sand (63 to 2,000 µm), silt (2 to 63 µm), clay (<2 µm); C_{org}, soil organic carbon content; N_{tot}, total soil N content, initial labile (*fBiom*) and inert (*fInert*) fraction of soil organic carbon.

The APSIM model (v 7.5)

APSIM is a daily time-step, point-scale cropping system model that uses a modular design around a central engine to drive the simulation process and ensure the communication between all modules, and is described in detail by Holzworth *et al.* (2014). In this study, key modules included the rice module ORYZA (Gaydon *et al.*, 2012a) that was developed based on physiological routines of the ORYZA2000 model (Bouman *et al.*, 2001), and the POND module (Gaydon *et al.*, 2012b) that simulates key chemical and biological processes under temporarily or permanently ponded conditions. Other modules included SOILWAT for soil water balancing, SOILN for soil C and N transformations and SURFACEOM for the fate and conversion of surface residues (Probert *et al.*, 1998).

APSIM parameterisation, calibration & validation protocol

APSIM was run continuously as a rice-fallow system for three-years without re-setting soil N, soil water and soil organic matter (SOM) parameters after initialisation at both study sites. Using the replications average per field position and treatment, the third season of experimental data was used for model calibration and determination of genotype-specific parameters and coefficients, while the two remaining seasons of independent experimental data were used for model validation. Considering all field positions and management treatments, observed vs. simulated key phenological stages, biomass accumulation and partitioning, N uptake, and grain yields were statistically compared.

APSIM parameterisation & calibration

Following the parameterisation procedure as set out by Gaydon *et al.* (2021), APSIM requires empirical local input data to drive the simulation process, i.e., daily climate such as minimum and maximum temperatures (°C), solar radiation (MJ m^{-2}) and rainfall (mm). Additionally, measurable soil physical and chemical parameters are required, i.e., layer-wise pH, bulk density, and soil volumetric water contents at saturation (SAT), field capacity (DUL) and permanent wilting point (LL15), as well as initial soil organic carbon (C$_{org}$) and mineral N (NO$_3^-$, NH$_4^+$) contents (**Table 5.1**). Macroflow conductivity and the vertical water flow through macropores was specified by measured saturated percolation rates (Ks, mm day^{-1}), while soil water conductivity, i.e., the proportion of water exceeding DUL and draining daily into the subsequent soil layer is specified via the *swcon* coefficient. *Swcon* varies depending on soil texture, i.e., typically <0.5 for heavy clay and >0.8 for sandy soils from greater water conductivity (Probert *et al.*, 1998). Not directly measurable parameters required iterative calibration as described below.

Crop phenology and assimilate partitioning: Following Jones & Kiniry (1986), APSIM uses growing degree days (GDD; °C day^{-1}) to determine the phenological development of rice, explained by Bouman & Van Laar (2006). Genotype-specific GDD constants and partitioning coefficients for SARO-5 and NERICA-4 were calibrated from observed key phenological stages and corresponding biomass accumulation and partitioning data. Similarly, field data was used to determine leaf maximum and minimum relative growth rates, maximum individual grain weight at maturity, and specific leaf area. Results were further fine-tuned to match observed data best (**Table A.B2**).

SOM mineralisation: APSIM requires initial layer-wise soil organic carbon (C_{org}), NO_3^- and NH_4^+ contents as well as parameter values for *fBiom* (fraction of soil microbial biomass (biom)) and *fInert* (fraction of inert humic material (hum)) to initialise the proportions of SOM pools and their mineralisation capacities, i.e., the fresh organic matter (*fom*), the more labile *biom* and the more inert *hum* pools. Values for *fInert* and *fBiom* were incrementally adjusted within physically plausible bounds (Probert *et al.*, 1998), and until observed and simulated crop yields of the non-amended baseline treatment (0N) provided a good match (**Table 5.1**). Additionally, APSIM was set to treat residues and weeds according to field management, i.e., incorporation in mid-November in the floodplain and full aboveground removal after rice harvest in the inland valley. Following field observations, APSIM's weed cultivar '*perennial_grass*' was planted and allowed to grow during the fallow period before being incorporated during field preparation.

Ponding and water table dynamics: Vertical water flow was restricted at around 30 cm depth to account for the plough-pan under puddled conditions and Ks values calibrated by matching observed and simulated ponds and soil water contents. In APSIM, ponded conditions and perched water tables result from restricted vertical water flow and *in-situ* rainfall and/or irrigation. Maximum pond depth is user-defined (*max_pond*) and excess water subjected to runoff, while a perched water table is defined as the proportion of soil water between DUL and SAT in a soil layer directly adjacent to a saturated layer (Asseng *et al.*, 1998). In wetlands, however, water tables are mutually affected by *in-situ* rainfall and/or irrigation and catchment-scale processes (rainfall, lateral and subsurface inflows) (Leemhuis *et al.*, 2016). Therefore, we used daily measured water table data to drive the simulation process. Variable aquifer depths and soil properties in the inland valley, however, caused high spatial-temporal water table fluctuations within field positions (Gabiri *et al.*, 2017). Therefore, plot-level soil moisture measurements were assumed to be the better indicator for local soil water conditions. Thus, daily measured water tables were adjusted by a fixed factor within the aquifer range, i.e., lowered daily by 32, 3 and 30 cm in the valley-fringe, mid-valley and valley-bottom position, respectively.

APSIM validation

Occasionally, poor initial validation performance required re-visitation of parameterisation and calibration procedures, until acceptable model performance was achieved, i.e., within the experimental uncertainty. APSIM's ability to simulate cropping system 'carry-over' effects was further evaluated, i.e., continuous comparison of observed and simulated soil moisture contents, and soil carbon dynamics and indigenous soil N supply via non-amended baseline yields (0 N) without seasonal re-setting of variables after initialisation.

APSIM water & N deficit factors

APSIM calculates crop water and N deficit factors to simulate the effects of water and N stress on crop growth and development. Following model validation, daily water and N stress factors were, therefore, used to assess the relative effects of wetland type and field position on rice yields (1= no stress, 0= severe stress). While water stress (*lestrs*) is calculated as a function of the upper and lower soil-water tensions in the root zone, i.e., water deficits from actual to potential soil water contents (Boling *et al.*, 2007), N stress (*rnstrs*) is calculated from crop N contents, i.e., N deficits from the ratio of potential (*ancrpt*) to actual (*ancr*) crop N content (Bouman & Van Laar, 2006). Both water and N stress affect the rate of relative leaf growth, i.e., reducing the relative leaf growth and thus the rates of photosynthesis and yield up until flowering, while accelerating leaf senescence after flowering. A detailed description of the processes and modelling logics is provided in Bouman *et al.* (2001).

Statistical analysis

Paired observed (O_i) and simulated (S_i) data-points were combined to determine the slope (α), intercept (β) and coefficient of determination (r^2) of the linear regression. A slope α of 0, and intercept β and r^2 of 1 indicate a perfect model fit. The Student's *t*-test of means was used assuming unequal variance; a P(t) ≥0.05 indicates no significant differences exist between observed and simulated values. Additional statistical measures included the absolute and normalised root mean square error (RMSEa, Mg ha^{-1}, Eq. (1), and RMSEn, %, Eq. (2)), modelling efficiency (EF, -, Eq. (3)), and the mean absolute error (MAE, Mg ha^{-1}, Eq. (4)) (Hagi-Bishow & Bonnell, 2000; Willmott & Matsuura, 2005):

$$\text{RMSEa} = \sqrt{\sum_{i=1}^{n} (O_i\text{-}S_i)^2 / n} \qquad (1)$$

$$\text{RMSEn} = \sqrt{\sum_{i=1}^{n} (O_i\text{-}S_i)^2 / n} * 100/\bar{O} \qquad (2)$$

$$EF = 1 - \sum_{i=1}^{n} (S_i-O_i)^2 \Big/ \sum_{i=1}^{n} (O_i-\bar{O})^2 \qquad\qquad (3)$$

$$MAE = \sum_{i=1}^{n} \left| S_i-O_i \right| / n \qquad\qquad (4)$$

Where S_i and O_i are the simulated and observed values, respectively; and n equals the number of data-pairs and $\bar{O}$ the mean of the observed values. The RMSEa is ideally similar to or smaller than the standard deviation (SD) of the observed values while the RMSEn is ideally similar to the coefficient of variation (CV) of the observed values. The EF value compares the simulated values to the mean of the observed values. EF of 1 indicates a perfect model fit and equals a mean squared error (MSE) of 0, while a value of 0 indicates the MSE is equal to the variability of the observed data. A negative EF value indicates that the mean of the observed data is a better predictor than the model. The MAE shows the absolute difference of simulated to observed values; a MAE of 0 denoting a perfect model fit and positive or negative MAEs the quantification of model over- or underestimation. Where applicable, multiple mean comparisons were performed using the Tukey's HSD test at a 95% confidence level.

5.1.3 Results

Seasonal weather conditions

Annual rainfall during the study period ranged between 1,060 and 1,319 mm in the floodplain (2015-2017) and between 775 and 1,300 mm in the inland valley (2014-2017) (**Figure 5.1**). During the main rice-growing periods from March to May, 790, 562 and 918 mm of rainfall were received at the floodplain's fringe, and 701, 537 and 1,033 mm at the floodplain's middle position in 2015, 2016 and 2017, respectively. In the El Niño year of 2016, irregular rainfall patterns were observed. While the rainy season started comparatively early and about 493 mm were received in January and February alone, the rains also ceased early with only about 30 mm being received in May. In the inland valley, 332, 519 and 233 mm of rainfall were received during the main rice-growing periods (September to November) in 2014, 2015, and 2016, respectively. Low seasonal rainfall of 2016 was most pronounced in October where only 35 mm were received against 84 and 243 mm in 2014 and 2015, respectively. Daily maximum and minimum temperatures varied only slightly during the rice-growing periods, with averages of 33.4° and 21.1°C in the floodplain, and 28.6° and 17.7°C in the inland valley, respectively (**Figure 5.1**).

Rice yields in contrasting lowland systems

Rice grain yields varied between 1.9 and 9.2 Mg ha^{-1}, depending on wetland type, field position, year and treatment. Yields were generally lower in the inland valley than the floodplain, with mean yields of 3.8 and 6.2 Mg ha^{-1}, respectively. Rainfall variability led to higher mean yields of 6.3 Mg ha^{-1} with favourable rainfall conditions in 2017 and to lower mean yields of 5.6 Mg ha^{-1} with unfavourable rainfall conditions in 2016 in the floodplain. Similarly, mean yields of 4.6 in 2014 and of 3.2 Mg ha^{-1} in 2016 were related to variable seasonal rainfall in the inland valley. Toposequential yield trends were not significant in the inland valley, while yields were significantly higher in the floodplain's fringe (6.5 Mg ha^{-1}) as compared to the middle position (5.9 Mg ha^{-1}) (**Table 5.2**). Baseline yields of non-amended rice (0N) were higher in the floodplain (4 Mg ha^{-1}) than the inland valley (2.7 Mg ha^{-1}), and more so in the floodplain's fringe (4.3 Mg ha^{-1}) than middle position (3.8 Mg ha^{-1}). In both wetlands, rice responded significantly to applied mineral N fertiliser (**Table 5.2**). Mean attainable yields were 8.7 and 7.6 Mg ha^{-1} in the floodplain's fringe and middle position, respectively, and about 5.2 Mg ha^{-1} with little variation among field positions in the inland valley.

Table 5.2 Effect of field position and management treatment on measured average grain and biomass yields and standard deviations (SD) at the floodplain (2015-2017) and the inland valley (2014-2016) sites. Values are the means of four replicates.

Site	Source of variation	n	Grain yield (SD) [Mg ha^{-1}]	Biomass yield (SD) [Mg ha^{-1}]	Site	Source of variation	n	Grain yield (SD) [Mg ha^{-1}]	Biomass yield (SD) [Mg ha^{-1}]
	Field position (FP)					Field position (FP)			
	fringe	36	6.5 (2.0)	13.0 (4.0)		valley-fringe	36	3.9 (1.4)	10.0 (3.3)
	middle	36	5.9 (1.7)	12.1 (4.1)		mid-valley	36	3.6 (1.5)	9.5 (4.1)
						valley-bottom	36	3.9 (1.5)	10.2 (3.6)
	Management treatment (M)					Management treatment (M)			
	0N	24	4.0 (0.8)	8.5 (1.4)		0N	36	2.7 (1.0)	7.2 (2.4)
Floodplain, Tanzania	60N	24	6.3 (0.7)	12.2 (2.1)	Inland valley, Uganda	60N	36	3.5 (1.1)	9.1 (2.8)
	120N+PK+I	24	8.1 (0.9)	17.0 (2.7)		120N+PK+I	36	5.2 (1.1)	13.4 (2.6)
	Year					Year			
	2015	24	6.5 (1.8)	12.1 (3.5)		2014	36	4.6 (1.4)	11.2 (3.7)
	2016	24	5.6 (1.9)	11.2 (3.8)		2015	36	3.5 (1.0)	10.0 (2.5)
	2017	24	6.3 (1.7)	14.3 (4.3)		2016	36	3.2 (1.6)	8.5 (4.2)
	Anova probabilities for the effects of					*Anova probabilities for the effects of*			
	Field position (FP)	72	0.010	NS		Field position (FP)	108	NS	NS
	Management (M)	72	0.001	0.001		Management (M)	108	0.001	0.001
	FP × M	144	0.100	NS		FP × M	216	NS	NS

SD, standard deviation*; NS*, not significant.

APSIM calibration & validation

Model veracity was assessed by statistically comparing observed and simulated soil moisture dynamics and crop parameters, i.e., phenology, sequential biomass accumulation and partitioning, N uptake and grain yield in response to wetland type, field position and management treatment.

Crop phenology

APSIM underestimated key phenological stages of the lowland rice variety SARO-5 in Tanzania during model calibration on average by 5 days for flowering and overestimated maturity by 2 days (**Figure A.B3**). During model validation, the upper whiskers indicated large deviations of >20 days to flowering and >11 days to maturity, while the median indicated deviations of 11 and 2 days to flowering and maturity, respectively. In Uganda, time to flowering and maturity of the rainfed rice variety NERICA-4 was underestimated on average by <7 days during both model calibration and validation (**Figure A.B3**).

Biomass accumulation & grain yield

During model validation, observed and simulated values correlated strongly at both study sites, showing a small MAE of <0.5 Mg ha^{-1} for grain and biomass yields (**Table 5.3**). In the floodplain, an RMSEa of 0.92 Mg ha^{-1} for grain and of 1.71 Mg ha^{-1} for biomass yield compared favourably to the SD among the observed data (1.84 Mg ha^{-1} for grain and 3.36 Mg ha^{-1} for biomass yield). Additionally, simulated and observed grain and biomass yields correlated strongly, i.e., with an r^2= 0.76, α= 0.82 and β= 1.20 for grain and an r^2= 0.76, α= 0.75 and β= 3.40 for biomass yield. Sound model performance was further endorsed by EF values of 0.75 and 0.74 for grain and biomass yield, respectively. In the inland valley, an RMSEa of 0.78 Mg ha^{-1} for grain and 1.42 Mg ha^{-1} for biomass yield compared similarly well to the SD among the observed data (1.11 Mg ha^{-1} for grain and 2.46 Mg ha^{-1} for biomass yield). Observed and simulated data-pairs also showed a strong correlation for grain and biomass yield (r^2= 0.71 and 0.72) with low bias (α= 0.91 and 0.88, β= 0.79 and 1.60), respectively. Furthermore, an EF of 0.51 and 0.67 for grain and biomass yields, respectively, supported sound model performance. At both study sites and field positions, the paired *t*-test additionally confirmed that no differences exist between simulated and observed non-amended baseline yields (0N) (data not shown). **Table 5.3** provides a detailed overview on model performance statistics during calibration and validation .

Table 5.3 Statistical measures for observed vs simulated grain yield, biomass accumulation and partitioning for the calibration and validation period at the study sites in the floodplain and the inland valley.

Site	Model evaluation	Parameter	n	Xobs (SD) [Mg ha^{-1}]	Ysim (SD) [Mg ha^{-1}]	α [ ]	β [Mg ha^{-1}]	r^2 [0-1]	P(t)*	CV [%]	RMSEa [Mg ha^{-1}]	RMSEn [%]	EF [ ]	MAE [Mg ha^{-1}]
Floodplain, Tanzania	calibration	biomass	6	14.29 (4.12)	13.30 (4.23)	0.97	-0.49	0.88	0.19	28.8	1.76	12.3	0.82	-0.99
		grain	6	6.30 (1.57)	6.88 (2.76)	1.67	-3.66	0.90	0.38	25.0	1.48	30.3	0.12	0.58
		stem	6	5.34 (2.15)	4.17 (0.98)	0.36	2.26	0.62	-	40.2	1.91	39.1	0.21	-1.17
		leaf	6	0.90 (0.44)	2.08 (0.50)	0.60	1.54	0.28	-	49.0	1.27	141.3	-7.31	1.18
	validation	biomass	12	11.69 (3.36)	12.11 (2.88)	0.75	3.40	0.76	0.41	28.7	1.71	14.6	0.74	0.42
		grain	12	6.08 (1.84)	6.21 (1.74)	0.82	1.20	0.76	0.66	30.3	0.92	15.2	0.75	0.13
		stem	12	3.79 (1.23)	4.00 (1.04)	0.71	1.33	0.70	-	32.4	0.71	18.7	0.67	0.21
		leaf	12	1.42 (0.50)	1.74 (0.51)	0.74	0.70	0.52	-	35.3	0.50	35.3	0.00	0.32
Inland valley, Uganda	calibration	biomass	9	8.52 (3.88)	8.08 (3.73)	0.88	0.55	0.85	0.44	45.6	1.58	18.5	0.83	-0.44
		grain	9	3.25 (1.45)	3.48 (1.61)	1.00	0.21	0.82	0.37	44.7	0.72	22.2	0.75	0.23
		stem	9	2.38 (1.04)	2.92 (1.32)	1.13	0.25	0.79	-	43.9	0.83	34.7	0.37	0.54
		leaf	9	1.40 (0.56)	1.62 (0.77)	1.28	-0.17	0.86	-	39.8	0.39	28.2	0.50	0.22
	validation	biomass	18	10.52 (2.46)	10.86 (2.55)	0.88	1.60	0.72	0.32	23.4	1.42	13.5	0.67	0.34
		grain	18	4.06 (1.11)	4.48 (1.20)	0.91	0.79	0.71	0.02	27.4	0.78	19.2	0.51	0.42
		stem	-	-	-	-	-	-	-	-	-	-	-	-
		leaf	-	-	-	-	-	-	-	-	-	-	-	-

n, number of data pairs; Xobs, mean of observed values; Xsim, mean of simulated values; SD, standard deviation; CV, coefficient of variance; P(t)*, significance of Student's paired t-test assuming unequal variances; α, slope of linear regression; β, y-intercept of linear regression; r^2, square of linear correlation; RMSEa and RMSEn, absolute and normalised root mean squared error; EF, modelling efficiency; MAE, mean absolute error.

* values greater than 0.05 indicate simulated and observed values are the same at 95% confidence level

Additionally, a linear regression of observed and simulated data-pairs for grain yield illustrates model performance from both externally supplied and internally simulated perched water tables, and the treatment effect on yield (**Figure 5.2**). In the floodplain, the linear regression from externally supplied water tables showed a strong correlation (r^2= 0.94) with a low bias (α= -0.20, β= 1.08), despite indicating a slight overestimation of the 0N yield in the fringe and the 120N+PK+I yield in the middle position (**Figure 5.2**). In contrast, the linear regression from internally simulated perched water tables showed a strong underestimation of yields (α= -1.95, β= 0.99) and rainfed yields were underestimated on average by 2 Mg ha^{-1}. In the inland valley, model performance from externally supplied water tables showed a similarly strong correlation (r^2= 0.88, α= -0.03, β= 1.1) and only the mid-valley's 60N yields were visibly overestimated. Model performance from internally simulated perched water tables, however, also showed a distinct underestimation of rainfed yields across all field positions (α= -2.12, β= 1.49). On average, yields were underestimated by 0.8 Mg ha^{-1} that, however, increased to 2.1 Mg ha^{-1} in 2016 with low seasonal rainfall. Furthermore, standard errors of observed yields were comparatively large in the inland valley, indicating a strong seasonal effect on yield (**Figure 5.2**).

Rice N uptake

Additionally, a linear regression of observed and simulated data-pairs for rice N uptake at physiological maturity illustrates sounds model performance at both study sites. In the floodplain, the linear regression showed a strong correlation (r^2= 0.95) and a high level of accuracy for the non-amended baseline treatment (0N), however, indicating an increasing overestimation of rice N uptake with increasing mineral N fertiliser application (α= -14.84, β= 1.4) (**Figure 5.3**). In the inland valley, model performance showed a similarly strong correlation (r^2= 0.79) with only the mid-valley's 60N and 120N+PK+I rice N uptake showing a visible overestimation (α= -5.56, β= 1.13) (**Figure 5.3**).
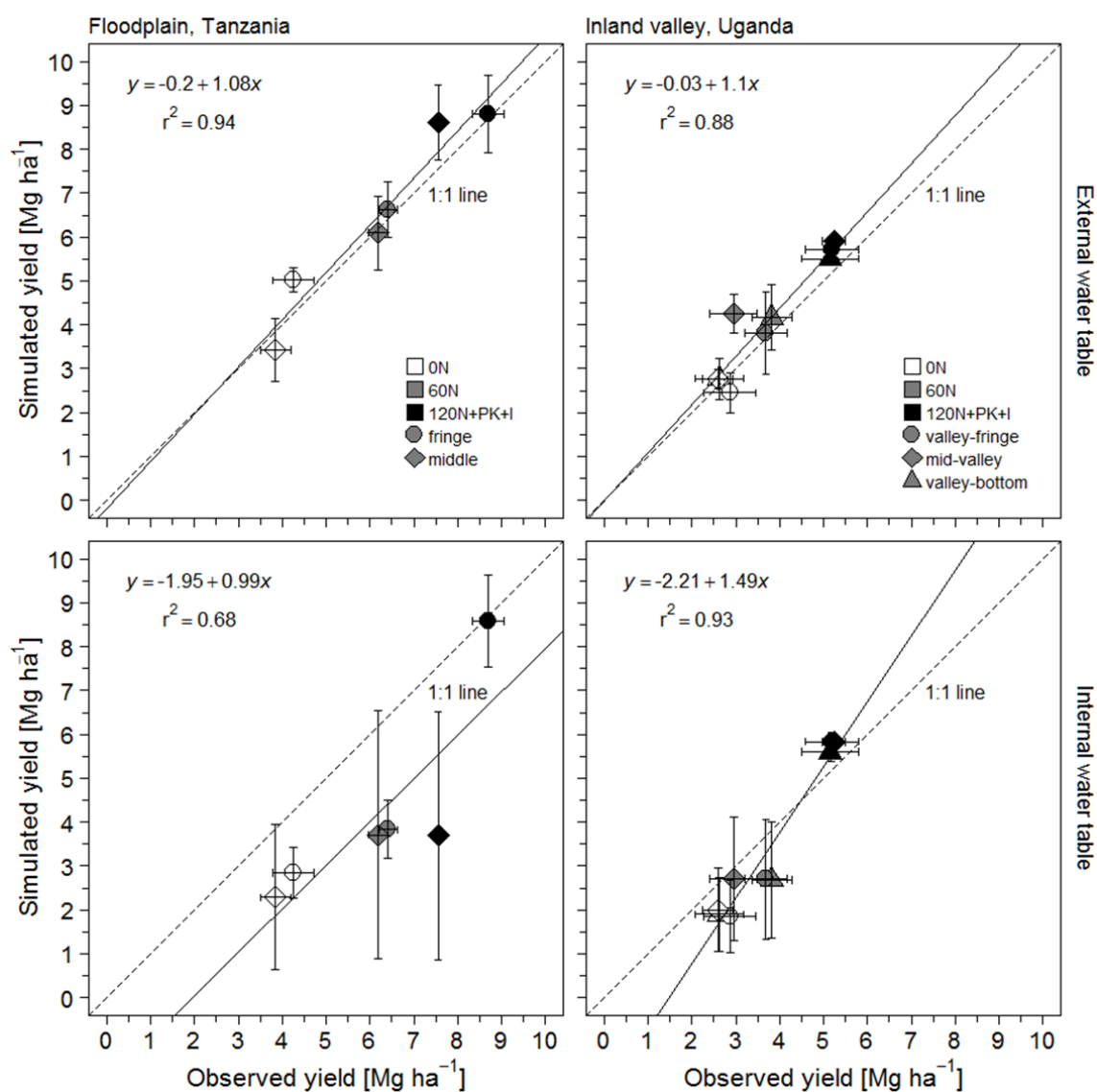
Figure 5.2 Comparison of observed and simulated grain yields from externally supplied (top) and internally simulated (bottom) water tables according to field position and management treatment at the study sites in the floodplain (left) and the inland valley (right), bars indicate standard errors of means over the study period (n= 3).
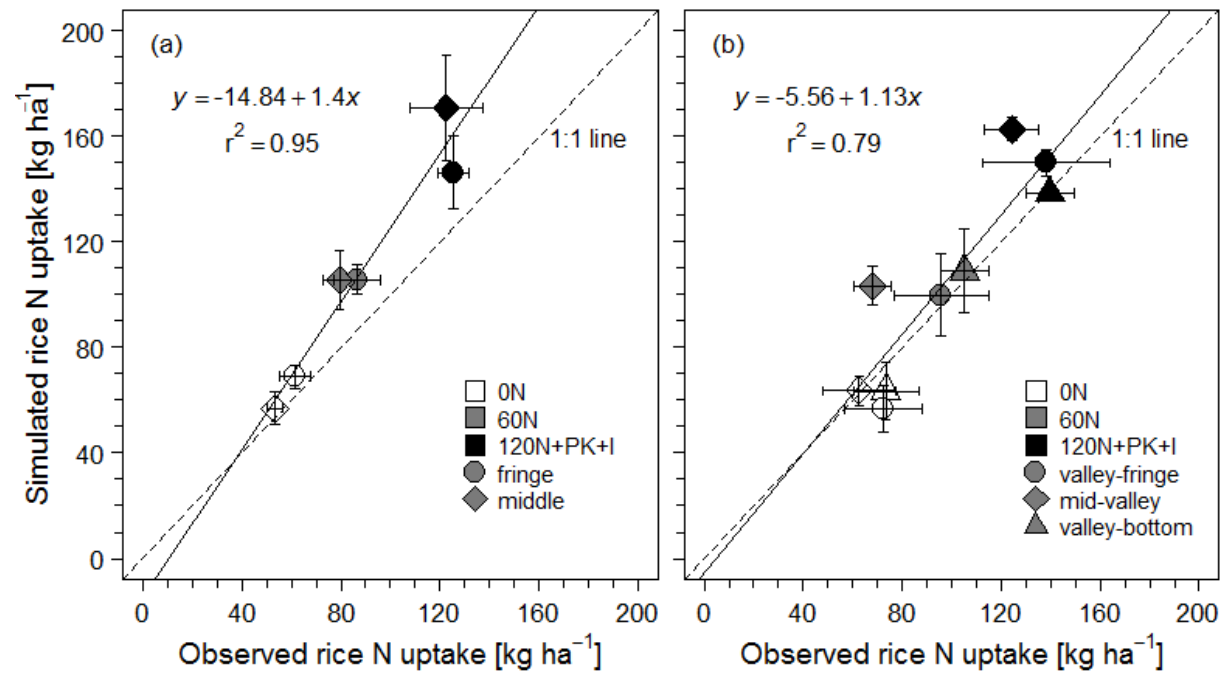
Figure 5.3 Comparison of observed and simulated rice N uptake at physiological maturity according to field position and management treatment at the study sites in (a) the floodplain and (b) the inland valley, bars indicate standard errors of means over the study period (*n*= 3).

Soil moisture dynamics

APSIM simulated the measured soil moisture dynamics in the floodplain with a high level of accuracy at 10 and 30 cm soil depths and throughout the 3-year study period, and with r^2 of 0.87 and 0.81 at 10 cm depth (**Figure 5.4**) and with r^2 of 0.85 and 0.66 at 30 cm depth (**Figure A.B4**) for the fringe and middle positions, respectively. Soil moisture dynamics in the inland valley were simulated satisfactorily at 10 cm depth and with r^2 of 0.59, 0.59 and 0.45 throughout the study period (**Figure 5.5**), and with r^2 of 0.19, 0.30 and 0.36 at 30 cm depth (**Figure A.B5**) in the valley-fringe, mid-valley and valley-bottom positions, respectively.

APSIM water & N stress factors by wetland type & field position

Wetland type- and field position-specific yield determinants were subsequently examined via APSIM water and N stress factors in the non-amended baseline treatment (0N). In both wetlands, N stress during the reproductive stage from PI to flowering was more severe and, hence, yield-affecting than water stress. Water stress, however, was more pronounced in the inland valley as compared to the floodplain (**Figure 5.6, Figure 5.7**). However, N and water deficits additionally varied as affected by field position and year. During the reproductive stage, N stress was lower (<0.3 at PI) while water stress higher (<0.85 at PI) in the floodplain's fringe as compared to the middle position (<0.1 for N stress and >0.95 for water stress at PI) (**Figure 5.6**). In toposequential comparison, N stress was lower (<0.85 at PI) and water stress higher (0.6 at PI) in the inland valley's valley-fringe position during the reproductive stage (**Figure 5.7**). N stress subsequently increased from the inland valley's mid-valley (>0.8 at PI) to the valley-bottom position (0.75 at PI), while water stress decreased from the valley-bottom (>0.7 at PI) to the mid-valley position (>0.8 at PI).
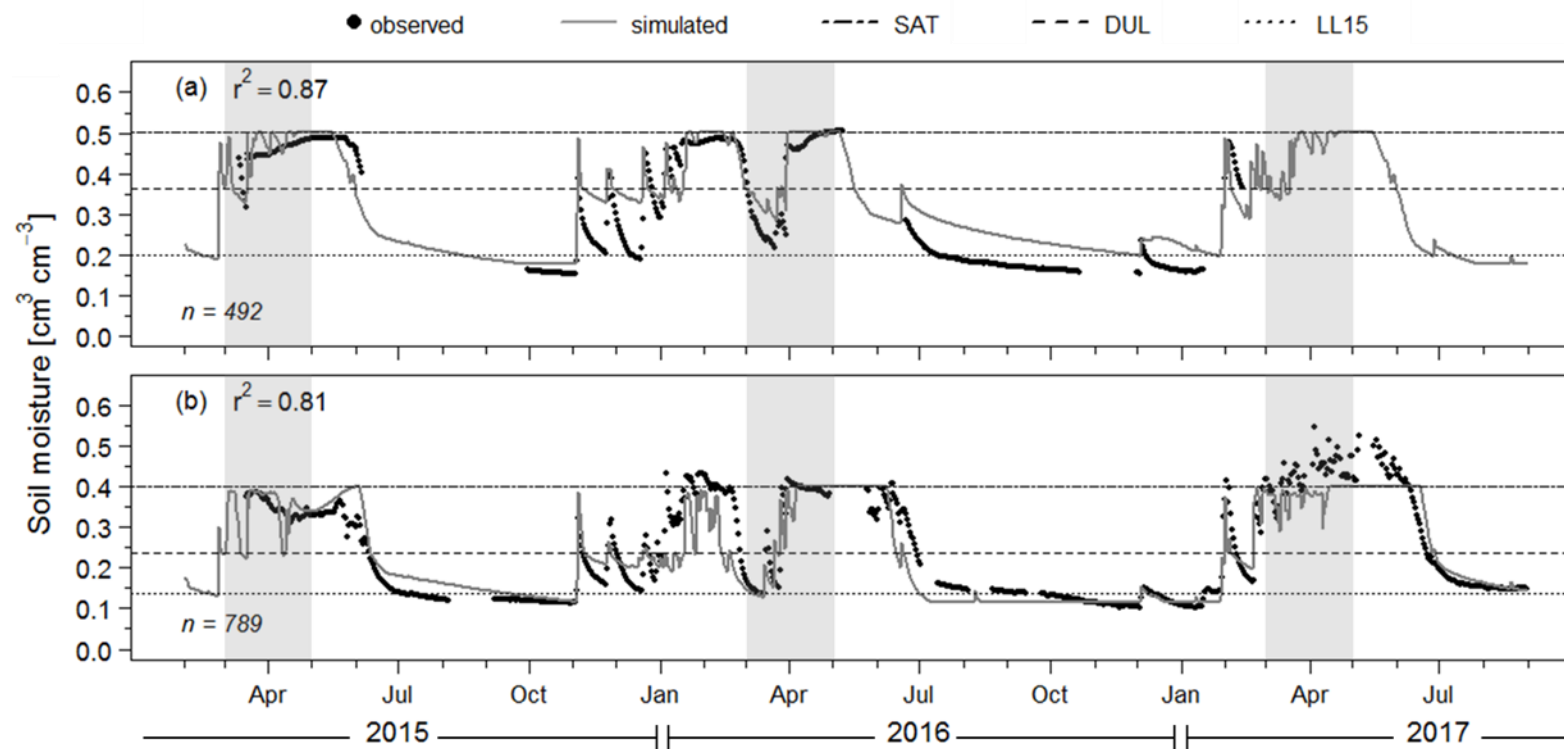
Figure 5.4 Observed (points, un-replicated) and simulated (lines) soil moisture dynamics in the non-amended baseline treatment (0N) and 10 cm depth at the floodplain's (a) fringe and (b) middle positions (2015-2017); volumetric water content at saturation (SAT), field capacity (DUL) and wilting point (LL15); the shaded areas (grey) indicate the main rice-growing periods (March to May).
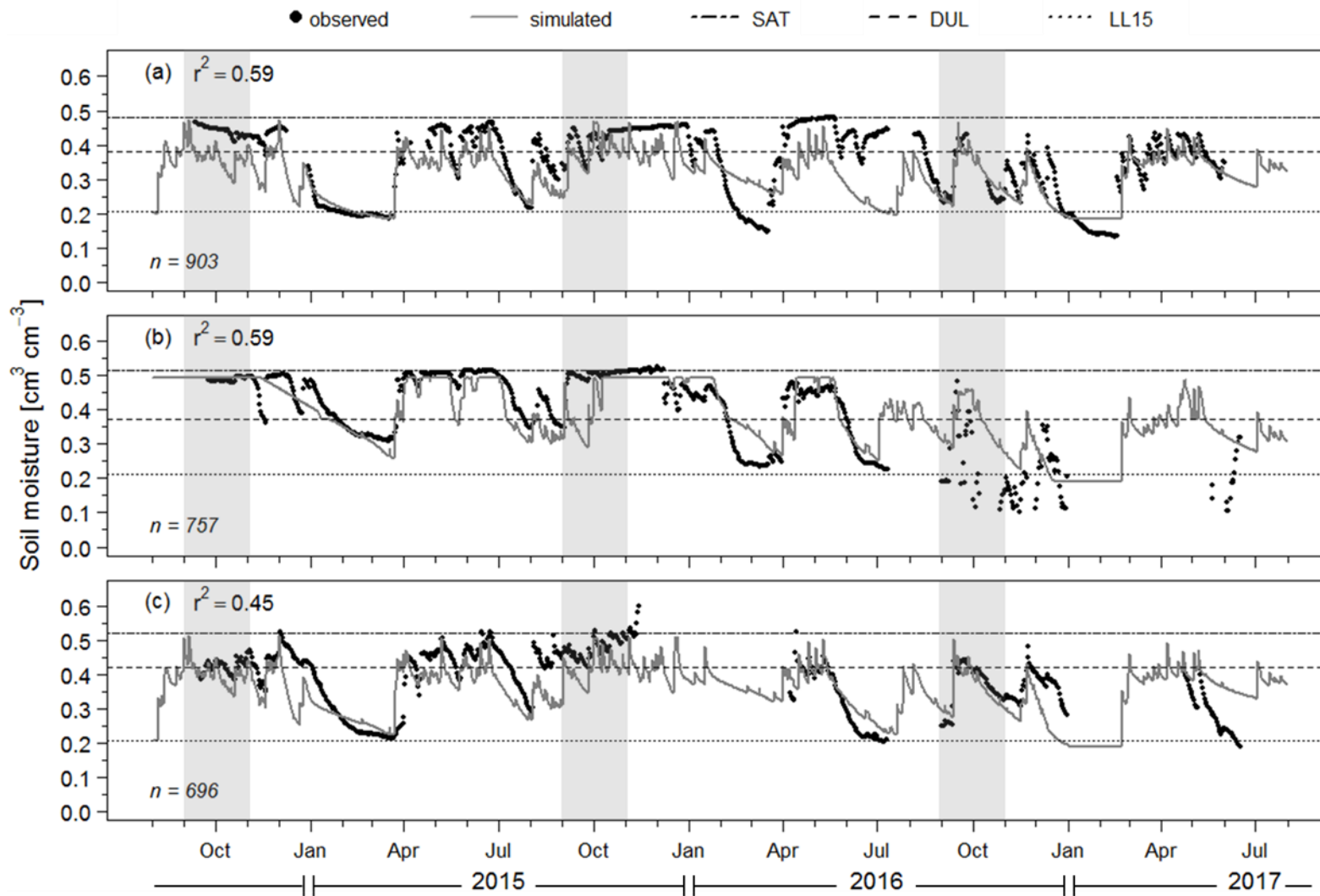
Figure 5.5 Observed (points, un-replicated) and simulated (lines) soil moisture dynamics in the non-amended baseline treatment (0N) and 10 cm depth at the inland valley's (a) valley-fringe, (b) mid-valley and (c) valley-bottom positions (2014-2017); volumetric water content at saturation (SAT), field capacity (DUL) and wilting point (LL15); the shaded areas (grey) indicate the main rice-growing periods (September to November).
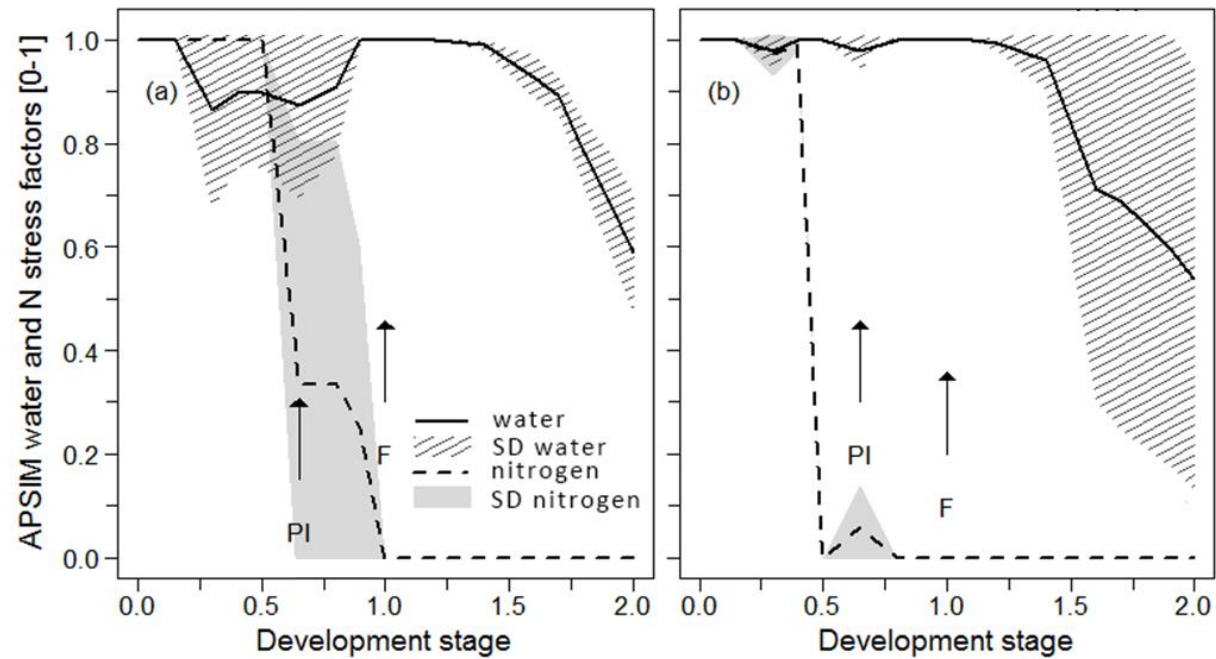
Figure 5.6 Simulated mean factor for water (solid line) and N stress (dotted line) (1= no stress, 0= severe stress) and the standard deviation (SD) according to phenological development stage in the non-amended baseline treatment (0N) at the floodplain's (a) fringe and (b) middle positions. Results based on the study period from 2015-2017 (*n*= 3). PI, panicle initiation; F, flowering.
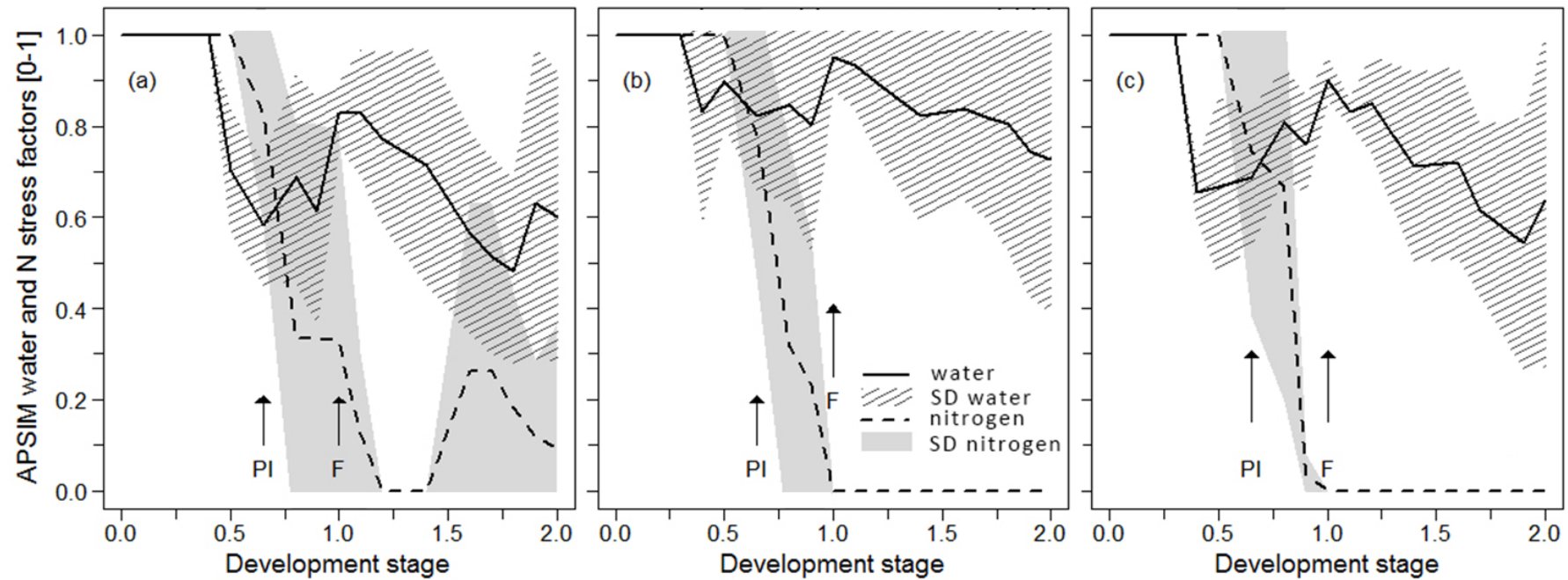
Figure 5.7 Simulated mean factor for water (solid line) and N stress (dotted line) (1= no stress , 0= severe stress) and the standard deviation (SD) according to phenological development stage in the non-amended baseline treatment (0N) at the inland valley's (a) valley-fringe, (b) mid-valley and (c) valley-bottom positions. Results based on the study period from 2014-2016 (*n*= 3). PI, panicle initiation; F, flowering.

5.1.4 Discussion

Evaluation of APSIM in contrasting lowland rice systems

APSIM performed well within the experimental uncertainty at both wetland types, field positions and treatments. Sound model performance was supported by several goodness-of-fit measures, e.g., a RMSEa of 0.92 and 0.78 Mg ha^{-1} for grain yield, comparing favourably to the observed standard deviation of 1.84 and 1.11 Mg ha^{-1} in the floodplain and inland valley, respectively. Similarly, total rice N uptake was simulated at a high level of accuracy particularly in the non-amended baseline treatments at both study sites, with r^2 of 0.95 and 0.79 in the floodplain and inland valley, respectively. Furthermore, the paired *t*-test confirmed that observed and simulated non-amended baseline yields were the same at a 95% confidence level, indicating that soil carbon dynamics and subsequent soil N supply were simulated accurately, which is considered a key performance criterion for cropping system models in low-input environments (Gaydon *et al.*, 2017).

Despite being a point-scale model, APSIM has further shown to perform accurately both in a temporally highly variable but spatially fairly homogenous floodplain as well as in a spatial-temporal highly heterogeneous inland valley provided external water table data were available as model input. Accurate depiction of soil water conditions in the floodplain, for example, was supported by the high level of accuracy in soil moisture simulation throughout the study period, with r^2 exceeding 0.85 in the fringe and 0.65 in the middle positions and in both 10 and 30 cm soil depth. Without the use of external water table data, APSIM underestimated rainfed rice yields on average by 2 Mg ha^{-1} in the floodplain and by 0.8 Mg ha^{-1} in the inland valley that, however, increased to 2.1 Mg ha^{-1} for the dry 2016 season with only 233 mm of seasonal rainfall. Therefore, results emphasised the importance of seasonally shallow water tables for rainfed lowland rice production and lowland rice modelling as they evidently mitigated extreme drought events in years of low and variable seasonal rainfall. Similarly, seasonally shallow water tables have shown to supply water for crop growth even during dry seasons in Southeast Asia (Belder *et al.*, 2007), and have been recognised as important water sources in lowland rice systems in West Africa (Schmitter *et al.*, 2015) and China (Cabangon *et al.*, 2004). Modelling lowland rice systems, local water table data may thus be provided from measurements or simulation using hydrological models like Hydrus-1D (Šimůnek *et al.*, 2013).

Reduced predictive accuracy, however, was observed in the simulation of certain phenological key stages in the floodplain and soil moisture dynamics in the inland valley but may be explained from seasonal abnormalities and experimental design limitations.

During the El Niño year of 2016, phenological predictions thus showed large deviations (>11 days) of key stages in the floodplain's fringe position. Irregular rainfall amount and distribution in 2016, comparatively early transplantation (about 3 weeks) of old seedlings (30 days) and a prolonged time to flowering and maturity (10-20 additional days) have been reported by Kwesiga *et al.* (2019). In slightly photoperiod-sensitive varieties, variation in sowing time and seedling age as well as low temperatures have shown to affect the time to flowering and thus maturity (Fukai, 1999). Due to the complexity of irregularities, however, a conclusive explanation of observed phenology is difficult. Serial planting trials could, therefore, help ascertain the interactions of temperature and photoperiod on the phenological development of SARO-5 and hence improve phenological development parameters in APSIM. Overall, however, model predictions were acceptable in 83% of all observations. In the inland valley, phenological and yield predictions were more accurate than the simulation of soil moisture dynamics, though temporal trends and magnitudes were simulated quite well. In a similar study, Feng *et al.* (2007) have related inaccurate soil moisture simulation to the time of state variable integration in the model. The time of integration in APSIM is one day and rainfall events may have occurred before or after integration of state variables. Furthermore, inaccurate soil moisture simulation has been related to spatially heterogeneous soil properties in inland valleys in Benin, particularly during dry periods, i.e., from a greater variability in soil properties as compared to crop variables (Worou *et al.*, 2012). While the coefficients of variances in measured crop yields ranged between 33-43%, measured variability in soil properties amounted to 24-80% (Gabiri *et al.*, 2017). Soil moisture measurements, however, were recorded un-replicated in a discrete field location and not causally related to soil properties, and were thus much harder to simulate at a high level of accuracy. The present study, however, lacked a high spatial resolution of field-level data to systematically explain or avoid such uncertainties. Additionally, lateral and subsurface inflows have shown to be important water balance components in sloped lowlands (Tsubo *et al.*, 2006). In the inland valley. lateral inflows evidently affected topsoil moisture dynamics, particularly in the valley-fringe position (Gabiri *et al.*, 2017) but were not available for model input. We, therefore, recommend to causally relate field-level soil texture, soil moisture, lateral inflow and water table data to improve yield and soil water predictions in highly heterogeneous and sloped lowlands. However, this would require extensive field instrumentation and data collection that might not be feasible for cash-limited research projects.

Despite such uncertainties from field data, APSIM performed well within the experimental uncertainty in both wetlands which is a key measure of acceptable model

performance (Gaydon *et al.*, 2017), and suggested that N x water stress interactions and their effects on yield were simulated adequately.

Effects of wetland type, field position & treatment on yield

In general, results have shown that improved cultural practices alone (varietal selection, row-transplanting, bunding, levelling and timely weeding) can increase regional yields substantially (4 Mg ha^{-1} compared to 1.8-2.2 Mg ha^{-1} in the floodplain, 2.7 Mg ha^{-1} compared to 1.8-1.9 Mg ha^{-1} in the inland valley), and reduce the current large yield gaps in floodplains (Senthilkumar *et al.*, 2020) and inland valleys (Nhamo *et al.*, 2014). Particularly bunding has been reported to reduce production risks from improved water retention during variable rainfall years in Tanzania (Raes *et al.*, 2007). Additionally, bunding has been reported to increase yields by about 1 Mg ha^{-1} in an inland valley in Benin (Worou *et al.*, 2013), and to improve rice N-responsiveness and reduce weed biomass in a small savanna valley in Côte d'Ivoire (Touré *et al.*, 2009).

In both wetlands, yields showed significant responses to applied mineral N fertiliser while only yields in the floodplain's fringe were significantly higher than the middle position and no toposequential effect on yield was observed in the inland valley. The lack thereof is likely the result of greater intra- than inter-toposequential yield variability from high observed standard deviations that can be explained by heterogeneous soil properties, a microscale topography and large spatial-temporal fluctuations of shallow water tables (Gabiri *et al.*, 2017). Therefore, yield pattern in the inland valley resulted from field- rather than toposequence-specific conditions, with differential responses to management and season as the seasonal rainfall variability was high (233-519 mm). Similar findings have been reported from inland valleys in Indonesia and Thailand (Boling *et al.*, 2008), and India (Cornish *et al.*, 2020). Meanwhile, attainable yields of >7.2 Mg ha^{-1} in the floodplain and of about 5.2 Mg ha^{-1} in the inland valley, were still substantially lower than simulated yield potentials of up to 10.5 and 7.3 Mg ha^{-1} in the floodplain and inland valley, respectively (Kwesiga *et al.*, 2020b). Overall higher yields and yield responses to applied N fertiliser in the floodplain as compared to the inland valley were associated to more favourable rainfall and hydro-edaphic conditions and varietal differences, i.e., greater inherent yield potentials of the lowland rice cv. SARO-5 as compared to the short-season, drought-resistant rainfed rice cv. NERICA-4.

However, the validated model can help to further differentiate the effects of hydro-edaphic field conditions on yield via spatial-temporal patterns of simulated water and N stress factors, and thus help guide management interventions (Inthavong *et al.*, 2011) and

assess risks to production (Boling *et al.*, 2007). In both wetlands, N stress exceeded water stress but varied from edaphic conditions, while water stress was more pronounced in the inland valley than the floodplain. These findings correspond to other studies that identified soil N deficiency coupled with low external N fertiliser rates as a main constraint to lowland rice productivity in East Africa (Tsujimoto *et al.*, 2019). Higher baseline yields in the wetlands' fringes were associated with lower N stress factors and correspond to more favourable topsoil C/N ratios. Furthermore, variations in soil aeration status could have stimulated SOM decomposition, resulting in higher soil N supply capacities (Kwesiga *et al.*, 2019). Moderate application of 60 kg N ha^{-1} resulted in significant and average yield gains of >2 and >0.8 Mg ha^{-1} while 120 kg N ha^{-1} and supplemental irrigation further increased yields by about 1.8 and 1.7 Mg ha^{-1} in the floodplain and in the inland valley, respectively. High N-responsiveness, particularly in the floodplain, was associated with sufficient soil P and K levels and the so-called priming effect in which applied N fertiliser helps overcome soil mineralisation barriers for increased plant N uptake (Liu *et al.*, 2017). Similarly, Niang *et al.* (2018) reported that N rather than P and K limit yields in rainfed lowlands in Benin.

Generally lower water stress in the floodplain than the inland valley was associated with higher seasonal rainfall amounts (562-1,033 mm) and higher water table supply capacities from greater hydraulic head gradients and soil water holding capacities (Bouman *et al.*, 2007). Spatial-temporal water stress patterns, however, indicated that supplemental irrigation is likely most beneficial during the vegetative and early reproductive stages in the floodplain's fringe and during the late reproductive and ripening stages in the floodplain's middle position. In the inland valley, spatial-temporal water stress patterns suggested beneficial effects of supplemental irrigation during the vegetative and reproductive stages in all field positions. However, the determination of both water and N stress factors inherently relies on experimentally-derived estimates in the model, i.e., the upper and lower soil-water tension limits for leaf expansion and potential crop N contents (Bouman *et al.*, 2001). Therefore, they encompass a certain level of uncertainty when used for new edaphic conditions and varieties but would otherwise require extensive additional field data collection that would have gone beyond the resources of this study.

Additionally, hydrological processes linked to seasonally shallow water tables at both wetland types and field positions potentially entail differential risks to crop production (Osujieke *et al.*, 2017), i.e., temporary drought-risk in the inland valley fringes and crop submergence risk in the floodplain's riparian from overbank flow. Subsurface interflows

from adjacent mountain ranges and overbank flows from a direct hydraulic connection to the river control seasonally shallow water tables in the floodplain's fringe and middle position, respectively (Burghof *et al.*, 2018). Therefore, the middle position is likely more prone to prolonged crop submergence with increasing river discharge amounts and to more erratic water table fluctuations in response to river water levels (Gabiri *et al.*, 2018b). Unfavourable rainfall pattern and erratic water table fluctuations may thus explain the high variability of late-season water stress factors that could have affected yields from increased spikelet sterility (Boling *et al.*, 2004). In the inland valley, seasonally shallow water tables resulted from lateral and subsurface inflows of adjacent valley slopes and local discharges from a deep groundwater table but showed high temporal and intra-toposequential variabilities and no distinct delineation (Gabiri *et al.*, 2019). Particularly lateral inflows are potentially benefiting upper toposequence positions, while higher water availabilities are usually reported from lower toposequence positions (Tsubo *et al.*, 2005). Additionally, Schmitter *et al.* (2015) ascertained higher production risks from prolonged crop submergence in the valley bottoms. However, no prolonged crop submergence was observed in the inland valley position during the study period which was likely the result of stream diversion for irrigation and/or drainage purposes from the original flow path and the subsequent effects on stream discharge amounts (Gabiri *et al.*, 2017).

5.1.5 Conclusion

This study showed that APSIM performed well within the bounds of the experimental error simulating rice responses to management treatments and variable hydro-edaphic conditions in two East African wetlands, provided external water table data (measured or simulated) were available as model input. While hydro-edaphic field conditions favoured the floodplain's fringe position, the lack of toposequential effect on yield from large spatial-temporal variabilities in the inland valley implied that management recommendations should be field- not toposequence-specific. The validated model can subsequently help to evaluate long-term effects of management and hydro-edaphic field conditions on yield, yield variability and associated production risks, and thus help to identify trade-offs between agronomic efficiencies and economic incentives of N fertiliser use for widespread adoption. Since this study, however, was restricted to two discrete study sites, management by hydro-edaphic interactions will likely differ within other East African lowland rice systems.

Highlights: Improved cultural practices can boost East African lowland rice yields substantially. The APSIM model adequately simulated rice performance using water table input

data. Low soil N was the main yield constraint but fertiliser responses were significant. Water stress was more pronounced in the inland valley and irrigation more beneficial. Hydro-edaphic field conditions modulated rice yields, particularly in the floodplain.

Author contributions: Conceptualization (K.G., D.G., M.B.), Methodology, (K.G., D.G., M.B.), Software (K.G., D.G.), Validation (K.G., D.G.), Formal analysis (K.G.), Investigation (K.G., S.Z., J.K.), Data curation (K. G., S.Z., J.K.), Writing-original draft preparation (K.G.), Writing-review and editing (K.G., D.G., M.B., M.L., S.Z., J.K., S.K., A.W.), Visualization (K.G.), Supervision (M.B.), Funding acquisition (M.B., M.L.), Resources (M.B., S.K.), Project administration (M.B.).

Conflicts of interest: The authors declare no conflict of interest. The founding sponsors had no role in the design of the study; in the collection, analyses, or interpretation of data; in the writing of the manuscript; or in the decision to publish the results.

5.2 Model-based evaluation of rainfed lowland rice responses to N fertiliser in variable hydro-edpahic wetlands of East Africa

Abstract

In East Africa, rainfed lowland rice is primarily produced by smallholders in alluvial floodplains of the lowlands and inland valley swamps of the highlands. These wetlands differ in terms of their dominant soil types and water regimes that vary seasonally, inter-annually and between field positions. Therefore, yield responses to mineral nitrogen (N) fertiliser likely vary between wetland types, field positions and years from variable hydro-edaphic conditions, and thus differentially affect agronomic yield gains and profitability of N fertiliser. The locally-validated APSIM model was thus used to simulate yield responses to mineral N fertiliser rates (0, 30, 60, 90, 120, and 150 kg N ha^{-1}) and supplemental irrigation at different field positions in a floodplain in Tanzania (fringe and middle positions) and an inland valley in Uganda (valley-fringe, mid-valley and valley-bottom positions) over a 30-year period. Average agronomic yield gains and N use efficiencies were high, ranging between 1.7-4.5 Mg ha^{-1} and 27-70 kg kg^{-1} in the floodplain and between 1.0-3.2 Mg ha^{-1} and 18-34 kg kg^{-1} in the inland valley, depending on field position, N rate and year, respectively. N fertiliser use was generally profitable in both wetlands, with value/cost ratios ≥4 and marginal rates of returns >150%. In the floodplain, profitable N rates were 30-120 kg N ha^{-1} in the fringe and 30-90 kg N ha^{-1} in the middle position in 100% of years, and 60-150 kg N ha^{-1} across all field positions in the inland valley in 77-100% of years. N fertiliser use among field positions in the inland valley, however, was comparatively riskier in the valley-fringe position. Since supplemental irrigation, however, increased yields substantially beyond N rates of 60 kg N ha^{-1} it may thus help boost N fertiliser use efficiencies and profitability. Additionally, spatial-temporal water stress pattern may help guide efficient irrigation scheduling.

Keywords: APSIM, floodplain, inland valley, mineral N fertiliser, *Oryza* spp.

5.2.1 Introduction

Across East Africa, wetlands are considered sites of largely untapped potential for lowland rice intensification from sustained water supply and comparatively fertile soils (Haefele *et al.*, 2013). Covering about 3-5% of the total land area, predominant wetland types are alluvial floodplains and narrow inland valleys (Leemhuis *et al.*, 2016). Alluvial floodplains are characterised by periodic flooding regimes from river spill-overs, while inland valleys are characterised by seasonal water-logging from subsurface interflows and surface run-off from adjacent valley slopes (Sakané *et al.*, 2014). Both wetland types are generally considered favourable for lowland rice production (Balasubramanian *et al.*, 2007). However, indiscriminate agricultural use of wetlands must be avoided in view of minimizing the risks of soil degradation, hydrological alterations and diminishment of ecosystem services (Rodenburg, 2013; Rodenburg *et al.*, 2014).

Regional focal areas for lowland rice intensification are the Kilombero floodplain in Tanzania and the numerous valley bottomlands in central Uganda. While the Kilombero floodplain is Tanzania's largest rice-growing area (Senthilkumar *et al.*, 2018), rice production in Uganda has only recently started shifting into inland valleys (Sakané *et al.*, 2013). Current average rice yields remain low, ranging between 1.1 and 1.8 Mg ha^{-1} under rainfed and between 1.4 and 1.9 Mg ha^{-1} under irrigated lowland conditions in Tanzania and Uganda, respectively (Diagne *et al.*, 2013). Meanwhile, yield gaps of 30-90% have been reported, i.e. the gap between actual and potential yields, emphasising the substantial scope to increase lowland rice production (Senthilkumar *et al.*, 2020). Commonly, yield gaps are associated to sub-optimal crop, land and soil fertility management (Mghase *et al.*, 2010; Miyamoto *et al.*, 2012). Thus, soil N deficiency a main production constraint (Saito *et al.*, 2019), accelerated regionally from zero to marginal mineral N fertiliser use, with maximum applied mineral N rates of <50 kg N ha^{-1} (Fungo *et al.*, 2013; Senthilkumar *et al.*, 2020).

Limited mineral N fertiliser use is associated with lack of credit, while investments are further discouraged by volatile markets, high input prices and unreliable returns from high yield variabilities (Crawford *et al.*, 2003). Therefore, regional lowland rice farmers are generally risk-averse (Ruhinduka *et al.*, 2020), and fertiliser recommendations need to consider the economic viability to increase widespread adoption (Daudu *et al.*, 2018; Posner & Crawford, 1992). Meanwhile, lowland rice in the Kilombero floodplain and the inland valleys of central Uganda is predominantly produced under rainfed conditions (Haneishi *et al.*, 2013a; Senthilkumar *et al.*, 2018), and thus reliant on water supply from seasonal rainfall and shallow water tables (Diagne *et al.*, 2013). However, field-level water

regimes vary between and within wetlands and years from variable hydro-edaphic conditions, both in floodplain (Kwesiga *et al.*, 2019) and inland valley wetlands (Touré *et al.*, 2009). Consequently, variable water regimes differentially affect soil-forming processes through erosion, leaching and deposition (Haefele *et al.*, 2008), and often lead to soil fertility gradients within the upland-lowland continuum (Boling *et al.*, 2008). Similarly, the risks of seasonal drought and/or submergence vary from field-level water regimes (Schmitter *et al.*, 2015), particularly since water-control structures from simple field bunding to drainage channels are largely absent at both focal areas (Haneishi *et al.*, 2013c; Raes *et al.*, 2007). In fact, unprofitable fertiliser use related to unreliable water regimes and sub-optimal crop management have been widely reported across rainfed lowland rice systems in SSA (Touré *et al.*, 2009), emphasising the insufficiency of blanket fertiliser recommendations (Arouna *et al.*, 2021; Nhamo *et al.*, 2014).

Meanwhile, long-term agronomic field data is generally scare in both focal areas since studies are usually only conducted for a limited number of seasons, management practices and environmental conditions (Kwesiga *et al.*, 2019). Since rainfed lowland rice production is particularly vulnerable to temporal rainfall variability (Niang *et al.*, 2018), well-adapted management recommendations are difficult to derive from short-term field experiments (Akponikpè *et al.*, 2010). Well-tested crop models, however, can be time- and cost-efficient tools to complement experimental results from site-specific studies by simulating most important biophysical processes (crop growth, soil water and N dynamics) (Mohanty *et al.*, 2020). Using long-term historical climate data, validated crop models can thus simulate differentiated yield responses to imposed management practices and environmental conditions (Khaliq *et al.*, 2019), and aid the identification of optimum management practices (Balwinder-Singh *et al.*, 2016). The Agricultural Production System Simulator (APSIM) is one such crop model that has been validated and used to simulate rice responses to a broad range of soils, climates and management practices worldwide (e.g. Gaydon *et al.*, 2017; Poulton *et al.*, 2015; Subash *et al.*, 2015). However, to date, APSIM has not been used for long-term scenario analyses of N fertiliser use rates in variable hydro-edaphic rainfed lowland rice systems of East Africa. This, however, seems to be of particular importance since field positions within the respective lowland system are anticipated to differentially affect rice responses to mineral N applications and thus modulate agronomic efficiencies and economic incentives for N fertiliser adoption. Therefore, the objectives of this study were to use the locally-validated APSIM model (Grotelüschen *et al.*, 2021) to assess (i) the agronomic efficiencies of N rates and fertiliser profitability under rainfed conditions, (ii) the effects of field positions and seasonal water

availabilities on crop water stress and yield, and (iii) the effects of supplemental irrigation on yield in two representative variable hydro-edaphic lowland rice systems of East Africa.

5.2.2 Material and Methods

Research locations

Simulation experiments were performed in (i) an alluvial floodplain in Ifakara in south-central Tanzania (8.10°-8.18°S and 36.67°-36-76°E, 255 masl), and (ii) an inland valley swamp at the Namulonge *National Crops Resources Research Institute* (NaCRRI) in central Uganda (0.519°-0.522°N and 32.640°-32.644°E, 1,105 masl). The Kilombero floodplain in Tanzania covers 7,967 km^2 within a 40,240 km^2 catchment area and is surrounded by the Udzungwa Mountains to the northwest and the Mahenge Highlands and Mbarika Mountains to the southwest (Msofe *et al.*, 2019). Rice production is the most important economic activity, followed by sugarcane production, fishing and livestock husbandry (Thonfeld *et al.*, 2020). The inland valley in Uganda covers about 4.5 km^2 within a 31.1 km^2 catchment area and is one of the headwater micro-catchments of the Lake Kyoga basin (Gabiri *et al.*, 2020). The regional landscape is undulating with flat-topped hills dissected by swampy bottomlands (Nsubuga *et al.*, 2011). Located along a rural-urban gradient, the inland valleys have increasingly been exposed to human activities with a mosaic-type agricultural land use and management (Gabiri *et al.*, 2017).

The APSIM model (v. 7.5)

APSIM is a modular simulation framework allowing the versatile specification of management options and simulation of agricultural system performance (Gaydon *et al.*, 2021). For rice-based cropping systems, the five modules used were Oryza, SurfaceOM, SoilWat, SoilN and Pond. Oryza integrates rice physiological routines of the ORYZA2000 model (Bouman *et al.*, 2001) to simulate rice development, growth, water- and N-uptake, abiotic stresses (water, N and temperature stress), and the responses thereof (Zhang *et al.*, 2007). However, Oryza is using the APSIM soil modules rather than the original ORYZA2000 soil routines (Gaydon *et al.*, 2012b; Gaydon *et al.*, 2012a). SurfaceOM was developed by Probert *et al.* (1995) and is described in detail by Thorburn *et al.* (2001). SoilWat is a cascading water balance model and SoilN simulates soil C and N transformations, described in detail by Probert *et al.* (1998). For temporarily or permanently flooded soil conditions, both SoilWat and SoilN were modified (Gaydon *et al.*, 2012a), and Pond developed to simulate key chemical and biological processes under ponded conditions (Gaydon *et al.*, 2012b).

Simulations

The locally calibrated and validated APSIM model (Grotelüschen *et al.*, 2021) was used to study the effects of N rates, variable hydro-edaphic field conditions and supplemental irrigation on rice performance and N fertiliser profitability in contrasting rainfed lowland rice systems of East Africa using long-term climate data.

The simulations were performed over 30-years of historic daily climate data (1980-2010) obtained from the *Kilombero Agricultural Training and Research Institute* (KATRIN) in Ifakara and Sokoine University in Morogoro, Tanzania for the floodplain wetland, and from the NaCRRI in Namulonge, Uganda for the inland valley wetland. **Table 5.4** presents mean monthly data during the main rice-growing season at both research locations.

The model was calibrated for the lowland rice variety SARO-5 in the floodplain and the rainfed rice variety NERICA-4 in the inland valley, and variety-specific phenological development parameters and partitioning coefficients are provided in Grotelüschen *et al.* (2021). Rice nurseries were established with the onset of the rainy seasons in alignment with common local practices, i.e., after ≥50 mm of rainfall from the end of January in the floodplain and ≥35 mm from mid-August in the inland valley over a 7-day period. Rice seedlings were transplanted 21 days after sowing with two seedlings per hill at 20x20 cm spacing in the floodplain and three seedlings per hill at 15x30 cm spacing in the inland valley. Prior to transplanting, fields were ploughed, puddled and irrigated once (40 mm). The effects of a plough-pan from puddling on soil properties were considered both by reducing the vertical water flow rate (by a factor of two), and by increasing the bulk density by 5% at 30 cm depth (Gathala *et al.*, 2011). According to field observations, weeds were allowed to grow simultaneously during the rice-growing season and as a weedy fallow. The APSIM weed cultivar '*perennial_grass*' was planted at an density of 20 and 15 plants m^{-2} at the beginning and at the end of the rice-growing season in the floodplain and inland valley, respectively. During the rice-growing season, weeds were removed at 3, 6 and 9 weeks after transplanting at an efficiency of 80%, mimicking manual hand-weeding. Post-harvest and pre-sowing, rice, weed and algae residues were incorporated to 30 cm depth, assuming a C/N ratio of 80 for rice and 20 for weed and algae residues.

Within each wetland, different hydrological and toposequence field positions were considered, i.e. with increasing distance to the river at the fringe and middle positions in the floodplain (Kwesiga *et al.*, 2019), and as a toposequence valley cross-section at the valley-fringe, mid-valley and valley-bottom positions in the inland valley (Gabiri *et al.*, 2017). Soil properties of the heavy-textured Fluvisols in the floodplain and the loamy-textured Gleysols in the inland valley are presented in Grotelüschen *et al.* (2021). The

Fluvisols had a plant-available water capacity (PAWC) of 53 and 35 mm in the puddled soil profile (0-30 cm) in the floodplain's fringe and middle positions, respectively. The Gleysols had a PAWC of 48, 44 and 64 mm in the valley-fringe, mid-valley and valley-bottom positions, respectively. Among both wetland sites and field positions, soil N contents were generally low but slightly above the critical N content for rice growth of 2 g kg^{-1}, similarily plant-available P and exchangeable K contents were above the critical limits of <8 mg P kg^{-1} and <60 mg K kg^{-1}, respectively (Senthilkumar *et al.*, 2018). Previously, Grotelüschen *et al.* (2021) emphasised the importance of field-level water table data as model input for sound model performance in rainfed lowland rice systems. Due to the lack of long-term water table data, simulations used measured daily field-level water table data from the floodplain (2015-2017) and the inland valley (2015-2016) as model input (Grotelüschen *et al.*, 2021). Measured daily water table data were reproduced recurrently over the 30-year simulation period (sequence 1) and additionally by alternating the data record by one year to account for year-to-year variability (sequence 2).

Scenario analysis

Six different mineral N fertiliser rates were simulated: 0, 30, 60, 90, 120, and 150 kg ha^{-1}. N rates were selected in alignment with previous studies (Grotelüschen *et al.*, 2021), however, additionally including decrement or increment rates of 30 kg ha^{-1} below and above 60 and 120 kg ha^{-1}. N was applied as urea-N (46% N) in two equal split applications at transplanting and panicle initiation (PI). Rice responses to N rates were determined under rainfed and irrigated production conditions. Under irrigated conditions, supplemental irrigation was triggered as soon as the ponded water level receded to 0 cm, and 30 mm of water were applied per irrigation event between transplanting and two-weeks prior physiological maturity.

Table 5.4 Mean monthly maximum and minimum temperatures and solar radiation, and mean monthly total rainfall during the main rice-growing season between 1980 and 2010 at the floodplain, Tanzania (top) and the inland valley, Uganda (bottom).

Site	Month	Temperature [°C]				Radiation [MJ m^{-2} day^{-1}]		Rainfall [mm]		
		maximum		minimum						% annual rainfall
Floodplain, Tanzania [a]	February	32.5	(30.9 - 34.6) [c]	22.2	(20.8 - 23.9) [c]	21.0	(14.6 - 24.4) [c]	207	(14 - 470) [c]	13.0
	March	31.9	(30.8 - 33.8)	22.1	(21.2 - 23.2)	19.9	(17.3 - 24.2)	345	(56 - 617)	21.2
	April	30.2	(28.6 - 32.1)	21.6	(19.9 - 22.6)	17.5	(14.0 - 19.4)	392	(160 - 565)	24.2
	May	28.9	(27.4 - 30.8)	20.0	(18.7 - 21.2)	15.7	(12.9 - 18.3)	140	(2 - 309)	8.8
	June	28.0	(26.7 - 31.4)	17.2	(15.2 - 18.8)	16.1	(13.5 - 17.9)	21	(0 - 79)	1.3
Inland valley, Uganda [b]	August	28.0	(26.4 - 30.7) [c]	16.4	(14.9 - 17.9) [c]	18.3	(16.6 - 20.0) [c]	96	(45 - 169) [c]	7.7
	September	28.3	(27.0 - 30.0)	16.6	(15.0 - 18.2)	19.1	(16.2 - 22.1)	128	(49 - 224)	10.2
	October	28.4	(26.9 - 30.9)	17.0	(16.1 - 18.1)	18.2	(16.5 - 20.2)	154	(92 - 255)	12.3
	November	28.4	(27.2 - 30.2)	17.1	(15.9 - 18.6)	18.1	(14.8 - 20.2)	141	(61 - 265)	11.0
	December	28.9	(27.4 - 31.7)	17.0	(15.9 - 19.5)	19.2	(16.3 - 21.4)	82	(34 - 188)	6.5

[a] for the study site in the floodplain (Tanzania), rainfall data were obtained from the KATRIN in Ifakara, and temperature and radiation data from the Sokoine University in Morogoro.

[b] for the study site in the inland valley (Uganda), climate data were obtained from the NaCRRI in Namulonge.

[c] values in parenthesis represent the range.

Assessment of model variables

Agronomic efficiency & yield stability analysis

Analysed model outputs included grain yield and daily water deficit factors. Thus, agronomic yield gains (Mg ha^{-1}, Eq. (1)) (Saito *et al.*, 2021), agronomic N use efficiencies (NUE$_a$, kg kg^{-1}, Eq. (2)) (Feng *et al.*, 2020), and the yield instability index (INI, -, Eq. (3)) (Bahri *et al.*, 2019) were calculated as:

$$\text{Agronomic yield gain} = GY_x - GY_0 \tag{1}$$

$$NUE_a = \left[(GY_x - GY_0)/x \right] \tag{2}$$

$$INI = CV * \sqrt{1 - r^2} \tag{3}$$

With GY$_x$ – the grain yield with mineral N fertiliser application (Mg ha^{-1}), GY$_0$ – the grain yield without mineral N fertiliser application (Mg ha^{-1}), x – the urea-N fertiliser rate (kg ha^{-1}), CV - the coefficient of variation (%), and r^2 - the coefficient of determination (%). The INI measures the degree of deviation from the underlying trend, indicating whether yields are becoming more stable or instable over time. Yield instability is defined as 'low' between 0 and 15, as 'medium' between >15 and <30, and as 'high' >30 (Sihmar, 2014). Additionally, daily simulated water deficit factors and their spatial-temporal pattern were assessed (1 = no stress, 0 = severe stress). Water stress is expressed as a reduction in leaf expansion and calculated as a function of the soil-water tension in the root zone, i.e., water deficits from actual to potential water contents (Boling *et al.*, 2007). Up until flowering, water stress affects the relative leaf growth and thus the photosynthesis rates and yield, while it accelerates leaf senescence after flowering (Bouman *et al.*, 2001). Under rainfed conditions, seasonal water availabilities (mm) during the reproductive phase from PI to flowering were additionally determined from the simulated extractable soil water in the soil profile at PI plus the rainfall from PI to flowering.

Partial gross margin analysis

A partial gross margin analysis on the use of mineral N fertiliser rates was performed. The analysis included the calculation of marginal costs (MC, USD ha^{-1} season^{-1}), considering the costs of fertiliser purchase, transport, application and additional harvesting costs that were assumed to equal half of the harvesting costs, and marginal revenues (MR, USD ha^{-1} season^{-1}), considering regionally reported paddy rice farm-gate prices (farm-gate, USD Mg^{-1}) (**Table 5.5**). At both sites, the input/output ratio, i.e., the ratio of kg N fertiliser costs to

kg grain price, was thus favourably low (between 4-5) and below the critical threshold of 10 (Yanggen *et al.*, 1998). Evaluated economic indicators included net returns (NR, USD ha^{-1} season^{-1}, Eq. (4)), marginal rates of return (MRR, %, Eq. (5)), and the value/cost ratio (VCR, -, Eq. (6)) (Evans, 2005; Fermont *et al.*, 2010), and were calculated as:

$$NR = (GY * \text{farm-gate}) - MC \tag{4}$$

$$MRR = ((MR_x - MR_{x-1})/(MC_x - MC_{x-1})) * 100 \tag{5}$$

with

$$MC = (\text{fertiliser purchase} + \text{transport} + \text{application} + \text{extra harvesting costs})$$

$$MR = (GY_x - GY_0) * \text{farm-gate}$$

$$VCR = (MR_x/MC_x) \tag{6}$$

With GY – the grain yield under the respective management (Mg ha^{-1}), GY_x – the grain yield with N fertiliser (Mg ha^{-1}), GY_0 - the gain yield without mineral N fertiliser application (Mg ha^{-1}), x - the N fertiliser rate under comparison (kg ha^{-1}), x-1 - the respective lower N fertiliser rate (kg ha^{-1}). MRR (%) was expressed as a percentage, and considered favourable when ≥150% (Evans, 2005). For smallholder farmers in developing countries, a VCR ≥2 is often considered sufficient incentive to adopt a new management practice (Fermont *et al.*, 2010), although also depending on the absolute profit margins. In high-risk production environments, however, a VCR ≥4 has been reported a more appropriate threshold for successful adoption (Okebalama *et al.*, 2016).

Statistical analysis

Model outputs were analysed in terms of agronomic yield gains, NUEa, INI and partial gross margins of N rates (VCR, MRR), and yield responses to supplemental irrigation among field positions in an East African floodplain and inland valley wetland. Data were subjected to an analysis of variance (ANOVA), using the R software (3.6.3) with a factorial design, keeping N rates and field positions as factors and seasons as replicates. Differences between field positions and N rates were additionally evaluated using Tukey's HSD test for multiple mean comparison at a 95% confidence level (p ≤0.05). Data analysis over the simulation period included the number of seasons (n= 31 in the floodplain in Tanzania, n= 30 in the inland valley in Uganda), treatments (n= 6), and water table sequences (n= 2).

Table 5.5 Marginal costs and marginal revenues considered for the partial gross margin analysis for fertiliser use at the floodplain in Tanzania (top) and the inland valley in Uganda (bottom).

Site	Marginal costs (MC)		Marginal revenues (MR)		Exchange rate to 1 USD [c]
Floodplain, Tanzania [a]	50 kg urea-N	60,000 TZS	farm-gate	650,000 TZS Mg^{-1}	1,998 TZS
	transport	1,998 TZS/50 kg N			
	application	14,000 TZS			
	harvest	60,000 TZS			
Inland valley, Uganda [b]	50 kg urea-N	115,000 UGX	farm-gate	1,000,000 UGX Mg^{-1}	3,137 UGX
	transport	3,137 UGX/50 kg N			
	application	32,500 UGX			
	harvest	181,500 UGX			

[a] personal communication, Michael Winklmaier, AfricaRice (2014).
[b] personal communication, Masao Kikuchi, Chiba University, Japan (2010), Miyamoto *et al.*, 2012.
[c] average exchange rate between 2015-2017.

5.2.3 Results

Agronomic efficiencies of N rates & fertiliser profitability

Agronomic yield gains from N fertiliser use varied between >0.5 and <7.0 Mg ha^{-1}, depending on wetland type, field position, N rate and season (**Figure 5.8**, **Figure 5.9**). Agronomic yield gains were generally lower but less variable in the inland valley than the floodplain, with average agronomic yield gains of 2.2 and 3.6 Mg ha^{-1}, respectively (**Figure 5.8, Figure 5.9**).

In the floodplain, the effect of field position on average agronomic yield gains was marginal and not significant (**Figure 5.8**). However, while the application of 30 kg N ha^{-1} resulted in higher average agronomic yield gains in the middle (2.1 Mg ha^{-1}) than fringe position (1.8 Mg ha^{-1}), average agronomic yields gains with increasing N rates were generally higher in the fringe as compared to the middle position (**Figure 5.8**). Agronomic yield gains, however, were only marginal and not significant from N rates beyond 120 kg ha^{-1} in the fringe and 90 kg ha^{-1} in the middle position (**Figure 5.8**). Yields were generally highest and less variable with 150 kg N ha^{-1}, and higher in the fringe (8.4 Mg ha^{-1}) with a CV of 8.8% than the middle position (7.9 Mg ha^{-1}) with a CV of 11.5% (**Table 5.6**). NUE$_a$ were highest at the lowest N rate of 30 kg ha^{-1} (59 and 70 kg kg^{-1} in the fringe and middle position, respectively), and decreased subsequently, while the INI indicated highest yield instability with 30-60 kg N ha^{-1} with values of between 16.4 to 12.4 (**Table 5.6**). MRR were highest with 60 kg N ha^{-1} at the fringe (>2,400%) and with 30 kg N ha^{-1} at the middle position (>2,200%), while the highest VCRs were attained with 90 kg N ha^{-1} in the fringe (14.3) and 60 kg N ha^{-1} in the middle position (14.5) (**Table 5.6**). Generally, however, all N rates obtained average VCR's ≥4 in >100% of years (**Table 5.6**).

In contrast, the effect of field position on average agronomic yield gains was significant in the inland valley, with average agronomic yield gains of 2.0, 2.3 and 2.3 Mg ha^{-1} in the valley-fringe, mid-valley and valley-bottom position (**Figure 5.9**). Average agronomic yield gains from 30 kg N ha^{-1} varied only slightly among field positions with about 1.0 Mg ha^{-1}, while agronomic yield gains from 150 kg N ha^{-1} were substantially higher in the mid-valley position (3.2 Mg ha^{-1}) as compared to the valley-fringe (2.7 Mg ha^{-1}) and valley-bottom positions (3.0 Mg ha^{-1}) (**Figure 5.9**). Additionally, average agronomic yield gains were significant up to N rates of 150 kg ha^{-1} across all field positions (**Figure 5.9**). Maximum yields amounted to 5.2 Mg ha^{-1} at the valley-fringe, 5.7 Mg ha^{-1} at the valley-bottom and 6.4 Mg ha^{-1} at the mid-valley position from 150 kg N ha^{-1} (**Table 5.7**). Maximum NUE$_a$ were obtained with 30 kg N ha^{-1}, ranging between 31 and 34 kg kg^{-1}

across field positions (**Table 5.7**). The INI indicated yields were becoming more instable in the valley-fringe and -bottom positions and more stable in the mid-valley position with increased N rates (**Table 5.7**). Highest MRR were uniformly obtained from 60 kg N ha^{-1} (>1,150%), while the VCR was highest between 90-120 kg N ha^{-1} and ranged between 5.0 and 5.9 (**Table 5.7**). Obtained VCRs were highest in the mid-valley position, but did not exceed the minimum threshold of 4 with 30 kg N ha^{-1} across all field positions. Comparatively lower VCRs and higher percentage of years with a VCR <4 were attained in the valley-fringe position **(Table 5.7)**.
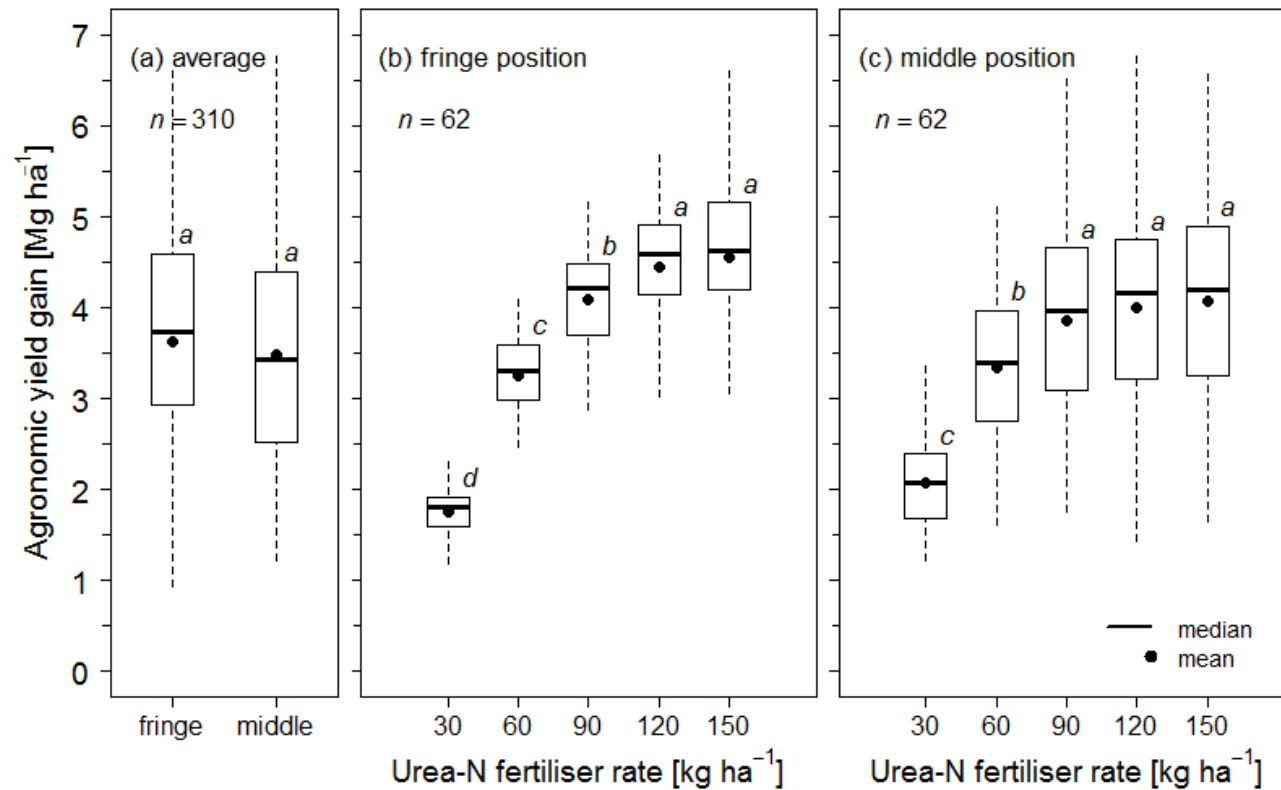
Figure 5.8 Average agronomic yield gains from mineral N fertiliser use under rainfed conditions in the floodplain in Tanzania. Different letters indicate significant differences according to the Tukey`s HSD test ($p \leq 0.05$) at (a) the average yield responses to field position, and yield responses from field position, and yield responses to mineral N fertiliser rates at the (b) fringe and (c) middle position.
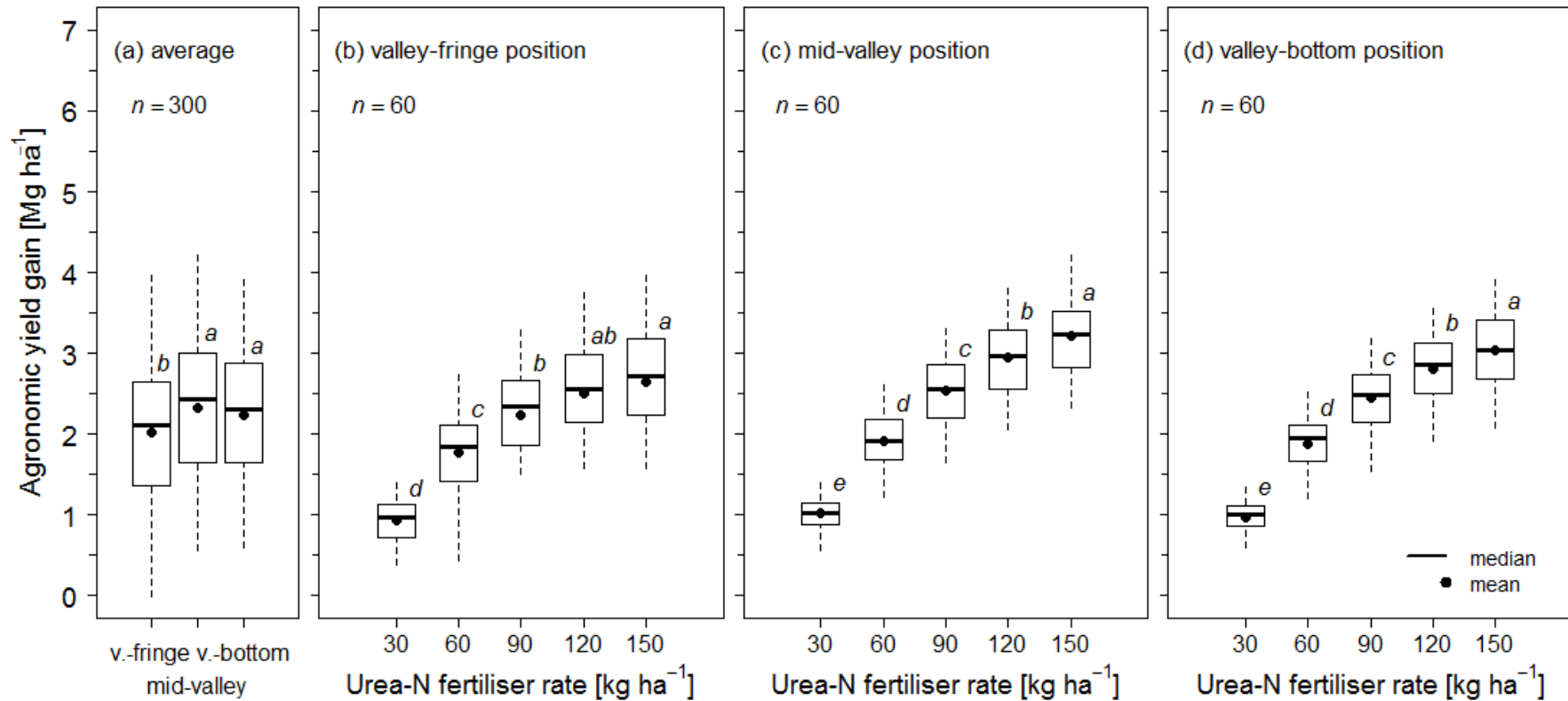
Figure 5.9 Average agronpomic yield gains from mineral N fertiliser use under rainfed conditions in the inland valley in Uganda. Different letters indicate significant differences according to the Tukey's HSD test ($p \leq 0.05$) at (a) the average yield responses from field position, and yield responses to mineral N fertiliser rates at the (b) valley-fringe, (c) mid-valley and (d) valley-bottom position.

Table 5.6 Average agronomic and economic evaluation of mineral N fertiliser rates under rainfed conditions during the simulation period (1980-2010), and according to field positions in the floodplain in Tanzania.

Field position	urea-N	Grain yield		NUE$_a$		INI	NR	MRR	VCR	Years with VCR ≥4
	[kg ha^{-1}]	Mean [Mg ha^{-1}]	CV [%]	[kg kg^{-1}]		[-]	[US\$ season^{-1} ha^{-1}]	[%]	[-]	[%]
fringe	0	3.9 e	18.6	-		17.5	1,240.2	-	-	-
	30	5.6 d	15.2	58.5 a		14.9	1,773.4	1,916.4	10.2	100.0
	60	7.1 c	12.6	54.4 b		12.4	2,244.6	2,468.5	14.1	100.0
	90	8.0 b	10.3	45.5 c		10.1	2,497.6	1,403.2	14.3	100.0
	120	8.3 ab	9.2	37.1 d		8.9	2,596.1	516.3	12.9	100.0
	150	8.4 a	8.8	30.4 e		8.4	2,609.4	74.0	11.4	100.0
middle	0	3.8 d	22.5	-		21.9	1,229.8	-	-	-
	30	5.9 c	16.8	69.5 a		16.4	1,870.3	2,249.7	12.1	100.0
	60	7.2 b	12.8	55.8 b		12.6	2,263.0	2,057.7	14.5	100.0
	90	7.7 a	11.7	42.9 c		11.7	2,412.3	827.9	13.5	100.0
	120	7.8 a	11.9	33.4 d		11.9	2,440.7	148.7	11.6	100.0
	150	7.9 a	11.5	27.2 e		11.5	2,444.5	21.4	10.2	100.0
Anova probabilities for the effects of										
Field position (E)		0.001	-	NS		NS	0.001	0.010	NS	-
Fertiliser-N (M)		0.001	-	0.001		0.001	0.001	0.001	0.001	-
E x M		0.010	-	0.001		0.001	0.010	0.010	0.001	-

CV, coefficient of variation; NUE$_a$, agronomic N use efficiency; INI, yield instability index; NR, net return; MRR, marginal rate of return; VCR, value/cost ratio.

Table 5.7 Average agronomic and economic evaluation of mineral N fertiliser rates under rainfed conditions during the simulation period (1980-2010), and according to field positions in the inland valley in Uganda.

Field position	urea-N	Grain yield		NUE$_a$		INI	NR	MRR	VCR	Years with VCR ≥4
	[kg ha^{-1}]	Mean [Mg ha^{-1}]	CV [%]	[kg kg^{-1}]		[-]	[US$ season^{-1} ha^{-1}]	[%]	[-]	[%]
valley-fringe	0	2.5 e	14.7	-		13.6	770.7	-	-	-
	30	3.5 d	14.0	31.0	a	14.0	1,009.9	813.3	3.2	30.0
	60	4.3 c	15.8	29.5	a	15.4	1,254.0	1,162.2	4.9	80.0
	90	4.8 b	16.1	24.9	b	15.6	1,382.7	685.0	5.2	90.0
	120	5.0 ab	16.7	20.9	c	16.1	1,446.6	377.8	5.0	86.7
	150	5.2 a	17.4	17.6	c	18.4	1,467.2	193.8	4.7	76.7
mid-valley	0	3.2 f	10.7	-		9.8	975.2	-	-	-
	30	4.2 e	6.9	33.9	a	7.0	1,242.2	886.8	3.6	20.0
	60	5.1 d	5.7	31.9	a	5.5	1,505.6	1,245.8	5.3	100.0
	90	5.7 c	5.9	28.2	b	5.5	1,683.2	907.6	5.9	100.0
	120	6.1 b	6.2	24.6	c	5.5	1,789.4	561.9	5.9	100.0
	150	6.4 a	6.7	21.4	d	6.0	1,851.2	381.2	5.6	100.0
valley-bottom	0	2.7 e	12.8	-		10.1	825.7	-	-	-
	30	3.7 d	10.2	32.5	a	9.7	1,079.6	845.8	3.4	20.0
	60	4.6 c	10.6	31.5	a	10.2	1,347.2	1,264.0	5.3	90.0
	90	5.1 b	10.8	27.2	b	10.4	1,504.3	814.4	5.7	100.0
	120	5.5 a	10.7	23.4	c	10.2	1,595.3	495.9	5.6	100.0
	150	5.7 a	11.1	20.2	d	13.9	1,645.8	329.8	5.3	100.0
Anova probabilities for the effects of										
Field position (E)	0.001		-	0.001		0.001	0.001	0.001	0.001	-
Fertiliser-N (M)	0.001		-	0.001		0.001	0.001	0.001	0.001	-
E x M	0.001		-	NS		NS	0.001	0.050	0.001	-

CV, coefficient of variation; NUE$_a$, agronomic N use efficiency; INI, yield instability index; NR, net return; MRR, marginal rate of return; VCR, value/cost ratio.

Production risks from seasonal water stress & rainfall

In APSIM, water deficit factors closer to 1 indicate lower water stress, while water deficit factors closer to 0 indicate more severe water stress. Generally, simulated water stress was more pronounced in the inland valley as compared to the floodplain (**Figure 5.10Figure 5.11**). In the floodplain, average water stress patterns from PI to flowering were similar among field positions, with averages of 0.90 at the time of PI (**Figure 5.10**). In the inland valley, average water stress incrementally increased from the time of PI to flowering across all field positions, but more so in the valley-fringe (from 0.80 to 0.65) followed by the valley-bottom (from 0.90 to 0.85) and mid-valley positions (from 0.80 to 0.75) (**Figure 5.11**).

Consequently, yields correlated more with seasonal water availabilities in the inland valley as compared to the floodplain (**Figure 5.12**). Findings indicate yields largely plateau beyond 700 mm of seasonally available water (**Figure 5.12**). In comparison, average rainfall during the main rice-growing season alone largely exceeded 750 mm in the floodplain against below 425 mm in the inland valley (**Table 5.4**), thus, yield responses were less correlated to seasonal water availabilities in the floodplain (**Figure 5.12**). In the inland valley, asymptotic yield increase was most pronounced in the valley-fringe position, and yields highest between 600-700 mm and lowest between 400-500 mm of available water during the reproductive phase (**Figure 5.12**).
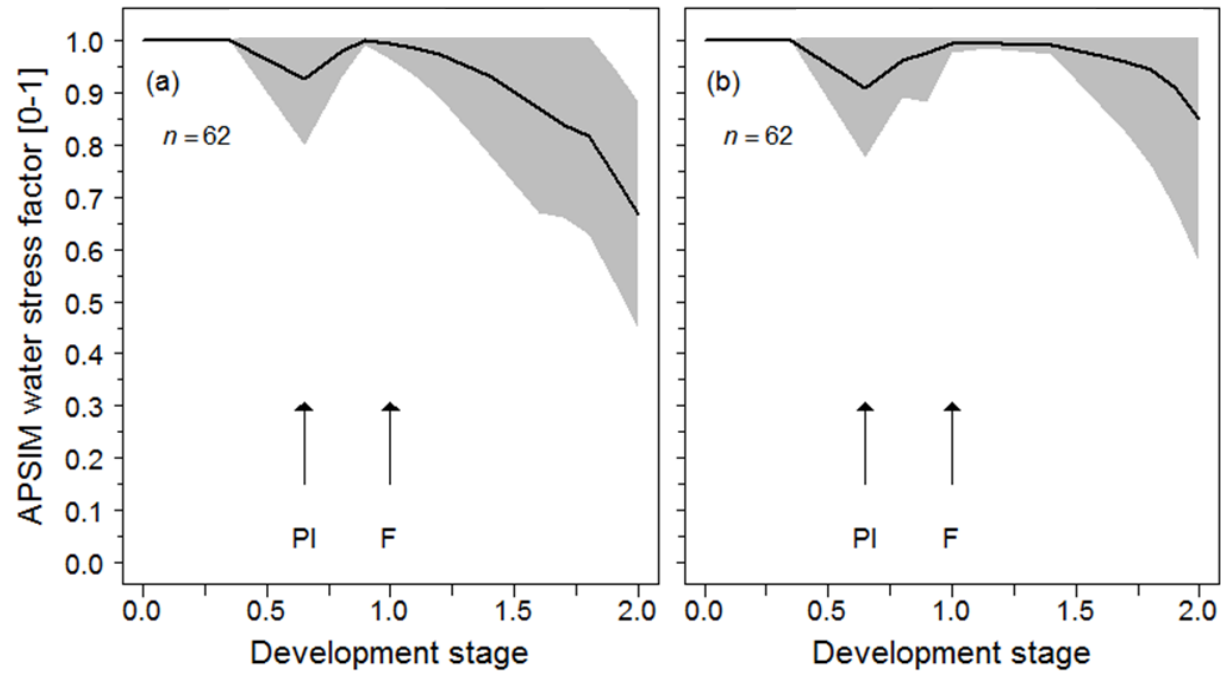
Figure 5.10 Simulated water-stress factor for leaf expansion under rainfed conditions as the mean (line) and standard deviation (grey) according to phenological development stage at the (a) fringe and (b) middle position in the floodplain in Tanzania. Results are based on APSIM simulations (1980-2010) and mineral N fertiliser rate of 150 kg ha^{-1}; PI= panicle initiation, F= flowering.
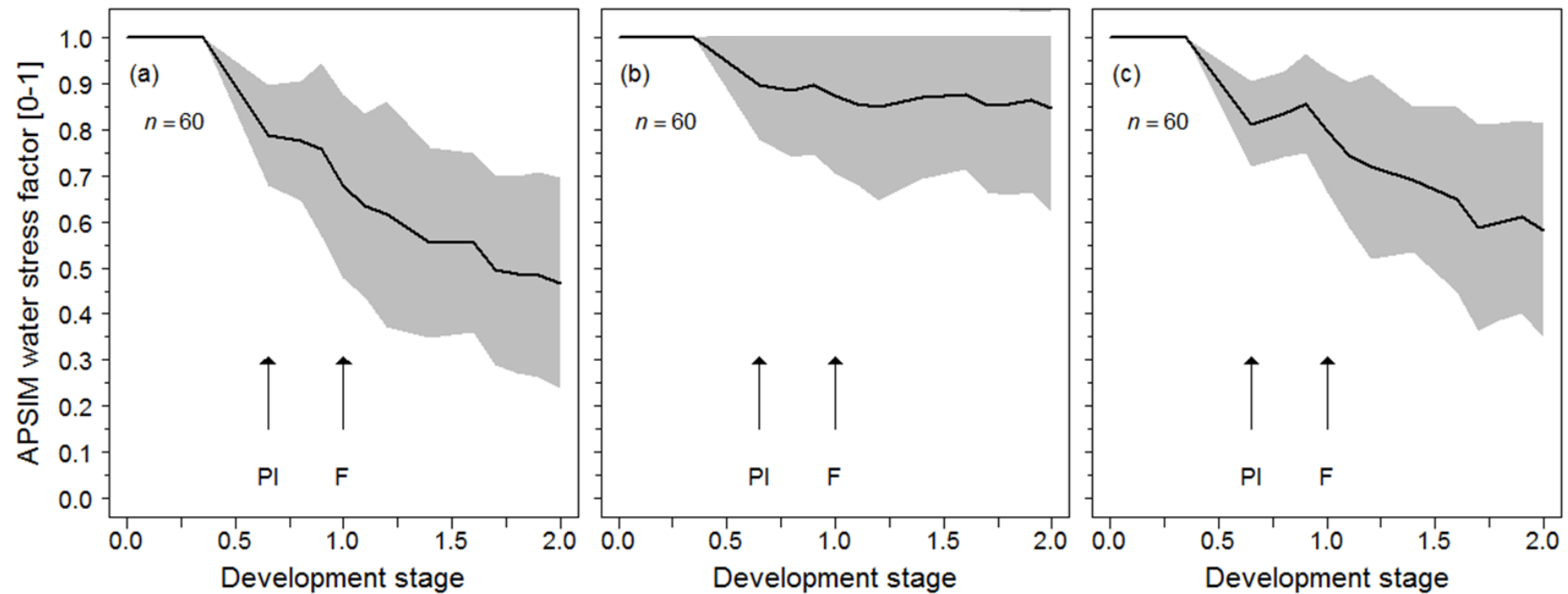
Figure 5.11 Simulated water-stress factor for leaf expansion under rainfed conditions as the mean (line) and standard deviation (grey) according to phenological development stage at the (a) valley-fringe, (b) mid-valley and (c) valley-bottom position in the inland valley in Uganda. Results are based on APSIM simulations (1980-2010) and mineral N fertiliser rate of 150 kg ha^{-1}; PI= panicle initiation, F= flowering.
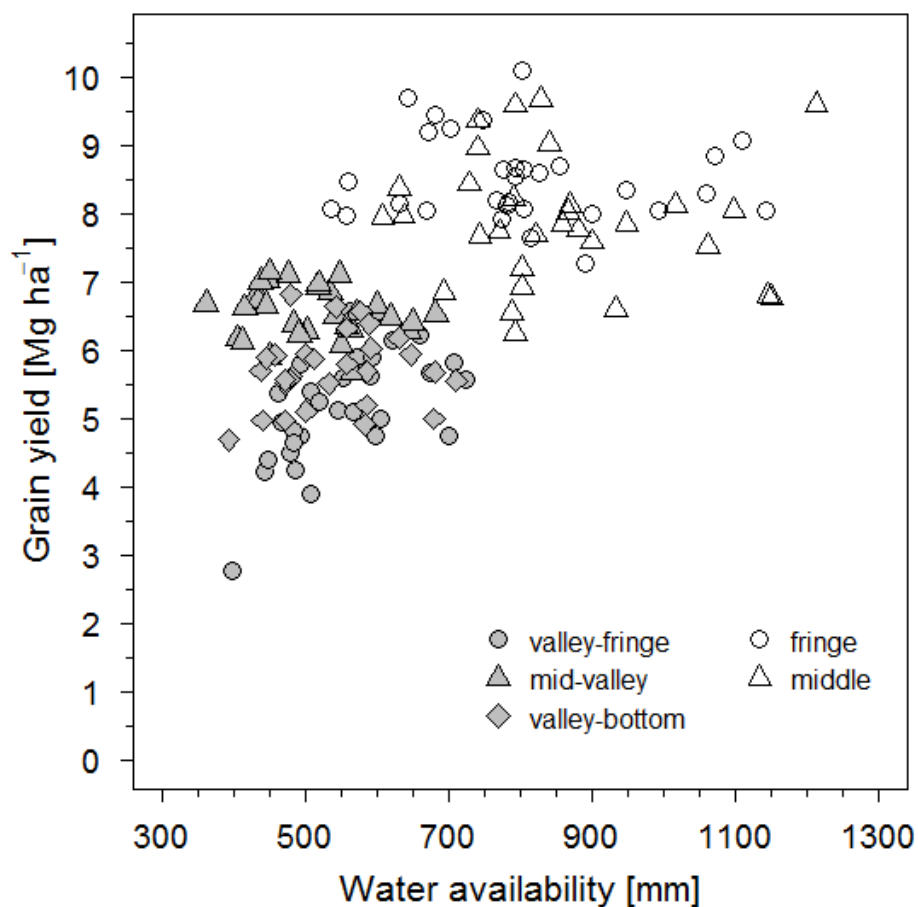
Figure 5.12 Water availability from PI to flowering under rainfed conditions vs. rice grain yield according to field position in the floodplain in Tanzania (unfilled points) and the inland valley in Uganda (filled points). Mineral N fertiliser rate was 150 kg ha^{-1}.

Yield responses to supplemental irrigation

Yield gains from supplemental irrigation similarly varied between wetland type, field position, N rate and year. Overall, supplemental irrigation increased yields on average by >1.5 Mg ha^{-1} in the floodplain and by >0.4 Mg ha^{-1} in the inland valley (**Figure 5.13**, **Figure 5.14**).

In the floodplain, average yield gains from supplemental irrigation amounted to 1.5 Mg ha^{-1} in the fringe and 1.4 Mg ha^{-1} in the middle position (**Figure 5.13**). Without fertiliser application, supplemental irrigation increased average yields by 1.6 and 0.3 Mg ha^{-1} in the fringe and middle position, respectively (**Figure 5.13**). Yield responses subsequently varied between field positions and increasing N rates, with additional yield gains decreasing to 1.3 Mg ha^{-1} in the fringe and increasing to 1.8 Mg ha^{-1} in the middle position from 150 kg N

ha^{-1} (**Figure 5.13**). Thus, supplemental irrigation was particularly beneficial at lower N rates in the fringe and at higher N rates in the middle position (**Figure 5.13**).

In the inland valley, average yield gains from irrigation amounted to 0.3 Mg ha^{-1} in the valley-fringe, 0.7 Mg ha^{-1} in the mid-valley and 0.3 Mg ha^{-1} in the valley-bottom positions (**Figure 5.14**). Similarly to the floodplain, field positions affected yield responses to supplemental irrigation and N rates. In contrast to the floodplain, however, supplemental irrigation exceeded rainfed yields only beyond N rates of 60 kg ha^{-1} in the valley-fringe and 30 kg ha^{-1} in the valley-bottom positoin, while always exceeding rainfed yields in the mid-valley position (**Figure 5.14**). At an N rate of 150 kg ha^{-1}, yield gains from supplemental irrigation were highest in the valley-fringe (1.3 Mg ha^{-1}), followed by the valley-bottom (1.0 Mg ha^{-1}) and the mid-valley position (0.9 Mg ha^{-1}) (**Figure 5.14**). Additionally, supplemental irrigation generally reduced yield variability substantially among field positions, particularly at the valley-fringe position (**Figure 5.14**).
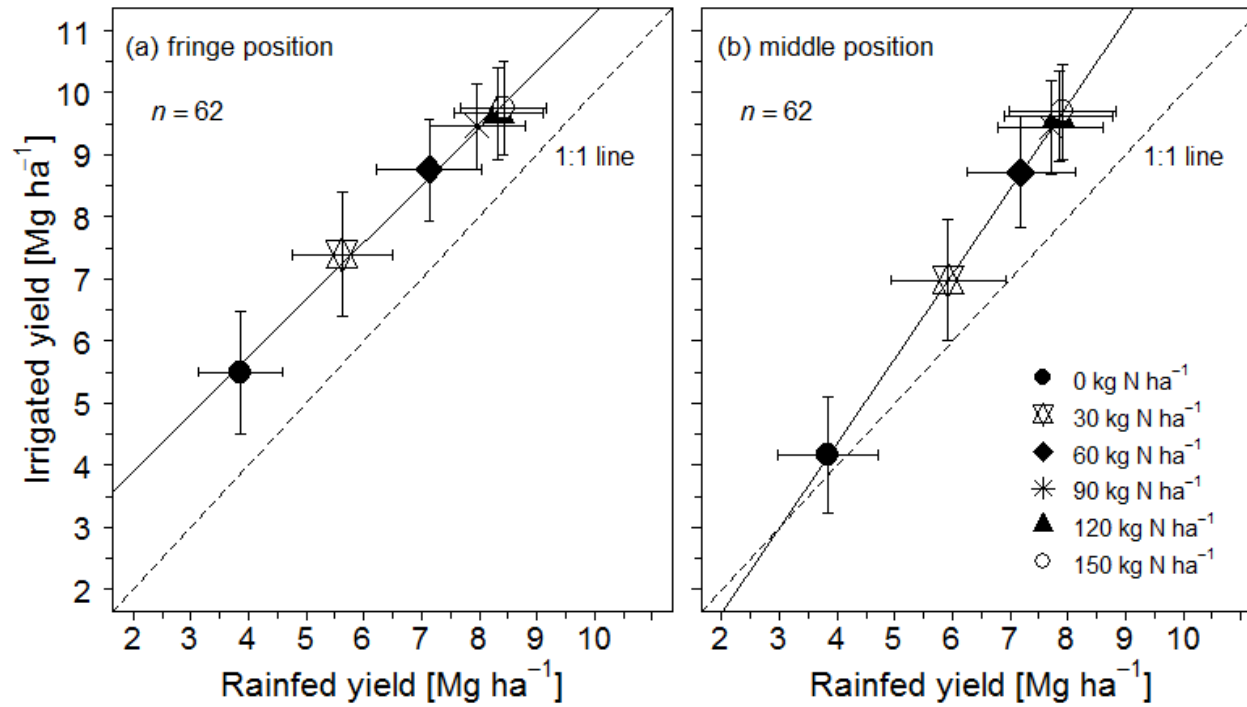
Figure 5.13 Comparison of rainfed and irrigated rice yields according to mineral N fertiliser rate in the floodplain in Tanzania at the (a) the fringe and (b) the middle position, bars indicate the standard deviations of means over the simulation period (1980-2010).
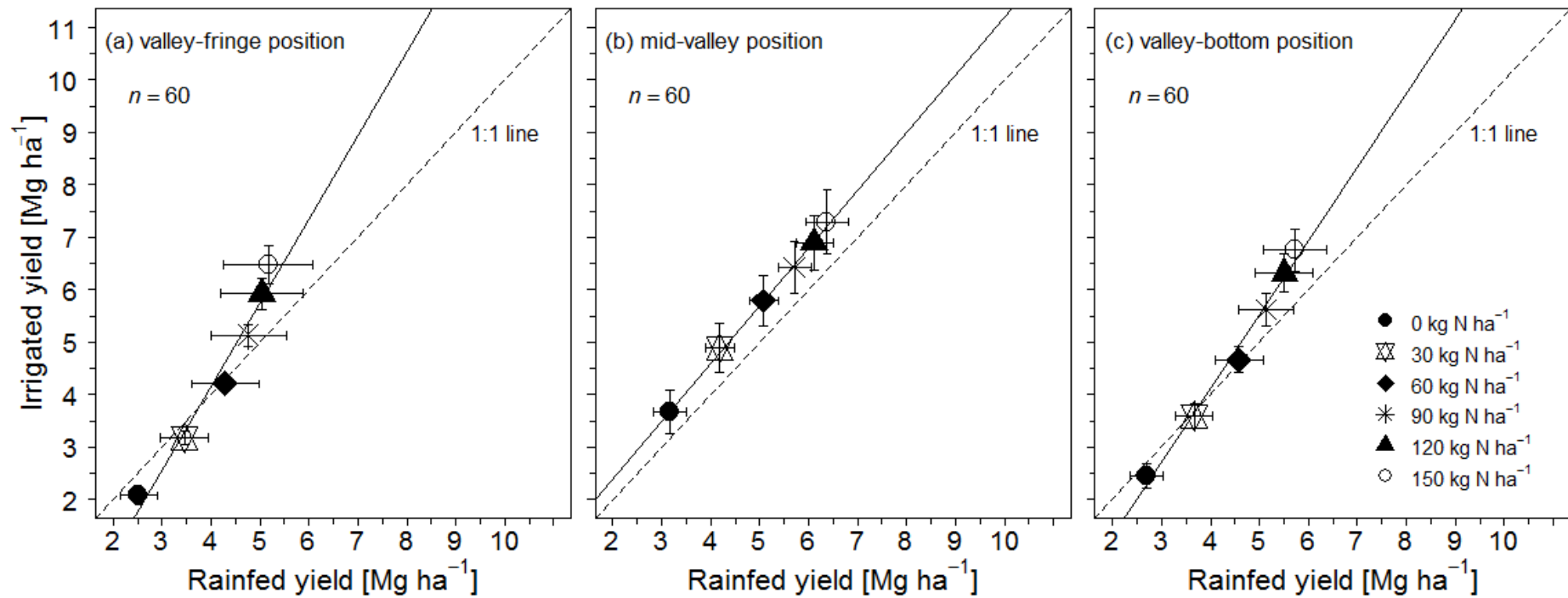
Figure 5.14 Comparison of rainfed and irrigated rice yields according to mineral N fertiliser rate in the inland valley in Uganda at the (a) the valley-fringe, (b) the mid-valley and (c) the valley-bottom position, bars indicate the standard deviations of means over the simulation period (1980-2010).

5.2.4 Discussion

Effects of mineral N rates on yield & fertiliser profitability

Typically, soil N deficiency coupled with low mineral N applications constitute major constraints to increased rainfed lowland rice productivity in East Africa (Tsujimoto *et al.*, 2019). Improved land and water management from field levelling and bunding, and timely and efficient weeding, however, may increase N use efficiencies and subsequently the profitability of mineral N fertiliser (Kwesiga *et al.*, 2020; Rodenburg & Johnson, 2009; Touré *et al.*, 2009).

Average simulated grain yields ranged between 3.8-8.4 Mg ha^{-1} in the floodplain and between 2.5-6.4 Mg ha^{-1} in the inland valley, depending on N rate, field position and year. Thus, agronomic yield gains from N fertiliser use were high, with 1.7-4.5 Mg ha^{-1} in the floodplain and 1.0-3.2 Mg ha^{-1} in the inland valley, and highlight the substantial scope to increase regional rainfed lowland rice productivity. Simulated gain yields compared favourably to experimental field data from both research locations, with average yields ranging between 4.0-8.1 Mg ha^{-1} in the floodplain and between 2.7-5.2 Mg ha^{-1} in the inland valley (Grotelüschen *et al.*, 2021). Additionally, simulated yield levels compared favourably to a participatory research study by Senthilkumar *et al.* (2018) that ascertained a maximum yield with 'Good Agricultural Practice' of 8.5 Mg ha^{-1} in the Kilombero region in Tanzania, and by Miyamoto *et al.* (2012) with 6.8 Mg ha^{-1} in an inland valley of central Uganda. Additionally, average rainfed lowland rice yields across 555 locations in West Africa ranged between 2.0-6.5 Mg ha^{-1} (Niang *et al.*, 2017), while irrigated lowland rice yields of 7.8 Mg ha^{-1} in Benin (Tanaka *et al.*, 2013), 7.3 Mg ha^{-1} in Côte d'Ivoire (Becker & Johnson, 1999) and 9.0 Mg ha^{-1} in Senegal (Krupnik *et al.*, 2012) were reported. However, variable hydro-edaphic field conditions have shown to modulate yield responses to fertiliser use (Haefele *et al.*, 2013; Niang *et al.*, 2018), and favoured the floodplain's fringe and inland valley's mid-valley positions during the simulations. Similar observations were reported from field experimental trials in the Kilombero floodplain (Kwesiga *et al.*, 2019) and an inland valley in Côte d'Ivoire (Touré *et al.*, 2009).

Furthermore, simulated NUE$_a$ were high from high agronomic yield gains, ranging between 27-70 kg kg^{-1} in the floodplain and between 18-34 kg kg^{-1} in the inland valley. Since simulated yields favourably compared to yields from experimental field trials at the research locations, attained NUE$_a$ were similarly high. Several factors have been related to high NUEa, including inherently low soil N supply capacities (Cassman *et al.*, 2002), minimal losses of applied N from matching crop N demand to supply through timely split

applications (Singh *et al.*, 2014), and efficient N partitioning into grains of improved rice varieties (Mae *et al.*, 2006). In fact, soil N contents were ascertained as being only slightly above the critical soil N content for rice growth of 2 g kg^{-1} and N fertiliser split application at transplanting and PI may have led to minimal N losses (Grotelüschen *et al.*, 2021). High harvest indexes of the improved lowland rice variety SARO-5 and rainfed rice variety NERICA-4 were additionally reported by Kwesiga *et al.* (2019) and Alou *et al.* (2018), respectively. Furthermore, soil organic C and clay contents beyond 13 g kg^{-1} and 19%, respectively, have been associated with improved fertiliser use efficiencies from enhanced soil nutrient-holding capacities (Tsujimoto *et al.*, 2017). Comparatively higher NUE$_a$ in the floodplain as compared to the inland valley under experimental conditions were additionally attributed to the so-called 'priming effect' where N fertiliser helps overcome soil mineralization barriers for increased plant N uptake (Liu *et al.*, 2017). Additionally, prolonged periods of ponded water during the simulations may have favoured the growth of cyanobacteria and led to substantial C and N inputs from aquatic microbial biomass and biologically-fixed N$_2$ (BNF) (Gaydon *et al.*, 2012a). Pampolino *et al.* (2008) have shown that BNF by free-living microorganisms can account for N inputs of 19-44 kg N ha^{-1} crop^{-1} in submerged soils, particularly at low N fertiliser application rates. Since APSIM assumes a maximum cyanobacteria growth rate of 20 kg ha^{-1} day^{-1} without environment-specific calibration (Gaydon *et al.*, 2012b), simulated BNF may be under- or overestimated. Only site- and/or environment-specific calibration of cyanobacteria growth rates, however, can avoid such model uncertainties. Since simulated yield levels, however, compared favourably to site-specific experimental field data (Grotelüschen *et al.*, 2021), simulated yield responses and efficiencies were assumed adequate. In comparison, however, simulated NUE$_a$ were substantially higher than those generally reported from rainfed lowland rice systems in West Africa (3-17 kg kg^{-1}) (Becker & Johnson, 2001) and Côte d'Ivoire (22-23 kg kg^{-1}) (Touré *et al.*, 2009), but favourably compared to the NUEa of 46 kg kg^{-1} reported by Miyamoto *et al.* (2012) from another inland valley in Uganda.

Following high agronomic yield gains, the partial gross margin analysis additionally indicated profitable N fertiliser use in both wetlands. However, N fertiliser use was less risky in the floodplain compared to the inland valley, with differences from field positioning within the respective wetland. In the floodplain, the MRR and VCR suggested profitable N rates of between 30-120 kg N ha^{-1} in the fringe and 30-90 kg N ha^{-1} in the middle position during the simulation period. Similarly, Senthilkumar *et al.* (2021) have shown profitable fertiliser use in the Kilombero floodplain provided yields are not constraint by water stress. Across field positions in the inland valley, the N rate of 30 kg N ha^{-1} attained average

VCRs of below 4 and VCR ≥4 in only 20-30% of years, making it highly risky. N rates of between 60-150 kg N ha^{-1}, however, indicated sufficient economic incentives for fertiliser adoption. Comparatively lower VCRs in the valley-fringe and higher seasonal variability (years with VCR ≥4 ranged between 77-90%) indicated that fertiliser use is comparably more risky. Supplemental irrigation may thus be required to boost N use efficiencies and profitability. Similarly, unprofitable and/or risky fertiliser use in the inland valley fringes have been reported in West Africa from lower and more variable yields (Touré *et al.*, 2009), and in Eastern Uganda from unfavourable input/output ratios of NPK fertilisers (Awio *et al.*, 2021). Therefore, fertiliser profitability is also vulnerable to changes in input/output ratios (Haefele *et al.*, 2010) while fertiliser subsidies have shown to improve the profitability and adoption of fertiliser use (Koussoubé & Nauges, 2016).

Adoption of improved management practices, i.e., adequate weed, land and water management, however, have shown to be crucial for profitable fertiliser use (Becker & Johnson, 2001; Tippe *et al.*, 2020). Simultaneously, improved management practices require additional labour which will consequently increase the overall costs of production and strain seasonal labour availabilities (Krupnik *et al.*, 2012). Other factors affecting the agronomic efficiencies and profitability of N fertiliser use may include biotic stressors (Kouassi *et al.*, 2005), nutrient deficiencies and/or toxicities other than N (Tsujimoto *et al.*, 2019), but could not be considered in this study due to model limitations.

Effects of hydro-edaphic conditions & irrigation

Simulated spatial-temporal water stress patterns indicated higher production risks from seasonal droughts in the inland valley as compared to the floodplain. Particularly during the reproductive phase from panicle initiation to flowering, water stress has been reported to affect grain yields most severely (Alou *et al.*, 2018).

Particularly in the inland valley, water stress was comparatively more pronounced at the fringes (Boling *et al.*, 2008) since seasonal water availabilities vary more distinct (Johnson & Kent, 2001). Therefore, yields correlated most strongly to seasonal water availabilities, indicating less hydrological resilience towards variable seasonal rainfall conditions (Boling *et al.*, 2010). In contrast, comparatively lower water stress factors in the floodplain and inland valley's mid-valley positions indicated greater water table supply capacities (Tsubo *et al.*, 2006), that may also reduce water requirements under irrigated conditions (Schmitter *et al.*, 2015).

Simulated spatial-temporal water stress patterns may thus help guide efficient irrigation scheduling (Inthavong *et al.*, 2011). Irrigation scheduling based on spatial-

temporal water stress patterns or implementation of alternate wetting and drying (AWD) systems can, therefore, potentially save irrigation water, sustain rice productivity and manage yield variability (Dang *et al.*, 2018). Water savings from AWD might be marginal at field-level, but can be substantial on an area-basis (Cabangon *et al.*, 2004), and thus contribute to a more sustainable agricultural wetland use. In the absence of irrigation structures, simple on-farm water holding structures might be useful to manage transient water stress, i.e., micro- and macro-catchments, and/or ponds, small reservoirs or earth dams to store rainfall, runoff and floodwater (Hatibu *et al.*, 2000; Nhamo *et al.*, 2014). Additionally, a study by De Bauw *et al.* (2019) have shown that in addition to water management strategies, micro-dose P placements can reduce the adverse effects of water stress on rainfed lowland rice yields.

However, hydrological processes further affect flooding regimes within lowland systems (Osujieke *et al.*, 2017), and since the floodplain's middle position has a direct hydraulic connection to the river (Gabiri *et al.*, 2018), the risks of prolonged crop submergence are inherently higher. While no prolonged crop submergence was observed during the experimental period (Kwesiga *et al.*, 2019), the implementation of water control infrastructures like drainage channels may be required to manage risks long-term (Balasubramanian *et al.*, 2007). In inland valleys, submergence risks are generally assumed to increase towards the valley bottoms as they intercept lateral and subsurface runoff (Tsubo *et al.*, 2006), while valley slopes and fringes loose rainfall water through runoff and seepage (Wade *et al.*, 1999). At our study site, however, a microscale topography and past human activities, i.e., irrigation and drainage channels from stream diversion, have altered hydrological characteristics and water pathways, and subsequently reduced submergence risks in the valley bottom (Gabiri *et al.*, 2017).

5.2.5 Conclusion

East African smallholders are among the most heterogeneous in the world (Fan & Rue, 2020). Therefore, overall fertiliser profitability will vary depending on the farms' opportunity costs, post-harvest decisions, resource endowment and labour availability to adopt improved management practices as well as market incentives to invest in mineral N fertilisers. Nevertheless, this study highlighted the substantial scope to increase rainfed lowland rice production from N fertiliser use under improved land and water management in predominant wetland types of East Africa. Improved land and water management included field levelling and bunding, row-transplanting of improved rice varieties, and timely and efficient weeding. Consequently, N fertiliser use was generally profitable, but recommendable rates varied from hydro-edaphic field attributes within both wetlands.

Further research on variable input/output prices, whole-farm gross margins and labour demand, however, may prove crucial for widespread adoption of improved management practices and N fertiliser use.

Highlights: APSIM showed substantial yield gains from N fertiliser in two East African wetlands. Yields increased by 1.7-4.5 Mg ha^{-1} (floodplain) and 1.0-3.2 Mg ha^{-1} (inland valley). Hydro-edaphic conditions modulated yield responses and fertiliser profitability. N fertiliser was generally profitable but comparatively riskier in the inland valley. Supplemental irrigation to boost use efficiencies and profitability of N fertiliser.

Author contributions: Conceptualization (K.G., D.G., M.B.), Methodology, (K.G., D.G.), Software (K.G., D.G.), Formal analysis (K.G.), Investigation (K.G.), Data curation (K. G.), Writing-original draft preparation (K.G.), Writing-review and editing (K.G., M.B., D.G., S.K., M.L.), Visualization (K.G.), Supervision (M.B.), Funding acquisition (M.B., M.L.), Resources (M.B, S.K.), Project administration (M.B.).

Conflicts of interest: The authors declare no conflict of interest. The founding sponsors had no role in the design of the study; in the collection, analyses, or interpretation of data; in the writing of the manuscript; or in the decision to publish the results.

6.   General discussion & conclusions

The major constraints to increased lowland rice productivity in representative wetland types of East Africa have been identified and addressed in this study using experimental and modelling approaches. Yield determinants, i.e., spatial-temporal water and N stress patterns, varied from hydro-edaphic field conditions in both wetlands, and thus modulated yield responses to improved management practices and the profitability of mineral N fertiliser use. Addressing soil N deficiency was found to be crucial for sustainable rice intensification efforts in both wetlands that, combined with improved land and crop management, led to a substantial rise in productivity. Meanwhile, supplemental irrigation may help boost N fertiliser use efficiencies and profitability, particularly in the inland valley. In-depth discussions and conclusions are presented in **chapter 5**. However, a brief summary on the main research findings with regard to the research hypotheses, insights on experimental and modelling approaches in lowland rice systems, and finally an outlook with recommendations are provided in the following sections.

6.1   Research hypotheses & findings

This thesis aimed at evaluating four integral research hypotheses. The related research findings are summarized in a nutshell here:

 Improved land and crop management can boost regional lowland rice yields substantially.

In comparison to regional rainfed lowland rice management practices (**see chapter 2.2**) and average yields of about 1.8-2.2 Mg ha^{-1} in the floodplain in southeast Tanzania and 1.8-1.9 Mg ha^{-1} in the inland valleys of central Uganda, improved management practices have shown to increase yields substantially. Application of improved management practices (i.e., land preparation, timely and efficient weeding, row-transplanting of improved rice varieties) resulted in average yields of 4 and 2.7 Mg ha^{-1} in the floodplain and inland valley, respectively. The regionally recommended fertiliser application of 60 kg N ha^{-1} resulted in average yields of 6.3 and 3.5 Mg ha^{-1}, and attainable yields (i.e., from 120 kg N ha^{-1}, 60 kg PK ha^{-1} and supplemental irrigation) averaged at 8.1 and 5.2 Mg ha^{-1} in the floodplain and inland valley, respectively. Therefore, the results demonstrated the substantial scope to increase regional lowland rice production and highlight the importance of disseminating improved management practices to regional farmers to help guide sustainable agricultural wetland use and align wetland conservation targets.

The APSIM model is a useful tool to simulate rice responses to management practices in variable hydro-edaphic lowland systems.

Agronomic field data from three consecutive seasons was used to extensively calibrate and validate the APSIM model using a multi-criteria approach, i.e., goodness-of-fit measures for the simulation of rice phenology, sequential biomass accumulation and partitioning, grain yield, plant N uptake, and so-called 'carry-over' effects (soil moisture contents, and soil carbon dynamics and indigenous soil N supply). Model inputs included field-level soil physical and chemical properties (layer-wise soil texture, bulk density, and organic matter, organic carbon and total N contents), daily weather (rainfall, minimum and maximum temperatures, and radiation), and water table data to drive the simulation process. APSIM performed well within the experimental uncertainty in simulating rice responses to management and hydro-edaphic field conditions in both wetlands, supported by a number of goodness-of-fit measures, e.g., RMSEa of 0.92 and 0.78 Mg ha^{-1} (comparing favourably to observed standard deviations of 1.74 and 1.20 Mg ha^{-1}), EF of 0.75 and 0.51 and MAE of 0.13 and 0.42 Mg ha^{-1} for grain yield during model validation in the floodplain and inland valley, respectively. Similarly, soil moisture dynamics were simulated satisfactorily, e.g., in the floodplain with r^2 exceeding 0.85 in the fringe and 0.65 in the middle positions and in both 10 and 30 cm soil depth. Additionally, the paired *t*-test confirmed that observed and simulated non-amended baseline grain yields were the same at a 95% confidence level, indicating that soil carbon dynamics and indigenous soil N supply were simulated accurately. This is considered a key model performance criterion for low-input systems. Results further emphasized the importance of seasonally shallow water tables for rainfed lowland rice production and model performance as they evidently attenuated extreme drought events in years of low and variable seasonal rainfall. This was highlighted as rice yields were underestimated on average by 2 Mg ha^{-1} in the floodplain and 0.8 Mg ha^{-1} in the inland valley that, however, increased to 2.1 Mg ha^{-1} during the dry season of 2016 (233 mm rainfall) when the model was driven not by externally supplied but internally simulated perched water tables.

Yield benefits from mineral N fertiliser use and supplemental irrigation vary from field positioning within the lowland system.

Agronomic field data highlighted differential yield responses to management practices, i.e., mineral N fertiliser rates and supplemental irrigation, from variable hydro-edaphic field conditions within both wetlands. In the floodplain, average non-amended baseline yields and yield responses were generally higher in the fringe as compared to the middle position, i.e., average baseline yields of 4.3 and 3.8 Mg ha^{-1}, and average marginal yield

gains of 2.2 and 2.3 Mg ha^{-1} from 60 kg N ha^{-1}, and average yield gains of 4.4 and 3.7 Mg ha^{-1} from 120 kg N ha^{-1}, 60 kg PK ha^{-1} and supplemental irrigation in the fringe and middle positions, respectively. In the inland valley, average non-amended baseline yields were generally higher in the valley-fringe (2.9 Mg ha^{-1}) followed by the valley-bottom (2.7 Mg ha^{-1}) and the mid-valley positions (2.6 Mg ha^{-1}), while average marginal yield gains ranged from 0.8, 0.4 and 1.1 Mg ha^{-1} with 60 kg N ha^{-1} to 2.3, 2.7 and 2.4 Mg ha^{-1} with 120 kg N ha^{-1}, 60 kg PK ha^{-1} and supplemental irrigation in the valley-fringe, mid-valley and valley-bottom positions, respectively. The validated APSIM model, however, provided further insights on differential yield responses and abiotic yield determinants from field positioning within both wetlands (N and water stress). Generally, soil N deficiency was the main yield constraint and water stress relatively more pronounced in the inland valley. Field positioning, however, modulated yield determinants, delineating relatively higher drought risks against lower N stress from greater mineralization capacities in both wetlands' fringes (i.e., from more favourable topsoil C/N ratios and alternating soil wetting and drying). Comparatively higher drought risks in the inland valley were attributed to lower seasonal rainfall (233-519 mm) as compared to the floodplain (537-1,033 mm), and to lower water table supply capacities. Therefore, supplemental irrigation was generally more beneficial in the inland valley, while both wetlands' fringes benefited comparatively more due to higher water stress factors.

Long-term, model-based evaluation of mineral N fertiliser rates can help identify trade-offs between agronomic benefits and economic incentives for fertiliser use, and help assess production risks from hydro-edaphic and climatic conditions.

Model-based evaluation of long-term (30 years) yield responses to and partial gross margins of N fertiliser rates highlighted variable agronomic benefits and profitability of mineral N fertiliser use between and within both wetlands. Generally, N fertiliser use efficiencies were high, resulting in yield gains of between 1.7-4.5 Mg ha^{-1} in the floodplain and between 1.0-3.2 Mg ha^{-1} in the inland valley, depending in field position, N rate and year. Partial gross margins of N fertiliser additionally indicated profitable use at rates of 30-120 kg N ha^{-1} in the fringe and 30-90 kg N ha^{-1} in the middle position of the floodplain, and of 60-150 kg N ha^{-1} in the inland valley. However, N fertiliser use was comparatively riskier in the valley-fringe position of the inland valley from high seasonal yield variability. Consequently, supplemental irrigation was particularly beneficial and may help boost fertiliser use efficiency and profitability. Additionally, hydrological processes in the floodplain's middle position indicate that water control structures may be needed to efficiently manage production risks from prolonged crop submergence.

6.2 Experimental & modelling approaches in lowland rice systems

Rice-based farming systems are comparatively more complex to simulate from anaerobic soil conditions and/or alternating aerobic and anaerobic soil conditions with subsequent effects on soil organic matter decomposition, plant N availability and potential N losses. Several biophysical models have been developed and are continuously being improved for rice-based farming systems, e.g., the EPIC model for the effects of fertiliser application and bunding on soil water dynamics and rice performance in inland valley systems of West Africa (Worou *et al.*, 2012), the ORYZA2000 model for the evaluation of water-saving technologies in lowland rice systems of Asia (Belder *et al.*, 2007), and the CERES-Rice model for the identification of best management practices in aerobic rice-maize cropping systems of India (Kadiyala *et al.*, 2015). Despite having been developed for dryland farming systems (Keating *et al.*, 2003), the APSIM framework has recently been improved for the application in permanently and/or temporarily flooded rice-based systems (Gaydon *et al.*, 2012b; Gaydon *et al.*, 2012a). Consequently, APSIM is increasingly being used for various rice-based systems worldwide, e.g., simulating Boro rice production strategies in the saline coastal zone of Bangladesh (Gaydon *et al.*, 2021), balancing water and crop productivity for rice, maize and mung bean in rice-based cropping systems of Sri Lanka (Amarasingha *et al.*, 2017), and identifying groundwater-saving management strategies for irrigated rice-wheat systems of India (Balwinder-Singh *et al.*, 2015). Similarly, this study has shown that APSIM performed well within the experimental uncertainty in simulating rice responses to management and variable hydro-edaphic field conditions in two representative wetland types of East Africa and was successfully used in a long-term (30-years) scenario analysis.

However, the identification of this studys' strengths and weaknesses may aid the design of similar research projects and science-based model improvements:

Soil water dynamics. Several studies have emphasised the importance of shallow water tables for lowland rice production, including studies from Southeast Asia (Belder *et al.*, 2007), China (Cabangon *et al.*, 2004) and West Africa (Schmitter *et al.*, 2015). Similarly, field-level water table data have proven crucial for model performance in this study as they evidently attenuated seasonal drought events. Generally, however, both shallow and perched water tables, and mutual recharge processes may occur in puddled and coarse-textured soils (Tsubo *et al.*, 2005), and suggest multi-dimensional simulation routines of water table dynamics may be necessary. Additionally, water control and

irrigation structures are largely absent in lowland rice systems of East Africa (Senthilkumar *et al.*, 2018). Therefore, water table-induced flooding poses serious hydrological risks depending on the water regime at field-level (Inthavong *et al.*, 2011). Currently, however, water table-induced flooding and subsequent effects on crop development and yield are not routinely simulated in APSIM. While water table data can be used to replace the perched water table routine via the manager module, ponding is simulated in the SoilWat module based on saturated soil layers, vertical percolation rates and user-defined bund heights. Actual submergence depths, however, may be higher. While Gaydon *et al.* (2017) described a 'work-around' by comparing *crop_height* and *pond_depth* daily and pausing phenological development and biomass accumulation when *pond_depth* ≥ (*crop_height* * 0.9), generic algorithms to describe submergence damage on rice i.a. as a function of time, crop stage, and submergence depth are currently missing but would improve risk assessments substantially. This would further require daily data collection of pond depths and plant heights. Additionally, this study has shown that a higher spatial resolution of hydrological key data, i.e., directly relating field-level water table, soil moisture and soil property data, may be needed to limit model uncertainties in highly heterogeneous environments like the inland valley. Similarly, the quantification of lateral inflows in sloped lowlands may further improve model accuracy (Tsubo *et al.*, 2006). Under temporarily and/or permanently ponded field conditions, APSIM assumes a maximum algae growth rate (*maxrate_PAB*) of 20 kg ha^{-1} day^{-1} (Gaydon *et al.*, 2012b). Site- and/or environment-specific calibration of *maxrate_PAB* may, however, improve the simulation of biologically-fixed N_2 (BNF) that can led to substantial C and N inputs (Pampolino *et al.*, 2008).

Soil properties. Reduced predictive accuracy of soil moisture dynamics in the inland valley have been associated i.a. with a high variability in soil properties, similarly also shown in a study from Benin (Worou *et al.*, 2012). Therefore, a higher spatial resolution of soil property data may be needed in heterogeneous environments to conclusively explain observed yield patterns and improve predictions of soil water contents and N dynamics. Additionally, implementing simulation routines for inter-seasonal soil property changes form soil tillage and puddling (i.e., effective Ks and bulk density (Gathala *et al.*, 2011)) would ease model application in mixed-crop systems (Gaydon *et al.*, 2017).

Phenological development. Reduced predictive accuracy of key phenological stages in the floodplain's fringe position during the 2016 season were associated to several seasonal abnormalities (late transplanting of old seedlings, irregular rainfall pattern). To conclusively explain model inaccuracies, serial-planting trials may help to

assess the interaction of photoperiod and temperature on the phenological development in slightly photoperiod-sensitive rice varieties like SARO-5 (Fukai, 1999), and thus improve phenological model parameters and predictions.

While a more detailed field data collection and instrumentation are likely to improve model veracity in wetland systems, model complexity vs applicability needs to be balanced under consideration of monetary resources, processing power and against the main goals of the research project.

6.3   Outlook & recommendations

Widespread adoption of improved management practices in lowland rice systems of East Africa will be crucial in order to improve and eventually attain rice self-sufficiency, with subsequent effects on household food security and national economies. In 2009, rainfed lowland rice was produced on about 677,806 ha by 251,506 rice-farming households in Tanzania and on about 72,109 ha by 133,852 rice-farming households in Uganda (Diagne *et al.*, 2013). Hence, increasing currently low regional rainfed lowland rice yields will have substantial effects on rice self-sufficiency and likely make further land expansion into unexploited and/or fragile wetland areas redundant.

This study's findings have shown that improved land and crop management alone, i.e., field levelling, puddling and bunding, timely weeding and row-transplanting of improved rice varieties, can increase average regional rainfed lowland rice yields by around 100 and 46% in the floodplain in Tanzania and an inland valley in central Uganda, respectively. Sustainable intensification efforts, however, need to further address the negative nutrient balances as soils are inherently N deficient, exacerbated by continued crop-residue removal, and zero to low organic and/or inorganic amendments (Senthilkumar *et al.*, 2020). Kwesiga *et al.* (2020a) have shown niches for pre- and/or post-rice legume cultivation in order to address nutrient balances and increase yields, while the application of mineral N fertiliser has resulted in additional average yields of 58-103% and 30-93% depending on N fertiliser rate and combination with P and K fertiliser and supplemental irrigation in the floodplain and inland valley, respectively. Meanwhile, hydro-edaphic field conditions modulated yield responses to and profitability of N fertiliser rates, and should thus replace blanket N fertiliser recommendations for lowland rice systems. The insufficiency of blanket fertiliser recommendations have previously been reported from rainfed lowland rice systems across SSA (Arouna *et al.*, 2021) and Southeast Asia (Boling *et al.*, 2007).

The paradigm of sustainable rice intensification in smallholder farming systems, however, does not only encompass biophysical, but also socio-economic and institutional constraints. Therefore, only a holistic, integrative and participatory approach is likely to attain widespread adoption of improved management practices including fertiliser use, and thus translate into the urgently needed rise in production (Rugumamu, 2014). Since regional lowland rice is predominantly produced by risk-averse smallholders (Ruhinduka *et al.*, 2020), fertiliser profitability is imperative for widespread adoption. This study's findings have shown via a partial gross margin analysis of mineral N fertiliser rates that N fertiliser use was generally profitable at both wetland sites, supported by favourable input/output ratios (I/O) of below the threshold of 10 (Yanggen *et al.*, 1998), value/costs ratios (VCR) ≥4 for successful adoption in risky environments (Okebalama *et al.*, 2016), and marginal rates of returns (MRR) ≥150% (Evans, 2005). Fertiliser profitability, however, is particularly vulnerable to changes in I/O ratios (Haefele *et al.*, 2010). Volatile markets, therefore, pose serious risks to fertiliser profitability (Crawford *et al.*, 2003), while fertiliser subsidies may be beneficial to attenuate market-related risks (Koussoubé & Nauges, 2016). Since, however, opportunity costs, post-harvest decisions, resource endowment and labour availability vary among smallholders, whole-farm gross margin analysis may be needed to comprehensively evaluate fertiliser profitability at farm-level.

Similarly, the adoption of improved management practices has proven crucial for profitable fertiliser use (Tippe *et al.*, 2020; Touré *et al.*, 2009). Improved management practices, i.e., systems like System of Rice Intensification (SRI), Conservation Agriculture (CA) and Integrated Rice Management (IRM) comprise row-transplanting or dribbling of improved rice varieties, field levelling and bunding, and timely and effective weed control among others (Krupnik *et al.*, 2012; Nhamo *et al.*, 2014; Zenna *et al.*, 2017). The systems' implementation and maintenance, however, is comparatively labour-intensive (Krupnik *et al.*, 2012). Meanwhile, farm power is often a 'forgotten resource', and as mechanization levels remain low, the adoption of improved management practices often leads to increased labour drudgery that particularly disadvantages women (Baudron *et al.*, 2015). Human muscle power currently accounts for about 80% of the farm power in smallholder farming systems across SSA (Mlengera *et al.*, 2015) but is increasingly in decline from rural-urban migration and alternative non-farm livelihoods (Dahlin & Rusinamhodzi, 2019). Additionally. seasonal labour bottlenecks often lead to late and poor land preparation, late planting, untimely and sub-optimal weeding, and thus in poor crop performance (Mlengera *et al.*, 2015). Post-harvest losses are additionally high, ranging between 30-50% from untimely harvesting (grain shattering) and poor storage facilities (spoilage from moisture, mycotoxin and pest infestations) (Rickman *et al.*, 2013).

In order to address on-farm labour constraints and post-harvest losses, 'farm-to-plate' labour-saving and cost-efficient technologies that can be (largely) produced and maintained locally are urgently needed (Johnson *et al.*, 2018; Rickman *et al.*, 2013). An initiative to facilitate and promote mechanization tailored to smallholder farming systems is the *AfricaRice*-lead 'Mechanization Task Force' in collaboration with National Agricultural Research Systems (NARS) institutions. The task force aims to identify and adopt small-scale machinery such as mechanical weeders, harvesters and threshers to be sold to smallholders via trained private manufacturers (Zenna *et al.*, 2017). Versatile usability of small-scale machinery may additionally increase adoption as smallholders seldom only cultivate one crop (Kuivanen *et al.*, 2016). In order to maximize the outreach, existing networks should additionally be used, e.g., via well-established NGOs like One Acre Fund (*www.oneacrefund.org*) that operates across ESA (Burundi, Kenya, Malawi, Rwanda, Tanzania, Uganda and Ethiopia) and currently serves 1.34 million smallholders.

In concluding this thesis, the following recommendations may be considered by regional policy makers and stakeholders to sustainably increase smallholder lowland rice production across East African wetlands:

Participatory land-use planning. Identify 'best-bet' wetlands for agricultural use including all stakeholders based on biophysical and socio-economic criteria. Delineate priority production sites for locally-built and -maintained infrastructure (field contours, water control and/or irrigation). Employ biophysical models (e.g., APSIM, EPIC, CERES) and GIS to help prioritize production potentials and constraints, and assess management options on crop, farm and/or wetland level.

'farm-to-plate' mechanization & capacity building. Promote mechanization from planting to harvest to ease labour demand and bottlenecks, and promote capacity building on improved management practices through farmer schools, radio, instruction videos, technical drawings, and/or demonstration farms using regional structures (e.g., via NARCs, NGOs, public-private partnerships, vocational institutes).

Farmer associations. Encourage the organization of smallholders to improve their access to credits, inputs, markets, improved representation and knowledge, and increase the level of mechanization, e.g., through collective ownership.

Infrastructural advances. Boost infrastructural advances along the rice value-chain, e.g., rural road networks to improve access to markets and to facilitate more cost-efficient distribution of inputs, development of input and milling enterprise networks and storage facilities, organization of formal and informal markets.

References

Akponikpè, P.B.I., Gérard, B., Michels, K. and Bielders, C. (2010). Use of the APSIM model in long term simulation to support decision making regarding nitrogen management for pearl millet in the Sahel. *Eur. J. Agron.* 32 (2), 144–154. doi:10.1016/j.eja.2009.09.005.

Alibu, S., Neuhoff, D., Senthilkumar, K., Becker, M. and Köpke, U. (2019). Potential of cultivating dry season maize along a hydrological gradient of an Inland Valley in Uganda. *Agronomy* 9 (10), 606. doi:10.3390/agronomy9100606.

Amarasingha, R.P.R.K., Suriyagoda, L.D.B., Marambe, B., Rathanayake, W.M.U.K., Gaydon, D.S., Galagedara, L.W., Punyawardena, R., Silva, G.L.L.P., Nidumolu, U. and Howden, M. (2017). Improving water productivity in moisture-limited rice-based cropping systems through incorporation of maize and mungbean: A modelling approach. *Agric. Water Manag.* 189, 111–122. doi:10.1016/j.agwat.2017.05.002.

Arouna, A., Fatognon, I.A., Saito, K. and Futakuchi, K. (2021). Moving toward rice self-sufficiency in sub-Saharan Africa by 2030: Lessons learned from 10 years of the Coalition for African Rice Development. *World Dev. Perspect.* 21, 100291. doi:10.1016/j.wdp.2021.100291.

Asseng, S., Keating, B.A., Fillery, I.R.P., Gregory, P.J., Bowden, J.W., Turner, N.C., Palta, J.A. and Abrecht, D.G. (1998). Performance of the APSIM-wheat model in Western Australia. *Field Crops Res.* 57 (2), 163–179. doi:10.1016/S0378-4290(97)00117-2.

Asseng, S., Keating, B.A., Huth, N.I. and Eastham, J. (1997). *Simulation of perched water tables in a duplex soil.* Proceedings of the International Conference on Modelling and Simulation, 8-10 December, The Modelling and Simulation Society of Australia, Tasmania, Australia, Vol. 2, pp. 538-543.

Bahri, H., Annabi, M., M'Hamed, H.C. and Frija, A. (2019). Assessing the long-term impact of conservation agriculture on wheat-based systems in Tunisia using APSIM simulations under a climate change context. *Sci. Total Environ.* 692, 1223–1233. doi:10.1016/j.scitotenv.2019.07.307.

Balasubramanian, V., Sie, M., Hijmans, R.J. and Otsuka, K. (2007). Increasing rice production in Sub-Saharan Africa: challenges and opportunities. *Adv. Agron.* 94, 55–133. doi:10.1016/S0065-2113(06)94002-4.

Balwinder-Singh, Humphreys, E., Gaydon, D.S. and Eberbach, P.L. (2016). Evaluation of the effects of mulch on optimum sowing date and irrigation management of zero till wheat in central Punjab, India using APSIM. *Field Crops Res.* 197, 83–96. doi:10.1016/j.fcr.2016.08.016.

Balwinder-Singh, Humphreys, E., Sudhir, Y. and Gaydon, D.S. (2015). Options for increasing the productivity of the rice–wheat system of North-West India while reducing groundwater depletion. Part 1. Rice variety duration, sowing date and inclusion of mungbean. *Field Crops Res.* 173, 68–80. doi:10.1016/j.fcr.2014.11.018.

Bamwesigye, D., Doli, A., Adamu, K.J. and Mansaray, S.K. (2020). A review of the political economy of agriculture in Uganda: women, property rights, and other challenges. *Univers. J. Agric.* 8 (1), 1–10. doi:10.13189/ujar.2020.0.

Baudron, F., Sims, B., Justice, S., Kahan, D.G., Rose, R., Mkomwa, S., Kaumbutho, P., Sariah, J., Nazare, R., Moges, G. and Gérard, B. (2015). Re-examining appropiate mechanization in Eastern and Southern Africa: two-wheel tractors, conservation agriculture, and private sector involvement. *Food Sec.* (7), 889–904. doi:10.1007/s12571-015-0476-3.

Behn, K., Becker, M., Burghof, S., Möseler, B.M., Kyalo, D.W. and Alvarez, M. (2018). Using vegetation attributes to rapidly assess degradation of East African wetlands. *Ecol. Indic.* 89, 250–259. doi:10.1016/j.ecolind.2018.02.017.

Belder, P., Bouman, B.A.M. and Spiertz, J.H.J. (2007). Exploring options for water savings in lowland rice using a modelling approach. *Agric. Syst.* 92 (1-3), 91–114. doi:10.1016/j.agsy.2006.03.001.

Belder, P., Bouman, B.A.M., Spiertz, J.H.J., Peng, S., Castañeda, A.R. and Visperas, R.M. (2005). Crop performance, nitrogen and water use in flooded and aerobic rice. *Plant Soil* 273 (1-2), 167–182. doi:10.1007/s11104-004-7401-4.

Birch, C.J., Carberry, P.S., Muchow, R.C., McCown, R.L. and Hargreaves, J.N.G. (1990). Development and evaluation of a sorghum model based on CERES-Maize in a semi-arid tropical environment. *Field Crops Res.* 24 (1-2), 87–104. doi:10.1016/0378-4290(90)90023-5.

Boling, A.A., Bouman, B.A.M., Tuong, T.P., Murty, M.V.R. and Jatmiko, S.Y. (2007). Modelling the effect of groundwater depth on yield-increasing interventions in rainfed lowland rice in Central Java, Indonesia. *Agric. Syst.* 92 (1-3), 115–139. doi:10.1016/j.agsy.2006.05.003.

Boling, A.A., Tuong, T.P., Jatmiko, S.Y. and Burac, M.A. (2004). Yield constraints of rainfed lowland rice in central Java, Indonesia. *Field Crops Res.* 90 (2-3), 351–360. doi:10.1016/j.fcr.2004.04.005.

Boling, A.A., Tuong, T.P., Suganda, H., Konboon, Y., Harnpichitvitaya, D., Bouman, B.A.M. and Franco, D.T. (2008). The effect of toposequence position on soil properties, hydrology, and yield of rainfed lowland rice in Southeast Asia. *Field Crops Res.* 106 (1), 22–33. doi:10.1016/j.fcr.2007.10.013.

Bouman, B.A.M., Feng, L., Tuong, T.P., Lu, G., Wang, H. and Feng, Y. (2007). Exploring options to grow rice using less water in northern China using a modelling approach: II. Quantifying yield, water balance components, and water productivity. *Agric. Water Manag.* 88, 23–33. doi:10.1016/j.agwat.2006.10.005.

Bouman, B.A.M., Kropff, M.J., Tuong, T.P., Wopereis, M.C.S., Ten Berge, H.F.M. and Van Laar, H.H. (2001). *ORYZA2000: modeling lowland rice.* International Rice Research Institute (IRRI)/Wageningen University and Research Centre, Los Baños, Philippines/Wageningen, Netherlands.

Bouman, B.A.M., Van Keulen, H., Van Laar, H.H. and Rabbinge, R. (1996). The 'School of de Wit' crop growth simulation models: a pedigree and historical overview. *Agric. Syst.* 52 (2/3), 171–198. doi:10.1016/0308-521X(96)00011-X.

Bouman, B.A.M. and Van Laar, H.H. (2006). Description and evaluation of the rice growth model ORYZA2000 under nitrogen-limited conditions. *Agric. Syst.* 87, 249–273. doi:10.1016/j.agsy.2004.09.011.

Burghof, S. (2017). *Hydrogeology and water quality of wetlands in East Africa - case studies of a floodplain and a valley bottom wetland.* Dissertation, Bonn, Germany.

Burghof, S., Gabiri, G., Stumpp, C., Chesnaux, R. and Reichert, B. (2018). Development of a hydrogeological conceptual wetland model in the data-scarce north-eastern region of Kilombero Valley, Tanzania. *Hydrogeol. J.* 26 (1), 267–284. doi:10.1007/s10040-017-1649-2.

Cabangon, R.J., Tuong, T.P., Castillo, E.G., Bao, L.X., Lu, G., Wang, G.H., Cui, Y., Bouman, B.A.M., Li, Y., Chen, C. and Wang, J. (2004). Effect of irrigation method and N-fertilizer management on rice yield, water productivity and nutrient-use efficiencies in typical lowland rice conditions in China. *Paddy Water Environ.* 2 (4), 195–206. doi:10.1007/s10333-004-0062-3.

Carberry, P.S., Muchow, R.C. and McCown, R.L. (1989). Testing the CERES-Maize simulation model in a semi-arid tropical environment. *Field Crops Res.* 20 (4), 297–315. doi:10.1016/0378-4290(89)90072-5.

Chapman, L.J., Balirwa, J., Bugenyi, F.W.B., Chapman, C. and Crisman, T.L. (2001). Wetlands of East Africa: biodiversity, exploitation, and policy perspectives. In: Gopal, B., Junk, W.J., Davis, J.A. (Eds.) *Biodiversity in Wetlands: Assessment, Function and Conservation, Vol. 2.* Backhuys Publishers, Leiden, Netherlands, pp. 101–131.

Chapman, S.C., Hammer, G.L. and Meinke, H. (1993). A sunflower simulation model. I. Model development. *Agron. J.* 85 (3), 725–735. doi:10.2134/agronj1993.00021962008500030038x.

Cornish, P.S., Kumar, A. and Das, S. (2020). Soil fertility along toposequences of the East India plateau and implications for productivity and sustainability. *Soil* 6 (2), 325–336. doi:10.5194/soil-2019-92.

Crawford, E.W., Kelly, V., Jayne, T.S. and Howard, J. (2003). Input use and market development in Sub-Saharan Africa: an overview. *Food Policy* 28 (4), 277–292. doi:10.1016/j.foodpol.2003.08.003.

Daconto, G., Games, I., Lukumbuzya, K. and Raijmakers, F. (2018). *Integrated management plan for the Kilombero Valley Ramsar site.* Ministry of Natural Resources and Tourism, Dar es Salaam, Tanzania.

Dahlin, A.S. and Rusinamhodzi, L. (2019). Yield and labor relations of sustainable intensification options for smallholder farmers in sub-Saharan Africa. A meta-analysis. *Agron. Sustain. Dev.* 39 (3), 1–18. doi:10.1007/s13593-019-0575-1.

Dalgliesh, N.P., Hochman, Z., Huth, N.I. and Holzworth, D.P. (2016). *A protocol for the development of APSoil parameter values for use in APSIM.* CSIRO Publishing, Towoomba, Australia.

Daudu, C.K., Ugbaje, E.M., Oyinlola, E.Y., Tarfa, B.D., Yakubu, A.A., Amapu, I.Y. and Wortmann, C.S. (2018). Lowland rice nutrient responses for the Guinea and Sudan savannas of Nigeria. *Agron. J.* 110 (3), 1079–1088. doi:10.2134/agronj2017.08.0469.

De Datta, S.K. (1981). *Principles and Practices of Rice Production.* Wiley, New York, USA.

Demont, M. and Ndour, M. (2015). Upgrading rice value chains: experimental evidence from 11 African markets. *Glob. Food. Sec.* 5, 70–76. doi:10.1016/j.gfs.2014.10.001.

Diagne, A., Amovin-Assagba, E., Futakuchi, K. and Wopereis, M.C.S. (2013). Estimation of cultivated area, number of farming households and yield for major rice-growing environments in Africa. In: Wopereis, M.C.S., Johnson, D.E., Ahmadi, N., Tollens, E., Jalloh, A. (Eds.) *Realizing Africa's Rice Promise*. CAB International, Wallingford, UK, pp. 35–45.

Dinesen, L. (2016). Kilombero Valley Floodplain (Tanzania). In: Finlayson, C.M., Everard, M., Irvine, K., Middleton, A.B., Dinesen, L., Davidson, N.C. (Eds.) *The Wetland Book*. Springer, Dordrecht, Netherlands, pp. 1–8.

Dixon, A.B. and Wood, A.P. (2003). Wetland cultivation and hydrological management in eastern Africa: matching community and hydrological needs through sustainable wetland use. *Nat. Resour. Forum* 27, 117–129. doi:10.1111/1477-8947.00047.

Drenth, H., Ten Berge, H.F.M. and Riethoven, J.J.M. (1994). *ORYZA simulation models for potential and nitrogen limited rice production.* SARP Research Proceedings, IRRI/AB-DLO, Wageningen, Netherlands.

Dutta, S.K., Laing, A.M., Kumar, S., Gathala, M.K., Singh, A.K., Gaydon, D.S. and Poulton, P.L. (2020). Improved water management practices improve cropping system profitability and smallholder farmers' incomes. *Agric. Water Manag.* 242 (1), 106411. doi:10.1016/j.agwat.2020.106411.

Evans, E.A. (2005). *Marginal analysis: an economic procedure for selecting alternative technologies/practices.* Institute of Food and Agricultural Sciences (IFAS), University of Florida, Gainsville, Florida, USA.

FAO (2014). *World reference base for soil resources 2014: international soil classification system for naming soils and creating legends for soil maps.* Food and Agriculture Organization of the United Nations (FAO), Rome, Italy.

Feng, J., Hussain, H.A., Hussain, S., Shi, C., Cholidah, L., Men, S., Ke, J. and Wang, L. (2020). Optimum water and fertilizer management for better growth and resource use efficiency of rapeseed in rainy and drought seasons. *Sustainability* 12 (2), 703. doi:10.3390/su12020703.

Feng, L., Bouman, B.A.M., Tuong, T.P., Cabangon, R.J., Li, Y., Lu, G. and Feng, Y. (2007). Exploring options to grow rice using less water in northern China using a modelling approach. *Agric. Water Manag.* 88 (1-3), 1–13. doi:10.1016/j.agwat.2006.10.006.

Fermont, A.M., Tittonell, P.A., Baguma, Y., Ntawuruhunga, P. and Giller, K.E. (2010). Towards understanding factors that govern fertilizer response in cassava: lessons from East Africa. *Nutr. Cycling Agroecosyst.* 86 (1), 133–151. doi:10.1007/s10705-009-9278-3.

Fukai, S. (1999). Phenology in rainfed lowland rice. *Field Crops Res.* 64 (1-2), 51–60. doi:10.1016/S0378-4290(99)00050-7.

Fungo, B., Kabanyoro, R., Mugisa, I.O. and Kabiri, S. (2013). Narrowing yield-gap of rice through soil fertility management in the Lake Victoria Crescent agro-ecological zone, Uganda. *AJAR* 8 (23), 2988–2999. doi:10.5897/AJAR12.2068.

Gabiri, G. (2018a). *Multi-scale modeling of water resources in a tropical inland valley and a tropical floodplain catchment in East Africa*. Dissertation, Bonn, Germany.

Gabiri, G., Burghof, S., Diekkrüger, B., Leemhuis, C., Steinbach, S. and Näschen, K. (2018b). Modeling spatial soil water dynamics in a tropical floodplain, East Africa. *Water* 10 (2), 191. doi:10.3390/w10020191.

Gabiri, G., Diekkrüger, B., Burghof, S., Näschen, K., Asiimwe, I. and Bamutaze, Y. (2017). Determining hydrological regimes in an agriculturally used tropical inland valley wetland in central Uganda using soil moisture, groundwater, and digital elevation data. *Hydrol. Process.* 32 (3), 349–362. doi:10.1002/hyp.11417.

Gabiri, G., Diekkrüger, B., Näschen, K., Leemhuis, C., Van der Linden, R., Majaliwa, J.-G., M. and Obando, J.A. (2020). Impact of climate and land use/land cover change on the water resources of a tropical inland valley catchment in Uganda, East Africa. *Climate* 8 (7), 83. doi:10.3390/cli8070083.

Gabiri, G., Leemhuis, C., Diekkrüger, B., Näschen, K., Steinbach, S. and Thonfeld, F. (2019). Modelling the impact of land use management on water resources in a tropical inland valley catchment of central Uganda, East Africa. *Sci. Total Environ.* 653, 1052–1066. doi:10.1016/j.scitotenv.2018.10.430.

Gathala, M.K., Ladha, J.K., Saharawat, Y.S., Kumar, V., Kumar, V. and Sharma, P.K. (2011). Effect of tillage and crop establishment methods on physical properties of a medium-textured soil under a seven-year rice−wheat rotation. *SSSAJ* 75 (5), 1851–1862. doi:10.2136/sssaj2010.0362.

Gaydon, D.S., Balwinder-Singh, Wang, E., Poulton, P.L., Ahmad, B., Ahmed, F., Akhter, S., Ali, I., Amarasingha, R.P.R.K., Chaki, A.K., Chen, C., Kumar, P.V., Khan, A.S.M.M.R., Laing, A.M., Liu, L., Malaviachichi, M.A.P.W.K., Mohapatra, K.P., Muttaleb, M.A., Power, B., Radanielson, A.M., Rai, G.S., Rashid, M.H., Rathanayake, W.M.U.K., Sarker, M.M.R., Sena, D.R., Shamim, M., Subash, N., Suriadi, A., Suriyagoda, L.D.B., Wang, G.H., Wang, J., Yadav, R.K. and Roth, C.H. (2017). Evaluation of the APSIM model in cropping systems of Asia. *Field Crops Res.* 204, 52–75. doi:10.1016/j.fcr.2016.12.015.

Gaydon, D.S., Lisson, S.N. and Xevi, E. (2006). *Application of APSIM 'multi-paddock' to estimate whole-of-farm water-use efficiency, system water balance and crop production for a rice-based operation in the Coleambally Irrigation District, NSW.* Proceedings of the 13th Australian Society of Agronomy Conference, 10-14 September, Perth, Australia.

Gaydon, D.S., Probert, M.E., Buresh, R.J., Meinke, H., Suriadi, A., Dobermann, A., Bouman, B.A.M. and Timsina, J. (2012a). Rice in cropping systems - Modelling transitions between flooded and non-flooded soil environments. *Eur. J. Agron.* 39, 9–24. doi:10.1016/j.eja.2012.01.003.

Gaydon, D.S., Probert, M.E., Buresh, R.J., Meinke, H. and Timsina, J. (2012b). Modelling the role of algae in rice crop nutrition and soil organic carbon maintenance. *Eur. J. Agron.* 39, 35–43. doi:10.1016/j.eja.2012.01.004.

Gaydon, D.S., Radanielson, A.M., Chaki, A.K., Sarker, M.M.R., Rahman, M.A., Rashid, M.H., Kabir, M.J., Khan, A.S.M.M.R., Gaydon, E.R. and Roth, C.H. (2021). Options for increasing Boro rice production in the saline coastal zone of Bangladesh. *Field Crops Res.* 264, 108089. doi:10.1016/j.fcr.2021.108089.

Godwin, D.C. and Singh, U. (1991). Modelling nitrogen dynamics in rice cropping systems. In: Deturk, P., Ponnamperuma, F.N. (Eds.) *Rice Production on Acid Soils of the Tropics*. Institute of Fundamental Studies, Kandy, Sri Lanka, pp. 287–294.

Godwin, D.C. and Singh, U. (1998). Nitrogen balance and crop response to nitrogen in upland and lowland cropping systems. In: Tsuji, G.Y., Hoogenboom, G., Thornton, P.K. (Eds.) *Understanding options for agricultural production*. Kluwer Academic Publishers, London, UK, pp. 55–77.

Gosh, B.C. and Bhat, R. (1998). Environmental hazards of nitrogen loading in wetland rice fields. *Environ. Pollut.* 102 (S1), 123–126.

Grotelüschen, K., Gaydon, D.S., Langensiepen, M., Ziegler, S., Kwesiga, J., Senthilkumar, K., Whitbread, A.M. and Becker, M. (2021). Assessing the effects of management and hydro-edaphic conditions on rice in contrasting East African wetlands using experimental and modelling approaches. *Agric. Water Manag.* 258, 107146. doi:10.1016/j.agwat.2021.107146.

Haefele, S.M., Jabbar, S.M.A., Siopongco, J.D.L.C., Tirol-Padre, A., Amarante, S.T., Sta Cruz, P.C. and Cosico, W.C. (2008). Nitrogen use efficiency in selected rice (*Oryza sativa* L.) genotypes under different water regimes and nitrogen levels. *Field Crops Res.* 107 (2), 137–146. doi:10.1016/j.fcr.2008.01.007.

Haefele, S.M., Saito, K., N'Diaye, K.M.N., Mussgnug, F., Nelson, A. and Wopereis, M.C.S. (2013). Increasing rice productivity through improved nutrient use in Africa. In: Wopereis, M.C.S., Johnson, D.E., Ahmadi, N., Tollens, E., Jalloh, A. (Eds.) *Realizing Africa's Rice Promise*. CAB International, Wallingford, UK, pp. 250–264.

Haefele, S.M., Sipaseuth, N., Phengsouvanna, V., Dounphady, K. and Vongsouthi, S. (2010). Agro-economic evaluation of fertilizer recommendations for rainfed lowland rice. *Field Crops Res.* 119 (2-3), 215–224. doi:10.1016/j.fcr.2010.07.002.

Hagi-Bishow, M. and Bonnell, R.B. (2000). Assessment of LEACHM-C Model for semi-arid saline irrigation. *ICID Journal (Journal on Irrigation and Drainage)* 49 (1), 29–42.

Hammer, G.L. and Muchow, R.C. (1991). Quantifying climatic risk to sorghum in Australia's semiarid tropics and subtropics: model development and simulation. In: Muchow, R.C., Bellamy, J.A. (Eds.) *Climatic risk in crop production: models and management for the semiarid tropics and subtropics*. CAB International, Wallingford, UK, pp. 205–232.

Haneishi, Y., Maruyama, A., Asea, G., Okello, S.E., Tsuboi, T., Takagaki, M. and Kikuchi, M. (2013a). Exploration of rainfed rice farming in Uganda based on a nationwide survey: regionality, varieties and yield. *AJAR* 8 (29), 4038–4048. doi:10.5897/AJAR12.121.

Haneishi, Y., Maruyama, A., Miyamoto, K., Matsumoto, S., Okello, S.E., Asea, G., Tsuboi, T., Takagaki, M. and Kikuchi, M. (2013b). Introduction of NERICA into an upland farming system and its impacts on farmers' income: a cast study of Namulonge in central Uganda. *Trop. Agr. Develop.* 57 (2), 61–73. doi:10.11248/jsta.57.61.

Haneishi, Y., Okello, S.E., Asea, G., Tsuboi, T., Maruyama, A., Takagaki, M. and Kikuchi, M. (2013c). Exploration of rainfed rice farming in Uganda based on a nationwide survey: Evolution, regionality, farmers and land. *AJAR* 8 (25), 3318–3329. doi:10.5897/AJAR12.120.

Hoffmann, M.P., Jacobs, A. and Whitbread, A.M. (2015). Crop modelling based analysis of site-specific production limitations of winter oilseed rape in northern Germany. *Field Crops Res.* 178, 49–62. doi:10.1016/j.fcr.2015.03.018.

Hoffmann, M.P., Swanepoel, C.M., Nelson, W.C.D., Beukes, D.J., Van der Laan, M., Hargreaves, J.N.G. and Rötter, R.P. (2020). Simulating medium-term effects of cropping system diversification on soil fertility and crop productivity in southern Africa. *Eur. J. Agron.* 119, 126089. doi:10.1016/j.eja.2020.126089.

Holzworth, D.P., Huth, N.I., deVoil, P.G., Zurcher, E.J., Herrmann, N.I., McLean, G., Chenu, K., Van Oosterom, E.J., Snow, V.O., Murphy, C., Fainges, J., Bell, L.W., Peake, A.S., Poulton, P.L., Hochman, Z., Thorburn, P.J., Gaydon, D.S., Dalgliesh, N.P., Rodriguez, D., Cox, H., Chapman, S.C., Doherty, A., Teixeira, E.I., Sharp, J., Cichota, R., Vogeler, I., Li, F.Y., Wang, E., Hammer, G.L., Robertson, M.J., Dimes, J.P., Whitbread, A.M., Hunt, J., Van Rees, H., McClelland, T., Carberry, P.S., Hargreaves, J.N.G., MacLeod, N., McDonald, C., Harsdorf, J., Wedgwood, S. and Keating, B.A. (2014). APSIM – Evolution towards a new generation of agricultural systems simulation. *Environ. Modell. Softw.* 62, 327–350. doi:10.1016/j.envsoft.2014.07.009.

Inthavong, T., Tsubo, M. and Fukai, S. (2011). A water balance model for characterization of length of growing period and water stress development for rainfed lowland rice. *Field Crops Res.* 121 (2), 291–301. doi:10.1016/j.fcr.2010.12.019.

IRRI (2004). *IRRI's Environmental Agenda - an Approach Toward Sustainable Development.* International Rice Research Institute (IRRI), Los Baños, Philippines.

Jama, B., Kimani, D., Harawa, R., Mavuthu, A.K. and Sileshi, G.W. (2017). Maize yield response, nitrogen use efficiency and financial returns to fertilizer on smallholder farms in southern Africa. *Food Sec.* 9 (3), 577–593. doi:10.1007/s12571-017-0674-2.

Jätzold, R. and Baum, E. (1968). *The Kilombero Valley (Tanzania): characteristic features of the economic geography of a semi-humid East African floodplain and its margins.* Weltforum-Verlag GmbH, Munich, Germany.

Jing, Q., Van Keulen, H. and Hengsdijk, H. (2010). Modeling biomass, nitrogen and water dynamics in rice–wheat rotations. *Agric. Syst.* 103 (7), 433–443. doi:10.1016/j.agsy.2010.04.001.

Johansson, E.L. and Abdi, A.M. (2020). Mapping and quantifying perceptions of environmental change in Kilombero Valley, Tanzania. *Ambio* 49, 557–568. doi:10.1007/s13280-019-01226-6.

Johnson, J.-M., Rodenburg, J., Tanaka, A., Senthilkumar, K., Ahouanton, K., Dieng, I., Klotoe, A., Akakpo, C., Segda, Z., Yameogo, L.P., Gbakatchetche, H., Acheampong, G.K., Bam, R.K., Bakare, O.S., Kalisa, A., Gasore, E.R., Ani, S., Ablede, K.A. and Saito, K. (2018). Farmers' perceptions on mechanical weeders for rice production in sub-Saharan Africa. *Exp. Agric.* 55 (1), 117–131.

Jones, A., Breuning-Madsen, H., Brossard, M., Dampha, A., Deckers, J., Dewitte, O., Gallali, T., Hallet, S., Jones, R., Kilasara, M., Le Roux, P., Micheli, E., Montanarealla, L., Spaargaren, O., Thiombiano, L., Van Ranst, E., Yemefack, M. and Zougmore, R. (2013). *Soil Atlas of Africa.* Publication Office of the European Union, Luxembourg.

Jones, C.A., Dyke, P.T., Williams, J.R., Kiniry, J.R., Benson, V.W. and Griggs, R.H. (1991). EPIC: an operational model for evaluation of agricultural sustainability. *Agric. Syst.* 37 (4), 341–350. doi:10.1016/0308-521X(91)90057-H.

Jones, C.A. and Kiniry, J.R. (1986). *CERES-Maize: a simulation model of maize growth and development.* Texas A&M University Press, College Station, Texas, USA.

Jones, M.P., Dingkuhn, M., Aluko, G.K. and Semon, M. (1997). Interspecific *Oryza sativa* L. x O. *glaberrima* Steud. progenies in upland rice improvement. *Euphytica* 94 (2), 237–246. doi:10.1023/A:1002969932224.

Kabumbuli, R. and Kiwazi, F.W. (2009). Participatory planning, management and alternative livelihoods for poor wetland-dependent communities in Kampala, Uganda. *Afr. J. Ecol.* 47, 154–160. doi:10.1111/j.1365-2028.2008.01063.x.

Kadiyala, M.D.M., Jones, J.W., Mylavarapu, R.S., Li, Y.C. and Reddy, M.D. (2015). Identifying irrigation and nitrogen best management practices for aerobic rice–maize cropping system for semi-arid tropics using CERES-rice and maize models. *Agric. Water Manag.* 149, 23–32. doi:10.1016/j.agwat.2014.10.019.

Kafiriti, E.M., Dondeyne, S., Msomba, S., Deckers, J. and Raes, D. (2003). Variations in agronomic characteristics of irrigated rice varieties: Lessons from participatory trials in south eastern Tanzania. *JFAE* 1 (2), 273–277.

Kangalawe, R.Y.M. and Liwenga, E.T. (2005). Livelihoods in the wetlands of Kilombero Valley in Tanzania: opportunities and challenges to integrated water resource

management. *Phys. Chem. Earth* 30 (11-16), 968–975. doi:10.1016/j.pce.2005.08.044.

Kansiime, F., Kateyo, E., Oryem-Origa, H. and Mucunguzi, P. (2007). Nutrient status and retention in pristine and disturbed wetlands in Uganda: management implications. *Wetlands Ecol. Manage.* 15 (6), 453–467. doi:10.1007/s11273-007-9054-6.

Kato, F. (2007). Development of a major rice cultivation area in the Kilombero Valley, Tanzania. *Afr. Stud. Monogr.* 36, 3–18. doi:10.14989/68498.

Kaye, D.K. (2006). Community perceptions and experiences of domestic violence and induced abortion in Wakiso District, Uganda. *Qual. Health Res.* 16 (8), 1120–1128. doi:10.1177/1049732306292172.

Kaye, D.K., Mirembe, F., Ekstrom, A.M., Kyomuhendo, G.B. and Johansson, A. (2005). Implications of bride price on domestic violence and reproductive health in Wakiso District, Uganda. *Afr. Health Sci.* 5 (4), 300–303.

Keating, B.A., Carberry, P.S., Hammer, G.L., Probert, M.E., Robertson, M.J., Holzworth, D.P., Huth, N.I., Hargreaves, J.N.G., Meinke, H., Hochman, Z., McLean, G., Verburg, K., Snow, V.O., Dimes, J.P., Silburn, D.M., Wang, E., Brown, S., Bristow, K.L., Asseng, S., Chapman, S.C., McCown, R.L., Freebairn, D.M. and Smith, C.J. (2003). An overview of APSIM, a model designed for farming systems simulations. *Eur. J. Agron.* 18, 267–288. doi:10.1016/S1161-0301(02)00108-9.

Keddy, P.A., Fraser, L.H., Solomeshch, A.I., Junk, W.J., Campbell, D.R., Arroyo, M.K.T. and Alho, C.J.R. (2009). Wet and wonderful: the world's largest wetlands are conservation priorities. *BioScience* 59 (1), 39–51. doi:10.1525/bio.2009.59.1.8.

Khaliq, T., Gaydon, D.S., Ahmad, M.D., Cheema, M.J.M. and Gull, U. (2019). Analyzing crop yield gaps and their causes using cropping systems modelling–A case study of the Punjab rice-wheat system, Pakistan. *Field Crops Res.* 232, 119–130. doi:10.1016/j.fcr.2018.12.010.

Kijima, Y. (2013). The adoption of NERICA rice varieties at the initial stage of the diffusion process in Uganda. *Afr. J. Agric. Resour. Econ.* 8 (1), 45–56. doi:10.22004/ag.econ.156984.

Kijima, Y., Ito, Y. and Otsuka, K. (2012). Assessing the impact of training on lowland rice productivity in an African setting: evidence from Uganda. *World Dev.* 40 (8), 1610–1618. doi:10.1016/j.worlddev.2012.04.008.

Kijima, Y., Otsuka, K. and Sserunjuuma, D. (2008). Assessing the impact of NERICA on income and poverty in central and western Uganda. *Agric. Econ.* 38, 327–337. doi:10.1111/j.1574-0862.2008.00303.x.

Kiniry, J.R., Rosenthal, W.D., Jackson, B.S. and Hoogenboom, G. (1990). Predicting leaf development of crop plants. In: Hodges, T. (Ed.) *Predicting Crop Phenology*. CRC Press, Boca Raton, USA, pp. 29–42.

Knisel, W.G. (1980). *CREAMS: a field-scale model for chemicals, runoff, and erosion from agricultural management systems.* US Department of Agriculture, Conservation Research Report no. 26, Washington, DC, USA.

Koussoubé, E. and Nauges, C. (2016). Returns to fertiliser use: Does it pay enough? Some new evidence from Sub-Saharan Africa. *Eur. Rev. Agric. Econ.* 44 (2), 183–210. doi:10.1093/erae/jbw018.

Koutsouris, A.J., Chen, D. and Lyon, S.W. (2016). Comparing global precipitation data sets in eastern Africa: a case study of Kilombero Valley, Tanzania. *Int. J. Climatol.* 36 (4), 2000–2014. doi:10.1002/joc.4476.

Kropff, M.J., Van Laar, H.H. and Matthews, R.B. (1994). *ORYZA1: an ecophysiological model for irrigated rice production.* SARP Research Proceedings, IRRI/AB-DLO, Wageningen, Netherlands.

Krupnik, T.J., Shennan, C., Settle, W.H., Demont, M., Ndiaye, A.B. and Rodenburg, J. (2012). Improving irrigated rice production in the Senegal River Valley through experiential learning and innovation. *Agric. Syst.* 109, 101–112. doi:10.1016/j.agsy.2012.01.008.

Kuivanen, K.S., Alvarez, S., Michalscheck, M., Adjei-Nsiah, S., Descheemaeker, K., Mellon-Bedi, S. and Groot, J.C.J. (2016). Characterising the diversity of smallholder farming systems and their constraints and opportunities for innovation: A case study from the Northern Region, Ghana. *NJAS - Wageningen Journal of Life Sciences* 78, 153–166. doi:10.1016/j.njas.2016.04.003.

Kwesiga, J. (2021). *Assessing and targeting management options for smallholder rice-based systems in Kilombero floodplain, Tanzania*. Dissertation, Bonn, Germany.

Kwesiga, J., Grotelüschen, K., Neuhoff, D., Senthilkumar, K., Döring, T.F. and Becker, M. (2019). Site and management effects on grain yield and yield variability of rainfed lowland rice in the Kilombero floodplain of Tanzania. *Agronomy* 9 (10), 632–648. doi:10.3390/agronomy9100632.

Kwesiga, J., Grotelüschen, K., Senthilkumar, K., Neuhoff, D., Döring, T.F. and Becker, M. (2020a). Effect of organic amendments on the productivity of rainfed lowland rice in the Kilombero floodplain of Tanzania. *Agronomy* 10 (9), 1280. doi:10.3390/agronomy10091280.

Kwesiga, J., Grotelüschen, K., Senthilkumar, K., Neuhoff, D., Döring, T.F. and Becker, M. (2020b). Rice yield gaps in smallholder systems of the Kilombero floodplain in Tanzania. *Agronomy* 10 (8), 1135. doi:10.3390/agronomy10081135.

Lankford, B. and Franks, T. (2000). The sustainable coexistence of wetlands and rice irrigation: a case study from Tanzania. *J. Environ. Dev.* 9 (2), 119–137. doi:10.1177/107049650000900202.

Leemhuis, C., Amler, E., Diekkrüger, B., Gabiri, G. and Näschen, K. (2016). East African wetland-catchment data base for sustainable wetland management. *PIAHS* 374, 123–128. doi:10.5194/piahs-374-123-2016.

Leemhuis, C., Thonfeld, F., Näschen, K., Steinbach, S., Muro, J., Strauch, A., López, A., Daconto, G., Games, I. and Diekkrüger, B. (2017). Sustainability in the food-water-ecosystem nexus: the role of land use and land cover change for water resources and ecosystems in the Kilombero wetland, Tanzania. *Sustainability* 9 (9), 1513. doi:10.3390/su9091513.

Lind, E.M., Morrison, M.E.S. and Hamilton, A.C. (1974). *East African vegetation.* Longman Group Limited, London, UK.

Littleboy, M., Silburn, D.M., Freebairn, D.M., Woodruff, D.R. and Hammer, G.L. (1989). *PERFECT - A computer simulation model of productivity erosion runoff functions to evaluate conservation techniques.* Bulletin-Queensland Department of Primary Industries, Toowoomba, Australia.

Liu, X.-J.A., Van Groenigen, K.J., Dijkstra, P. and Hungate, B.A. (2017). Increased plant uptake of native soil nitrogen following fertilizer addition – not a priming effect? *Appl. Soil Ecol.* 114, 105–110. doi:10.1016/j.apsoil.2017.03.011.

Lyon, S.W., Koutsouris, A.J., Scheibler, F., Jarsjö, J., Mbanguka, R., Tumbo, M., Robert, K.K., Sharma, A.N. and van der Velde, Y. (2015). Interpreting characteristic drainage timescale variability across Kilombero Valley, Tanzania. *Hydrol. Process.* 29 (8), 1912–1924. doi:10.1002/hyp.10304.

Materu, S.F. and Heise, S. (2019). Eco-toxicity of water, soil, and sediment from agricultural areas of Kilombero Valley Ramsar wetlands, Tanzania. *EHS* 5 (1), 256–269. doi:10.1080/20964129.2019.1695545.

Mbaga, H.R., Mrema, J.P. and Msanya, B.M. (2017). Response of rice to nitrogen and phosphorus applied on typical soils of Dakawa irrigation scheme, Morogoro, Tanzania. *IJIR* 3 (6), 378–384.

McCartney, M.P. and Houghton-Carr, H.A. (2009). Working wetland potential: an index to guide the sustainable development of African wetlands. *Nat. Resour. Forum* 33, 99–110. doi:10.1111/j.1477-8947.2009.01214.x.

McCown, R.L., Hammer, G.L., Hargreaves, J.N.G., Holzworth, D.P. and Freebairn, D.M. (1996). APSIM: a novel software system for model development, model testing and simulation in agricultural systems research. *Agric. Syst.* 50, 255–271. doi:10.1016/0308-521X(94)00055-V.

McCown, R.L., Hammer, G.L., Hargreaves, J.N.G., Holzworth, D.P. and Huth, N.I. (1995). APSIM: an agricultural production system simulation model for operational research. *Math. Comput. Simul.* 39, 225–231.

McCown, R.L. and Williams, J.R. (1989). AUSIM: a cropping systems model for operational research. In: SSA ImACS (Ed.) *Biennial Conference on Modelling and Simulation.* Australian National University, Canberra, Australia, pp. 25–27.

Mghase, J.J., Shiwachi, H., Nakasone, K. and Takahashi, H. (2010). Agronomic and socio-economic constraints to high yield of upland rice in Tanzania. *AJAR* 5 (2), 150–158. doi:10.5897/AJAR09.459.

Mitsch, W.J., Bernal, B. and Hernandez, M.E. (2015). Ecosystem services of wetlands. *Int. J. Biodivers. Sci. Ecosyst. Serv. Manag.* 11 (1), 1–4. doi:10.1038/387253a0.

Miyamoto, K., Maruyama, A., Haneishi, Y., Matsumoto, S., Tsuboi, T., Asea, G., Okello, S.E., Takagaki, M. and Kikuchi, M. (2012). NERICA cultivation and its yield determinants: the case of upland rice farmers in Namulonge, central Uganda. *J. Agric. Sci.* 4 (6), 120–135. doi:10.5539/jas.v4n6p120.

Mlengera, N., Wanjala, N., Tegambwage, W., Kakema, T., Kayeke, J. and Ndunguru, A. (2015). Promotion of labour saving rice mechanization technologies in rain-fed low land and irrigated ecologies of Tanzania and Kenya. *J. Nat. Sci. Res.* 5 (20), 52–59.

Mohanty, M., Sinha, N.K., Somasundaram, J., McDermid, S.S., Patra, A.K., Singh, M., Dwivedi, A.K., Reddy, K.S., Rao, C.S., Prabhakar, M., Hati, K.M., Jha, P., Singh, R.K., Chaudhary, R.S., Kumar, S.N., Tripathi, P., Dalal, R.C., Gaydon, D.S. and Chaudhari, S.K. (2020). Soil carbon sequestration potential in a Vertisol in central India- results from a 43-year long-term experiment and APSIM modeling. *Agric. Syst.* 184, 102906. doi:10.1016/j.agsy.2020.102906.

Mokus, V. (1972). *National engineering handbook section 4: hydrology.* USDA, Soil Conservation Service, Washington DC, USA.

Mombo, F., Speelman, S., Hella, J. and Van Huylenbroeck, G. (2013). How characteristics of wetlands resource users and associated institutions influence the sustainable management of wetlands in Tanzania. *Land Use Policy* 35, 8–15. doi:10.1016/j.landusepol.2013.04.010.

Monson, J.P. (2000). Memory, migration and the authority of history in southern Tanzania, 1860-1960. *J. Afr. Hist.* 41 (3), 347–372. doi:10.1017/S0021853700007763.

Moritz, S. and Bartz-Beielstein, T. (2017). imputeTS: time series missing value imputation in R. *R J.* 9 (1), 207. doi:10.32614/rj-2017-009.

Mruma, A.H. (2002). Structural evolution of the Kilombero rift basin in central Tanzania. *Tanz. J. Sci.* 28 (2), 55–68. doi:10.4314/tjs.v28i2.18354.

Msanya, B.M., Kaaya, A.K., Araki, S., Otsuka, H. and Nyadizi, G.I. (2003). Pedological characteristics, general fertility and classification of some benchmark soils of Morogoro district, Tanzania. *AJST* 4 (2), 101–112. doi:10.4314/ajst.v4i2.15309.

Msofe, N., Sheng, L. and Lyimo, J. (2019). Land use change trends and their driving forces in the Kilombero Valley Floodplain, south-eastern Tanzania. *Sustainability* 11 (2), 505. doi:10.3390/su11020505.

Mugisa, I.O., Fungo, B., Adur, S.O., Ssemalulu, O., Molly, A., Atim, J., Nakyagaba, W., Kizza, T., Kabanyoro, R., Sseruwu, G. and Akello, B.O. (2017). Urban and peri-urban crop farming in central Uganda: characteristics, constraints and opportunities for household food security and income. *AJPS* 11 (7), 264–275. doi:10.5897/AJPS2016.1477.

Mwalyosi, R.B.B. (1990). Resource potentials of Tanzania Basin, the Rufiji River. *Ambio* 19, 16–20.

Mwongera, C., Shikuku, K.M., Winowiecki, L., Okolo, W., Twyman, J. and Läderach, P. (2014). *Climate smart agriculture rapid appraisal (CSA-RA) report from the southern agricultural growth corridor of Tanzania (SAGCOT).* International Fund for Agricultural Development (IFAD), Rome, Italy.

Näschen, K. (2020). *Impact assessment of global change on wetland-catchment interactions in a tropical East African catchment.* Dissertation, Bonn, Germany.

Näschen, K., Diekkrüger, B., Evers, M., Höllermann, B., Steinbach, S. and Thonfeld, F. (2019). The impact of land use/land cover change (LULCC) on water resources in a tropical catchment in Tanzania under different climate change scenarios. *Sustainability* 11 (24), 7083. doi:10.3390/su11247083.

Näschen, K., Diekkrüger, B., Leemhuis, C., Steinbach, S., Seregina, L., Thonfeld, F. and Van der Linden, R. (2018). Hydrological modeling in data-scarce catchments: the Kilombero floodplain in Tanzania. *Water* 10 (5), 599. doi:10.3390/w10050599.

Nasrin, S., Bergman, L.J., Jirström, M., Holmquist, B., Andersson Djurfeldt, A. and Djurfeldt, G. (2015). Drivers of rice production: evidence from five Sub-Saharan African countries. *Agric. Food Secur.* 4 (1), 1–19. doi:10.1186/s40066-015-0032-6.

Nhamo, N., Rodenburg, J., Zenna, N., Makombe, G. and Luzi-Kihupi, A. (2014). Narrowing the rice yield gap in East and Southern Africa: using and adapting existing technologies. *Agric. Syst.* 131, 45–55. doi:10.1016/j.agsy.2014.08.003.

Niang, A., Becker, M., Ewert, F., Tanaka, A., Dieng, I. and Saito, K. (2018). Yield variation of rainfed rice as affected by field water availability and N fertilizer use in central Benin. *Nutr. Cycling Agroecosyst.* 110 (2), 293–305. doi:10.1007/s10705-017-9898-y.

Nicholson, S.E. (2017). Climate and climatic variability of rainfall over eastern Africa. *Rev. Geophys.* 55 (3), 590–635. doi:10.1002/2016RG000544.

Nindi, S.J., Maliti, H., Bakari, S., Kija, H. and Machoke, M. (2014). Conflicts over land and water resources in the Kilombero valley floodplain, Tanzania. *Afr. Stud. Monogr.* 50, 173-190. doi:10.14989/189720.

Nsubuga, F.N.W., Namutebi, E.N. and Nsubuga-Ssenfuma, M. (2014). Water resources of Uganda: an assessment and review. *JWARP* 6 (14), 1297–1315. doi:10.4236/jwarp.2014.614120.

Nsubuga, F.N.W., Olwoch, J.M. and Rautenbach, C.W. de (2011). Climatic trends at Namulonge in Uganda: 1947-2009. *IGG* 3 (1), 119–131. doi:10.5539/jgg.v3n1p119.

Nurulhuda, K., Gaydon, D.S., Jing, Q., Zakaria, M.P., Struik, P.C. and Keesman, K.J. (2018). Nitrogen dynamics in flooded soil systems: an overview on concepts and performance of models. *J. Sci. Food Agric.* 98 (3), 865–871. doi:10.1002/jsfa.8683.

Ogallo, L.A. (1993). Dynamics of the East African climate. *Earth Planet Sci.* 102 (1), 203–217. doi:10.1007/BF02839191.

Ojara, M.A., Lou, Y., Aribo, L., Namumbya, S. and Uddin, M.J. (2020). Dry spells and probability of rainfall occurrence for Lake Kyoga Basin in Uganda, East Africa. *Nat. Hazards* 100 (2), 493–514. doi:10.1007/s11069-019-03822-x.

Okebalama, C.B., Safo, E.Y., Yeboah, E., Abaidoo, R.C. and Logah, V. (2016). Fertilizer microdosing in the humid forest zone of Ghana: an efficient strategy for increasing maize yield and income in smallholder farming. *Soil Sci. Soc. Am. J.* 80 (5), 1254–1261. doi:10.2136/sssaj2016.03.0065.

Oonyu, J. (2011). Upland rice growing: a potential solution to declining crop yields and the degradation of the Doho wetlands, Butaleja district, Uganda. *AJAR* 6 (12), 2774–2783. doi:10.5897/AJAR10.806.

Oosterbaan, R.J., Gunneweg, H.A. and Huizing, A. (1986). *Water control for rice cultivation in small valleys of West Africa.* International Institute for Land Reclamation and Improvement (ILRI), Wageningen, Netherlands.

Osujieke, D.N., Imadojemu, P.E. and Igbojionu, J.N. (2017). Characterization and variability of soils formed on a toposequential floodplain in Uratta, south eastern Nigeria. *FTSTJ* 2 (1), 628–632.

Pampolino, M.F., Laureles, E.V., Gines, H.C. and Buresh, R.J. (2008). Soil carbon and nitrogen changes in long-term continuous lowland rice cropping. *Soil Sci. Soc. Am. J.* 72 (3), 798–807. doi:10.2136/sssaj2006.0334.

Parton, W.J., Schimel, D.S., Cole, C.V. and Ojima, D.S. (1987). Analysis of factors controlling soil organic matter levels in great plains grasslands. *Soil Sci. Soc. Am. J.* 51 (5), 1173–1179.

Peel, M.C., Finlayson, B.L. and McMahon, T.A. (2007). World map of the Köppen-Geiger climate classification updated. *Hydrol. Earth Syst. Sci.* 11, 1633–1644. doi:10.1127/0941-2948/2006/0130.

Penning de Vries, F.W.T., Jansen, D.M., Ten Berge, H.F.M. and Bakema, A. (1989). *Simulation of eco-physiological processes of growth in several annual crops.* International Rice Research Institute (IRRI)/Pudoc, Los Baños, Philippines/Wageningen, Netherlands.

Penning de Vries, F.W.T., Van Laar, H.H. and Kropff, M.J. (1991). *Simulation and systems analysis for rice production (SARP).* Pudoc, Wageningen, Netherlands, 371 pp.

Penning de Vries, F. W. and Van Laar, H.H. (1982). *Simulation of plant growth and crop production.* Pudoc, Wageningen, The Netherlands.

Philippon, N., Camberlin, P. and Fauchereau, N. (2002). Empirical predictability study of October–December East African rainfall. *Q. J. R. Meteorol. Soc.* 128 (585), 2239–2256. doi:10.1256/qj.01.190.

Posner, J.L. and Crawford, E.W. (1992). Improving fertilizer recommendations for subsistance farmers in West Africa: The use of agro-economic analysis of on-farm trials. *Nutr. Cycling Agroecosyst.* 32 (3), 333–342. doi:10.1007/bf01050371.

Poulton, P.L., Vesna, T., Dalgliesh, N.P. and Seng, V. (2015). Applying simulation to improve rice varieties in reducing the on-farm yield gap in Cambodian lowland rice ecosystems. *Exp. Agric.* 51 (2), 264–284. doi:10.1017/S0014479714000271.

Probert, M.E., Dimes, J.P., Keating, B.A., Dalal, R.C. and Strong, W.M. (1998). APSIM's water and nitrogen modules and simulation of the dynamics of water and nitrogen in fallow systems. *Agric. Syst.* 56 (1), 1–28. doi:10.1016/S0308-521X(97)00028-0.

Probert, M.E., Keating, B.A., Thompson, J.P. and Parton, W.J. (1995). Modelling water, nitrogen, and crop yield for a long-term fallow management experiment. *Aust. J. Exp. Agric.* 35 (7), 941–950. doi:10.1071/ea9950941.

Raes, D., Kafiriti, E.M., Wellens, J., Deckers, J., Maertens, A., Mugogo, S., Dondeyne, S. and Descheemaeker, K. (2007). Can soil bunds increase the production of rain-fed

lowland rice in South Eastern Tanzania? *Agric. Water Manag.* 89 (3), 229–235. doi:10.1016/j.agwat.2007.01.005.

Ragasa, C. and Chapoto, A. (2017). Limits to Green Revolution in rice in Africa: The case of Ghana. *Land Use Policy* 66, 304–321. doi:10.1016/j.landusepol.2017.04.052.

Rebelo, L.M., McCartney, M.P. and Finlayson, C.M. (2010). Wetlands of Sub-Saharan Africa: distribution and contribution of agriculture to livelihoods. *Wetlands Ecol. Manage.* 18 (5), 557–572. doi:10.1007/s11273-009-9142-x.

Rickman, J., Moreira, J., Gummert, M., Wopereis, M.C.S., Johnson, D.E., Ahmadi, N., Tollens, E. and Jalloh, A. (2013). Mechanizing Africa's rice sector. In: Wopereis, M.C.S., Johnson, D.E., Ahmadi, N., Tollens, E., Jalloh, A. (Eds.) *Realizing Africa's Rice Promise.* CAB International, Wallingford, UK, pp. 332–342.

Ritchie, J.T. (1972). A model for predicting evaporation from a row crop with incomplete cover. *Water Resour. Res.* 8 (5), 1204–1213. doi:10.1029/WR008i005p01204.

Ritchie, J.T. and Otter, S. (1985). Description and performance of CERES Wheat : A user-oriented wheat yield model. In: Willis, W.O. (Ed.) *ARS Wheat Yield Project.* USDA, Agricultural Research Service, Missouri, USA, pp. 159–175.

Rodenburg, J. (2013). Inland Valleys: Africa's future food baskets. In: Wopereis, M.C.S., Johnson, D.E., Ahmadi, N., Tollens, E., Jalloh, A. (Eds.) *Realizing Africa's Rice Promise.* CAB International, Wallingford, UK, pp. 276–293.

Rodenburg, J., Saito, K., Irakiza, R., Makokha, D.W., Onyuka, E.A. and Senthilkumar, K. (2015). Labor-saving weed technologies for lowland rice farmers in sub-Saharan Africa. *Weed Technol.* 29 (4), 751–757. doi:10.1614/WT-D-15-00016.1.

Rodenburg, J., Zwart, S.J., Kiepe, P., Narteh, L.T., Dogbe, W. and Wopereis, M.C.S. (2014). Sustainable rice production in African inland valleys: Seizing regional potentials through local approaches. *Agric. Syst.* 123, 1–11. doi:10.1016/j.agsy.2013.09.004.

Roger, P.A. (1996). *Biology and management of the floodwater ecosystem in rice fields.* International Rice Research Institute (IRRI), Los Baños, Philippines.

Ross, P.J. (1990). *SWIM: a simulation model for soil water infiltration and movement: reference manual.* CSIRO Division of Soils, Canberra, Australia.

Ruane, A.C., Goldberg, R. and Chryssanthacopoulos, J. (2015). Climate forcing datasets for agricultural modeling: Merged products for gap-filling and historical climate series estimation. *Agric. For. Meteorol.* 200, 233–248. doi:10.1016/j.agrformet.2014.09.016.

Rugumamu, C.P. (2014). Empowering smallholder rice farmers in Tanzania to increase productivity for promoting food security in Eastern and Southern Africa. *Agric. Food Secur.* 3 (1), 1–8. doi:10.1186/2048-7010-3-7.

Ruhinduka, R.D., Alem, Y., Eggert, H. and Lybbert, T. (2020). Smallholder rice farmers' post-harvest decisions: preferences and structural factors. *Eur. Rev. Agric. Econ.* 47 (4), 1587–1620. doi:10.1093/erae/jbz052.

Sabiiti, E.N. and Katongole, C.B. (2016). Role of peri-urban areas in the food system of Kampala, Uganda. In: Maheshwari, B., Singh, V.P., Thoradeniya, B. (Eds.) *Balanced Urban Development: Options and strategies for liveable cities*. Springer, Cambridge, UK, pp. 387–392.

Saito, K., Nelson, A., Zwart, S.J., Niang, A., Sow, A., Yoshida, H. and Wopereis, M.C.S. (2013). Towards a better understanding of biophysical determinants of yield gaps and the potential for expansion of the rice area in Africa. In: Wopereis, M.C.S., Johnson, D.E., Ahmadi, N., Tollens, E., Jalloh, A. (Eds.) *Realizing Africa's Rice Promise*. CAB International, Wallingford, UK, pp. 188–203.

Saito, K., Six, J., Komatsu, S., Snapp, S., Rosenstock, T., Arouna, A., Cole, S., Taulya, G. and Vanlauwe, B. (2021). Agronomic gain: Definition, approach, and application. *Field Crops Res.* 270, 108193. doi:10.1016/j.fcr.2021.108193.

Saito, K., Vandamme, E., Johnson, J.-M., Tanaka, A., Senthilkumar, K., Dieng, I., Akakpo, C., Gbaguidi, F., Segda, Z., Bassoro, I., Lamare, D., Gbakatchetche, H., Abera, B.B., Jaiteh, F., Bam, R.K., Dogbe, W., Sékou, K., Rabeson, R., Kamissoko, N., Mossi, I.M., Tarfa, B.D., Bakare, O.S., Kalisa, A., Baggie, I., Kajiru, G.J., Ablede, K.A., Ayeva, T., Nanfumba, D. and Wopereis, M.C.S. (2019). Yield-limiting macronutrients for rice in sub-Saharan Africa. *Geoderma* 338, 546–554. doi:10.1016/j.geoderma.2018.11.036.

Sakané, N., Becker, M., Langensiepen, M. and Van Wijk, M.T. (2013). Typology of smallholder production systems in small East-African wetlands. *Wetlands* 33 (1), 101–116. doi:10.1007/s13157-012-0355-z.

Sakané, N., Van Wijk, M.T., Langensiepen, M. and Becker, M. (2014). A quantitative model for understanding and exploring land use decisions by smallholder agrowetland households in rural areas of East Africa. *Agric. Ecosyst. Environ.* 197, 159–173. doi:10.1016/j.agee.2014.07.011.

Schmitter, P., Zwart, S.J., Danvi, A. and Gbaguidi, F. (2015). Contributions of lateral flow and groundwater to the spatio-temporal variation of irrigated rice yields and water productivity in a West-African inland valley. *Agric. Water Manag.* 152, 286–298. doi:10.1016/j.agwat.2015.01.014.

Schulthess, U. and Ritchie, J.T., 1996. Simulation of tillage and crop residue dynamics with the SALUS-model. 26th Annual Crop Simulation Workshop, 9 April 1996, Fort Collins, USA.

Sekiya, N., Oizumi, N., Kessy, T.T., Fimbo, K.M.J., Tomitaka, M., Katsura, K. and Araki, H. (2020). Importance of market-oriented research for rice production in Tanzania. A review. *Agron. Sustain. Dev.* 40 (1), 1–16. doi:10.1007/s13593-020-0611-1.

Seligman, N.G. and Van Keulen, H. (1981). PAPRAN: a simulation model of annual pasture production limited by rainfall and nitrogen. In: Frissel, M.J., Van Veen, J.A. (Eds.) *Simulation of Nitrogen Behaviour of Soil-Plant Systems*. Pudoc, Wageningen, Netherlands, pp. 192–221.

Senthilkumar, K., Rodenburg, J., Dieng, I., Vandamme, E., Sillo, F.S., Johnson, J.-M., Rajaona, A., Ramarolahy, J.A., Gasore, E.R., Abera, B.B., Kajiru, G.J., Mghase, J.J., Rabeson, R., Lamo, J. and Saito, K. (2020). Quantifying rice yield gaps and their causes in Eastern and Southern Africa. *J. Agron. Crop Sci.* 206, 478–490. doi:10.1111/jac.12417.

Senthilkumar, K., Sillo, F.S., Rodenburg, J., Dimkpa, C.O., Saito, K., Dieng, I. and Bindraban, P.S. (2021). Rice yield and economic response to micronutrient application in Tanzania. *Field Crops Res.* 270, 108201. doi:10.1016/j.fcr.2021.108201.

Senthilkumar, K., Tesha, B.J., Mghase, J.J. and Rodenburg, J. (2018). Increasing paddy yields and improving farm management: results from participatory experiments with good agricultural practices (GAP) in Tanzania. *Paddy Water Environ.* 16 (4), 749–766. doi:10.1007/s10333-018-0666-7.

Shaffer, M.J., Gupta, S.C., Linden, D.R., Molina, J.A.E., Clapp, C.E. and Larson, W.E. (1991). Simulation of nitrogen, tillage, and residue management effects on soil fertility. In: Jørgensen, S.E. (Ed.) *Developments in Environmental Modelling*. Elsevier, Amsterdam, Netherlands, pp. 525–544.

Sihmar, R. (2014). Growth and instability in agricultural production in Haryana: A district level analysis. *Int. J. Sci. Res.* 4 (7), 1–12.

Šimůnek, J., Šejna, M., Saito, H., Sakai, M. and Van Genuchten, M.T. (2013). *The HYDRUS-1D Software Package for Simulating the One-Dimensional Movement of Water, Heat, and Multiple Solutes in Variably Saturated Media, Manual Version 4.17,* University of California, Riverside, California, USA.

Singh, R.K., Murori, R., Ndayiragije, A., Bigirimana, J., Kimani, J.M., Kanyeka, Z.L., Surpong, S. and Singh, Y.P. (2013). Rice breeding activities in Eastern and Southern Africa. *SABRAO J. Breed. Genet.* 45 (1), 73–83.

Sommer, H., Kröner, A. and Lowry, J. (2017). Neoproterozoic eclogite- to high-pressure granulite-facies metamorphism in the Mozambique belt of east-central Tanzania: A petrological, geochemical and geochronological approach. *Lithos* 284, 666–690. doi:10.1016/j.lithos.2017.05.010.

Subash, N., Shamim, M., Singh, V.K., Gangwar, B., Singh, B., Gaydon, D.S., Roth, C.H., Poulton, P.L. and Sikka, A.K. (2015). Applicability of APSIM to capture the effectiveness of irrigation management decisions in rice-based cropping sequence in the Upper-Gangetic plains of India. *Paddy Water Environ.* 13 (4), 325–335. doi:10.1007/s10333-014-0443-1.

Taylor, R.G. and Howard, K.W.F. (1998). Post-Palaeozoic evolution of weathered landsurfaces in Uganda by tectonically controlled deep weathering and stripping. *Geomorphology* 25 (3-4), 173–192. doi:10.1016/s0169-555x(98)00040-3.

Ten Berge, H.F.M. and Kropff, M.J. (1995). Founding a systems research network for rice. In: Bouma, J., Kuyvenhoven, A., Bouman, B.A.M., Luyten, J.C., Zandstra, H.G. (Eds.) *Eco-regional Approaches for Sustainable Land Use and Food Production. Systems Approaches for Sustainable Agricultural Development, vol 4.* Kluwer Academic Publishers, Dordrecht, Netherlands, pp. 263–282.

Thonfeld, F., Steinbach, S., Muro, J. and Kirimi, F. (2020). Long-Term land use/land cover change assessment of the Kilombero catchment in Tanzania using random forest classification and robust change vector analysis. *Remote Sens.* 12 (7), 1057. doi:10.3390/rs12071057.

Thorburn, P.J., Probert, M.E. and Robertson, F.A. (2001). Modelling decomposition of sugarcane surface residues with APSIM–Residue. *Field Crops Res.* 70 (3), 223–232. doi:10.1016/s0378-4290(01)00141-1.

Tippe, D.E., Bastiaans, L., van Ast, A., Dieng, I., Cissoko, M., Kayeke, J., Makokha, D.W. and Rodenburg, J. (2020). Fertilisers differentially affect facultative and obligate parasitic weeds of rice and only occasionally improve yields in infested fields. *Field Crops Res.* 254, 107845. doi:10.1016/j.fcr.2020.107845.

Touré, A.A., Becker, M., Johnson, D.E., Koné, B., Kossou, D.K. and Kiepe, P. (2009). Response of lowland rice to agronomic management under different hydrological regimes in an inland valley of Ivory Coast. *Field Crops Res.* 114 (2), 304–310. doi:10.1016/j.fcr.2009.08.015.

Tsubo, M., Basnayake, J., Fukai, S., Sihathep, V., Siyavong, P., Sipaseuth and Chanphengsay, M. (2006). Toposequential effects on water balance and productivity in rainfed lowland rice ecosystem in Southern Laos. *Field Crops Res.* 97 (2-3), 209–220. doi:10.1016/j.fcr.2005.10.004.

Tsubo, M., Fukai, S., Basnayake, J., Tuong, T.P., Bouman, B.A.M. and Harnpichitvitaya, D. (2005). Estimating percolation and lateral water flow on sloping land in rainfed lowland rice ecosystem. *Plant Prod. Sci.* 8 (3), 354–357. doi:10.1626/pps.8.354.

Tsujimoto, Y., Rakotoson, T., Tanaka, A. and Saito, K. (2019). Challenges and opportunities for improving N use efficiency for rice production in sub-Saharan Africa. *Plant Prod. Sci.* 22 (4), 413–427. doi:10.1080/1343943X.2019.1617638.

Turyahabwe, N., Tumusiime, D.M., Kakuru, W. and Barasa, B. (2013). Wetland use/cover changes and local perceptions in Uganda. *SAR* 2 (4), 95–105. doi:10.22004/ag.econ.230546.

UBOS (2018). *2018 Statistical abstract.* Uganda Bureau of Statistics (UBOS), Kampala, Uganda.

van Campenhout, B., Walukano, W. and van Asten, P.J.A. (2016). *Addressing knowledge gaps in rice growing in eastern Uganda.* International Food Policy Research Institute (IFPRI), Washington DC, USA.

Van Ittersum, M.K., Leffelaar, P.A., Van Keulen, H., Kropff, M.J., Bastiaans, L. and Goudriaan, J. (2003). On approaches and applications of the Wageningen crop models. *Eur. J. Agron.* 18 (3-4), 201–234. doi:10.1016/S1161-0301(02)00106-5.

Van Keulen, H., de Vries, F.P. and Drees, E.M. (1982). A summary model for crop growth. In: Penning de Vries, F.W.T., Van Laar, H.H. (Eds.) *Simulation of Pant Gowth and Cop Poduction.* Pudoc, Amsterdam, Netherlands, pp. 87–97.

Van Keulen, H. and Wolf, J. (1987). Modelling of agricultural production: weather, soils and crops. *Field Crops Res.* 17, 319–320. doi:10.1016/0378-4290(87)90043-8.

Van Oort, P.A.J., Saito, K., Tanaka, A., Amovin-Assagba, E., van Bussel, L.G.J., Van Wart, J., De Groot, H., Van Ittersum, M.K., Cassman, K.G. and Wopereis, M.C.S. (2015). Assessment of rice self-sufficiency in 2025 in eight African countries. *Glob. Food. Sec.* 5, 39–49. doi:10.1016/j.gfs.2015.01.002.

Van Soest, M. (2018). *The political ecology of malaria - emerging dynamics of wetland agriculture at the urban fringe in central Uganda.* Dissertation, Cologne, Germany.

Verburg, K. (1996). *Methodology in soil water and solute balance modelling: an evaluation of the APSIM-SoilWat and SWIMv2 models. Divisional Report No 131.* CSIRO Division of Soils, Adelaide, Australia.

Wade, L.J., Fukai, S., Samson, B.K., Ali, A. and Mazid, M.A. (1999). Rainfed lowland rice: physical environment and cultivar requirements. *Field Crops Res.* (64), 3–12. doi:10.1016/S0378-4290(99)00047-7.

Walshaw, S.C. (2010). Converting to rice: urbanization, Islamization and crops on Pemba Island, Tanzania, AD 700–1500. *World Archaeol.* 42 (1), 137–154. doi:10.1080/00438240903430399.

Westerhof, A.B., Härmä, P., Isabirye, E., Katto, E., Koistinen, T., Kuosmanen, E., Lehto, T., Lehtonen, M.I., Mäkitie, H., Manninen, T., Mänttäri, I., Pekkala, Y., Pokki, J.,

Saalmann, K. and Virransalo, P. (2014). *Geology and Geodynamic Development of Uganda with Explanation of the 1: 1,000,000 Scale Geological Map.* Special Paper, Geological Survey of Finland 55, Espoo, Finland, 387 pp.

Williams, J.R. (1983). *EPIC, The Erosion-Productivity Impact Calculator, Volume 1. Model Documentation.* USDA, Agricultural Research Service, Beltsville, USA.

Williams, J.R., Jones, C.A., Kiniry, J.R. and Spanel, D.A. (1989). The EPIC crop growth model. *Trans. ASAE* 32 (2), 497–511. doi:10.13031/2013.31032.

Willmott, C.J. and Matsuura, K. (2005). Advantages of the mean absolute error (MAE) over the root mean square error (RMSE) in assessing average model performance. *Clim. Res.* 30 (1), 79–82. doi:10.3354/cr030079.

Wilson, E., McInnes, R., Mbaga, D.P. and Ouedaogo, P. (2017). *Kilombero Valley, United Republic of Tanzania. Ramsar Site No. 1173.* Ramsar Advisory Mission Report, Gland, Switzerland.

Windmeijer, P.N. and Andriesse, W. (1993). *Inland valleys in West Africa: an agro-ecological characterization of rice-growing environments.* International Institute for Land Reclamation and Improvement (ILRI), Wageningen, Netherlands.

Wood, A.P. and Van Halsema, G.E. (2008). *Scoping agriculture–wetland interactions: towards a sustainable multiple-response strategy.* Food and Agriculture Organization of the United Nations (FAO), Rome, Italy.

Wopereis, M.C.S., Bouman, B.A.M., Tuong, T.P., Ten Berge, H.F.M. and Kropff, M.J. (1996). *ORYZA_W: rice growth model for irrigated and rainfed environments.* SARP Research Proceedings, IRRI/AB-DLO, Wageningen, Netherlands.

Worou, N.O., Gaiser, T., Saito, K., Goldbach, H. and Ewert, F. (2012). Simulation of soil water dynamics and rice crop growth as affected by bunding and fertilizer application in inland valley systems of West Africa. *Agric. Ecosyst. Environ.* 162, 24–35. doi:10.1016/j.agee.2012.07.018.

Worou, N.O., Gaiser, T., Saito, K., Goldbach, H. and Ewert, F. (2013). Spatial and temporal variation in yield of rainfed lowland rice in inland valley as affected by fertilizer application and bunding in north-west Benin. *Agric. Water Manag.* 126, 119–124. doi:10.1016/j.agwat.2013.04.007.

Yanggen, D., Kelly, V.A., Reardon, T. and Naseem, A. (1998). *Incentives for fertilizer use in Sub-Saharan Africa: a review of empirical evidence on fertilizer response and profitability,* International Development Working Paper No. 70, Michigan State University, East Lansing, USA.

Zakaria, S., Matsuda, T., Tajima, S. and Nitta, Y. (2002). Effect of high temperature at ripening stage on the reserve accumulation in seed in some rice cultivars. *Plant Prod. Sci.* 5 (2), 160–168. doi:10.1626/pps.5.160.

Zenna, N., Senthilkumar, K. and Sie, M. (2017). Rice Production in Africa. In: Chauhan, B.S., Jabran, K., Mahajan, G. (Eds.) *Rice Production Worldwide.* Springer International Publishing, Berlin/Heidelberg, Germany, pp. 117–135.

Zhang, X., Lee, J.H., Abawi, Y., Kim, Y.H., McClymont, D. and Kim, H.D. (2007). Testing the simulation capability of APSIM-ORYZA under different levels of nitrogen fertiliser and transplanting time regimes in Korea. *Aust. J. Exp. Agric.* 47 (12), 1446–1454. doi:10.1071/EA05363.

List of publications

Peer-reviewed journal publications

Grotelüschen, K., Gaydon, D.S., Ziegler, S., Kwesiga, J., Langensiepen, M., Senthilkumar, S., Whitbread, A.M. and Becker, M. (2021). Assessing the effects of management and hydro-edaphic conditions on rice in contrasting East African wetlands using experimental and modelling approaches. *Agric. Water Manag.* 258, 107146. 10.1016/j.agwat.2021.107146.

Grotelüschen, K., Gaydon, D.S., Senthilkumar, K., Langensiepen, M. and Becker, M. (2021). Model-based evaluation of rainfed lowland rice responses to N fertiliser in variable hydro-edaphic wetlands of East Africa. *Field Crops Res.* (in revision).

Kwesiga, J., Grotelüschen, K., Senthilkumar, K., Neuhoff, D., Döring, T.F. and Becker, M. (2020). Rice Yield Gaps in Smallholder Systems of the Kilombero Floodplain in Tanzania. *Agronomy* 10(8), 1135-1149. 10.3390/agronomy10081135.

Kwesiga, J., Grotelüschen, K., Senthilkumar, K., Neuhoff, D., Döring, T.F. and Becker, M. (2020). Effect of organic amendments on the productivity of rainfed lowland rice in the Kilombero floodplain of Tanzania. *Agronomy* 10(9), 1280-1298. 10.3390/agronomy10091280.

Kwesiga, J., Grotelüschen, K., Neuhoff, D., Senthilkumar, K., Döring, T.F. and Becker, M. (2019). Site and management effects on grain yield and yield variability of rainfed lowland rice in the Kilombero floodplain of Tanzania. *Agronomy* 9(10), 632-648. doi:10.3390/agronomy9100632.

Conference contributions

Grotelüschen, K.; Langensiepen, M.; Ziegler, S.; Kwesiga, J.; Glasner, B.; Gabiri, G.; Senthilkumar, K., Becker, M. (2018). Unlocking Rice Potentials in Contrasting Wetlands in East Africa. Presented at 'Global food security and food safety: the role of universities', Tropentag, 17-19 Sep. 2018, Ghent University, Ghent, Belgium.

Kwesiga, J., Neuhoff, D., Gabiri, G.; Grotelüschen, K., Senthilkumar, K., Köpke, U., Becker, M. (2018). Grain Yield and Yield Variability of Rainfed Lowland Rice with 'Good Agricultural Practices' in the Kilombero Floodplain of Tanzania. Presented at 'Global food security and food safety: the role of universities', Tropentag, 17-19 Sep. 2018, Ghent University, Ghent, Belgium.

Ziegler, S.; Neuhoff, D.; Senthilkumar, K.; Namugalu, M.; Grotelüschen, K.; Glasner, B.; Becker, M., Köpke, U. (2017). Increasing Crop Productivity in Rainfed Rice Systems

of Central Uganda. Poster presented at 'Future Agriculture: Socio-ecological transitions and bio-cultural shifts', Tropentag, 20-22 September 2017, Bonn University, Bonn, Germany.

Grotelüschen, K.; Sennhenn, A.; Whitbread, A.; Maass, B.L., Njarui, D.M.G. (2014). *Lablab purpureus* (L) Sweet: A promising multipurpose legume for enhanced drought resistance in smallholder farming-systems of eastern Kenya. Poster presented at 'Bridging the gap between increasing knowledge and decreasing resources', Tropentag, 17-19 Sep. 2014, Czech University of Life Sciences, Prague, Czech Republic.

Grotelüschen, K.; Sennhenn, A., Whitbread, A. (2013). Nitrogen-Use-Efficiency in Maize-Based Farming Systems in Malawi: A Simulation and Meta-Analysis of Literature. Poster presented at 'Agricultural development within the rural-urban continuum', Tropentag, 17-19 Sep. 2013, Hohenheim University, Stuttgart, Germany.

Annex

Annex A: Field impressions

    A_1 Field experimental site in the floodplain near Ifakara, Tanzania.

    A_2 Field experimental site in the inland valley near Namulonge, Uganda.

Annex B: Supplemental material (chapter 5.1)

    B_1 Measured water table dynamics in the floodplain in Tanzania and the inland valley in Uganda.

    B_2 Variety-specific phenological development parameters and partitioning coefficients.

    B_3 Mean absolute errors of simulated to observed key phenological stages.

    B_4 Observed and simulated soil moisture dynamics at 30 cm soil depth in the floodplain in Tanzania.

    B_5 Observed and simulated soil moisture dynamics at 30 cm soil depth in the inland valley in Uganda.

Annex C: APSIM input files and manager scripts

    C_1 Oryza.xml input file for the lowland rice cv. SARO-5.

    C_2 Oryza.xml input file for the rainfed rice cv. NERICA-4.

    C_3 Logic commands for the scenario analysis in the floodplain in Tanzania.

    C_4 Logic commands for the scenario analysis in the inland valley in Uganda.

Annex A$_1$: Field experimental site in the floodplain near Ifakara, Tanzania

Plate 1: View into the Kilombero floodplain in Tanzania. Picture taken from *www.ambero.de*.

Plate 2: Rice nursery.

Plate 3: Field preparation (surface levelling).

Plate 4: Rice transplanting.

Plate 7: Rice stand at physiological maturity.

Plate 8: The team.

Annex A$_2$: Field experimental site in inland valley near Namulonge, Uganda

Plate 9: View into experimental site in the inland valley swamp in Namulonge, Uganda.

Plate 10: Rice nursery.

Plate 11: Rice transplanting.

Plate 12: Freshly transplanted rice.

Plate 13: Rice stand during the vegetative growth stage.

Plate 14: Rice stand at 50% flowering.

Plate 15: Rice stand at physiological maturity.

Plate 16: Lozio Makesa, our field manager without whom this study would have not been possible.

Annex B$_1$: Measured water table dynamics in the floodplain in Tanzania and the inland valley in Uganda
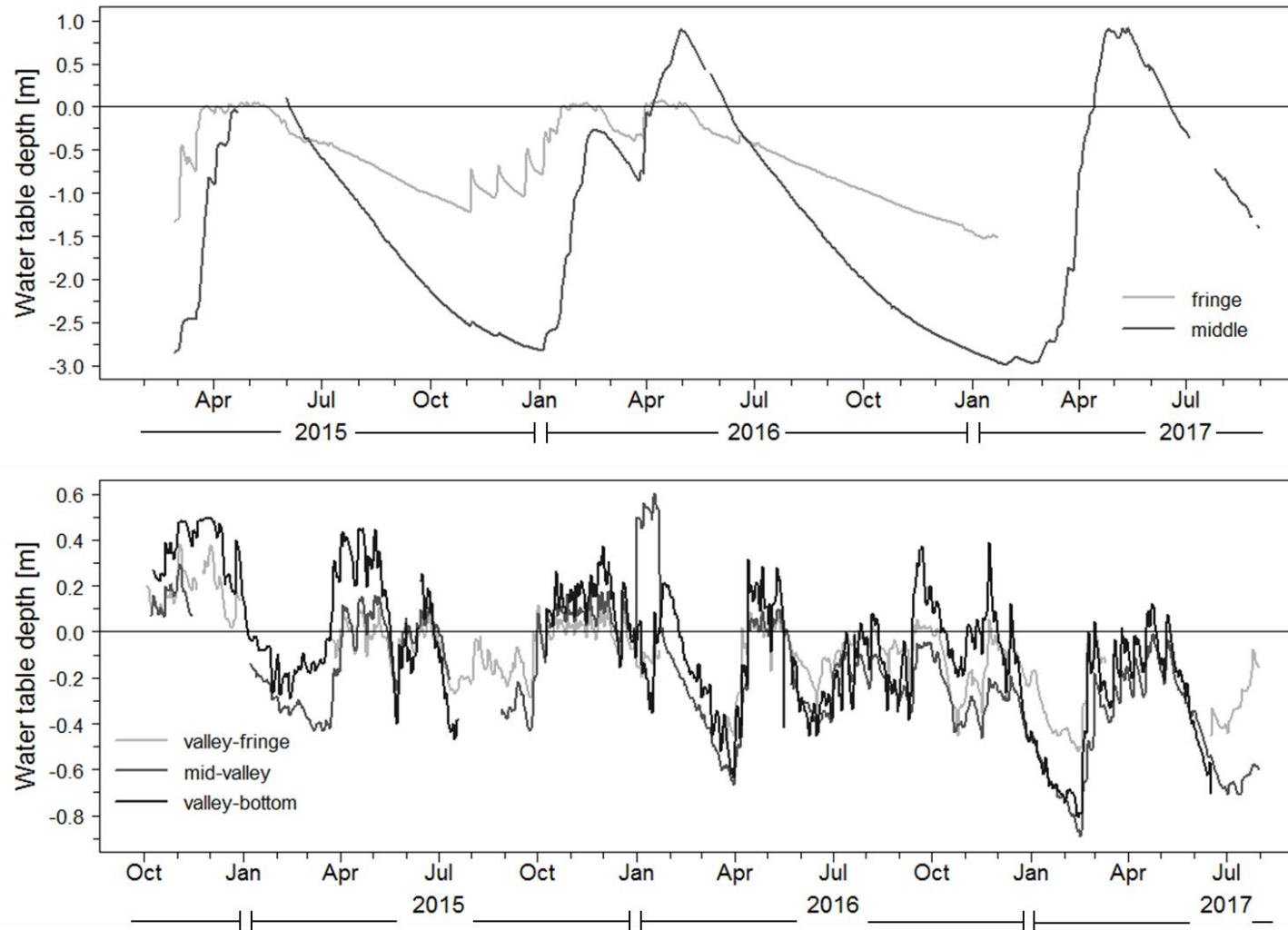
Figure A.1 Measured daily depth to water table during the study period (2014-2017) at the study sites and field positions in the floodplain in Tanzania (2015-2017) (top) and (b) the inland valley in Uganda (2014-2017) (bottom); solid zero line represents the surface level in the field; positive values are not implicitly related to water levels above the surface (floods); modified from Gabiri *et al.* 2017, 2018.

Annex B$_2$: Variety-specific phenological development parameters and partitioning coefficients

Table A.1 Phenological development parameters and biomass partitioning coefficients for the two rice varieties.

Parameter	Acronym	Unit	lowland rice cv. SARO-5	rainfed rice cv. NERICA-4
Development rate in the juvenile phase	DVRJ	(°C day^{-1})	0.000866	0.001131
Development rate in the photoperiod-sensitive phase	DVRI	(°C day^{-1})	0.000758	0.000758
Development rate in the panicle development phase	DVRP	(°C day^{-1})	0.000692	0.000624
Development rate in the reproductive phase	DVRR	(°C day^{-1})	0.001400	0.001835
Min. value of the relative growth rate of the leaf area	RGRLMN	(°C day^{-1})	0.0040	0.0035
Max. value of the relative growth rate of the leaf area	RGRLMX	(°C day^{-1})	0.0085	0.0070
Maximum individual grain weight	WGRMX	(mg grain^{-1})	30.6	26.2
Development stage	DVS	(0-2)	[0.00; 0.60; 0.85; 1.00; 1.40; 2.00]	[0.00; 0.55; 0.80; 1.00; 1.50; 2.00]
Fraction of shoot dry matter to leaves	FLV	(0-1)	[0.55; 0.44; 0.24; 0.15; 0.00; 0.00]	[0.60; 0.54; 0.37; 0.21; 0.00; 0.00]
Fraction of shoot dry matter to stems	FST	(0-1)	[0.45; 0.56; 0.76; 0.50; 0.00; 0.00]	[0.40; 0.46; 0.63; 0.69; 0.00; 0.00]
Fraction of shoot dry matter to storage organs	FSO	(0-1)	[0.00; 0.00; 0.00; 0.35; 1.00; 1.00]	[0.00; 0.00; 0.00; 0.10; 1.00; 1.00]
Specific green leaf area	SLA	(m^2 leaf kg leaf^{-1})	[0.0045; 0.0045; 0.0035; 0.0018; 0.0015; 0.0015; 0.0015]	[0.0035; 0.0030; 0.0025; 0.0018; 0.0018; 0.0018; 0.0018]

Annex B$_3$: Mean absolute errors of simulated to observed key phenological stages
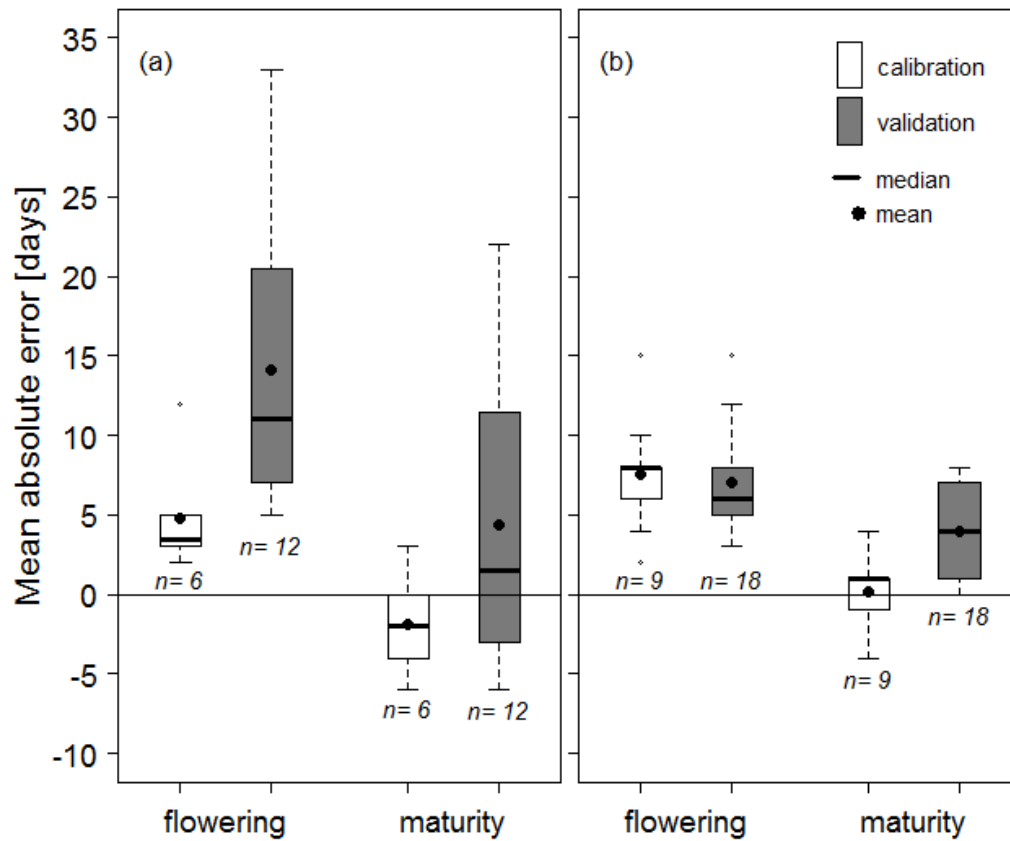
Figure A.2 Mean absolute errors of simulated to observed durations of key phenological stages during model calibration and validation in (a) the floodplain in Tanzania and (b) the inland valley in Uganda.

Annex B$_4$: Observed and simulated soil moisture dynamics at 30 cm soil depth in the floodplain in Tanzania
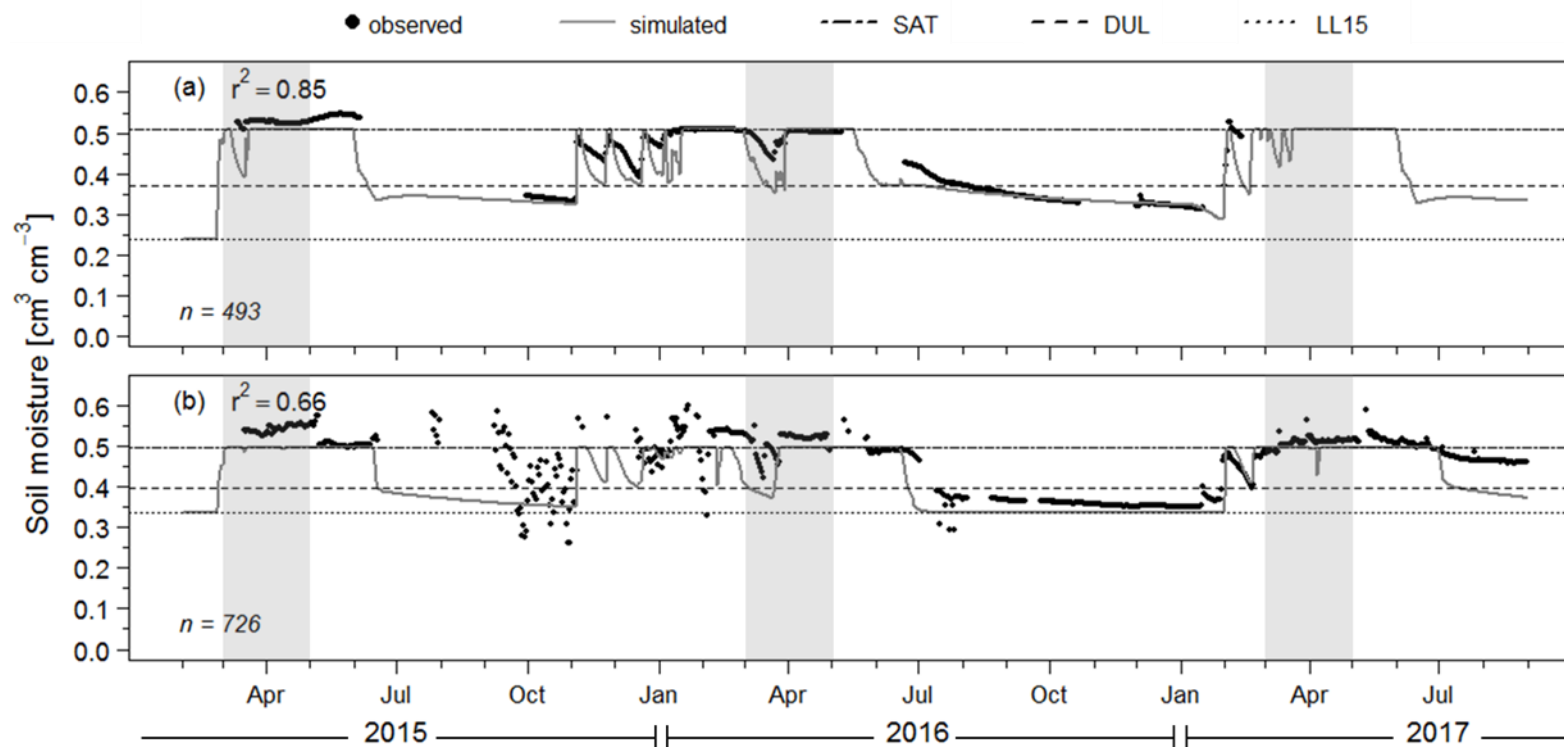
Figure A.3 Observed (points, un-replicated) and simulated (lines) soil moisture dynamics in the non-amended baseline treatment (0N) and 30 cm depth at the floodplain's (a) fringe and (b) middle positions (2015-2017); volumetric water content at saturation (SAT), field capacity (DUL) and wilting point (LL15); the shaded areas (grey) indicate the main rice-growing periods (March to May).

Annex B$_5$: Observed and simulated soil moisture dynamics at 30 cm soil depth in the inland valley in Uganda
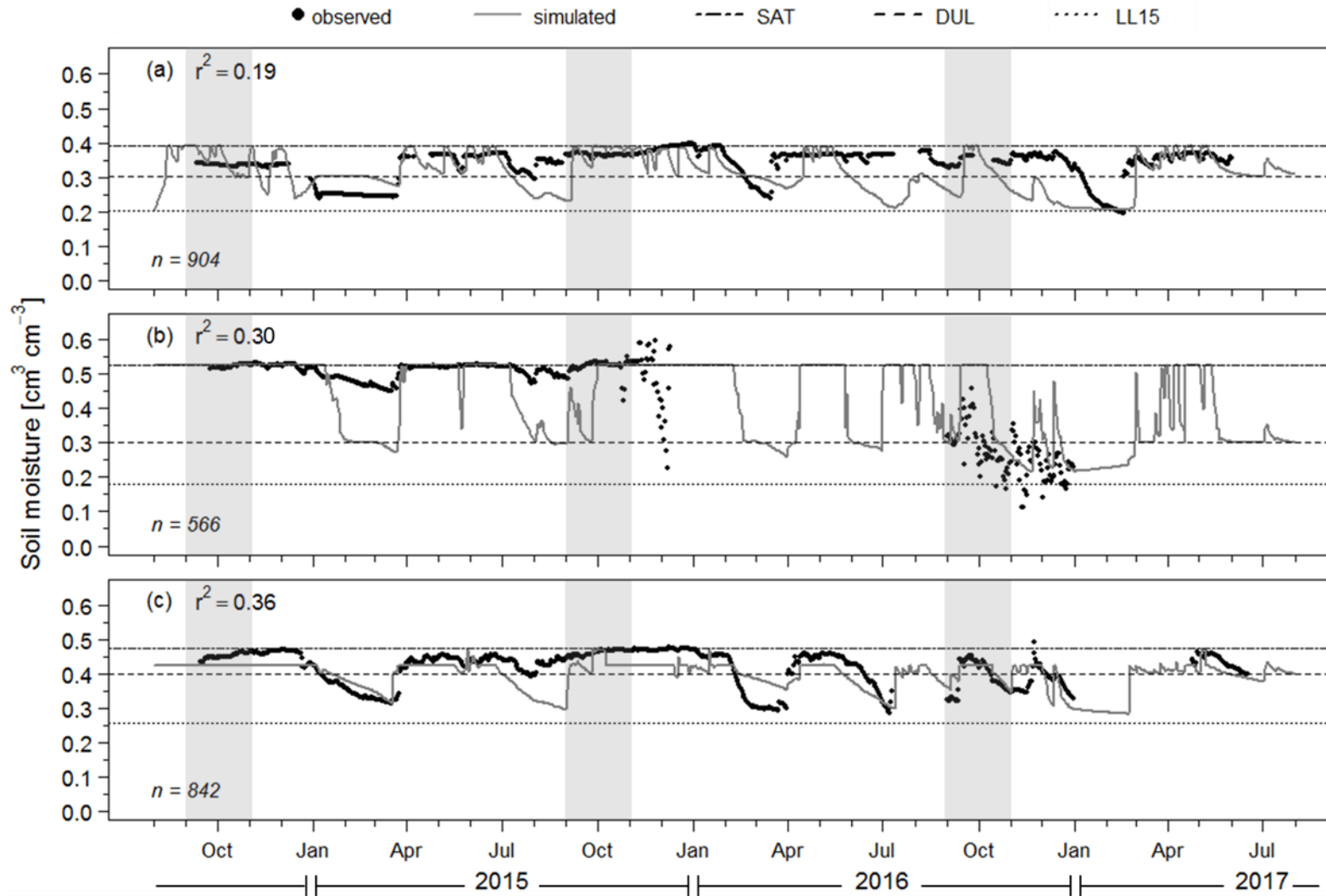
Figure A.4 Observed (points, un-replicated) and simulated (lines) soil moisture dynamics in the non-amended baseline treatment (0N) and 30 cm depth at the inland valley's (a) valley-fringe, (b) mid-valley and (c) valley-bottom positions (2014-2017); volumetric water content at saturation (SAT), field capacity (DUL) and wilting point (LL15); the shaded areas (grey) indicate the main rice-growing periods (September to November).

Annex C₁: Oryza.xml input file for the lowland rice cv. SARO-5

(only script sections with changes shown)

```
<!--  East African varieties -->
<txd306 cultivar="yes">
<DVRJ description="Development rate in juvenile phase (oCd-1)">.000866</DVRJ>
<DVRI description="Development rate in photoperiod-sensitive phase (oCd-1)">.000758</DVRI>
<DVRP description="Development rate in panicle development (oCd-1)">.000692</DVRP>
<DVRR description="Development rate in reproductive phase (oCd-1)">.001400</DVRR>
<MOPP description="Maximum optimum photoperiod (h)">11.50</MOPP>
<PPSE description="Photoperiod sensitivity (h-1)">0.0</PPSE>
</txd306>


<WGRMX description="Maximum individual grain weight (kg grain-1)">0.0000264 </WGRMX>
<!--  SLA determination -->
<ASLA description="(-)* SLA function parameters: (used when no sla table present..)">0.0024 </ASLA>
<BSLA description="(-)* SLA = ASLA + BSLA*EXP(CSLA*(DVS-DSLA)), and SLAMAX">0.0025 </BSLA>
<CSLA description="(-)">-4.5   </CSLA>
<DSLA description="(-)">0.14   </DSLA>
<SLAMAX description="maximum value of SLA (ha/kg)">0.0045 </SLAMAX>
<!--  Uncomment these to use this stick function instead of the above fn.
SLAT = 0.00   0.60   0.85   1.00   2.00   2.50   !
SLA =  0.0045 0.0045 0.0035 0.0018 0.0015 0.0015 ! -->
<RGRLMX description="Maximum relative growth rate of leaf area (oCd-1)">0.0085  </RGRLMX>
<RGRLMN description="Minimum relative growth rate of leaf area (oCd-1)">0.0040  </RGRLMN>
<ZRTMCW description="Maximum depth of roots if no drought stress (m)">0.25   </ZRTMCW>
<ZRTMCD description="Maximum depth of roots if drought (m)">0.47   </ZRTMCD>
<ZRTMS description="Maximum rooting depth in the soil (m)">1.0     </ZRTMS>


<!-- Table of fraction total dry matter partitioned to the shoot as a function of development stage (-; X value): -->
<FSHT>0.00 0.43 1.00 2.50 </FSHT>
<FSH>0.50 0.75 0.92 1.00 </FSH>
<!-- Table of fraction shoot dry matter partitioned to the leaves as a function of development stage (-; X value):  -->
<FLVT>0.00 0.60 0.85 1.00 1.55 2.00 2.50 </FLVT>
 <FLV>0.55 0.44 0.24 0.15 0.00 0.00 0.00</FLV>
<!-- Table of fraction shoot dry matter partitioned to the stems as a function of development stage (-; X value): -->
<FSTT>0.00 0.60 0.85 1.00 1.55 2.00 2.50 </FSTT>
<FST>0.45 0.56 0.76 0.50 0.00 0.00 0.00</FST>
<!--  Table of fraction shoot dry matter partitioned to the panicles as a function of development stage (-; X value): -->
<FSOT>0.00 0.60 0.85 1.00 1.55 2.00 2.50 </FSOT>
<FSO>0.00 0.00 0.00 0.35 1.00 1.00 1.00</FSO>
<!-- Table of leaf death coefficient (d-1; Y-value) as a function of development stage (-; X value): ->
<DRLVT>0.00  0.60  1.00  1.50  2.10  2.50   </DRLVT>
<DRLV>0.000 0.000 0.001 0.020 0.060 0.060  </DRLV>
```

Annex C$_2$: Oryza.xml input file for the rainfed rice cv. NERICA-4

(only script sections with changes shown)

```
<!-- East African varieties -->
<nerica4 cultivar="yes">
<DVRJ description="Development rate in juvenile phase (oCd-1)">.001131</DVRJ>
<DVRI description="Development rate in photoperiod-sensitive phase (oCd-1)">.000758</DVRI>
<DVRP description="Development rate in panicle development (oCd-1)">.000624</DVRP>
<DVRR description="Development rate in reproductive phase (oCd-1)">.001835</DVRR>
<MOPP description="Maximum optimum photoperiod (h)">11.50</MOPP>
<PPSE description="Photoperiod sensitivity (h-1)">0.0</PPSE>
</nerica4>

<WGRMX description="Maximum individual grain weight (kg grain-1)">0.0000219 </WGRMX>
<!-- SLA determination -->
<ASLA description="(-)* SLA function parameters: (used when no sla table present..)">0.0024
</ASLA>
<BSLA description="(-)* SLA = ASLA + BSLA*EXP(CSLA*(DVS-DSLA)), and SLAMAX">0.0025
</BSLA>
<CSLA description="(-)">-4.5   </CSLA>
<DSLA description="(-)">0.14   </DSLA>
<SLAMAX description="maximum value of SLA (ha/kg)">0.0035 </SLAMAX>
<!-- Uncomment these to use this stick function instead of the above fn.
SLAT = 0.00   0.55   0.80   1.00   2.00   2.50   !
SLA =  0.0035 0.0030 0.0035 0.0018 0.0018 0.0018 ! -->
<RGRLMX description="Maximum relative growth rate of leaf area (oCd-1)">0.0070  </RGRLMX>
<RGRLMN description="Minimum relative growth rate of leaf area (oCd-1)">0.0035  </RGRLMN>
<ZRTMCW description="Maximum depth of roots if no drought stress (m)">0.25  </ZRTMCW>
<ZRTMCD description="Maximum depth of roots if drought (m)">0.50   </ZRTMCD>
<ZRTMS description="Maximum rooting depth in the soil (m)">1.0     </ZRTMS>

<!-- Table of fraction total dry matter partitioned to the shoot as a function of development stage (-;
X value): -->
<FSHT>0.00 0.40 1.00 2.00 2.50 </FSHT>
<FSH>0.50 0.75 0.80 1.00 1.00</FSH>
<!-- Table of fraction shoot dry matter partitioned to the leaves as a function of development stage
(-; X value): -->
<FLVT>0.00 0.55 0.80 1.00 1.50 2.00 2.50 </FLVT>
<FLV>0.60 0.54 0.37 0.21 0.00 0.00 0.00 </FLV>
<!-- Table of fraction shoot dry matter partitioned to the stems as a function of development stage (-
; X value): -->
<FSTT>0.00 0.55 0.80 1.00 1.50 2.00 2.50 </FSTT>
<FST>0.40 0.46 0.63 0.69 0.00 0.00 0.00 </FST>
<!-- Table of fraction shoot dry matter partitioned to the panicles as a function of development
stage (-; X value): -->
<FSOT>0.00 0.55 0.80 1.00 1.50 2.00 2.50 </FSOT>
<FSO>0.00 0.00 0.00 0.10 1.00 1.00 1.00 </FSO>
<!-- Table of leaf death coefficient (d-1; Y-value) as a function of development stage (-; X value): ->
<DRLVT>0.00  0.86  1.00  1.50  2.10  2.50   </DRLVT>
<DRLV>0.000 0.001 0.010 0.025 0.050 0.050  </DRLV>
```

Annex C$_3$: Logic commands for the scenario analysis in the floodplain in Tanzania

```
! *************************************************************************************************
! ******* Saro-5 – Rainfed lowland rice, floodplain wetland in Tanzania *********************************
! *************************************************************************************************


! ******* init section *********************************************************************************
! Rice husbandry
    rice_sow_day = 0
    transplant_day = 0
    maturity_day = 0
    tot_fert = 0
    flag = 0
! Water use & supply
    crop_radn = 0
    season = 0
    crop_rain = 0
    tot_irrig = 0
    crop_water = 0
    irrig_count = 0
    cum_etd = 0
    PEP_rain = 0
    PEP_water = 0
! Weed management
    weed_sow_day = 0
    weed_1 = 0
    weed_2 = 0
    weed_3 = 0
    fallow_sow_day = 0
! N-availability & losses
    tot_N_uptake = 0
    cum_dnit = 0
    tot_NO3_leach = 0
    loss_NH4 = 0
! N- & waterstress
    waterstress_cum = 0
    wateravstress_rice = 0
    nstress_cum = 0
    navstress_rice = 0
! Rice phenology
    trip_1 = 0
    trip_2 = 0
    trip_3 = 0
    trip_4 = 0
    trip_5 = 0
    trip_6 = 0
    trip_7 = 0
    trip_8 = 0
    trip_9 = 0
    trip_10 = 0
    trip_11 = 0
    trip_12 = 0
    trip_13 = 0
    trip_14 = 0
```

```
! ******* start_of_day section ********************************************************************
! ****** Environmental Conditions & Stress Factors ***********************************************
if rice.plant_status = 'alive' and rice.dae>=1 then
    crop_rain = crop_rain + rain  ! in-season rainfall & radiation
    crop_radn = crop_radn + radn
    crop_water = crop_rain + tot_irrig
    cum_etd = cum_etd + etd  ! evapotranspiration
    waterstress_cum = waterstress_cum + lestrs  ! water- and N-stress
    wateravstress_rice = waterstress_cum/rice.dae
    nstress_cum = nstress_cum + rnstrs
    navstress_rice = nstress_cum/rice.dae
    tot_N_uptake   =   tot_N_uptake   +   nacr       !   N-losses   (plant   uptake   and
    denitrification/leaching/volatilisation)
    cum_dnit = cum_dnit + dnit()
    tot_NO3_leach = tot_NO3_leach + flow_NO3(13)
    loss_NH4 = amloss + loss_NH4
endif
! ****** Water supply between DVS 0.65 and 1.00 *********************************************
if dvs >= 0.64 and dvs <= 1.02 then
    PEP_rain = PEP_rain + rain
    PEP_water = cum_esw + PEP_rain
    cum_trw = cum_trw + trw
endif
!****** Seasonal rainfall categories ************************************************************
if rice.plant_status = 'alive' and crop_rain <= 1000 then
    season = 1
elseif crop_rain >= 1000 then
    season = 2
endif
! ****** Grow Weed Fallow – fringe position ****************************************************
if day = 200 and weed.stagename = 'out' then
    SurfaceOrganicMatter_fringe tillage type = tine, f_incorp = 1.0, tillage_depth = 300   !
    incorporate remaining rice residues
    weed sow cultivar = perennial, plants = 20 (/m2), crop_class = perennial_grass, sowing_depth
    = 20 (mm)
    crop_name = 'weed1'
    fallow_sow_day = day
endif
! ****** Grow Weed Fallow – middle position ***************************************************
if day = 200 and weed.stagename = 'out' then
    SurfaceOrganicMatter_mid tillage type = tine, f_incorp = 1.0, tillage_depth = 300  ! incorporate
    remaining rice residues
    weed sow cultivar = perennial, plants = 20 (/m2), crop_class = perennial_grass, sowing_depth
    = 20 (mm)
    crop_name = 'weed1'
    fallow_sow_day = day
endif
! ****** Rice Sowing & Transplanting **********************************************************
if day > 25 and day < 60 and rice.plant_status = 'out' and rain[7] >= 50 then
    rice sow cultivar = txd306, establishment = transplant, sbdur = 21, nplh = 2, nh = 25, nplsb =
    1000
    crop_name = 'rice'
    rice_sow_day = day
    transplant_day = rice_sow_day + 21
elseif day = 60 and rice.plant_status = 'out' then
    rice sow cultivar = txd306, establishment = transplant, sbdur = 21, nplh = 2, nh = 25, nplsb =
    1000
    crop_name = 'rice'
    rice_sow_day = day
```

```
    transplant_day = rice_sow_day + 21
endif
! ******* Field Management – fringe position ***********************************************************
if day = rice_sow_day then
    gwd_sequence = 1
    crop_name = 'weed2'
    weed harvest
    weed end_crop
    nit_tot_init = nit_tot()
    soc_init = oc()
    SurfaceOrganicMatter_fringe tillage type = tine, f_incorp = 1.0, tillage_depth = 300   !
    incorporate 100% of initial residues into soil
    max_pond = 400
    irrigation apply amount = 40
    'TZA - fringe Water' set ks = 799 33 52 43 30 28 28 27 27 27 27 27 27 27  ! reduced KS from
    puddling
    'TZA - fringe Water' set bd = 1.05 1.365 1.41 1.41 1.42 1.40 1.40 1.39 1.39 1.39 1.39 1.39 1.39
    1.39  ! increase BD of plough-pan by 5% as per Gathala et al. 2011
endif
! ******* Field Management – middle position ***********************************************************
if day = rice_sow_day then
    gwd_sequence = 1
    crop_name = 'weed2'
    weed harvest
    weed end_crop
    nit_tot_init = nit_tot()
    soc_init = oc()
    SurfaceOrganicMatter_mid tillage type = tine, f_incorp = 1.0, tillage_depth = 300  ! incorporate
    100% of initial residues into soil
    max_pond = 400
    irrigation apply amount = 40
    'TZA - mid Water' set ks = 945 170 59 27 67 34 11 31 34 34 34 34 34 34  ! reduced KS from
    puddling
    'TZA - mid Water' set bd = 1.34 1.3 1.34 1.3965 1.3 1.34 1.43 1.34 1.35 1.35 1.35 1.35 1.35
    1.35  ! increase BD of plough-pan by 5% as per Gathala et al. 2011
endif
! ****** Output Drought Stress at Key Phenological Stages ***********************************************
if day = rice_sow_day and trip_1 = 0 then
    trip_1 = 1
    waterstr_1 = lestrs
    nstr_1 = rnstrs
endif
if day = transplant_day and trip_2 = 0 then
    trip_2 = 1
    waterstr_2 = lestrs
    nstr_2 = rnstrs
endif
if dvs >= 0.64 and dvs <= 0.66 and trip_3 = 0 then
    trip_3 = 1
    waterstr_3 = lestrs
    nstr_3 = rnstrs
    cum_esw = esw  ! extractable water content at PI (for water supply calculation DVS 0.65-1.0)
endif
if dvs >= 0.78 and dvs <= 0.82 and trip_4 = 0 then
    trip_4 = 1
    waterstr_4 = lestrs
    nstr_4 = rnstrs
endif
if dvs >= 0.88 and dvs <= 0.92 and trip_5 = 0 then
```

```
    trip_5 = 1
    waterstr_5 = lestrs
    nstr_5 = rnstrs
endif
if dvs >= 0.98 and dvs <= 1.02 and trip_6 = 0 then
    trip_6 = 1
    waterstr_6 = lestrs
    nstr_6 = rnstrs
endif
if dvs >= 1.08 and dvs <= 1.12 and trip_7 = 0 then
    trip_7 = 1
    waterstr_7 = lestrs
    nstr_7 = rnstrs
endif
if dvs >= 1.18 and dvs <= 1.22 and trip_8 = 0 then
    trip_8 = 1
    waterstr_8 = lestrs
    nstr_8 = rnstrs
endif
if dvs >= 1.38 and dvs <= 1.42 and trip_9 = 0 then
    trip_9 = 1
    waterstr_9 = lestrs
    nstr_9 = rnstrs
endif
if dvs >= 1.58 and dvs <= 1.62 and trip_10 = 0 then
    trip_10 = 1
    waterstr_10 = lestrs
    nstr_10 = rnstrs
endif
if dvs >= 1.68 and dvs <= 1.72 and trip_11 = 0 then
    trip_11 = 1
    waterstr_11 = lestrs
    nstr_11 = rnstrs
endif
if dvs >= 1.78 and dvs <= 1.82 and trip_12 = 0 then
    trip_12 = 1
    waterstr_12 = lestrs
    nstr_12 = rnstrs
endif
if dvs >= 1.88 and dvs <= 1.92 and trip_13 = 0 then
    trip_13 = 1
    waterstr_13 = lestrs
    nstr_13 = rnstrs
endif
if dvs >= 2.00 and trip_14 = 0 then
    trip_14 = 1
    waterstr_14 = lestrs
    nstr_14 = rnstrs
    nit_tot_diff = nit_tot() - nit_tot_init
    soc_diff = oc() - soc_init
endif
! ****** Weed Sowing ***************************************************************************************
if day = transplant_day then
    weed sow cultivar = perennial, plants = 15 (/m2), crop_class = perennial_grass, sowing_depth
    = 20 (mm)
    crop_name = 'weed2'
    weed_sow_day = day
    weed_1 = weed_sow_day + 21
    weed_2 = weed_sow_day + 42
```

```
        weed_3 = weed_sow_day + 63
endif
! ****** Weed Manual Weeding *************************************************************************
if day = weed_1 then
        weed kill_crop, kill_fr = 0.8  ! 80% of weeds are killed as a result of hand-weeding
endif
if day = weed_2 then
        weed kill_crop, kill_fr = 0.8  ! 80% of weeds are killed as a result of hand-weeding
endif
if day = weed_3 then
        weed kill_crop, kill_fr = 0.8  ! 80% of weeds are killed as a result of hand-weeding
endif
! ****** Equal Fertiliser Split-Application ***************************************************************
! ****** fert_factor (0, 0.5, 1, 1.5, 2, 2.5)
fert_amount_1 = 30 * fert_factor
if day = transplant_day then
        fertiliser apply amount = fert_amount_1, type = urea_n
endif
fert_amount_2 = 30 * fert_factor
if dvs >= 0.65 and flag = 0 then
        fertiliser apply amount = fert_amount_2, type = urea_N
        flag = 1
        tot_fert = fert_amount_1 + fert_amount_2
endif
! ****** Rice Harvest and Parameter re-set – fringe position ***********************************************
if rice.plant_status = 'dead' then
        maturity_day = day - 1
        crop_name = 'rice'
        rice harvest
        rice end_crop
        crop_name = 'weed2'
        weed harvest
        weed end_crop
        nit_tot_end = nit_tot()
        soc_end = oc()
        SurfaceOrganicMatter_fringe tillage_single name = rice, type = user_defined, f_incorp = 0.45,
        tillage_depth = 0  ! remove residues according to average HI
        'TZA - fringe Water' set ks = 799 66 52 43 30 28 28 27 27 27 27 27 27 27  ! reverse KS from
        puddling
        'TZA - fringe Water' set bd = 1.05 1.30 1.41 1.41 1.42 1.40 1.40 1.39 1.39 1.39 1.39 1.39 1.39
        1.39  ! reverse increased BD of plough-pan by 5% as per Gathala et al. 2011
! ****** Rice Harvest and Parameter re-set – middle position ***********************************************
if rice.plant_status = 'dead' then
        maturity_day = day - 1
        crop_name = 'rice'
        rice harvest
        rice end_crop
        crop_name = 'weed2'
        weed harvest
        weed end_crop
        nit_tot_end = nit_tot()
        soc_end = oc()
        SurfaceOrganicMatter_mid tillage_single name = rice, type = user_defined, f_incorp = 0.45,
        tillage_depth = 0  ! remove residues according to average HI
        'TZA - mid Water' set ks = 945 170 59 54 67 34 11 31 34 34 34 34 34 34  ! reduced KS from
        puddling
        'TZA - mid Water' set bd = 1.34 1.3 1.34 1.33 1.3 1.34 1.43 1.34 1.35 1.35 1.35 1.35 1.35 1.35
        ! increase BD of plough-pan by 5% as per Gathala et al. 2011
```

```
! ****** Reset Section ***********************************************************************************
    rice_sow_day = 0
    transplant_day = 0
    weed_sow_day = 0
    weed_1 = 0
    weed_2 = 0
    weed_3 = 0
    fallow_sow_day = 0
    tot_fert = 0
    flag = 0
    season = 0
    crop_rain = 0
    crop_radn = 0
    crop_water = 0
    tot_irrig = 0
    irrig_count = 0
    cum_etd = 0
    PEP_rain = 0
    PEP_water = 0
    waterstress_cum = 0
    wateravstress_rice = 0
    nstress_cum = 0
    navstress_rice = 0
    tot_N_uptake = 0
    cum_dnit = 0
    tot_NO3_leach = 0
    loss_NH4 = 0
    cum_dnit = 0
    trip_1 = 0
    trip_2 = 0
    trip_3 = 0
    trip_4 = 0
    trip_5 = 0
    trip_6 = 0
    trip_7 = 0
    trip_8 = 0
    trip_9 = 0
    trip_10 = 0
    trip_11 = 0
    trip_12 = 0
    trip_13 = 0
    trip_14 = 0
endif


! ******* end_of_day section ******************************************************************************
water_table = gwd_fringe  !  reports the depth of gwd below surface from met file in mm; no water
table = 10000; gwd = 0 indicates ponding
water_table = gwd_mid   !  reports the depth of gwd below surface from met file in mm; no water
table = 10000; gwd = 0 indicates ponding
```

Annex C$_4$: Logic commands for the scenario analysis in the inland valley in Uganda

```
! ****************************************************************************************************
! ******* Nerica-4 – Rainfed lowland rice, inland valley wetland in Uganda ****************************
! ****************************************************************************************************


! ******* init section ******************************************************************************
! Rice husbandry
    rice_sow_day = 0
    transplant_day = 0
    maturity_day = 0
    tot_fert = 0
    flag = 0
! Water use & supply
    crop_radn = 0
    season = 0
    crop_rain = 0
    tot_irrig = 0
    crop_water = 0
    irrig_count = 0
    cum_etd = 0
    PEP_rain = 0
    PEP_water = 0
! Weed management
    weed_sow_day = 0
    weed_1 = 0
    weed_2 = 0
    weed_3 = 0
    fallow_sow_day = 0
! N-availability & losses
    tot_N_uptake = 0
    cum_dnit = 0
    tot_NO3_leach = 0
    loss_NH4 = 0
! N- & waterstress
    waterstress_cum = 0
    wateravstress_rice = 0
    nstress_cum = 0
    navstress_rice = 0
! Rice phenology
    trip_1 = 0
    trip_2 = 0
    trip_3 = 0
    trip_4 = 0
    trip_5 = 0
    trip_6 = 0
    trip_7 = 0
    trip_8 = 0
    trip_9 = 0
    trip_10 = 0
    trip_11 = 0
    trip_12 = 0
    trip_13 = 0
    trip_14 = 0
```

```
! ******* start_of_day section *******************************************************************
! ****** Environmental Conditions & Stress Factors **********************************************
if rice.plant_status = 'alive' and rice.dae>=1 then
    crop_rain = crop_rain + rain  ! in-season rainfall & radiation
    crop_radn = crop_radn + radn
    crop_water = crop_rain + tot_irrig
    cum_etd = cum_etd + etd  ! evapotranspiration
    waterstress_cum = waterstress_cum + lestrs  ! water- and N-stress
    wateravstress_rice = waterstress_cum/rice.dae
    nstress_cum = nstress_cum + rnstrs
    navstress_rice = nstress_cum/rice.dae
    tot_N_uptake    =    tot_N_uptake    +    nacr        !    N-losses    (plant    uptake    and
    denitrification/leaching/volatilisation)
    cum_dnit = cum_dnit + dnit()
    tot_NO3_leach = tot_NO3_leach + flow_NO3(13)
    loss_NH4 = amloss + loss_NH4
endif
! ****** Water supply between DVS 0.65 and 1.00 **********************************************
if dvs >= 0.64 and dvs <= 1.02 then
    PEP_rain = PEP_rain + rain
    PEP_water = cum_esw + PEP_rain
    cum_trw = cum_trw + trw
endif
!****** Seasonal rainfall categories ***********************************************************
if rice.plant_status = 'alive' and crop_rain <= 500 then
    season = 1
elseif crop_rain >= 500 then
    season = 2
endif
! ****** Grow Weed Fallow - valley-fringe position **********************************************
if day = 35 and weed.stagename = 'out' then
    SurfaceOrganicMatter_fringe tillage type = tine, f_incorp = 1.0, tillage_depth = 300   !
    incorporate remaining rice residues
    weed sow cultivar = perennial, plants = 15 (/m2), crop_class = perennial_grass, sowing_depth
    = 20 (mm)
    crop_name = 'weed1'
    fallow_sow_day = day
endif
! ****** Grow Weed Fallow – mid-valley position **********************************************
if day = 35 and weed.stagename = 'out' then
    SurfaceOrganicMatter_mid tillage type = tine, f_incorp = 1.0, tillage_depth = 300  ! incorporate
    remaining rice residues
    weed sow cultivar = perennial, plants = 15 (/m2), crop_class = perennial_grass, sowing_depth
    = 20 (mm)
    crop_name = 'weed1'
    fallow_sow_day = day
endif
! ****** Grow Weed Fallow – valley-bottom position *******************************************
if day = 35 and weed.stagename = 'out' then
    SurfaceOrganicMatter_center tillage type = tine, f_incorp = 1.0, tillage_depth = 300   !
    incorporate remaining rice residues
    weed sow cultivar = perennial, plants = 15 (/m2), crop_class = perennial_grass, sowing_depth
    = 20 (mm)
    crop_name = 'weed1'
    fallow_sow_day = day
endif
! ****** Rice Sowing & Transplanting *********************************************************
if day > 230 and day < 265 and rice.plant_status='out' and rain[7]>=35 then
```

```
    rice sow cultivar = nerica4, establishment = transplant, sbdur = 21, nplh = 3, nh = 22, nplsb =
    1000
    crop_name = 'rice'
    rice_sow_day = day
    transplant_day = rice_sow_day + 21
elseif day = 265 and rice.plant_status = 'out' then
    rice sow cultivar = nerica4, establishment = transplant, sbdur = 21, nplh = 3, nh = 22, nplsb =
    1000
    crop_name = 'rice'
    rice_sow_day = day
    transplant_day = rice_sow_day + 21
endif
! ******* Field Management – valley-fringe position *******************************************************
if day = rice_sow_day then
    gwd_sequence = 1
    crop_name = 'weed2'
    weed harvest
    weed end_crop
    nit_tot_init = nit_tot()
    soc_init = oc()
    SurfaceOrganicMatter_fringe tillage type = tine, f_incorp = 1.0, tillage_depth = 300
    max_pond = 400
    irrigation apply amount = 40
    'UGA - fringe Water' set ks = 950 276 483 425 151 65 65 60 60 60 60 60 60  ! reduced KS from
    puddling
    'UGA - fringe Water' set bd = 0.97 1.1865 1.33 1.68 1.68 1.68 1.68 1.25 1.25 1.25 1.25 1.25
    1.25  ! increase BD of plough-pan by 5% as per Gathala et al. 2011
endif
! ******* Field Management – mid-valley position *******************************************************
if day = rice_sow_day then
    gwd_sequence = 1
    crop_name = 'weed2'
    weed harvest
    weed end_crop
    nit_tot_init = nit_tot()
    soc_init = oc()
    SurfaceOrganicMatter_mid tillage type = tine, f_incorp = 1.0, tillage_depth = 300
    max_pond = 400
    irrigation apply amount = 40
    'UGA - mid Water' set ks = 743 113 65 17 18 18 7.4 7.4 7.4 7.4 7.4 7.4 7.4  ! reduced KS from
    puddling
    'UGA - mid Water' set bd = 1.05 1.365 1.51 1.48 1.52 1.52 1.5 1.5 1.5 1.5 1.5 1.5 1.5  !
    increase BD of plough-pan by 5% as per Gathala et al. 2011
endif
! ******* Field Management – valley-bottom position *******************************************************
if day = rice_sow_day then
    gwd_sequence = 1
    crop_name = 'weed2'
    weed harvest
    weed end_crop
    nit_tot_init = nit_tot()
    soc_init = oc()
    SurfaceOrganicMatter_center tillage type = tine, f_incorp = 1.0, tillage_depth = 300
    max_pond = 400
    irrigation apply amount = 40
    'UGA - center Water' set ks = 246 184 266 63 29 29 19 19 19 19 19 19 19  ! reduced KS from
    puddling
    'UGA - center Water' set bd = 1.10 1.1445 1.57 1.53 1.54 1.54 1.53 1.53 1.53 1.53 1.53 1.53
    1.53  ! increase BD of plough-pan by 5% as per Gathala et al. 2011
```

```
endif
! ****** Output Drought Stress at Key Phenological Stages *********************************************
if day = rice_sow_day and trip_1 = 0 then
    trip_1 = 1
    waterstr_1 = lestrs
    nstr_1 = rnstrs
endif
if day = transplant_day and trip_2 = 0 then
    trip_2 = 1
    waterstr_2 = lestrs
    nstr_2 = rnstrs
endif
if dvs >= 0.64 and dvs <= 0.66 and trip_3 = 0 then
    trip_3 = 1
    waterstr_3 = lestrs
    nstr_3 = rnstrs
    cum_esw = esw  ! extractable water content at PI (for water supply calculation DVS 0.65-1.0)
endif
if dvs >= 0.78 and dvs <= 0.82 and trip_4 = 0 then
    trip_4 = 1
    waterstr_4 = lestrs
    nstr_4 = rnstrs
endif
if dvs >= 0.88 and dvs <= 0.92 and trip_5 = 0 then
    trip_5 = 1
    waterstr_5 = lestrs
    nstr_5 = rnstrs
endif
if dvs >= 0.98 and dvs <= 1.02 and trip_6 = 0 then
    trip_6 = 1
    waterstr_6 = lestrs
    nstr_6 = rnstrs
endif
if dvs >= 1.08 and dvs <= 1.12 and trip_7 = 0 then
    trip_7 = 1
    waterstr_7 = lestrs
    nstr_7 = rnstrs
endif
if dvs >= 1.18 and dvs <= 1.22 and trip_8 = 0 then
    trip_8 = 1
    waterstr_8 = lestrs
    nstr_8 = rnstrs
endif
if dvs >= 1.38 and dvs <= 1.42 and trip_9 = 0 then
    trip_9 = 1
    waterstr_9 = lestrs
    nstr_9 = rnstrs
endif
if dvs >= 1.58 and dvs <= 1.62 and trip_10 = 0 then
    trip_10 = 1
    waterstr_10 = lestrs
    nstr_10 = rnstrs
endif
if dvs >= 1.68 and dvs <= 1.72 and trip_11 = 0 then
    trip_11 = 1
    waterstr_11 = lestrs
    nstr_11 = rnstrs
endif
if dvs >= 1.78 and dvs <= 1.82 and trip_12 = 0 then
```

```
        trip_12 = 1
        waterstr_12 = lestrs
        nstr_12 = rnstrs
endif
if dvs >= 1.88 and dvs <= 1.92 and trip_13 = 0 then
        trip_13 = 1
        waterstr_13 = lestrs
        nstr_13 = rnstrs
endif
if dvs >= 2.00 and trip_14 = 0 then
        trip_14 = 1
        waterstr_14 = lestrs
        nstr_14 = rnstrs
        nit_tot_diff = nit_tot() - nit_tot_init
        soc_diff = oc() - soc_init
endif
! ****** Weed Sowing ************************************************************************************
if day = transplant_day then
        weed sow cultivar = perennial, plants = 20 (/m2), crop_class = perennial_grass, sowing_depth
        = 20 (mm)
        crop_name = 'weed2'
        weed_sow_day = day
        weed_1 = weed_sow_day + 21
        weed_2 = weed_sow_day + 42
        weed_3 = weed_sow_day + 63
endif
! ****** Weed Manual Weeding *************************************************************************
if day = weed_1 then
        weed kill_crop, kill_fr = 0.8 ! 80% of weeds are killed as a result of hand-weeding
endif
if day = weed_2 then
        weed kill_crop, kill_fr = 0.8 ! 80% of weeds are killed as a result of hand-weeding
endif
if day = weed_3 then
        weed kill_crop, kill_fr = 0.8 ! 80% of weeds are killed as a result of hand-weeding
endif
! ****** Equal Fertiliser Split-Application *********************************************************
! ****** fert_factor (0, 0.5, 1, 1.5, 2, 2.5)
fert_amount_1 = 30 * fert_factor
if day = transplant_day then
        fertiliser apply amount = fert_amount_1, type = urea_n
endif
fert_amount_2 = 30 * fert_factor
if dvs >= 0.65 and flag = 0 then
        fertiliser apply amount = fert_amount_2, type = urea_N
        flag = 1
        tot_fert = fert_amount_1 + fert_amount_2
endif
! ****** Rice & Weed Harvest and Parameter re-set – valley-fringe position ***************************
if rice.plant_status = 'dead' then
        maturity_day = day - 1
        crop_name = 'rice'
        rice harvest
        rice end_crop
        crop_name = 'weed2'
        weed harvest
        weed end_crop
        nit_tot_end = nit_tot()
        soc_end = oc()
```

SurfaceOrganicMatter_fringe tillage_single name = rice, type = user_defined, f_incorp = 0.39, tillage_depth = 0 ! remove residues according to average HI
'UGA - fringe Water' set ks = 950 552 483 425 151 65 65 60 60 60 60 60 60 ! reduced KS from puddling
'UGA - fringe Water' set bd = 0.97 1.13 1.33 1.68 1.68 1.68 1.68 1.25 1.25 1.25 1.25 1.25 1.25 ! increase BD of plough-pan by 5% as per Gathala et al. 2011
! ****** Rice & Weed Harvest and Parameter re-set – mid-valley position ******************************
if rice.plant_status = 'dead' then
    maturity_day = day - 1
    crop_name = 'rice'
    rice harvest
    rice end_crop
    crop_name = 'weed2'
    weed harvest
    weed end_crop
    nit_tot_end = nit_tot()
    soc_end = oc()
    SurfaceOrganicMatter_mid tillage_single name = rice, type = user_defined, f_incorp = 0.39, tillage_depth = 0 ! remove residues according to average HI
    'UGA - mid Water' set ks = 743 229 65 17 18 18 7.4 7.4 7.4 7.4 7.4 7.4 7.4 ! reduced KS from puddling
    'UGA - mid Water' set bd = 1.05 1.3 1.51 1.48 1.52 1.52 1.5 1.5 1.5 1.5 1.5 1.5 1.5 ! increase BD of plough-pan by 5% as per Gathala et al. 2011
! ****** Rice & Weed Harvest and Parameter re-set – valley-bottom position **************************
if rice.plant_status = 'dead' then
    maturity_day = day - 1
    crop_name = 'rice'
    rice harvest
    rice end_crop
    crop_name = 'weed2'
    weed harvest
    weed end_crop
    nit_tot_end = nit_tot()
    soc_end = oc()
    SurfaceOrganicMatter_center tillage_single name = rice, type = user_defined, f_incorp = 0.39, tillage_depth = 0 ! remove residues according to average HI
    'UGA - center Water' set ks = 246 368 266 63 29 29 19 19 19 19 19 19 19 ! reduced KS from puddling
    'UGA - center Water' set bd = 1.10 1.19 1.57 1.53 1.54 1.54 1.53 1.53 1.53 1.53 1.53 1.53 1.53 ! increase BD of plough-pan by 5% as per Gathala et al. 2011

! ****** Reset Section **
    rice_sow_day = 0
    transplant_day = 0
    weed_sow_day = 0
    weed_1 = 0
    weed_2 = 0
    weed_3 = 0
    fallow_sow_day = 0
    tot_fert = 0
    flag = 0
    season = 0
    crop_rain = 0
    crop_radn = 0
    crop_water = 0
    tot_irrig = 0
    irrig_count = 0
    cum_etd = 0
    PEP_rain = 0

```
        PEP_water = 0
        waterstress_cum = 0
        wateravstress_rice = 0
        nstress_cum = 0
        navstress_rice = 0
        tot_N_uptake = 0
        cum_dnit = 0
        tot_NO3_leach = 0
        loss_NH4 = 0
        cum_dnit = 0
        trip_1 = 0
        trip_2 = 0
        trip_3 = 0
        trip_4 = 0
        trip_5 = 0
        trip_6 = 0
        trip_7 = 0
        trip_8 = 0
        trip_9 = 0
        trip_10 = 0
        trip_11 = 0
        trip_12 = 0
        trip_13 = 0
        trip_14 = 0
endif
```

```
! ******* end_of_day section *************************************************************************
water_table = gwd_fringe + 320 !  reports the depth of gwd below surface from met file in mm; no
water table = 10000; gwd = 0 indicates ponding
water_table = gwd_mid + 30 !  reports the depth of gwd below surface from met file in mm; no
water table = 10000; gwd = 0 indicates ponding
water_table = gwd_center + 300 !  reports the depth of gwd below surface from met file in mm; no
water table = 10000; gwd = 0 indicates ponding
```

© Sandra Grotelüschen